VISIBLE LIGHT EXCITABLE Eu^{3+}-β-DIKETONATE COMPLEXES: SYNTHESIS, CHARACTERIZATION, AND PHOTOPHYSICAL PROPERTIES

Thesis Submitted to AcSIR for the Award of the Degree of
DOCTOR OF PHILOSOPHY
in Chemical Sciences

By

USHA GANGAN T. V.

Registration No: 10CC11A39001

Under the supervision of

Dr. M. L. P. REDDY

CSIR-NATIONAL INSTITUTE FOR INTERDISCIPLINARY SCIENCE AND TECHNOLOGY (CSIR-NIIST)
THIRUVANANTHAPURAM-695 019, KERALA, INDIA

2016

Dedicated to

My Family

DECLARATION

I hereby declare that the Ph.D. thesis entitled: "**Visible light excitable Eu^{3+}-*β*-diketonate complexes: Synthesis, characterization, and photophysical properties**" is the result of the investigations carried out by me at the Materials Science and Technology Division, CSIR-National Institute for Interdisciplinary Science and Technology (CSIR-NIIST), Trivandrum, under the supervision of Dr. M. L. P. Reddy and the same has not been submitted elsewhere for any other degree.

In keeping with the general practice of reporting scientific observations, due acknowledgement has been made wherever the work described is based on the findings of other investigators.

USHA GANGAN T. V.

COUNCIL OF SCIENTIFIC & INDUSTRIAL RESEARCH
NATIONAL INSTITUTE FOR INTERDISCIPLINARY SCIENCE AND TECHNOLOGY (CSIR-NIIST)
Industrial Estate P.O., Trivandrum - 695 019, India

Dr. M. L. P. Reddy, FAPSc
Chief Scientist

Tel: 91-471-2515 360
Fax: +91-471-2491 712
E-mail: mlpreddy55@gmail.com

CERTIFICATE

This is to certify that the work incorporated in this Ph.D. thesis entitled "**Visible light excitable Eu^{3+}-β-diketonate complexes: Synthesis, characterization, and photophysical properties**" submitted by **Ms. USHA GANGAN T. V.** to Academy of Scientific and Innovative Research (AcSIR), in partial fulfilment of the requirements for the award of the **Degree of Doctor of Philosophy in Chemical Sciences**, embodies original research work under my supervision and guidance at the Materials Science and Technology Division of the CSIR-National Institute for Interdisciplinary Science and Technology (CSIR-NIIST), Trivandrum. I further certify that this work has not been submitted to any other University or Institution in part or full for the award of any degree or diploma. Research material obtained from other sources has been duly acknowledged in the thesis. Any text, illustration, table etc., used in the thesis from other sources, have been duly cited and acknowledged.

USHA GANGAN T. V.

Dr. M. L. P. REDDY
(Thesis Supervisor)

Thiruvananthapuram

December, 2016

ACKNOWLEDGEMENTS

This thesis is the culmination of a fabulous journey in obtaining my PhD. The thesis was made possible only by the support and encouragement of many people including my supervisor, co-workers, teachers, and family members. I would like to thank all those people who contributed in many ways to the success of this study and made this thesis a joyful experience.

First and foremost, I would like to express my sincere gratitude to my supervisor Dr. M. L. P. Reddy for the continuous support during my PhD study and related research, for his patience, motivation, and encouragement. His guidance helped me in all the time of research and writing of this thesis. The journey had lots of ups and downs, all through which you have been supportive and encouraging.

I am grateful to Dr. A. Ajayaghosh, Director, NIIST, and former Directors Dr. Suresh Das and Dr. Gangan Pratap, for providing the necessary facilities and infrastructure to carry out this investigation.

I would like to extend my sincere gratitude to Dr. R. Luxmi Varma and Dr. Mangalam S. Nair for their advise and helps during their tenure as AcSIR co-ordinators. I would like to express my deep sense of gratitude towards all AcSIR faculty. I would like to thank my DAC members, Dr. R. Luxmi Varma, Dr. Ananthakumar and Dr. Mangalam S. Nair for their support, advices and encouragement. I would like to thank Dr. Sunil Varughese for the fruitful discussions and advices. I am thankful to Dr. Jayamurthy for bio-imaging studies.

I am indebted to many of my colleagues for the support, fruitful discussions and help with the experiments. I would like to thank Dr. S. Biju, Dr. V. Divya, Dr. A. Balamurugan, Dr. S. Sarika, Dr. A. R. Ramya, Dr. Biju Francis, Dr. Sheethu Jose, Ms. P. Aiswaria, Mr. K. S. Bejoymohandas, Mr. T. M. George, Mrs. J. Anaswara, Mr. K. R. Ajay, Mr. S. Sreenadh, Mrs. M. V. Lucky, Mr. P. K. Thejus, Mr. Alikunhi, Mrs. S. Surya, Ms. Shanmugha Priya and all other friends at NIIST family for their help and cooperation. I am also thankful to all technical supportive staff of CSIR-NIIST for their timely help in the utilization of sophisticated analytical instruments.

There are a few special people for me in Trivandrum, to whom I owe a lot. Ramya & Linda, thank you very much for the sisterly affection, encouragement, love, care and all the helps both professional and personal. Thank you Sudhakshina, Maneesh, Vaisakhan Thampi, Lekshmi, Vijay, Bineesh, Sudheesh, Shaiju, Kiran, Gayathri and Malini for your friendship, love and care. Thank you Subha, Anupama, Sumi, Vineetha, for being amazing roommates. You people made me feel at home and never made me feel homesick. Thank you…

I would like to express my deep sense of gratitude to my teachers also, who encouraged me to take up science as my career.

I acknowledge University Grants Commission (UGC), New Delhi, Government of India for financial assistance.

Without the support of my lovely family, I wouldn't have been able complete my PhD and I would like to express my deep sense of gratitude to them also. Words are inadequate to express my happiness to have a partner like you, Sambhu who could perfectly understand my words, silence and even more. I wish to thank my parents for their unconditional love, encouragement and support all through my life, without whom I couldn't imagine being at this stage in my life. I would like to thank, my beloved sister Nisha, my brother in law Rajeev, their kids, Gayathri and Aravind, and all other relatives for their support and encouragement. I am also thankful to my mother in law, Subha, sister in law, Radhu, Sasidev & Devoos and all other family members for their love and support.

Above all, I thank Almighty for the blessings throughout my research work to complete the research successfully.

Usha Gangan T. V.

CONTENTS

	Page
Declaration	i
Certificate	iii
Acknowledgements	v
Contents	vii
List of Schemes	xiii
List of Figures	xv
List of Tables	xxiii
List of Abbreviations	xxv
Preface	xxix

CHAPTER 1:	**Visible-light sensitized luminescent europium(III)-*β*-diketonate complexes**	**01-32**

1.1.	Introduction	3
1.2.	Antenna effect	4
1.3.	Overview on visible light sensitized europium(III)–*β*-diketonate complexes-primary ligand modifications	9
1.3.1.	Luminescence properties of visible-light sensitized fluorene-based Eu^{3+}-*β*-diketonate complexes	9
1.3.2.	Visible-light excitable carbazole-based Eu^{3+}-*β*-diketonate complexes	13
1.3.3.	Luminescence properties of visible-light excitable phenanthrene-based Eu^{3+}-*β*-diketonate complexes	19
1.4.	Luminescent behavior of visible-light sensitized Eu^{3+}-*β*-diketonate complexes: Ancillary ligand modifications	21

1.5.	Objective of the present investigation	27
1.6	References	27

CHAPTER 2:	**Tuning of the excitation wavelength in Eu^{3+}-aminophenyl based polyfluorinated β-diketonate complexes: a red-emitting Eu^{3+}-complex encapsulated in a silica/polymer hybrid material excited by blue light**	**33-84**

2.1.	Abstract	35
2.2.	Introduction	37
2.3.	Experimental section	40
2.3.1.	Materials and instrumentations	40
2.3.2.	Synthetic procedures for the ketones	42
2.3.3.	Synthesis of the ligands	43
2.3.4.	Synthesis of binary complexes	45
2.3.5.	Synthesis of Eu^{3+} complexes 4–6	47
2.3.6.	Synthesis of $Eu(DPAPFP)_3(DDXPO)$-gel [EuC-Gel]	48
2.3.7.	Synthesis of polymer-$Eu(DPAPFP)_3(DDXPO)$-gel (EuC-PMMA-Gel)	49
2.4.	Results and discussion	49
2.4.1.	Synthesis and characterization of lanthanide complexes	49
2.4.2.	Electronic spectra of the aminophenyl based β-diketonate ligands and their corresponding Eu^{3+} complexes (1–6)	54
2.4.3.	Solid-state photophysical properties of Eu^{3+} complexes 1–6	56

2.4.4.	Energy transfer between ligands and Eu^{3+}	64
2.4.5.	Photostability of the $Eu(DPAPFP)_3DDXPO$ complex	67
2.5.	Synthesis, characterization and luminescence studies of the hybrid materials EuC-Gel and EuC-PMMA-Gel	67
2.5.	Conclusions	76
2.6.	References	77

CHAPTER 3:	**Visible-light excitable highly luminescent molecular plastic materials derived from Eu^{3+}-biphenyl based *β*-diketonate ternary complex and poly(methylmethacrylate)**	**85-128**

3.1.	Abstract	87
3.2.	Introduction	89
3.3.	Experimental Section	92
3.3.1.	Materials and Instrumentations	92
3.3.2.	Synthetic procedures for the ketones	94
3.3.3.	Synthesis of the ligands	95
3.3.4.	Synthesis of binary complexes	96
3.3.5.	Synthesis of ternary Eu^{3+} complexes 2 and 4	98
3.3.6.	Preparation of luminescent polymer films	99
3.4.	Results and Discussion	99
3.4.1.	Synthesis and characterization of ligands and their corresponding lanthanide complexes	99

3.4.2.	Electronic spectra of the Eu^{3+}-β-diketonate complexes	104
3.4.3.	Steady state photoluminescence	106
3.4.4.	Characterization and photophysical properties of $Eu(MeOBPhTFB)_3(TPY)$ doped PMMA polymer films	115
3.5.	Conclusions	121
3.6.	References	122

CHAPTER 4:	**Synthesis, characterization and photoluminescence properties of Eu^{3+}-β-diketonate complexes derived from 3-hydroxy-1-(4-methoxyphenyl)-3-(naphthalen-2-yl)prop-2-en-1-one and various bidentate nitrogen donors**	**127-163**

4.1.	Abstract	129
4.2.	Introduction	131
4.3.	Experimental Section	133
4.3.1.	Materials and Instrumentations	133
4.3.2.	Synthetic procedures for the ligand	135
4.3.3.	Synthesis of binary complexes 1-3.	136
4.3.4.	Synthesis of ternary complexes 4-5.	137
4.4.	Results and Discussion	140
4.4.1.	Synthesis and characterization of lanthanide complexes	140
4.4.2.	Electronic spectra of the ligand and Eu^{3+} complexes	143
4.4.3.	Steady-state photoluminescence	145

4.4.4.	Photoluminescence measurement of complex 5 in buffer solution [% DMSO: % PBS = 1: 99; c = 1 x 10^{-4} M]	152
4.4.5.	Photostability of the Eu^{3+} complex Eu(MeOPNP)$_3$(MeOBPY) (5) in buffer solution	155
4.5.	Conclusions	156
4.6.	References	157
	Papers Presented at Conferences	165
	List of Publications	167

List of Schemes

		Page
(1)	**Scheme 2.1.** Synthetic procedure for the *β*-diketonate ligands.	45
(2)	**Scheme 2.2.** Synthesis of Ln^{3+} (Ln = Eu, Gd) binary complexes.	48
(3)	**Scheme 2.3.** Synthesis of ternary Eu^{3+} complexes.	48
(4)	**Scheme 3.1.** Synthesis of the ligands.	96
(5)	**Scheme 3.2.** Synthesis of the Ln^{3+} (Ln = Eu, Gd) binary complexes.	97
(6)	**Scheme 3.3.** Synthesis of the Eu^{3+} ternary complexes **2** and **4**.	98
(7)	**Scheme 4.1.** Synthetic procedure for the *β*-diketonate ligand.	136
(8)	**Scheme 4.2.** Synthesis of Ln^{3+} (Ln = Eu, Gd, La) binary complexes.	139
(9)	**Scheme 4.3.** Synthesis of ternary Ln^{3+} (Ln = Eu, La) complexes **4**-**9**.	140

List of Figures

Page

(1) **Figure 1.1.** Applications of europium luminescent complexes. 4

(2) **Figure 1.2.** (A) Pictorial representation of antenna effect. (B) The energy transfer mechanism in europium complexes. The antenna harvests energy through high molar absorption to the singlet excited state. After undergoing intersystem crossing to the triplet state, the antenna transfers energy to the excited ^5D_J state of the lanthanide. The radiative transition of electrons from the excited ^5D_J state to the ^7F_J states results in luminescent emission from the lanthanide ion. Luminescent 4f-4f transitions of europium complexes and commonly observed emission wavelengths to emit red light is also represented. 6

(3) **Figure 1.3.** Pictorial representation of a d-f system and an energy level diagram. 8

(4) **Figure 1.4.** Molecular structures of $Eu(pffpd)_3(DDXPO)$ (left), $Eu(pffpd)_3(DPEPO)$ (right) and excitation and emission spectra of the complexes. 12

(5) **Figure 1.5.** Molecular structures and excitation emission spectra of $Eu(BFPD)_3(TBNPO)$, $Eu(NFPD)_3(TBNPO)$ and $Eu(BPFPD)_3(TBNPO)$. 12

(6) **Figure 1.6.** The structure of the carbazole rings system. 13

(7) **Figure 1.7.** The molecular structure of $EuL_3(phen)$ and emission spectra of the original InGaN LEDs without phosphor (broken line) and the LEDs with $EuL_3(phen)$ (solid line) under excitation of 20 mA forward bias. 14

(8) **Figure 1.8.** Excitation (a and c) and emission (b and d) spectra of 16

Eu(2-TFDBC)$_3$(phen) and Eu$_2$(2,7-BTFDBC)$_3$(phen)$_2$ respectively in the solid state (λ_{exc} = 429 nm and λ_{em} = 613 nm).

(9) **Figure 1.9.** (i) Molecular structure, (ii) Emission spectra and the photographs of the original InGaN LED without phosphor (a and left) and the LED with Eu(EMOCTFBD)$_3$(phen) (b and right) under excitation of 20 mA forward bias. Inset: photographs of the lighting LEDs. 17

(10) **Figure 1.10.** Molecular structures of Eu(L1)$_3$(DDXPO) (left) and Eu(L2)$_3$(DDXPO) (right). 18

(11) **Figure 1.11.** (i) Molecular structure of Eu(pfppd)$_3$(tpy), (ii) excitation and emission spectrum of Eu(pfppd)$_3$(tpy) and Eu(pfppd)$_3$(H_2O)$_2$ (a) An image of the H9c2 cells after 16 h incubation with Mitochondria tracker CellLight™ Mitochondria-GFP BacMam 2.0, (b) An image of the H9c2 cells after incubation with 30 μM of the Eu(pfppd)$_3$(tpy) complex for 30 min, (c) The merged image. Scale bars: 25 μm. 20

(12) **Figure 1.12.** The AFM, TEM images of the Eu(pfppd)$_3$(H_2O)$_2$ complex incorporated into multi-walled carbon nanotube excited at 415 nm (left). Excitation and emission spectra of Eu(pfppd)$_3$(H_2O)$_2$ (1) and luminescent composite (right). 21

(13) **Figure 1.13.** The molecular structure of Eu(fod)$_3$-MK. Corrected luminescence excitation (λ_{em} = 612 nm) and emission (λ_{exc} = 450 nm) spectra of a solution of 10^{-5} M Michler's ketone and 10^{-4} M Eu(fod)$_3$ in benzene. 23

(14) **Figure 1.14.** The molecular structure of Eu(tta)$_3$dpbt and Eu(tta)$_3$bpt**.** Energy-level diagram showing the energy-transfer pathways in complex Eu(tta)$_3$dpbt; isc denotes intersystem crossing. 24

(15)	**Figure 1.15.** The molecular structure of the ligands L_1-L_4.	25
(16)	**Figure 1.16.** The molecular structure of [Eu(tta)$_4$(DEASPI)].	26
(17)	**Figure 2.1.** Structures of the β-diketonate ligands.	39
(18)	**Figure 2.2.** Thermogravimetric curves for Eu^{3+} complexes **1** and **4**.	52
(19)	**Figure 2.3.** Thermogravimetric curves for Eu^{3+} complexes **2** and **5**.	52
(20)	**Figure 2.4.** Thermogravimetric curves for Ln^{3+} complexes **3** and **6**.	53
(21)	**Figure 2.5.** Thermogravimetric curves for Gd^{3+} complexes **7-9**.	53
(22)	**Figure 2.6**. UV-visible absorption spectra of the ligands HAPFP, HDMAPFP, HDPAPFP and DDXPO in THF (c = 5 × 10^{-6} M).	55
(23)	**Figure 2.7**. UV-visible absorption spectra of complexes **1**-**6** in THF (c = 5 × 10^{-6} M).	55
(24)	**Figure 2.8** Normalized excitation spectra of Eu^{3+} binary complexes **1**-**3** in solid state.	58
(25)	**Figure 2.9** Normalized excitation spectra of Eu^{3+} ternary complexes **4-6** in solid state.	59
(26)	**Figure 2.10.** 298 K emission spectra of Eu^{3+} complexes **1-6** in solid state.	59
(27)	**Figure 2.11** $^5D_0$ decay profiles for complexes **1** and **4** (solid-state) where emission monitored around 612 nm. The straight lines are the best fits (r^2 = 0.999) considering single-exponential behavior.	61

(28) **Figure 2.12.** $^5D_0$ decay profiles for complexes **2** and **5** (solid-state) where emission monitored around 612 nm. The straight lines are the best fits (r^2 = 0.999) considering single-exponential behavior**.** 61

(29) **Figure 2.13.** $^5D_0$ decay profiles for complexes **3** and **6** (solid-state) where emission monitored around 612 nm. The straight lines are the best fits (r^2 = 0.999) considering single-exponential behavior**.** 62

(30) **Figure 2.14.** UV-vis absorption spectra at 298 K (left), and 77 K phosphorescence spectra (right) of the complexes **7**-**9** in THF (c = 5×10^{-6} M). 66

(31) **Figure 2.15.** Schematic energy level diagram and energy transfer processes for the complex 6. S_1 represents the first excited singlet state and T_1 represents the first excited triplet state. 66

(32) **Figure 2.16.** Photoluminescence intensity of the complex $Eu(DPAPFP)_3DDXPO$ in solid state as a function of irradiation time. 67

(33) **Figure 2.17.** Photographs of the EuC-PMMA-Gel (left) and EuC-Gel (right) before (a) and after (b) UV irradiation. 68

(34) **Figure 2.18.** FT-IR spectra of the EuC-Gel and EuC-PMMA-Gel. 68

(35) **Figure 2.19.** XRD patterns of the EuC-Gel and EuC-PMMA-Gel. 69

(36) **Figure 2.20.** TG/DTA curves for (a) $Eu(DPAPFP)_3DDXPO$, (b) EuC-Gel and (c) EuC-PMMA-Gel. 70

(37) **Figure 2.21.** UV-visible absorption spectra of the gels (solid). 72

(38) **Figure 2.22.** Room temperature excitation and emission spectra of hybrid materials, EuC-Gel and EuC-PMMA-Gel (Inset 73

photographs show the gels coated on a glass plate).

(39) **Figure 2.23.** $^5D_0$ decay profiles for EuC-Gel and EuC-PMMA-Gel (solid-state) where emission monitored around 612 nm. The straight lines are the best fits (r^2 = 0.999) considering single-exponential behavior. 75

(40) **Figure 2.24**. Emission spectra of the blue emitting InGaN LED (left) and EuC-PMMA-Gel coated on an InGaN chip (right). Inset: photographs of the LEDs in working state. 75

(41) **Figure 3.1.** Structure of the ligands. 92

(42) **Figure 3.2.** ^1H NMR spectrum of $Eu(MeOBPhTFB)_3(H_2O)(C_2H_5OH)$ in $CDCl_3$. 101

(43) **Figure 3.3.** ^1H NMR spectrum of $Eu(BPhTFB)_3(H_2O)(C_2H_5OH)$ in $CDCl_3$. 101

(44) **Figure 3.4.** Thermogravimetric curves for Eu^{3+} complexes $Eu(MeOBPhTFB)_3(H_2O)(C_2H_5OH)$ (**1**) & $Eu(MeOBPhTFB)_3(TPY)$ (**2**). 103

(45) **Figure 3.5.** Thermogravimetric curves for Eu^{3+} complexes $Eu(BPhTFB)_3(H_2O)(C_2H_5OH)$ (**3**) & $Eu(BPhTFB)_3(TPY)$ (**4**). 103

(46) **Figure 3.6.** UV-visible absorption spectra of the ligands, HMeOBPhTFB, TPY and corresponding Eu^{3+} complexes (**1**-**2**) in THF ($c = 5 \times 10^{-6}$ M). 105

(47) **Figure 3.7.** UV-visible absorption spectra of the ligands, HBPhTFB, TPY and corresponding Eu^{3+} complexes (**3**-**4**) in THF ($c = 5 \times 10^{-6}$ M) 106

(48) **Figure 3.8.** (a) UV-vis absorption spectra at 298K and (b) 77K phosphorescence spectra of the $Gd(BPhTFB)_3(H_2O)(C_2H_5OH)$ (red) and $Gd(MeOBPhTFB)_3(H_2O)(C_2H_5OH)$ (blue) complexes. 109

(49) **Figure 3.9.** 298 K (a) excitation and (b) emission spectra of Eu^{3+} complexes $Eu(MeOBPhTFB)_3(H_2O)(C_2H_5OH)$ (**1**) and $Eu(MeOBPhTFB)_3(TPY)$ (**2**) in solid-state. 110

(50) **Figure 3.10.** 298 K (a) excitation and (b) emission spectra (b) of Eu^{3+} complexes $Eu(BPhTFB)_3(H_2O)(C_2H_5OH)$ (**3**) and $Eu(BPhTFB)_3(TPY)$ (**4**) in solid-state. 110

(51) **Figure 3.11.** CIE chromaticity diagram showing the colour of the $Eu(MeOBPhTFB)_3(TPY)$ complex (**2**). 111

(52) **Figure 3.12.** 298 K $^5D_0$ decay profiles for complexes $Eu(MeOBPhTFB)_3(H_2O)(C_2H_5OH)$ (**1**) and $Eu(MeOBPhTFB)_3(TPY)$ (**2**) (solid-state) where emission monitored around 615 nm. The straight lines are the best fits (r^2 = 0.999) considering single-exponential behavior. 111

(53) **Figure 3.13.** 298 K $^5D_0$ decay profiles for complexes $Eu(BPhTFB)_3(H_2O)(C_2H_5OH)$ (**3**) & $Eu(BPhTFB)_3(TPY)$ (**4**) (solid-state) where emission monitored around 615 nm. The straight lines are the best fits (r^2 = 0.999) considering single-exponential behavior. 112

(54) **Figure 3.14.** FT-IR Spectra for the PMMA film, 3, 5, 7 and 9 w/w% $Eu(MeOBPhTFB)_3(TPY)$ doped PMMA films. 116

(55) **Figure 3.15.** Thermogravimetric curves for pure PMMA (black) and Eu^{3+} complex doped PMMA film (PMMA@7Eu) (red). 116

(56) **Figure 3.16.** 298 K (a) excitation and (b) emission spectra of 3%, 5%, 7% and 9% $Eu(MeOBPhTFB)_3(TPY)$ doped PMMA films. 117

(57) **Figure 3.17.** 298 K excitation and emission spectra of Eu^{3+} complexes doped PMMA films (λ_{ex} = 385 nm). 119

(58) **Figure 3.18.** $^5D_0$ decay profiles for 3, 5, 7 and 9 w/w% 119

Eu(MeOBPhTFB)$_3$(TPY) doped PMMA films, where emission monitored around 615 nm. The straight lines are the best fits (r^2 = 0.999) considering single-exponential behavior.

(59) **Figure 3.19.** Photograph of the transparent PMMA film doped with 7 w/w% Eu(MeOBPhTFB)$_3$(TPY) a) before UV irradiation and b) after UV irradiation. 120

(60) **Figure 4.1.** Structures of the β-diketonate ligand. 132

(61) **Figure 4.2.** Structures of the ancillary ligands. 133

(62) **Figure 4.3.** Thermogravimetric curves for Eu^{3+} complexes **1** and **4-6**. 142

(63) **Figure 4.4**. Solid-state UV-vis absorption spectra of the β-diketonate ligand, HMeOPNP and Eu^{3+} complexes **4-6.** 144

(64) **Figure 4.5.** Room temperature excitation and emission spectra of Eu^{3+} complexes **1, 4-6** in the solid-state. 148

(65) **Figure 4.6** $^5D_0$ decay profiles for complexes **1** and **4-6** (solid-state) where emission monitored around 612 nm. The straight lines are the best fits (r^2 = 0.999) considering single-exponential behavior. 150

(66) **Figure 4.7.** UV-vis absorption spectra at 298 K (left), and 77 K phosphorescence spectra (right) of the complex **2** in THF ($c = 5 \times 10^{-6}$ M). 152

(67) **Figure 4.8**. UV-visible absorption spectra of the europium(III) complex **5** in buffer solution (%DMSO: %PBS = 1: 99, $c = 1\times10^{-4}$ M). 153

(68) **Figure 4.9.** Solution-state excitation (left) and emission spectra (right) Eu(MeOPNP)$_3$(MeOBPY) in a buffer solution of pH 7.4 [% DMSO : % PBS = 1: 99; $c = 1 \times 10^{-4}$ M] at 298 K, emission 154

monitored at around 612 nm (λ_{exc} = 405 nm). Inset: photograph of the complex **5** in buffer solution under day light and UV light with 365 nm excitation).

(69) **Figure 4.10.** The $^5D_0$ decay profile for the complex **5** in a buffer solution of pH 7.4 [% DMSO: % PBS =1: 99; c = 1 x 10^{-4} M] at 298 K, excited at 405 nm. The emission was monitored at 612 nm. 155

(70) **Figure 4.11.** Photoluminescence intensity of complex **5** at 612 nm in a buffer solution of pH 7.4 [% DMSO: % PBS = 1: 99; c = 1 x 10^{-4} M] at 298 K, as a function of irradiation time. λ_{exc} = 405 nm. 156

List of Tables

Page

(1) **Table 2.1** Molar absorption coefficient for the ligands and their corresponding Eu^{3+} complexes 56

(2) **Table 2.2.** The radiative **(A_{RAD})** and non-radiative **(A_{NR})** decay rates, $5D_0$ lifetime **(τ_{obs})**, intrinsic quantum yield **(Φ_{Ln}, %)**, energy transfer efficiency **(Φ_{sens}, %)**, and overall quantum yield **($\Phi_{overall}$, %)** for complexes **1**-**6** in the solid state 64

(3) **Table 2.3**. Luminescence intensities, content of the Eu^{3+} complex, radiative-nonradiative decay rates and the photoluminescence quantum yields of $Eu(DPAPFP)_3DDXPO$, EuC- PMMA-Gel and EuC-Gel samples 74

(4) **Table 3.1** Molar absorption coefficient for the ligands and their corresponding Eu^{3+} complexes **1-4**. 105

(5) **Table 3.2** The radiative (A_{RAD}, s^{-1}) and non-radiative (A_{NR}, s^{-1}) decay rates, $^5D_0$ lifetime (τ_{obs}, μs), intrinsic quantum yield (Φ_{Ln}, %), energy transfer efficiency (Φ_{sen}, %), overall quantum yield ($\Phi_{overall}$, %) and colour coordinates for Eu^{3+} complexes in the solid-state (λ_{exc} = 400 nm). 113

(6) **Table 3.3.** Comparison of the results of the current work with previous reports with respect to quantum yields ($\Phi_{overall}$, %) and excitation maxima (λ_{exc}, nm) of various Eu^{3+}- β-diketonate complexes. 114

(7) **Table 3.4** The radiative (A_{RAD}, s^{-1}) and non-radiative (A_{NR}, s^{-1}) decay rates, $^5D_0$ lifetime (τ_{obs}, μs), intrinsic quantum yield (Φ_{Ln}, 118

%), energy transfer efficiency (***Φ*sen, %**), overall quantum yield (***Φ*overall, %**) of 3%, 5%, 7% and 9% Eu^{3+} complex doped PMMA films (λ_{exc} = 400 nm).

(8) **Table 4.1** Molar absorption coefficient for the ligand and the corresponding Eu^{3+} complexes. 145

(9) **Table 4.2** The radiative (**A_{RAD}, s^{-1}**) and non-radiative (**A_{NR}, s^{-1}**) decay rates, $^5D_0$ lifetime (**τ_{obs}, μs**), intrinsic quantum yield (**Φ_{Ln}, %**), energy transfer efficiency (**Φ_{sen}, %**), overall quantum yield (**$\Phi_{overall}$, %**) and colour coordinates for Eu^{3+} complexes in the solid-state excited at their excitation maximum. 150

ABBREVIATIONS

UV	Ultra Violet
OLED	Organic Light Emitting Diode
MLCT	Metal–to–ligand charge transfer
MMLCT	Metal–metal-to-ligand charge transfer
ISC	Intersystem crossing
EL	Electroluminescence
PL	Photoluminescence
ET	Energy Transfer
Ln^{3+}	Trivalent Lanthanide ion
Eu^{3+}	Trivalent Europium ion
Gd^{3+}	Trivalent Gadolinium ion
S_1	Singlet
T_1	Triplet
XRD	X-Ray Diffraction
ESI-MS	Electro Spray Ionization Mass Spectroscopy
FT-IR	Fourier Transform Infrared spectrophotometer
NMR	Nuclear Magnetic Resonance
AFM	Atomic-force microscopy
TEM	Transmission electron microscopy
FAB-MS	Fast Atom Bombardment Mass Spectrometer
MALDI- TOF	Matrix Assisted Light Desorption/Ionization- Time Of Flight
TGA	Thermogravimetric Analysis
DTA	Differential thermal analysis
CIE	Commission Internationale de L′Eclairage
THF	Tetrahydrofuran
IR	Infrared
LED	Light Emitting Diode

DMSO	Dimethyl sulphoxide
NaH	Sodium hydride
HCl	Hydrochloric acid
$CHCl_3$	Chloroform
$CDCl_3$	Chloroform-*d*
PBS	Phosphate buffer saline
DMF	*N*,*N*-dimethylformamide
MCM-41	Mobil Composition of Matter No. 41
InGaN	Indium Gallium nitride
fod	6,6,7,7,8,8,8-heptafluoro-2,2-dimethyloctane-3,5-dione
TTA	Theonyltrifluoroacetylacetone
hpffpd	4,4,5,5,5-pentafluoro-1-(9H-fluoren-2-yl)-1,3-pentanedione
HBFPD	1-(1-phenyl)-3-(2-fluoryl)propanedione
HNFPD	1-(2-naphthyl)-3-(2-fluoryl)propanedione
HBPFPD	1-(4-biphenyl)-3-(2-fluoryl)propanedione
TBNPO	2,2′-bis(di-p-tolylphosphino)-1,1′-binaphthyl oxide
DPEPO	bis(2-(diphenylphosphino)phenyl) ether oxide
2-TFDBC	2-(4´4´4´-trifluoro-1´3´-dioxobutyl)-carbazole
2,7-BTFDBC	2,7-bis(4´4´4´-trifluoro-1´3´-dioxobutyl)-carbazole
Phen	1,10-phenanthroline
EMOCTFBD	1-(9-ethyl-7-methoxyl-9H-carbazol-2-yl)-4,4,4-trifluorobutane-1,3-dione
Hpfppd	4,4,5,5,5-pentafluoro-3-hydroxy-1-(phenanthren-3-yl)pent-2-en-1-one
CPFHP	1-(9*H*-Carbazol-2-yl)-4,4,5,5,5-pentafluoro-3-hydroxypent-2-en-1-one
DDXPO	4,5-bis(diphenylphosphino)-9,9-dimethylxanthene oxide
bpy	2,2′- bipyridine
MK	Michler’s ketone

dpbt	2-(N,N-diethylanilin-4-yl)-4,6-bis(3,5-dimethyl-pyrazol-1-yl)-1,3,5-triazine
bpt	2-(N,N-di-ethylanilin-4-yl)-4,6-bis(pyrazol-1-yl)-1,3,5-triazine
DEASPI	trans-4-[p-(N,N-diethylamino) styryl]-N-methylpyridinium
HAPFP	1-(4-aminophenyl)-4,4,5,5,5-pentafluoro-3-hydroxypent-2-en-1-one
HDMAPFP	1-(4-(Dimethylamino)phenyl)-4,4,5,5,5-pentafluoro-3-hydroxypent-2-en-1-one
HDPAPFP	1-(4-(Diphenylamino)phenyl)-4,4,5,5,5-pentafluoro-3-hydroxypent-2-en-1-one
HMeOBPhTFB	1-(4'-methoxy-[1,10-biphenyl]-4-yl)-4,4,4-trifluoro-3-hydroxybut-2-en-1-one
HMeOPNP	3-hydroxy-1-(4-methoxyphenyl)-3-(naphthalen-2-yl)prop-2-en-1-one
MeOBPY	4,4'-dimethoxy-2,2-bipyridine
PhBPY	4,4'-diphenyl-2,2-bipyridine
TPA	Two photon absorption
CT	Charge Transfer
PMMA	poly(methyl methacrylate)
MWCNT	Multi-walled Carbon Nanotubes
TEOS	Tetraethyl orthosilicate
Alq_3	tris-8-hydroxyquinolinolato aluminium

PREFACE

The fascinating optical properties of Eu^{3+} ions have promoted the use of their complexes in an increasing number of technological applications ranging from biomedical analysis to material science. The attractive features of Eu^{3+} ions as luminescent materials include their intense line like red photoluminescence emission, high quantum yield, long luminescence lifetime (µs–ms range) and low long-term toxicity. The major drawbacks for most of the luminescent Eu^{3+} complexes is that the optical excitation window is limited to the UV region. It would be necessary to extend the excitation window towards the visible region to decrease the effects of excitation phototoxicity especially in life sciences. Recently this field has become much more important because of the demand for less-harmful labelling reagents in the life sciences and low-voltage-driven pure-red emitters in optoelectronic technology. As a result, several longer-wavelength-sensitized Eu^{3+} complexes have been developed by several groups through the usual triplet pathway mechanism, with the use of suitably expanded π-conjugation in the complex molecules by appropriate molecular engineering. However, poor stability in polar solvents and low luminescence quantum yield (less than 10%) of these complexes make them unsuitable for many applications. Therefore, the objective of the current research work is to design and develop efficient visible-light excitable Eu^{3+}-β-diketonates with superior photophysical properties.

The thesis comprises of four chapters. The first introductory chapter highlights the need for the development of new class of antenna molecules based on novel β-diketonates for the visible-light sensitization of Eu^{3+} ions. Further, a detailed literature review on the recent advances on the photophysical properties of visible-light excited Eu^{3+}-β-diketonate complexes will be also be incorporated towards the end of this chapter.

Chapter 2 deals with the synthesis, characterization and photophysical properties of a series of europium complexes based on three aminophenyl based polyfluorinated β-diketonates, namely, 1-(4-aminophenyl)-4,4,5,5,5-pentafluoro-3-hydroxypent-2-en-1-one, 1-(4-(dimethylamino)phenyl)-4,4,5,5,5-pentafluoro-3-hydroxypent-2-en-1-one and 1-(4-(diphenylamino)phenyl)-4,4,5,5,5-pentafluoro-3-hydroxypent-2-en-1-one, and an ancillary ligand, 4,5-bis(diphenylphosphino)-9,9-dimethylxanthene oxide. The triphenylamine-based polyfluorinated Eu^{3+}-β-diketonate complexes dramatically red-shifted the excitation maximum to the visible region (λ_{exc}= 400 nm) with an impressive quantum yield (40%) as compared to the simple Eu^{3+}-aminophenyl-β-diketonate complexes (λ_{exc} = 370 nm). This can be explained based on the conjugation between nitrogen lone pair electrons and the phenyl π-electrons in the β-diketonate ligand system. On the other hand, the electron-donating dimethylamino group (Hammett constant: σ_p = −0.83) containing Eu^{3+}-β-diketonate complexes moderately shifted the excitation maximum in the UV region from 370 to 380 nm as compared to unsubstituted aminophenyl (Hammett constant: σ_p = −0.66) Eu^{3+} complexes. The displacement of water molecules in aminophenyl based Eu^{3+}-β-diketonate binary complexes by a rigid phosphine oxide ligand richly enhances the photoluminescence quantum yields as well as the excited state lifetime values of the corresponding ternary complexes. As an integral part of this work, hybrid materials have been developed through a sol–gel route by encapsulating a ternary Eu^{3+} compound in a silica/polymer hybrid for high-performance luminescence applications. In addition, a bright red-emitting diode was fabricated by coating the designed hybrid material onto a 400 nm emitting InGaN chip and the photoluminescence was examined. Notably, the current study clearly shows that the developed triphenylamine-based Eu^{3+}-β-diketonate complex is an interesting red-emitting material excited by blue light and therefore may find potential applications in the fields of biological and materials science.

A β-diketonate ligand, namely, 1-(4'-methoxy-[1,10-biphenyl]-4-yl)-4,4,4-trifluoro-3-hydroxybut-2-en-1-one (HMeOBPhTFB), which contains a conjugated methoxy-substituted biphenyl unit, as well as a polyfluorinated alkyl group, was synthesized and utilized for the construction of two new Eu^{3+} complexes $[Eu(MeOBPhTFB)_3(H_2O)(C_2H_5OH)]$ and $[Eu(MeOBPhTFB)_3(TPY)]$ where TPY denotes 2,2':6',2''-terpyridine. These results have been described in Chapter 3. The synthesized compounds were characterized by various spectroscopic techniques, and their solid-state photophysical properties were investigated. The results disclosed that the methoxy-substituted biphenyl based polyfluorinated Eu^{3+}-β-diketonate complexes significantly red-shifted the excitation maximum to the visible region (λ_{exc} = 400 nm) with promising solid-state quantum yield ($\Phi_{overall}$ = 62%) as compared to simple Eu^{3+}-biphenyl β-diketonate ternary complex (λ_{exc} = 382 nm). In this work, attempts also have been made to isolate luminescent molecular plastic materials by incorporating the unique photophysical properties of the developed visible-light excitable Eu^{3+}-β-diketonate complex with the mechanical, thermal, and chemical stability, and flexibility and a film-forming tendency of poly(methylmethacrylate) [PMMA]. The developed molecular plastic materials were characterized and evaluated their photoluminescence properties. Most importantly, the newly constructed polymer films exhibit remarkable quantum yields (75–79%) under blue-light excitation as compared to many of the existing Eu^{3+} based polymeric materials.

In Chapter 4, a visible-light excitable β-diketonate ligand, 3-hydroxy-1-(4-methoxyphenyl)-3-(naphthalen-2-yl)prop-2-en-1-one (HMeOPNP) was synthesized and utilized for the construction of a series of new Eu^{3+} complexes of the general formula $Eu(MeOPNP)_3(L)$ [where L = H_2O, 2,2-bipyridine (BPY), 4,4'-dimethoxy-2,2-bipyridine (MeOBPY) and 4,4'-diphenyl-2,2-bipyridine (PhBPY)] in the presence and the absence of various derivatives of bipyridines as ancillary ligands. The designed Eu^{3+} complexes have been characterized by various spectroscopic techniques and investigated their photophysical properties with a view to understanding the structure–property relationships in these systems. The substitution of conjugated naphthyl moiety as well as methoxyphenyl group at 1,3-positions, respectively of the β-diketonate ligand notably extended the excitation window of the binary complex $Eu(MeOPNP)_3(H_2O)_2$ to visible region (λ_{exc} = 410 nm) with a quantum yield of 6 %. In the presence of an electron-donating methoxy substituted bipyridine as an ancillary ligand, the excitation window of $Eu(MeOPNP)_3(MeOBPY)$ has been further shifted to longer wavelengths in the visible region [(λ_{exc} = 420 nm; $\Phi_{overall}$ = 32%)] with an enhanced luminescence intensity as compared to unsubstituted ternary complex $Eu(MeOPNP)_3(BPY)$ [(λ_{exc} = 412 nm; $\Phi_{overall}$ = 20%)]. The red-shifted excitation window is attributed to the presence of donating methoxy group, which allows the oxygen electrons to be a part of the whole delocalized system through resonance and enhances the conjugation of the chromophore. On the contrary, when electron-withdrawing phenyl groups substituted bipyridine used as an ancillary ligand, the excitation window of Eu(MeOPNP)$_3$(PhBPY) has been drastically shifted to the lower wavelength region (λ_{exc} = 400 nm) with diminished quantum yield ($\Phi_{overall}$ = 9%) as compared to Eu(MeOPNP)$_3$(BPY). This may be due to the fact that the bulky phenyl substituents on the 4,4'-position of the bipyridine system severely hinders co-planarity and as a result attenuate any extended π-interactions in this system. As an integral part of this work, the photophysical properties of the visible light excitable Eu^{3+} complex, Eu(MeOPNP)$_3$(MeOBPY) was investigated under biologically relevant pH conditions [pH 7.4, % DMSO: % PBS = 1: 99; c = 1 x 10^{-4} M].

Chapter 1

Chapter 1

Visible-light sensitized luminescent europium(III)-*β*-diketonate complexes

Introduction

Visible-light sensitized luminescent Eu^{3+} molecular materials are of considerable importance because their outstanding photoluminescence properties make them well suited as labels in fluorescence-based bioassays[1] and low-voltage driven pure red emitters in optoelectronic technology[2] (Figure 1.1). A major challenge in this field is the development of visible-light sensitizing ligands that can form highly emissive Eu^{3+} complexes with sufficient stability and aqueous solubility for practical applications.

Europium possess intrinsic luminescence that originates from f−f electron transitions in the 4f shell of the $[Xe]5s^25p^6$ configuration and offer unique properties for optical imaging contrast agents that address current limitations of their organic counterparts.[3] Due to shielding by the 5s and 5p orbitals, the 4f orbitals do not directly participate in chemical bonding. The emission wavelengths of europium are thus minimally perturbed by the surrounding matrix and ligand field, resulting in sharp, line-like emission bands with the same fingerprint wavelengths and narrow peak widths of the corresponding free Eu^{3+} salts. Moreover, the f−f transitions are formally forbidden by the spin and Laporte rule and feature long excited-state lifetimes in the milli- to microsecond range.[3,4] This property lends luminescent europium to time-gated or time-resolved live-cell or in vivo imaging. Such an approach enhances signal-to-noise ratios through the elimination of interferences from scattering and short-lived autofluorescence of biological constituents.

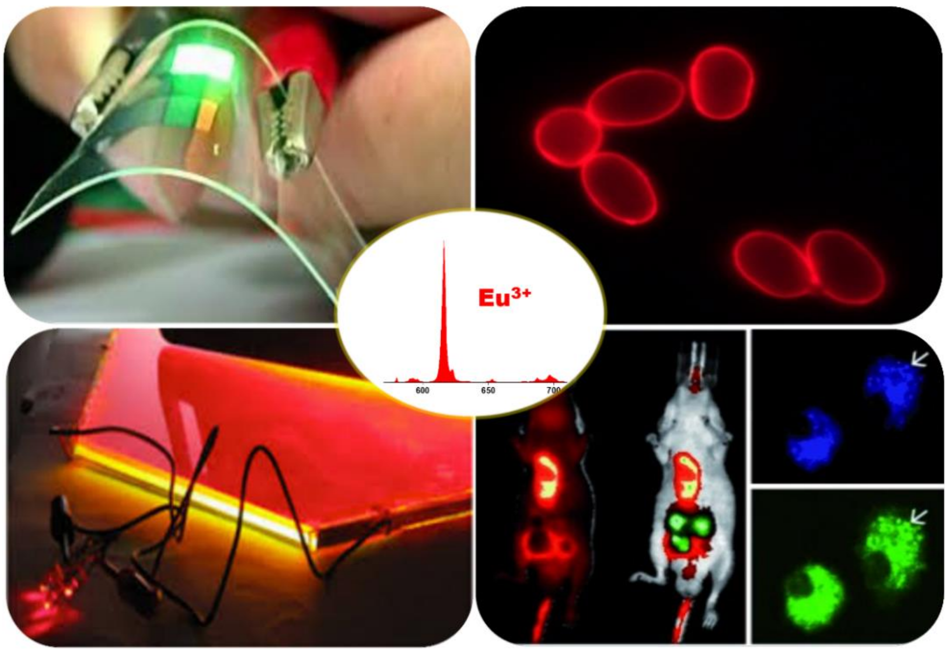

Figure 1.1. Applications of europium luminescent complexes.

1.1. Antenna effect

Although the excited-state lifetimes of Eu^{3+} are long, the forbidden f–f transitions suffer the consequence of weak intrinsic luminescence due to low molar absorptivity.[3,4] Intense light sources such as lasers are required to populate the excited states of Ln^{3+} ions by direct excitation and are impractical for most biological imaging applications. Attachment of a light-harvesting antenna circumvents this limitation by sensitizing the Eu^{3+} ion in what has been termed as the "antenna effect".[5] The antenna can be any aromatic or hetero-aromatic highly -conjugated system characterized by high efficiency of light absorption (high extinction coefficient) and high efficiencies of intersystem crossing and energy transfer processes.[4d] In 1942, Weissman[6] observed that the use of organic ligands in europium complexes increased the luminescence intensity from the lanthanide ion when such complexes were irradiated with ultraviolet (UV) light. The β-diketonate ligand class is emerging as one of the important "antennas" in terms of high harvest emissions because of the effectiveness of the energy transfer from this type of ligand to the Eu^{3+} cation.[7] Moreover, β-diketonates possess strong absorption over a substantial wavelength range for the π–π^* transition and can therefore sensitize the Eu^{3+} luminescence effectively.

The sensitization pathway in luminescent europium complexes consists of excitation of the ligands into their excited singlet states (S_1 = $^1\pi\pi^*$), subsequent intersystem crossing (ISC) of the ligands to their triplet states (T_1 = $^3\pi\pi^*$), and energy transfer (ET) from the triplet state to the ^5D_J manifold of the Eu^{3+} ion, followed by internal conversion to the emitting $^5D_0$ state and, finally, the Eu^{3+} ion emits when transition to the ground state occurs (Figure 1.2). Moreover, the electron transition from the higher excited states, such as $^5D_3$ (24,800 cm^{-1}), $^5D_2$ (21,200 cm^{-1}), and $^5D_1$ (19,000 cm^{-1}), to $^5D_0$ (17,250 cm^{-1}) becomes feasible by internal conversion, and most of the photophysical processes take place in this orbital. Consequently, most europium complexes give rise to typical Eu^{3+} emission bands at ∼580, 590, 612, 650, 690, 710 and 820 nm corresponding to the deactivation of the excited state $^5D_0$ to the ground states ^7F_J (J = 0–6) (Figure 1.2).[8] Thus, the energy level's match of the triplet state of the ligands to $^5D_0$ of Eu^{3+} is one of the key factors which affect the luminescent properties of the europium complexes. According to Latva's empirical rule,[9] an optimal ligand-to-metal transfer process for Eu^{3+} needs $\Delta E(^3\pi\pi^* - {}^5D_0)$ = 2500 cm^{-1}. The intersystem crossing process becomes effective when ($^{1}\pi\pi^{*}$ - $^{3}\pi\pi^{*}$) is at least 5000 cm^{-1} as per Reinhoudt's empirical rule.[10] The overall quantum yield for a sensitized Eu^{3+} complex is given by the equation:

$$\Phi_{\mathrm{overall}} = \Phi_{\mathrm{sens}} \times \Phi_{\mathrm{Ln}} = \Phi_{\mathrm{sens}} \times (\tau_{\mathrm{obs}}/\tau_{\mathrm{rad}})$$

where Φ_{overall} and Φ_{Ln} represent the ligand-sensitized and intrinsic luminescence quantum yields of Eu^{3+}; Φ_{sens} represents the efficiency of the ligand-to-metal energy transfer and $\tau_{\mathrm{obs}}/\tau_{\mathrm{rad}}$ are the observed and the radiative lifetimes of Eu^{3+} ($^{5}D_{0}$).

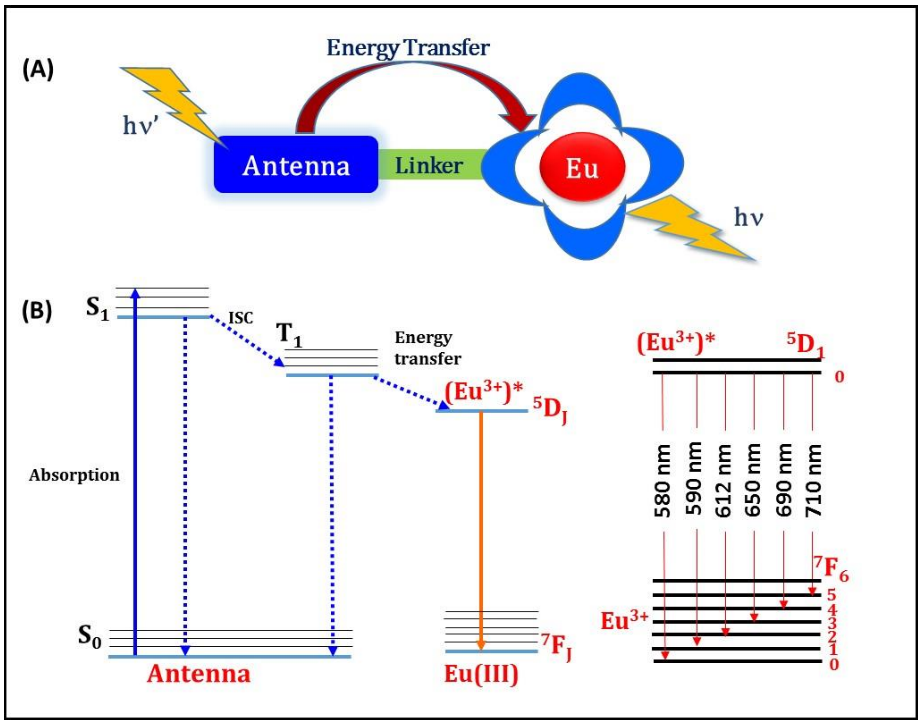

Figure 1.2. (A) Pictorial representation of antenna effect. (B) The energy transfer mechanism in europium complexes. Luminescent 4f-4f transitions of europium complexes and commonly observed emission wavelengths to emit red light are also represented.

For application in the biological field, luminescent Eu^{3+} complexes capable of being efficiently sensitized by long-wavelength light have been more focused, because the long-wavelength light is less harmful to biological tissue, allowing deep penetration, causing less background fluorescence.[10] However, in many of the reported Eu^{3+} complexes the excitation window appears to be limited to the near-UV region (generally below 380 nm) due to the energy constraints posed by the photophysics of sensitized europium luminescence, as highlighted by Reinhoudt and co-workers.[11] Furthermore, no cheap pump sources are available in the UV. Thus, challenge in the chemistry of the lanthanide ions is to develop luminescent Eu^{3+} complexes that can be sensitized by visible light and to determine the energy-transfer process in these systems. The commonly observed sensitization mechanism for luminescent europium complexes involves a triplet pathway, in which the transfer of the energy absorbed by the ligand to the Eu^{3+} ion takes place from the ligand-centered triplet excited state (T_1). With the use of antenna, chromophoric groups, which have a smaller energy gap between the lowest singlet excited state (S_1) and the triplet (T_1) state (e.g. acridone, diaryl ketones),[12] it has been demonstrated by several research groups that the excitation wavelength for Eu^{3+} complexes can be extended into the visible region through the usual triplet pathway. Another promising means of longer-wavelength sensitization of Eu^{3+} emission is through the singlet pathway, in which the excited-state energy of a chromophore is directly transferred from its S_1 state to the luminescent states of the Eu^{3+} center. In this way, the energetic constraints from the T_1 state of the ligand can be avoided.[13] But this mechanism has rarely been observed. There are mainly two strategies that can be adopted to achieve visible light excitation *via* the favorable triplet pathway. One of the approaches is to introduce a 4d- or 5d-transition metal ion such as Ir(III) or Pt(II) into the Eu^{3+} complex molecule, which exhibits an efficient energy transfer to the Ln^{3+} ion (Figure 1.3).[14]

Unfortunately, the photoluminescence efficiency of this kind of europium complex based on the ^{3}MMLCT (metal–metal-to-ligand charge transfer) or ^{3}MLCT (metal-to-ligand charge transfer) was always very low.[15] Another promising approach is to modify the ligand molecule with an appropriate expanded π-conjugated system to shift the excitation band of its Eu^{3+} complex to the visible region, and this expanded π-conjugated system cannot be either too small to absorb visible-light or too big to raise the triplet state of the ligand to a degree higher than $^{5}D_{0}$, the lowest excited state energy level of the central Eu^{3+} ion. The π-conjugation can be expanded either in the primary or in the ancillary ligands. Some of the examples for such π-conjugated moiety are Michler's ketone, phenanlenone, phenanthrene, substituted carbazole etc.[1j]

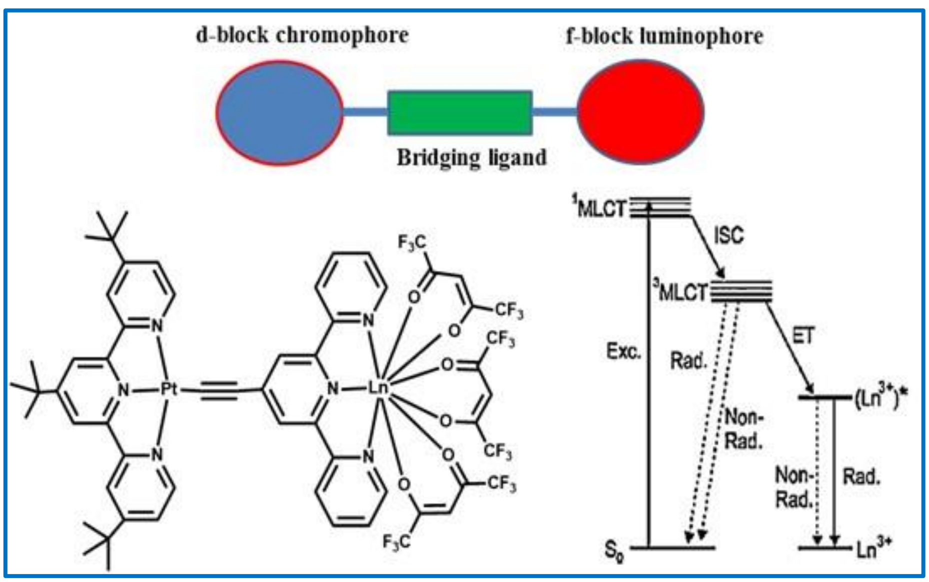

Figure 1.3. Pictorial representation of a d-f system and an energy level diagram.

1.3. Overview on visible light sensitized Eu^{3+}–β-diketonate complexes-primary ligand modifications

It is surprising to note that only very few investigations have been found in the literature on visible-light sensitized Eu^{3+} complexes despite their proven advantages. In 2010, Ma and Wang[1j] reviewed the syntheses, and luminescent properties of organic lanthanide complexes and have underlined basically the development of europium complexes capable of being efficiently excited by visible-light or multiphoton absorption of NIR light. Indeed, some of the recent reports have demonstrated that the excitation-window can be shifted to longer-wavelengths in Eu^{3+}-*β*-diketonate complexes by appropriate molecular engineering and suitably expanded *π*-conjugation in the primary *β*-diketonate ligand of the complex molecules. In 2013 Reddy and coworkers[16] have reviewed the latest innovations in the syntheses and photophysical properties of visible-light sensitized Eu^{3+}–*β*-diketonate complexes and on their application as bioprobes in cellular imaging.

1.3.1. Luminescence properties of visible-light sensitized fluorene-based Eu^{3+}-β-diketonate complexes

π-Conjugated polymers and oligomers based on fluorene building blocks have gained importance as the active materials in various types of organic optoelectronic devices, especially in organic light-emitting diodes.[17] Fluorene is one of the polycyclic aromatic hydrocarbon which is isoelectronic with carbazole which can be easily modified at 2,7-positions.[18] Inspired by these facts, Reddy and co-workers[19] designed a series of near-visible light sensitized europium complexes $Eu(pffpd)_3(C_2H_5OH)(H_2O)$,

$Eu(pffpd)_3(DDXPO)$ and $Eu(pffpd)_3(DPEPO)$ based on a novel β-diketonate ligand, 4,4,5,5,5-pentafluoro-1-(9H-fluoren-2-yl)-1,3-pentanedione (hpffpd), and a chelate phosphine oxide ligand [where DDXPO refers to 4,5-bis(diphenylphosphino)-9,9-dimethylxanthene oxide and DPEPO refers to bis(2-(diphenylphosphino)phenyl)ether oxide]. The single crystal X-ray diffraction analyses of $Eu(pffpd)_3(DDXPO)$ and $Eu(pffpd)_3(DPEPO)$ revealed that these complexes are mononuclear with a distorted square-antiprism structure. The central Eu^{3+} ion is surrounded by eight oxygen atoms, six of which are from the three bidentate fluorinated β-diketonates and the other two oxygen atoms from the chelate phosphine oxide. A broad excitation band between 250 and 450 nm (λ_{max} = 390 nm) was observed for the complexes, attributed to the singlet–singlet π–π* enol absorption of the β-diketonate ligand (Figure 1.4). The displacement of the solvent molecules from the complex $Eu(pffpd)_3(C_2H_5OH)(H_2O)$ by the chelating phosphine oxide, DDXPO, lead to significant enhancement in the emission intensity (absolute quantum yield 3 to 48%) and lifetime values (328 to 820 μs). This was attributed to strong coordination of P=O in DDXPO with the central Eu^{3+} ion (average Eu–O = 2.34 Å), which might enable efficient energy transfer. On the other hand, in the presence of DPEPO these values were only moderately enhanced (quantum yield = 28% and lifetime to 742 μs) due to weak binding of DPEPO to the central Eu^{3+} ion (average Eu–O = 2.38 Å).

In the subsequent studies, Reddy and co-workers[20] managed to further extend the excitation window to the visible region, and constructed a new class of efficient visible light sensitized antenna complexes of Eu^{3+} based on the highly conjugated β-diketonates, namely, 1-(1-phenyl)-3-(2-fluoryl)propanedione (HBFPD), 1-(2-naphthyl)-

3-(2-fluoryl)propanedione (HNFPD), 1-(4-biphenyl)-3-(2-fluoryl)propanedione (HBPFPD) and 2,2′-bis(di-p-tolylphosphino)-1,1′-binaphthyl oxide (TBNPO), as the ancillary ligand.[20] The substitution of the phenyl group with the naphthyl or biphenyl groups in the 3-position of the fluorenyl based β-diketonate ligand remarkably shifted the excitation window from 275–440 nm (λ_{exc} = 400 nm) for Eu^{3+} complexes containing HBFPD to the visible region 300–550 nm with an excitation maximum at 430 nm (for Eu^{3+} complexes containing HNFPD) and 440 nm (for Eu^{3+} complexes containing HBPFPD), respectively, in the corresponding Eu^{3+} complexes(Figure 1.5.). The extended π-conjugation in the β-diketonate ligand lead to shift in the excitation window of the Eu^{3+} complexes towards the visible region, with an important application in biomedical analysis and lighting devices. The luminescence intensity of the ternary Eu^{3+} complexes was greatly enhanced as compared to the hydrated europium β-diketonate complexes by the displacement of the solvent molecules from the complexes by the rigid chelating phosphine oxide TBNPO, which in turn reduces the high-frequency oscillators. Consequently, the quantum yields (19–43%) and lifetime values (769–877 μs) of the ternary Eu^{3+} complexes are found to be significantly enhanced as compared to precursor Eu^{3+} complexes (quantum yields = 2–7%, lifetime = 399–376 μs).

Further, the visible-light sensitized Eu^{3+} complex based on 1-(4-biphenyl)-3-(2-fluoryl)propanedione (HBPFPD) was used for the preparation of mesoporous nanomaterial by covalently immobilizing into the MCM-41 host.[21] The newly designed mesoporous hybrid material exhibited stronger red/orange intensity ratio, higher $^5D_0$ quantum efficiency, longer lifetimes, and better thermal stability than the precursor complex pointing to their prospective use as visible-light excitable red phosphors for luminescent applications.

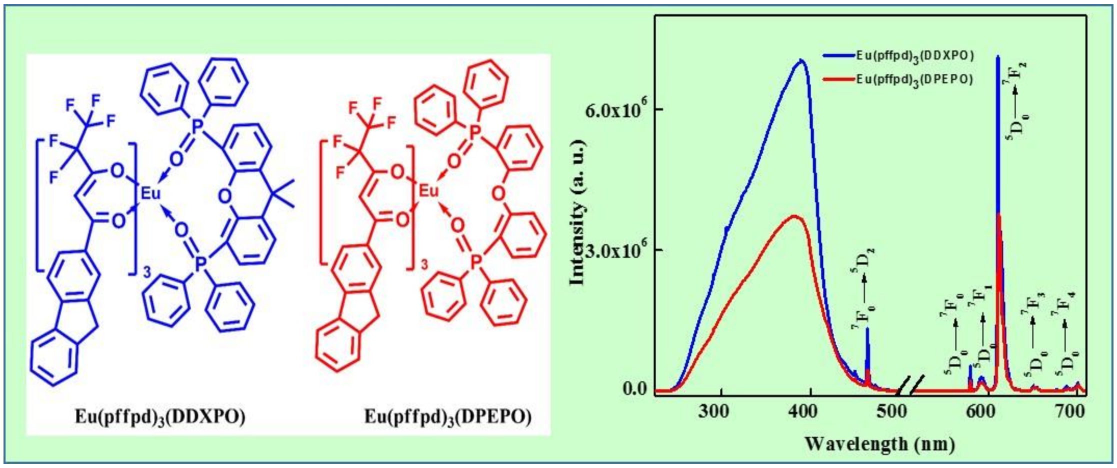

Figure 1.4. Molecular structures of Eu(pffpd)3(DDXPO) (left), Eu(pffpd)3(DPEPO) (right) and excitation and emission spectra of the complexes.

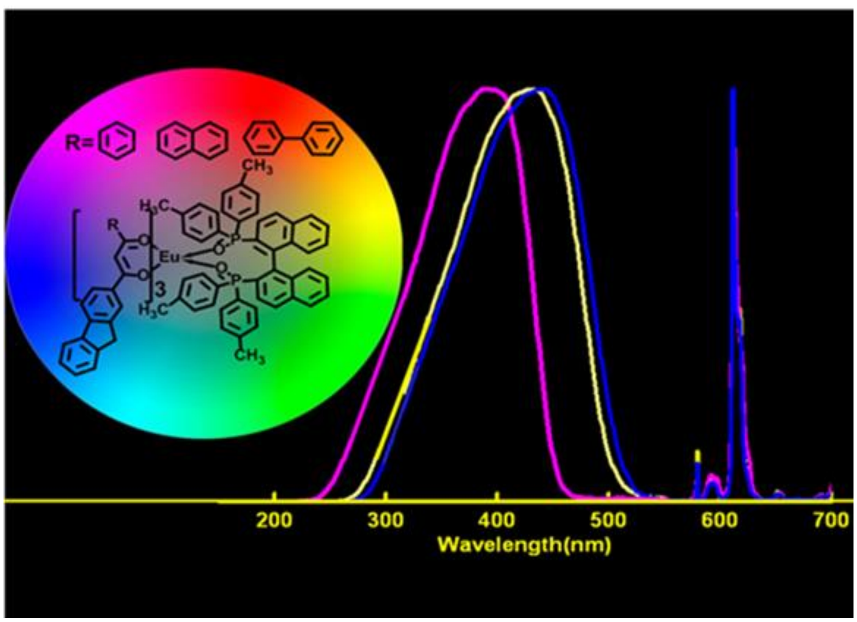

Figure 1.5. Molecular structures and excitation emission spectra of Eu(BFPD)3(TBNPO), Eu(NFPD)3(TBNPO) and Eu(BPFPD)3(TBNPO).

1.3.2. Visible-light excitable carbazole-based Eu^{3+}-*β*-diketonate complexes

The carbazole moiety displays unique advantages for application in optoelectronic devices because of inexpensive starting material, good chemical stability, and being tailored with a wide variety of functional groups to tune the optical and electrical properties.[22] The carbazole moiety can be easily modified via its *N*, C-3, and C-6 positions (Figure 1.6). There are substantial number of studies on 3,6-substituted carbazole derivatives and it was concluded that *β*-diketonates containing 1',3'-dioxobutyl linked at the 3- and 6- positions could slightly extend their excitation band to the visible region. In contrast, substitution at 2- or 7-position in the carbazole ring lead to a longer *π*-conjugation length, leading to bathochromic shift in the excitation band.[23] Until now very less research was done on 2,7-substituted carbazole derivatives, probably due to the lack of an efficient synthesis procedure for these compounds.

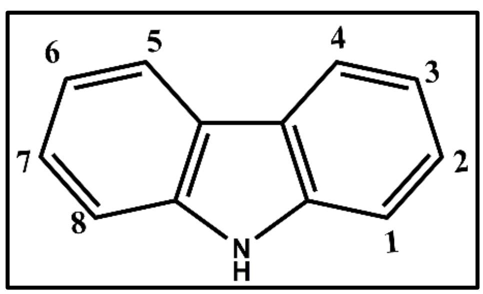

Figure 1.6. The structure of the carbazole rings system.

Liu and co-workers developed a new *β*-diketonate ligand containing carbazole group, 1-(7-(tert-butyl)-9-ethyl-9H-carbazol-2-yl)-4,4,4-trifluorobutane-1,3-dione (HL), and utilized it for the synthesis of a new complex, EuL_3(phen).[24] Photoluminescence measurements indicated that the Eu^{3+} complex exhibit intense red-emission and extend its excitation bands to the visible region. Compared with the similar 3-(*β*-diketonato)carbazole complexes, the excitation bands of the complex showed a bathochromic shift of about 30 nm and were extended to 500 nm. Complex EuL_3(phen) was employed as a phosphor to fabricate LEDs in a mass ratio of 1:20 of phosphor to silicone gel with 460 nm-emitting InGaN chips. The emission spectra of the original 460 nm LEDs without phosphor and the LED fabricated with the complex and a 460 nm chip under 20 mA forward bias are shown in Figure 1.7. The sharp peak at 613 nm is due to the Eu^{3+} emission from the complex in the LEDs chip.

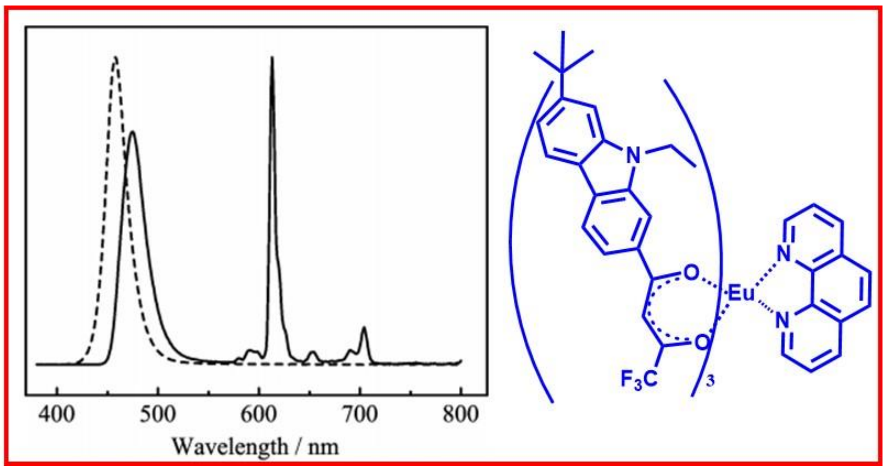

Figure 1.7. The molecular structure of EuL_3(phen) and emission spectra of the original InGaN LEDs without phosphor (broken line) and the LEDs with EuL_3(phen) (solid line) under excitation of 20 mA forward bias.

Gong and co-workers[25] were successful in designing two new carbazole-based *β*-diketonates with 2- or 2,7-substituted groups in the carbazole ring, 2-(4′,4′,4′-trifluoro-1′,3′-dioxobutyl)-carbazole (2-TFDBC) and 2,7-bis(4′,4′,4′-trifluoro-1′,3′-dioxobutyl)-carbazole (2,7-BTFDBC), and their Eu^{3+} ternary complexes Eu(2-TFDBC)$_3$(phen) and Eu_2(2,7-BTFDBC)$_3$(phen)$_2$. Compared with the similar *β*-diketonate complexes linked at

3- and 6-positions in the carbazole ring, the excitation bands of $Eu(2\text{-}TFDBC)_3(phen)$ and $Eu_2(2,7\text{-}BTFDBC)_3(phen)_2$ showed a remarkable red shift by about 30 nm and were extended to 500 nm because of the larger π-conjugation in the molecules (Figure 1.8). However, the strongest excitation peak of these two complexes was not long enough to avoid the photodecomposition efficiently. The ancillary ligand, phen, enhanced the luminescence intensity and thermal stabilities of the complexes and satisfies the high coordination number of the central Eu^{3+} ion. The quantum yields are found to be 28% for $Eu(2\text{-}TFDBC)_3(phen)$ and 10% for $Eu_2(2,7\text{-}BTFDBC)_3(phen)_2$. This quantum yield reduction can be explained by the closer Eu^{3+}-Eu^{3+} distance in the $Eu_2(2,7\text{-}BTFDBC)_3(phen)_2$ molecule than that in $Eu(2\text{-}TFDBC)_3(phen)$, and thus, the concentration quenching more easily happens in the former molecule. The decomposition temperatures of the complexes $Eu(2\text{-}TFDBC)_3(phen)$ and $Eu_2(2,7\text{-}BTFDBC)_3(phen)_2$ determined by thermo-gravimetric analysis were also quite high (361.4 and 367.3 °C in air, respectively), indicating the prospects of luminescence application for these complexes.

To minimize the photodecomposition and also to extend the excitation band to the blue region, in the subsequent studies, Gong and coworkers[26] introduced a methoxyl moiety at the 7-position of β-diketone; thus, a new organic ligand, 1-(9-ethyl-7-methoxyl-9H-carbazol-2-yl)-4,4,4-trifluorobutane-1,3-dione (EMOCTFBD), and its Eu^{3+} ternary complex $Eu(EMOCTFBD)_3(phen)$ were synthesized and their photophysical properties have been investigated. The introduction of a methoxyl in the 7-position of the carbazole ring remarkably enhanced the excitation band intensity in the blue region, and the complex exhibited intense red emission under blue-light excitation. The integrated emission intensity of Eu(EMOCTFBD)$_3$(phen) was enhanced by 60% as compared with the complex Eu(2-TFDBC)$_3$(phen) without a methoxyl at the 7-position of the ligand. Substitution of the 7-positional hydrogen atom with a methoxyl leads to the increase of the electronic density in the carbazole ring, and thus increases the electron transition probability, which in turn lead to enhanced excitation intensity. Finally, a bright red-emitting diode was fabricated by coating the complex phosphor onto a ~460 nm emitting InGaN chip (Figure 1.9). All the results indicated that Eu(EMOCTFBD)$_3$(phen) is an interesting red-emitting material excited by blue light, and therefore may be applied in many fields without UV radiation.

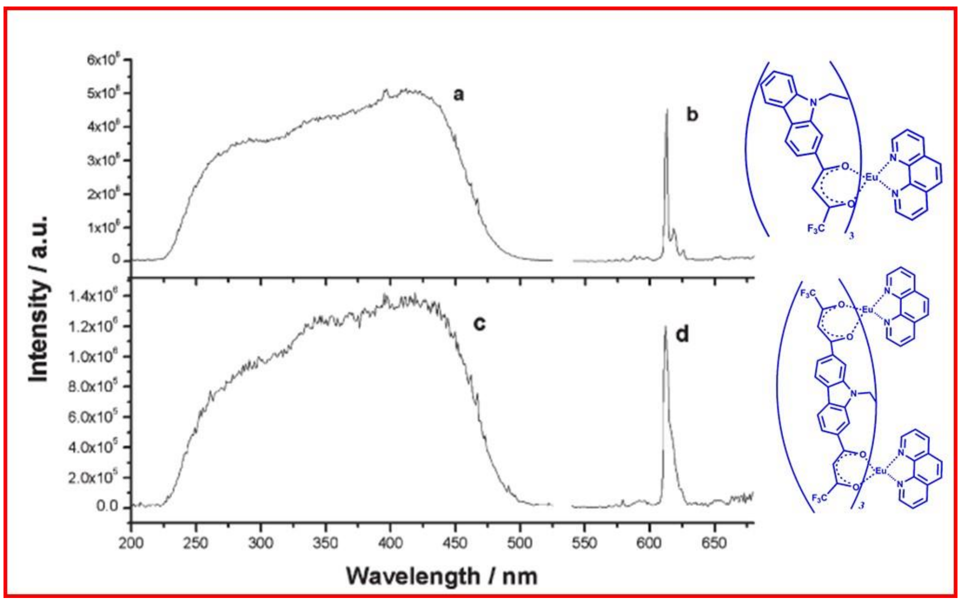

Figure 1.8. Excitation (a and c) and emission (b and d) spectra of Eu(2-TFDBC)$_3$(phen) and Eu$_2$(2,7-BTFDBC)$_3$(phen)$_2$ respectively in the solid state (λ_{exc} = 429 nm and λ_{em} = 613 nm).

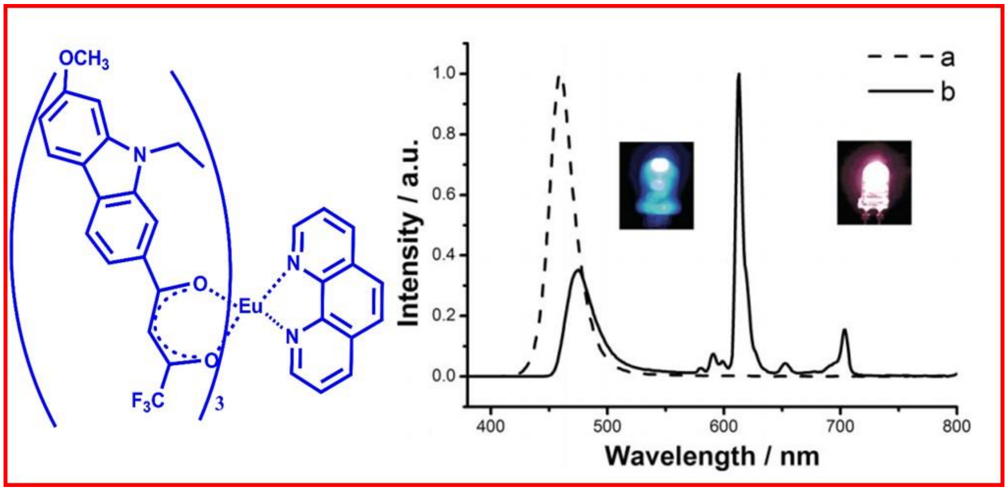

Figure 1.9. (i) Molecular structure, (ii) Emission spectra and the photographs of the original InGaN LED without phosphor (a and left) and the LED with $Eu(EMOCTFBD)_3(phen)$ (b and right) under excitation of 20 mA forward bias. Inset: photographs of the lighting LEDs.

Reddy and co-workers[27] synthesized a series of Eu^{3+} complexes based on novel carbazole-based fluorinated β-diketones, namely, 4,4,5,5,5-pentafluoro-3-hydroxy-1-(9-phenyl-9H-carbazol-2-yl)pent-2-en-1-one (L1) and 4,4,5,5,5-pentafluoro-3-hydroxy-1-(9-(4-methoxyphenyl)-9H-carbazol-2-yl)pent-2-en-1-one (L2) as primary ligands and a bidentate phosphine oxide molecule, 4,5-bis(diphenylphosphino)-9,9-dimethylxanthene oxide (DDXPO) as ancillary ligand (Figure 1.10). Using the Sparkle/PM3 model, the molecular geometries of the designed complexes were optimized and the luminescent parameters were calculated by the LUMPAC software. The results demonstrated that suitably expanded π-conjugation in the developed Eu^{3+}–carbazole-based β-diketonate complexes red-shifted the excitation maximum to the visible region (λ_{exc} = 420 nm) with an impressive quantum yield (34–42%). The obtained results were compared with their previously reported results of $Eu(CPFHP)_3(DDXPO)$, (henceforth, referred to as complex

A, CPFHP = 1-(9*H*-Carbazol-2-yl)-4,4,5,5,5-pentafluoro-3-hydroxypent-2-en-1-one λ_{exc} = 390 nm) and found superior.[28] The triplet state energy levels of L1 and L2 in the complexes were higher than that of the lowest excited level of Eu^{3+} ion, $^5D_0$, so the photoluminescence mechanism of the Eu^{3+} complexes was proposed as a ligand-sensitized luminescence process. The predicted luminescent parameters from the Sparkle/PM3 structures agreed with the experimental data, which confirming the efficacy of the theoretical models adopted in the study. The improvements in the photophysical properties and excitation window brought about by the introduction of extended conjugation and an ancillary ligand emphasize the significance of molecular engineering of ligand and complexes to achieve desired properties.

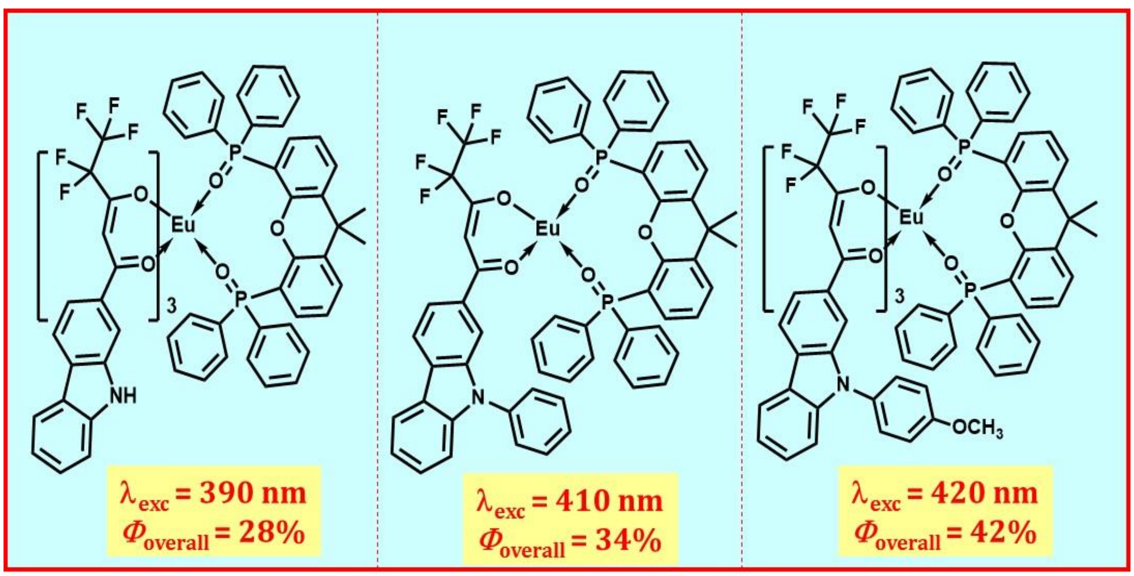

Figure 1.10. Molecular structures of $Eu(CPFHP)_3(DDXPO)$ (left), $Eu(L1)_3(DDXPO)$ (middle) and $Eu(L2)_3(DDXPO)$ (right).

1.3.3. Luminescence properties of visible-light excitable phenanthrene-based Eu^{3+}-β-diketonate complexes

Reddy and co-workers[29] developed a novel β-diketonate ligand, namely, 4,4,5,5,5-pentafluoro-3-hydroxy-1-(phenanthren-3-yl)pent-2-en-1-one (Hpfppd), by incorporating a highly conjugated phenanthrene moiety as well as a polyfluorinated alkyl group in the complex molecule with a view to improve the quantum efficiency and especially to shift the excitation window to longer wavelengths in Eu^{3+}–β-diketonate complexes for use in bioassays.[28] The synthesized ligand has been well characterized and utilized for the construction of two new europium complexes $Eu(pfppd)_3(H_2O)_2$ and $Eu(pfppd)_3(tpy)$ (where tpy = 2,2′:6,6″-terpyridine). The photophysical studies demonstrated that the introduction of conjugated phenanthrene moiety in 3-position of the β-diketonate ligand remarkably extends the excitation window of the Eu^{3+} complexes towards the visible region (500 nm). The replacement of high-energy oscillators O–H in $Eu(pfppd)_3(H_2O)_2$ with an ancillary ligand, terpyridine, lead to an impressive enhancement in both overall quantum yield (from 31 to 75%) and $^5D_0$ lifetime (from 0.51 to 1.04 ms) values. The newly developed Eu^{3+} complex also exhibited a strong photoluminescence (quantum yield = 41%) and a long lifetime (0.88 ms) under physiological pH conditions (7.4) when excited under blue light (403 nm) and selectively stains cellular mitochondria of the rat embryonic heart cell line, H9c2. The ternary Eu^{3+} complex permeates into the H9c2 cells and co-localizes with the mitochondria, as demonstrated by counterstaining experiments (Figure 1.11). The attractive feature of the developed Eu^{3+} complex was its chemical stability at ambient temperature and requiring less incubation time (30 min) compared to commercial Mitotracker, CellLight™

Mitochondria-GFP (16 h). On the other hand, the commercially available Mitotracker Green has the typical problem of thawing and freezing and must be stored at −20 °C due to chemical instability. These properties of the designed Eu^{3+} ternary complex, together with its good cell membrane permeability and fast cellular uptake, suggest its potential as mitochondria targeting probe excitable at visible light.

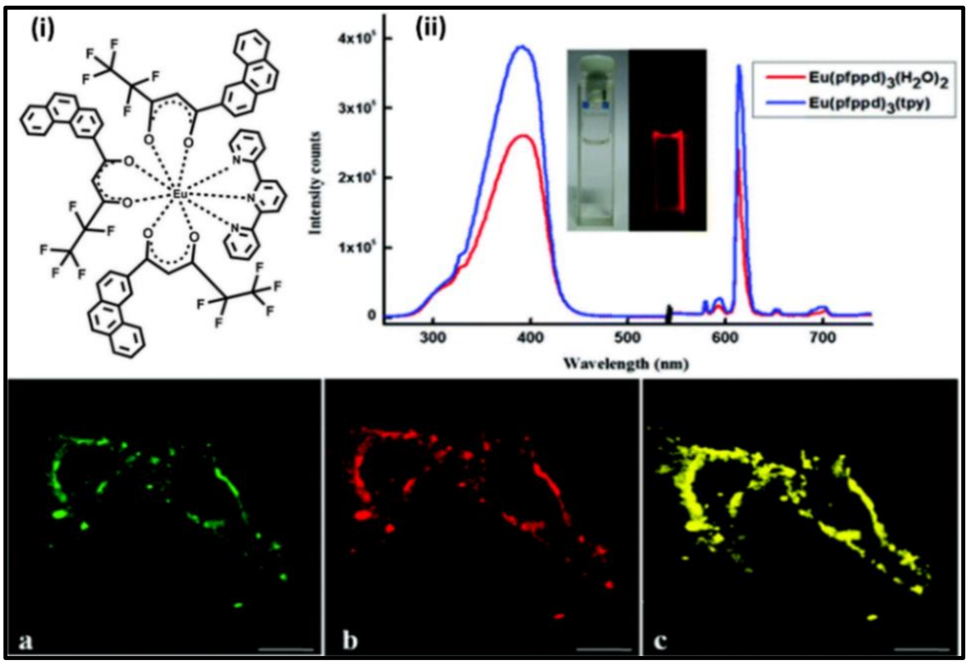

Figure 1.11. (i) Molecular structure of $Eu(pfppd)_3(tpy)$, (ii) excitation and emission spectrum of $Eu(pfppd)_3(tpy)$ and $Eu(pfppd)_3(H_2O)_2$ (a) An image of the H9c2 cells after 16 h incubation with Mitochondria tracker CellLight™ Mitochondria-GFP BacMam 2.0, (b) An image of the H9c2 cells after incubation with 30 μM of the $Eu(pfppd)_3(tpy)$ complex for 30 min, (c) The merged image. Scale bars: 25 μm.

Further, to improve the electrical, mechanical, and thermal properties, Reddy and co-workers derived a luminescent nanocomposite based on visible-light sensitized $Eu(pfppd)_3(H_2O)_2$ and carboxylate modified MWCNTs.[30] The designed luminescent nanocomposite material was characterized and exhibited intense red emissions with an overall quantum yield of 27% under a wide excitation range from UV to visible regions (330–460 nm) (Figure 1.12). Also, the high dispersibility of luminescent nanocomposites in polymer matrices make it a promising luminophore for possible application in OLEDs and in optical amplifiers and waveguides.

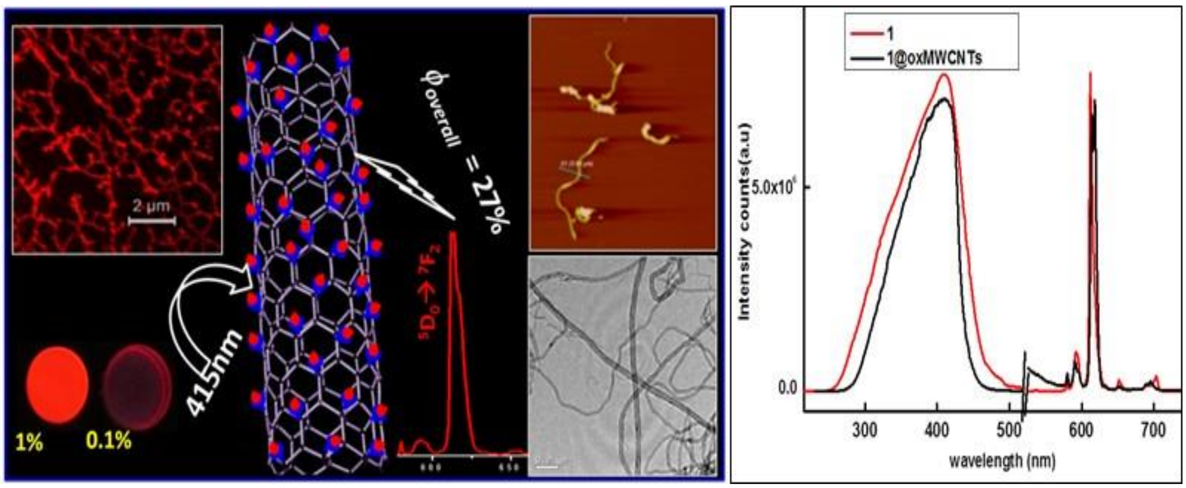

Figure 1.12. The AFM, TEM images of the $Eu(pfppd)_3(H_2O)_2$ complex incorporated into multi-walled carbon nanotube excited at 415 nm (left). Excitation and emission spectra of $Eu(pfppd)_3(H_2O)_2$ (**1**) and luminescent composite (right).

1.4. Luminescent behavior of visible-light sensitized Eu^{3+}-*β*-diketonate complexes: Ancillary ligand modifications

Werts and co-workers[31] were the first time to disclose that the electronic absorption of Michler's ketone (MK) and related push–pull sensitizers undergoes a strong red shift upon coordination with europium-tris(6,6,7,7,8,8,8-heptafluoro-2,2-dimethyloctane-3,5-dione) [$Eu(fod)_3$] (Figure 1.13), which enables efficient sensitization of Eu^{3+} luminescence for excitation at long wavelengths extending well into the visible region (>450 nm).[30] Michler's ketone and $Eu(fod)_3$ apparently form a ground state complex under the experimental conditions, most likely by the interaction of the electron rich carbonyl group with the positively charged Eu^{3+} ion. The new absorption band is probably due to a bathochromic shift of the first singlet–singlet transition of Michler's ketone occurring upon complexation. This π–π^* transition possesses charge-transfer character and in the process of excitation, electron density is moved towards the carbonyl group making the transition solvatochromic. Thus, it is quite likely that the transition energy is largely affected by the presence of the lanthanide ion. Upon closer inspection, the coordination of MK to lanthanide β-diketonates was found to occur only in non-coordinating solvents. The emission spectrum demonstrates that this red glow is Eu^{3+} luminescence and the sharp peaks are characteristic of lanthanide ion emission, Eu^{3+} usually having its most intense emission around 615 nm. The corresponding excitation spectrum is in accordance with the observation that this luminescence can be excited by visible-light. It extends well beyond 450 nm (λ_{max} = 414 nm, Figure 1.13). The quantum yield was found to be 0.17 in aerated solution and 0.20 after deoxygenation by four freeze-pump-thaw cycles (excitation at 420 nm, using quinine bisulfate in 1 M H_2SO_4). Further, these results clearly point to the occurrence of the 'usual' triplet pathway in the sensitization of Eu^{3+} by MK without resort to more exotic mechanisms.

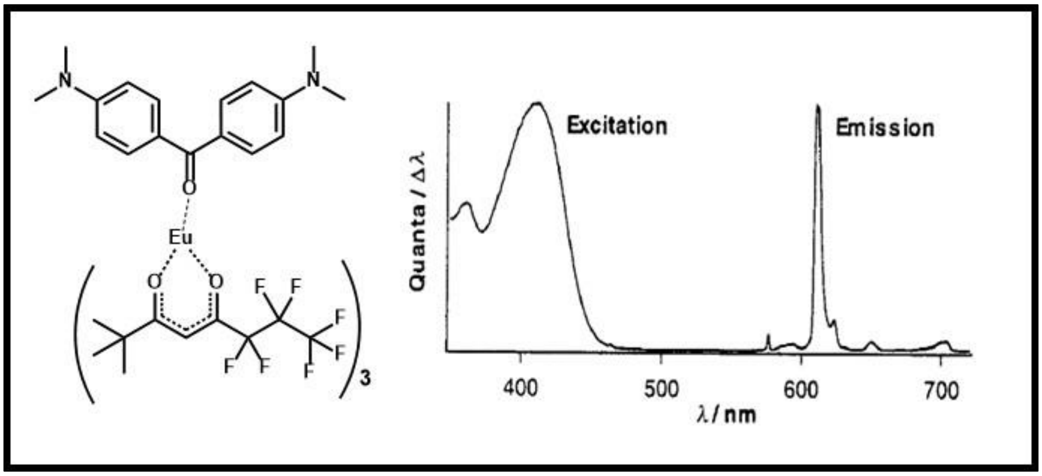

Figure 1.13. The molecular structure of $Eu(fod)_3$-MK. Corrected luminescence excitation (λ_{em} = 612 nm) and emission (λ_{exc} = 450 nm) spectra of a solution of 10^{-5} M Michler's ketone and 10^{-4} M $Eu(fod)_3$ in benzene.

It is well documented that longer-wavelength sensitization of Eu^{3+} emission can be achieved through the singlet pathway, in which the excited-state energy of a chromophore is directly transferred from its S_1 state (singlet state) to the luminescent states of the Eu^{3+} center. Thus, by this way, the energy constraints from the T_1 state (triplet state) of the ligand can be avoided. Wang and co-workers have demonstrated the singlet pathway mechanism for the first time in a visible-light-sensitized europium tris-thenoyltrifluoroacetonato-2-(N,N-diethylanilin-4-yl)-4,6-bis(3,5-dimethyl-pyrazol-1-yl)-1,3,5-triazine complex [$Eu(tta)_3(dpbt)$] (Figure 1.14).[12, 32] Upon selective excitation of the ligand CT band at room temperature, the emission spectrum of $Eu(tta)_3(dpbt)$ complex displays a broad band centered at 430 nm, derived from the coordinated ligand, and the characteristic sharp peaks associated with the $^5D_0 \rightarrow {}^7F_J$ transitions of the Eu^{3+} ion. The overall luminescence quantum yields for the emissions from the Eu^{3+} ion and the coordinated ligand in toluene are 52% and 27%, respectively (λ_{exc} = 402 nm).[32]

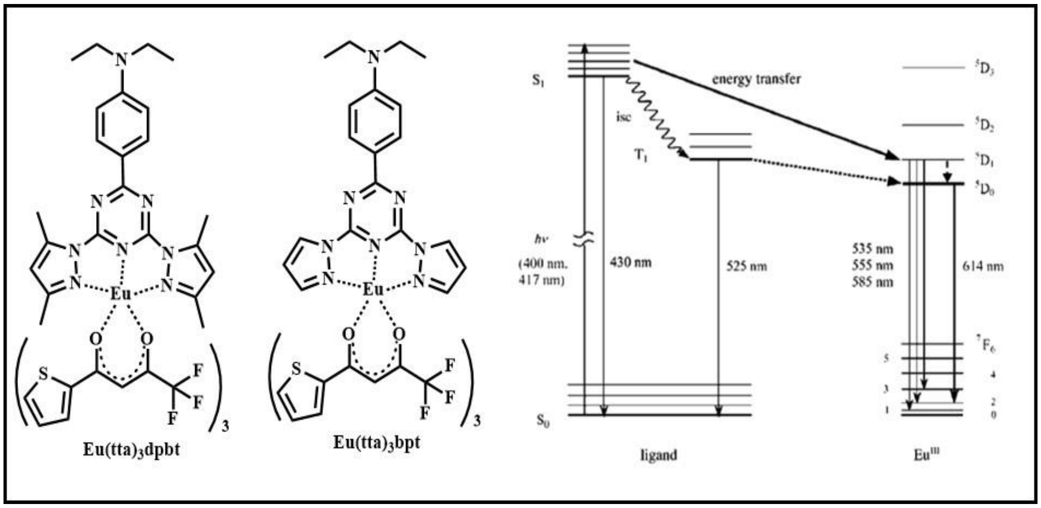

Figure 1.14. The molecular structure of Eu(tta)$_3$dpbt and Eu(tta)$_3$bpt**.** Energy-level diagram showing the energy-transfer pathways in complex Eu(tta)$_3$dpbt; isc denotes intersystem crossing.

Afterwards, Wang and co-workers[33] developed a new complex Eu(tta)$_3$(bpt) (tta = thenoyltrifluoroacetonate; bpt = 2-(N,N-di-ethylanilin-4-yl)-4,6-bis(pyrazol-1-yl)-1,3,5-triazine) with excellent long-wavelength sensitized luminescent properties, in which four hydrogen atoms replace the methyl groups at the 3,3′- and 5,5′-positions of the pyrazolyl rings in a previously reported complex Eu(tta)$_3$(dpbt). The excitation window of Eu(tta)$_3$(bpt) is much broader than that of Eu(tta)$_3$(dpbt) with a red edge extending up to 450 nm in a dilute toluene solution (1.0×10^{-5} M) and 500 nm in a concentrated toluene solution (1.0×10^{-2} M). Upon visible-light excitation (λ_{exc} = 410 nm) at 295 K, the quantum yield of Eu(tta)$_3$(bpt) complex was higher by 23% than that of Eu(tta)$_3$(dpbt). In addition, Eu(tta)$_3$(bpt) exhibits excellent two-photon-excitation luminescent properties. The different emitting-band shapes of Eu(tta)$_3$(bpt) and Eu(tta)$_3$(dpbt) (Figure 1.14) and their high capabilities of long-wavelength sensitized luminescence may be applicable in developing new multiplex probes for bioanalysis. Figure 1.14 also shows the singlet energy-transfer pathways in complex $Eu(tta)_3dpbt$.

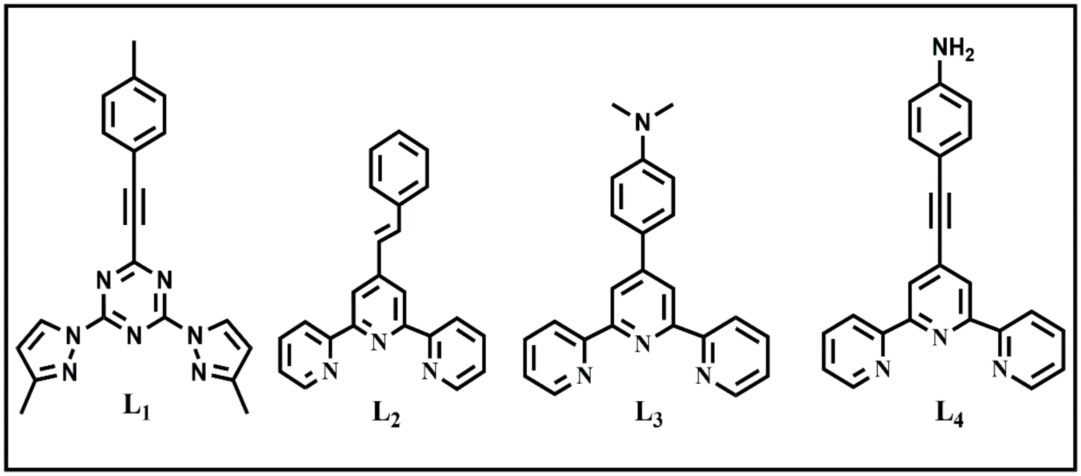

Figure 1.15. The molecular structure of the ligands L_1-L_4.

In order to improve the visible-light sensitization of luminescent europium complexes, Raymond Ziessel and co-workers[34] have designed a series of new europium complexes of formula $[EuL_n(TTA)_3]$ in which TTA refers to 2-thenoyltrifluoroacetonate and L_n to tridentate ligands with nitrogen containing heterocyclic structure (Figure 1.15), such as a 2,6-bis(3-methyl-pyrazolyl)-4-(p-toluoyl-ethynyl)-triazine for L_1, or terpyridine functionalized at the 4′ position by a phenyl-vinylene for L_2, a *p*-dimethylaminophenylene for L_3, or a *p*-aminophenyl-ethynylene for L_4 and examined their photophysical properties. Careful examination of the excitation spectra revealed the differences in the sensitization efficiencies of the ligands. For complexes of L_1 and L_2, excitation of europium is mainly achieved through the TTA moieties and the photophysical studies on $[EuL_1(TTA)_3]$ evidenced a weaker coordination of the bispyrazolyltriazine tridentate ligand, resulting from a partial decomplexation upon dilution. Complexes of L_3 and L_4 display intense excitation through the tridentate units, which extend down to 460 nm in the visible region. In the case of L_3, selective excitation reveals the presence of a ligand centered emission band at 520 nm which is likely ascribed to an L_3 centered charge transfer state.

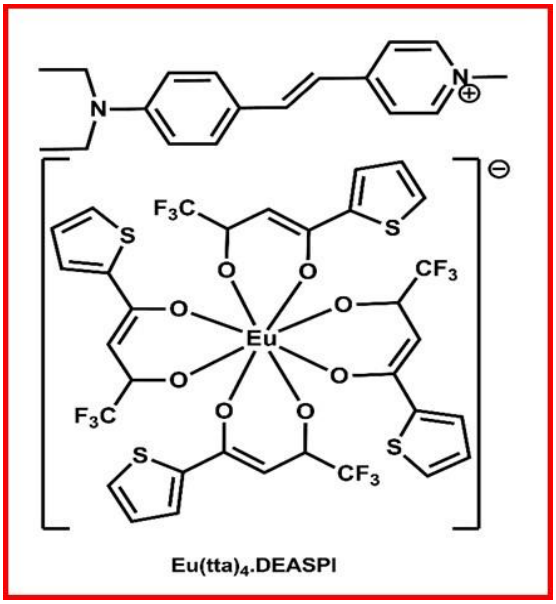

Figure 1.16. The molecular structure of [Eu(tta)$_4$(DEASPI)].

Shi and co-workers[35] described a novel Eu^{3+} complex [trans-4-[p-(N,N-diethylamino)styryl]-N-methylpyridiniumtetrakis(thenoyltrifluoroacetonato) Eu^{3+} [Eu(tta)$_4$(DEASPI)] (Figure 1.16) with efficient luminescence at the excitation wavelength of 1.06 μm. In this ternary complex, the important and innovative point is using trans-4-[p-(N,N-diethylamino) styryl]-N-methylpyridinium (DEASPI) as a one- and two-photon sensitizer for Eu^{3+} ion, which makes the excitation band of this Eu^{3+} complex cover the range from the near-infrared and visible to the ultraviolet. The photophysical properties also demonstrated that the energy transfer from DEASPI to Eu^{3+} is through the charge-transfer (CT) states of DEASPI. The luminescence of Eu^{3+} sensitized by TPA of

1.06 mm laser satisfies the need of less-harmful labeling and high-quality deep-penetrating bioimaging *in vivo*.

1.5. Objective of the present investigation

Research on the design of adequate ligands for both coordination and luminescence sensitization of trivalent europium ions has seen a tremendous development during the past two decades.[1-4] The unique photoluminescence properties of the trivalent europium ions have been found to be a great application in the design of bioprobes for live cell imaging. Thus, the development of europium coordination chemistry in the context of applied bioimaging has been profound. However, a challenge in the coordination chemistry of the lanthanide ions is to develop luminescent Eu^{3+} complexes that can be sensitized by visible-light and to determine the energy-transfer mechanism in these systems owing to the energetic constraints highlighted by Reinhoudt and co-workers.[10] Therefore one of the primary objectives of the present investigation is to design and develop novel visible-light excitable Eu^{3+}-β-diketonate coordination compounds and investigate their photophysical properties for possible use in the bioimaging applications.

1.6. References

1. (a) J.-C. G. Bünzli, *Chem. Rev*., 2010, **110**, 2729; (b) A. J. Amoroso and S. J. A. Pope, *Chem. Soc. Rev.*, 2015, **44**, 4723; (c) S. J. Butler, L. Lamarque, R. Pal and D. Parker, *Chem. Sci.*, 2014, **5**, 1750; (d) S. Faulkner, S. J. A. Pope and B. P. Burton-Pye, *Appl. Spectrosc. Rev.*, 2005, **40**, 1; (e) R. C. Leif, L. M. Vallarino, M. C. Becker and S. Yang, *Cytometry A*, 2006, **69**, 767; (f) C. P. Montgomery, B. S. Murray, E. J. New, R. Pal and D. Parker, *Acc.*

Chem. Res., 2009, **42**, 925; (g) K. H. Thompson and C. Orvig, *Chem. Soc. Rev.*, 2006, **35**, 499; (h) X. Wang, H. Chang, J. Xie, B. Zhao, B. Liu, S. Xu, W. Pei, N. Ren, L. Huang and W. Huang, *Coord. Chem. Rev.*, **0530**, 273; (i) S. V. Eliseeva and J.-C. G. Bünzli, *Chem. Soc. Rev.*, 2010, **39**, 189; (j) Y. Ma and Y. Wang, *Coord. Chem. Rev*., 2010, **254**, 972.

2. (a) H. Xu, Q. Sun, Z. An, Y. Wei and X. Liu, *Coord. Chem. Rev.,* 2015, **293-294**, 228; (b) J. M. Stanley and B. J. Holliday, *Coord. Chem. Rev.*, 2012, **256**, 1520; (c) A. de Bettencourt-Dias, *Dalton Trans.*, 2007, **22**, 2229; (d) J.-C. G. Bünzli, *Coord. Chem. Rev.*, 2015, **293-294**, 19; (e) J. Kido and Y. Okamoto, *Chem. Rev.*, 2002, **102**, 2357; (f) K. Kohtaro, in *Phosphor Handbook*, CRC Press, 2006. (f) L. Ozawa and M. Itoh, *Chem. Rev.*, 2003, **103**, 3835; (g) H. Xu, R. Chen, Q. Sun, W. Lai, Q. Su, W. Huang and X. Liu, *Chem. Soc. Rev.*, 2014, **43**, 3259.

3. (a) J.-C. G. Bünzli, S. V. Eliseeva, Lanthanide Luminescence: Photophysical, Analytical and Biological Aspects. In *Springer Series on Fluorescence*; P. Hänninen, H. Härmä, Eds.; Springer Verlag: Berlin,¨Heidelberg, 2011; Vol. 7, pp 1−46; (b) M. H. V. Werts, *Sci. Prog.*, 2005, **88**, 101; (c) J.-C. G. Bünzli, *Acc. Chem. Res.*, 2006, **39**, 53; (d) N. M. Shavaleev, S. V. Eliseeva, R. Scopelliti, J.-C.G. Bünzli, *Inorg. Chem.* 2015, **54**, 9166; (e) N. M. Shavaleev, S. V. Eliseeva, R. Scopelliti, J.-C. G. Bünzli, *Inorg. Chem.* 2010, **49**, 3927.

4. (a) J.-C. G. Bünzli, A.-S. Chauvin, H. K. Kim, E. Deiters, S. V. Eliseeva, *Coord. Chem. Rev.*, 2010, **254**, 2623; (b) J.-C. G. Bünzli and C. Piguet, *Chem. Soc. Rev.*, 2005, **34**, 1048; (c) M. C. Heffern, L. M. Matosziuk and T. J. Meade, *Chem. Rev.,* 2014, **196**, 4496 (d) L. Armelao, S. Quici, F. Barigelletti, G. Accorsi, G. Bottaro, M. Cavazzini and E. Tondello, *Coord. Chem. Rev.*, 2010, **254**, 487; (e) M. L. P. Reddy and S. Sivakumar, *Dalton Trans.*, 2013, **42**, 2663.

5. (a) W. T. Carnall, P. R. Fields and B. G. Wybourne, *J. Chem. Phys*., 1965, **42**, 3797; (b) Y. H. Kim, N. S. Baek and H. K. Kim, *ChemPhysChem*, 2006, **7**, 213; (c) W. T. Carnall, *J. Phys. Chem*., 1963, **67**, 1206; (c) N. Sabbatini, M. Guardigli and J.-M. Lehn, *Coord. Chem. Rev*., 1993, **123**, 201; (d) J.-M. Lehn, *Angew. Chem., Int. Ed. Engl*., 1990, **29**, 1304; (e) A. R. Ramya, D. Sharma, S. Natarajan and M. L. Reddy, *Inorg. Chem.*, 2012, **51**, 8818; (f) A. R. Ramya, M. L. Reddy, A. H. Cowley and K. V. Vasudevan, *Inorg. Chem.*, 2010, **49**, 2407
6. S. I. Weissman, *J. Chem. Phys*., 1942, **10**, 214.
7. (a) K. Binnemans, Handbook on the Physics and Chemistry of Rare Earths, Elsevier, Amsterdam, 2005, vol. 35, pp. 107; (b) D. B. A. Raj, S. Biju and M. L. P. Reddy, *Inorg. Chem*., 2008, **47**, 8091; (c) P. N. Remya, S. Biju, M. L. P. Reddy, A. H. Cowley and M. Findlater, Inorg. Chem., 2008, **47**, 7396; (d) S. Biju, M. L. P. Reddy, A. H. Cowley and K. V. Vasudevan, *Cryst. Growth Des*., 2009, **9**, 3562; (e) S. Biju, N. Gopakumar, J.-C. G. Bünzli, R. Scopelliti, H. K. Kim and M. L. P. Reddy, *Inorg. Chem*., 2013, **52**, 8750; (f) S. Biju, D. B. A. Raj, M. L. P. Reddy, C. K. Jayasankar, A. H. Cowley and M. Findlater, *J. Mater. Chem*., 2009, **19**, 1425; (g) B. Francis, D. B. Ambili Raj and M. L. P. Reddy, *Dalton Trans*., 2010, 39, 8084; (h) R. Pavithran, N. S. Saleesh Kumar, S. Biju, M. L. P. Reddy, S. A. Junior and R. O. Freire, *Inorg. Chem*., 2006, **45**, 2184.
8. M. H. V. Werts, R. T. F. Jukes and J. W. Verhoeven, *Phys. Chem. Chem. Phys*., 2002, **4**, 1542.
9. M. Latva, H. Takalo, V.-M. Mukkala, C. Matachescu, J. C. Rodriguez-Ubis and J. Kankare, *J. Lumin*., 1997, **75**, 149.
10. (a) S. Pandya, J. Yu and D. Parker, *Dalton Trans.*, 2006, 2757; (b) M. P. Coogan and V. F.-Moreira, *Chem. Commun*., 2014, **50**, 384.

11. F. J. Steemers, W. Verboom, D. N. Reinhoudt, E. B. VanderTol and J. W. Verhoeven, *J. Am. Chem. Soc*., 1995, **117**, 9408.
12. (a) A. Dadabhoy, S. Faulkner, P. G. Sammes, *J. Chem. Soc. Perkin Trans. 2* 2000, 2359; (b) A. Beeby, L. M. Bushby, D. Maffeo, J. A. G. Williams, *J. Chem. Soc. Perkin Trans. 2*, 2000, 1281; (c) Y. Bretonniere, M. J. Cann, D. Parker, R. Slater, *Chem. Commun.*, 2002, 1930.
13. C. Yang, L.-M. Fu, Y. Wang, J.-P. Zhang, W.-T. Wong, X.-C. Ai, Y.-F. Qiao, B.-S. Zou, and L.-L. Gui, *Angew. Chem. Int. Ed*., 2004, **43**, 5010.
14. (a) M. D. Ward, *Coord. Chem. Rev*., 2010, **254**, 2634; (b) M. D. Ward, *Coord. Chem. Rev.*, 2007, **251**, 1663; (c) F.-F. Chen, Z.-Q. Chen, Z.-Q. Bian and C.-H. Huang, *Coord. Chem. Rev*., 2010, **254**, 991; (d) F. Chen, Z. Bian, Z. Liu, D. Nie, Z. Chen and C. Huang, *Inorg. Chem*., 2008, **47**, 2507.
15. (a) R. Ziessel, S. Diring, P. Kadjane, L. Charbonnière, P. Retailleau and C. Philouze, *Chem.–Asian J*., 2007, 2, 975; (b) P. He, H. H. Wang, S. G. Liu, J. X. Shi, G. Wang and M. L. Gong, *Inorg. Chem*., 2009, **48**, 11382.
16. M. L. P. Reddy, V. Divya and R. Pavithran, *Dalton Trans*., 2013, **42**, 15249.
17. (a) S. Wang, B. S. Gaylord and G. C. Bazan, *J. Am. Chem. Soc.*, 2004, **126**, 5446; (b) M. H. V. Werts, S. Gmouh, O. Mongin, T. Pons and M. Blanchard-Desce, *J. Am. Chem. Soc.*, 2004, **126**, 16294; (c) P. N. Day, K. A. Nguyen and R. Pachter, *J. Phys. Chem. B*, 2005, **109**, 1803; (d) Z. Zou, L. Dang, P. Liu, and H. Wei, *J. Chem. Eng. Data,* 2007, **52***,* 1501.
18. M. Uekawa, Y. Miyamoto, H. Ikeda, K. Kaifu, T. Nakaya, *Synthetic Metals*, 1997, **91**, 259.
19. D. B. Ambili Raj, S. Biju and M. L. P. Reddy, *Dalton Trans.*, 2009, **36**, 7519.

20. V. Divya, R. O. Freire and M. L. P. Reddy, *Dalton Trans.*, 2011, **40**, 3257.
21. V. Divya, S. Biju, R. Luxmi Varma and M. L. P. Reddy, *J. Mater. Chem*., 2010, **20**, 5220.
22. (a) N. Blouin and M. Leclerc, *Acc. Chem. Res.,* 2008, **41**, 1110 (b) J. Yang, X. Tao, C. X. Yuan, Y. X. Yan, L. Wang, Z. Liu, Y. Ren and M. H. Jiang, *J. Am. Chem. Soc.*, 2005, **127**, 3278; (c) K. Hasnaoui, H. Zgou, M. Hamidi and M. Bouachrine, *Chin. Chem. Lett.*, 2008, **19**, 488; (d) W. Wong, C. Ho, Z. Gao, B. Mi, C. Chen, K. Cheah and Z. Lin, *Angew. Chem., Int. Ed.*, 2006, **45**, 7800; (e) W. Wong, *Coord. Chem. Rev.*, 2005, **249**, 971; (f) W. Wong and C. Ho, *Coord. Chem. Rev.*, 2006, **250**, 2627.
23. (a) J. Lia and A. C. Grimsdale, *Chem. Soc. Rev*., 2010, **39**, 2399; (b) J.-F. ois Morin, M. Leclerc, D. Ad es, A. Siove, *Macromol. Rapid Commun*., 2005, **26**, 761.
24. S.-g. Liu, W.-y. Su, R.-k. Pan and X.-p. Zhou, *Chin. J. Chem. Phys.*, 2012, **25**, 697.
25. P. He, H. H. Wang, S. G. Liu, J. X. Shi, G. Wang and M. L. Gong, *Inorg. Chem.*, 2009, **48**, 11382.
26. P. He, H. H. Wang, H. G. Yan, W. Hu, J. X. Shi and M. L. Gong, *Dalton Trans.*, 2010, **39**, 8919.
27. B. Francis, C. Heering, R. O. Freire, M. L. P. Reddy and C. Janiak, *RSC Adv.*, 2015, **5**, 90720.
28. D. B. A. Raj, B. Francis, M. L. P. Reddy, R. R. Butorac, V. M. Lynch and A. H. Cowley, *Inorg. Chem*., 2010, **49**, 9055
29. V. Divya, V. Sankar, K. G. Raghu and M. L. P. Reddy, *Dalton Trans.*, 2013, **42**, 12317.
30. V. Divya and M. L. P. Reddy, *J. Mater. Chem. C*, 2013, **1**, 160.
31. M. H. V. Werts, M. A. Duin, J. W. Hofstraat and J. W. Verhoeven, *Chem. Commun*., 1999, **9**, 799.

32. L.-M. Fu, X.-C. Ai, M.-Y. Li, X.-F. Wen, R. Hao, Y.-S. Wu, Y. Wang and J.-P. Zhang, *J. Phys. Chem. A*, 2010, **114**, 4494.

33. F. Xue, Y. Ma, L. Fu, R. Hao, G. Shao, M. Tang, J. Zhang and Y. Wang, *Phys. Chem. Chem. Phys*., 2010, **12**, 3195.

34. P. Kadjane, L. Charbonnière, F. Camerel, P. P. Lainé and R. Ziessel, *J. Fluoresc*., 2008, **18**, 119.

35. M. Shi, C. Ding, J. Dong, H. Wang, Y. Tian and Z. Hu, *Phys. Chem. Chem. Phys.*, 2009, **11**, 5119.

Chapter 2

Chapter 2

Tuning of the excitation wavelength in Eu^{3+}-aminophenyl based polyfluorinated β-diketonate complexes: a red-emitting Eu^{3+}-complex encapsulated in a silica/polymer hybrid material excited by blue light

2.1. Abstract

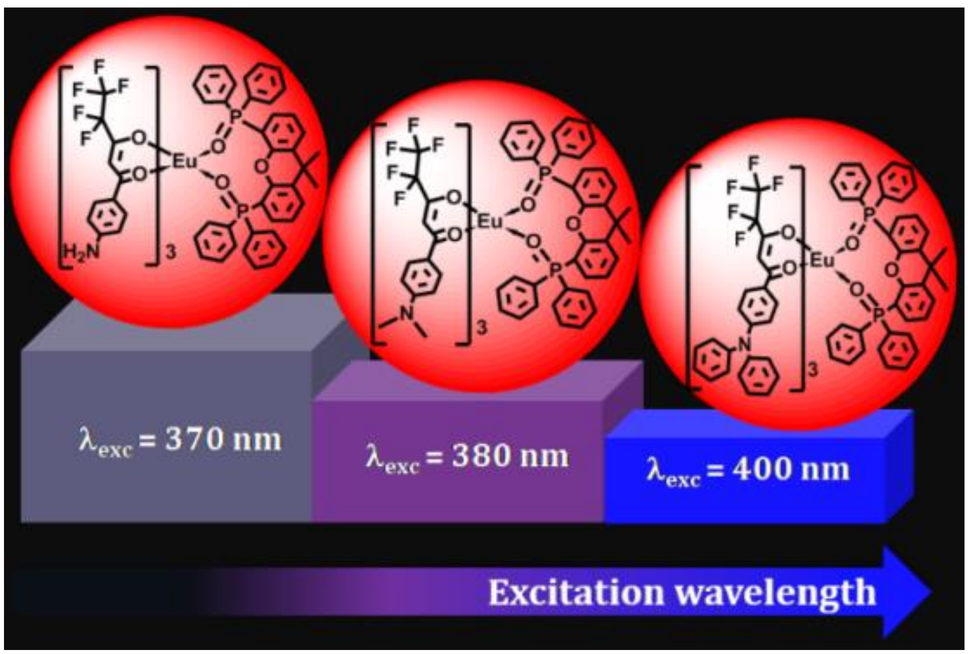

This chapter describes the synthesis, characterization and photophysical properties of a series of Eu^{3+} complexes based on three aminophenyl based polyfluorinated β-diketonates, namely, 1-(4-aminophenyl)-4,4,5,5,5-pentafluoro-3-hydroxypent-2-en-1-one, 1-(4 (dimethylamino)phenyl)-4,4,5,5,5-pentafluoro-3-hydroxypent-2-en-1-one and 1-(4 (diphenylamino)phenyl)-4,4,5,5,5-pentafluoro-3-hydroxypent-2-en-1-one, and an ancillary ligand, 4,5-bis(diphenylphosphino)-9,9-dimethylxanthene oxide. The results demonstrated

that the triphenylamine based polyfluorinated Eu^{3+}–β-diketonate complexes dramatically red-shifted the excitation maximum to the visible region (λ_{exc} = 400 nm) with an impressive quantum yield (40%) as compared to the simple Eu^{3+}–aminophenyl-β-diketonate complexes (λ_{exc} = 370 nm). This can be explained on the basis of the conjugation between nitrogen lone pair electrons and the phenyl π-electrons in the β-diketonate ligand system. On the other hand, the electron-donating dimethylamino group (Hammett constant: σ_p = −0.83) containing Eu^{3+}–β-diketonate complexes moderately shifted the excitation maximum in the UV region from 370 to 380 nm as compared to unsubstituted aminophenyl (Hammett constant: σ_p = −0.66) Eu^{3+} complexes. The displacement of water molecules in aminophenyl based Eu^{3+}–β-diketonate binary complexes by a rigid phosphine oxide ligand richly enhances the photoluminescence quantum yields as well as the excited state lifetime values of the corresponding ternary complexes. As an integral part of this work, hybrid materials have been developed through a sol–gel route by encapsulating a ternary Eu^{3+} compound in a silica/polymer hybrid for high performance luminescence applications. In addition, a bright red-emitting diode was fabricated by coating the designed hybrid material onto a 400 nm emitting InGaN chip and the photoluminescence was examined. Notably, the current study clearly shows that the developed triphenylamine based Eu^{3+}–β-diketonate complex is an interesting red-emitting material excited by blue light and therefore may find potential applications in the fields of biological and materials science.

T. V. Usha Gangan and M. L. P. Reddy, *Dalton Trans*., 2015, **44**, 15924–15937.

2.2. Introduction

The unique photoluminescence properties of Eu^{3+} complexes have been attracting tremendous interest for decades owing to their outstanding potential applications in medical diagnostics and organic light emitting diodes.[1–4] The shielding of the f orbitals by $5s^2$ and $5p^6$ closed shells results in narrow line-like emissions of optically pure colors with long radiative lifetimes. However, the f–f transitions that result in light emission from the lanthanide ions are both spin- and parity-forbidden, which, in turn, mandates the use of antenna molecules for the indirect excitation of the metal center. This indirect excitation, also known as the antenna effect, takes advantage of the coordinated ligands in the sense that energy transfer from the ligand-centered excited states to the metal center results in lanthanide ion luminescence.[4] The β-diketonate ligand class is emerging as one of the important antenna molecules in terms of high harvest emissions because of the effectiveness of the energy transfer from this ligand to the Ln^{3+} ion.[5]

Unfortunately, the excitation window appears to be limited to the near-UV region in many of the Eu^{3+}–β-diketonate complexes due to the energy constraints imposed by the photophysics of sensitized Eu^{3+} luminescence, as well documented by Reinhoudt and coworkers.[6] Therefore, one of the challenges in this field is to develop luminescent Eu^{3+} complexes that can be excited by visible-light and this field has become more important because of the increasing demand for less harmful reagents in life sciences and low voltage driven pure red emitters in optoelectronic applications. Indeed, some of the recent literature reports demonstrated that the excitation window can be shifted to the visible region in Eu^{3+}–β-diketonate complexes by appropriate molecular engineering of the ligand systems with suitably expanded π-conjugation in the complex molecules.[7-9] However, some of the Eu^{3+}–β-diketonate complexes reported exhibit poor quantum yields.[7,8a,b]

Triphenylamine derivatives are widely used as hole-transporting materials in Organic Light Emitting Diodes (OLEDs) due to their high charge mobility, light-harvesting unit and high thermal stability.[10] It is well documented that the replacement of C–H bonds in a β-diketonate ligand with lower-energy C–F oscillators is able to lower the vibration energy of the ligand, which decreases the energy loss caused by ligand vibration and enhances the emission intensity of the lanthanide ion. Further, due to the heavy-atom effect, which facilitates intersystem crossing, the lanthanide-centered luminescent properties are enhanced.[11] Based on the above considerations, we conceived a strategy that simultaneously incorporates highly conjugated triphenylamine and polyfluorinated alkyl groups into the β-diketonate ligand, expecting to obtain the resultant ligands possessing high luminescence efficiency and photochemical stability under visible-light excitation upon coordination with trivalent lanthanides. Thus, a series of novel aminophenyl based β-diketonate ligands (Figure 2.1), namely, 1-(4-aminophenyl)-4,4,5,5,5-pentafluoro-3-hydroxypent-2-en-1-one (HAPFP), 1-(4-(dimethylamino)phenyl)-4,4,5,5,5-pentafluoro-3-hydroxypent-2-en-1-one (HDMAPFP) and 1-(4-(diphenylamino)phenyl)-4,4,5,5,5-pentafluoro-3-hydroxypent-2-en-1-one (HDPAPFP), have been synthesized and utilized for the construction of Eu^{3+}–β-diketonate coordination compounds in the presence and absence of an ancillary ligand, 4,5-bis(diphenylphosphino)-9,9-dimethylxanthene oxide (DDXPO), with a view to shift the excitation window to the visible region. Herein, we demonstrate that these ligands are easily accessible, readily coordinate to europium, and efficiently sensitize its luminescence when excited under visible-light. The origin of the “amino conjugation effect” on the emission as well as other excited state properties in these complexes has also been elucidated and discussed.

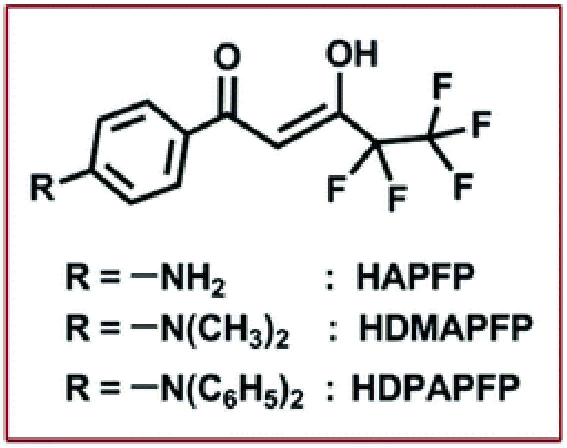

Figure 2.1. Structures of the *β*-diketonate ligands.

Due to their poor thermal resistivity, moisture sensitivity and feeble mechanical strength, the lanthanide complexes are difficult to directly utilize as luminescence sources in many optoelectronic applications. These inherent problems can be solved by encapsulating the lanthanide luminescent complexes in suitable solid matrixes including polymers,[2a,4d,8c,12] sol–gel silica,[2a,3c,4d,13] mesoporous materials[2a,4d,5g,8c,14] and even carbon nanotubes.[8d,15] The potential utility of these materials depends on exploiting the synergy between the excellent luminescence features of lanthanides and the intrinsic characteristics of sol–gel derived hybrid materials. These materials may find promising applications such as light emitting devices, active waveguides and biomedical actuators and sensors. In order to enhance the luminescent properties and improve the stability of the lanthanide complexes, herein a novel ternary Eu^{3+} luminescent complex was embedded into a silica/polymer hybrid material and characterized and its photoluminescence properties were examined. Additionally, a bright red emitting diode was fabricated by coating the luminescent hybrid material onto a 400 nm emitting InGaN chip and the photoluminescence was investigated.

2.3. Experimental section

2.3.1. Materials and instrumentation

The following chemicals were acquired commercially and used without further purification: europium(III) nitrate hexahydrate, 99.9% (Alfa-Aesar); gadolinium(III) nitrate hexahydrate, 99.9% (Sigma-Aldrich); triphenylamine, 98% (Sigma-Aldrich); 4-aminoacetophenone, 99% (Alfa-Aesar); sodium hydride, 60% dispersion in mineral oil (Sigma-Aldrich); ethyl pentafluoropropionate, 98% (Sigma-Aldrich); 4,5-bis(diphenylphosphino)-9,9-dimethylxanthene, 97% (Sigma-Aldrich); iodomethane, 98% (Alfa-Aesar); tetraethyl orthosilicate (TEOS), 98% (Sigma-Aldrich). All the other chemicals used were of analytical reagent grade without further purification.

Elemental analyses were performed with an Elementar – vario MICRO cube elemental analyzer. A Perkin-Elmer Spectrum Two FT-IR spectrometer using KBr was used to obtain the IR spectral data and a Bruker 500 MHz NMR spectrometer was used to record the ^{1}H NMR (500 MHz), $^{13}C\{^{1}H\}$ NMR (125.7 MHz) and $^{31}P\{^{1}H\}$ NMR (202.44 MHz) spectra of the new compounds in chloroform-d solution. The chemical shifts are reported in parts per million relative to tetramethylsilane, $SiMe_4$, for ^{1}H NMR and $^{13}C\{^{1}H\}$ NMR spectra and with respect to 85% phosphoric acid for $^{31}P\{^{1}H\}$ NMR spectra. Electrospray ionization (ESI) mass spectra were recorded on a Thermo Scientific

Exactive Benchtop LC/MS Orbitrap Mass Spectrometer. Matrix assisted laser desorption ionization time-of-flight (MALDI-TOF) mass spectra were recorded on a KRATOS analytical spectrometer (Shimadzu Inc.) and the thermogravimetric analyses were performed on a TG/DTA-6200 (SII Nano Technology Inc., Japan). Scanning electron microscopy (SEM) of EuC-PMMA-Gel and EuC-Gel was performed on a Zeiss EVO-18 Cryo-SEM instrument. X-ray powder patterns (XRD) were recorded in the 2θ range of 10–70° using Cu-K_α radiation (Philips X'pert Pro). The molar absorption coefficient (ε) of the ligands was measured in THF solution on a UV-vis spectrophotometer (Shimadzu, UV-2450). The photoluminescence (PL) spectra were recorded on a Spex-Fluorolog FL22 spectrofluorimeter equipped with a double grating 0.22 m Spex 1680 monochromator and a 450 W Xe lamp as the excitation source operating in the front face mode. The lifetime measurements were carried out at room temperature using a Spex 1040D phosphorimeter. The overall quantum yield (Φ_{overall}) was measured using an integrating sphere in a SPEX Fluorolog spectrofluorimeter.

The PL quantum yields of thin films (Φ_{overall}) were determined using a calibrated integrating sphere system. A Xe-arc lamp was used to excite the thin film samples that were placed in the sphere. All samples were prepared by drop casting the material placed between two glass cover slips. The quantum yields were determined by comparing the spectral intensities of the lamp and the sample emission as reported in the literature.[16] Using this experimental setup and the integrating sphere system, the solid state fluorescence quantum yield of a thin film of the standard green OLED material tris-8-hydroxyquinolinolato aluminium (Alq_3) was determined to be 0.40, which is consistent with previously reported values.[17] Several measurements were carried out for each sample, so that the presented value corresponds to the arithmetic mean value. The estimated error for the quantum yields is ±10%.

2.3.2 Synthetic procedures for the ketones

Synthesis of 1-(4-(dimethylamino)phenyl)ethenone: To a DMF solution of 4-aminoacetophenone (7.40 mmol), iodomethane (17 mmol) and K_2CO_3 (17 mmol) were added. The resultant mixture was stirred at 60 °C for 1 day, cooled at room temperature and quenched with a mixture of ice and water. The product was filtered and washed with water to afford the compound as a white solid. Yield: 82%. ^{1}H NMR ($CDCl_3$, 500 MHz) δ (ppm): 7.87 (d, 2H, J = 8.5 Hz), 6.65 (d, 2H, J = 8.5 Hz), 3.06 (s, 6H), 2.51 (s, 3H). ^{13}C{^{1}H} NMR ($CDCl_3$, 125.7 MHz) δ (ppm): 196.47, 153.17, 130.53, 125.33, 129.60, 110.59, 40.02, 25.98. m/z = 164 (M + H)$^+$.

Synthesis of 1-(4-(diphenylamino)phenyl)ethenone: Acetyl chloride (4.08 mmol) taken in a dichloromethane solution was added dropwise to a slurry of zinc chloride (4.08 mmol) suspended in a solution of triphenylamine (4.08 mmol). After the addition was completed, the mixture was heated under reflux for 24 h. The reaction mixture was then poured into cold, dilute hydrochloric acid. The organic layer was separated, washed with water until the wash water was neutral, and then dried over anhydrous sodium sulphate. The resulting residue was purified by column chromatography using ethyl acetate/hexane (10 : 90), thereby affording the desired product as a yellow solid. Yield: 60%. ^{1}H NMR ($CDCl_3$, 500 MHz) δ (ppm): 7.79 (d, 2H, J = 10 Hz), 7.30 (m, 4H), 7.14 (m, 6H), 6.98 (d, 2H, J = 9 Hz), 2.53 (s, 3H). ^{13}C{^{1}H} NMR ($CDCl_3$, 125.7 MHz) δ (ppm): 196.48, 152.17, 146.51, 129.88, 129.60, 125.96, 124.63, 119.68, 26.23. m/z = 288 (M + H)$^+$.

2.3.3. Synthesis of the ligands

A modified method of the typical Claisen condensation procedure is used for the synthesis of β-diketonate ligands (Scheme 2.1). The corresponding ketone (1.0 mmol) and ethyl pentafluoropropionate (1.0 mmol) were added to 20 mL of dry tetrahydrofuran (THF) and stirred for 10 min at 0 °C in an ice bath. To this reaction mixture, sodium hydride (60%) was added under an inert atmosphere and stirred for 30 min followed by further stirring at 65 °C for 24 h. To the resulting solution, 2 M HCl (25 mL) was added, and extracted thrice with dichloromethane (3 × 25 mL). The organic layer was separated and dried over Na_2SO_4, and the solvent was evaporated. The crude product thus obtained was then purified by column chromatography on silica gel with a mixture of ethyl acetate and hexane (5 : 95 for HAPFP and 2 : 98 for HDMAPFP and HDPAPFP) as the eluent to obtain the product.

1-(4-Aminophenyl)-4,4,5,5,5-pentafluoro-3-hydroxypent-2-en-1-one (HAPFP): Yield: 60%. Elemental analysis (%): calculated for $C_{11}H_8F_5NO_2$ (281.18): C 46.99, H 2.87, N 4.98; Found: C 46.74, H 2.84, N 4.76. ^{1}H NMR ($CDCl_3$, 500 MHz) δ (ppm): 15.28 (broad, enol–OH), 8.17 (s, 2H, NH_2), 8.04 (d, 2H, J = 9 Hz), 7.79 (d, 2H, J = 8.5 Hz), 6.64 (s, 1H). $^{13}C\{^1H\}$ NMR (125.7 MHz, $CDCl_3$) δ (ppm): 196.68, 183.78, 156.39, 139.88, 132.16, 127.21, 117.21, 112.14, 96.82, 77.26–76.75 ($CDCl_3$). IR (KBr) ν_{max} (cm^{-1}): 3346 (N–H), 1703, 1534, 1333, 1209, 1037, 794. m/z = 281 $(M)^+$.

1-(4-(Dimethylamino)phenyl)-4,4,5,5,5-pentafluoro-3-hydroxypent-2-en-1-one (HDMAPFP): Yield: 65%. Elemental analysis (%): calculated for $C_{13}H_{12}F_5NO_2$ (309.23): C 50.49, H 3.91, N 4.53; Found: C 50.64, H 4.06, N 4.58. ^{1}H NMR ($CDCl_3$, 500 MHz) δ (ppm):

15.97 (broad, enol–OH), 7.86 (d, 2H, J = 9.5 Hz), 6.68 (d, 2H, J = 10 Hz), 6.48 (s, 1H), 3.11 (s, 6H). $^{13}C\{^{1}H\}$ NMR ($CDCl_3$, 125.7 MHz) δ (ppm): 185.68, 175.78, 154.39, 133.88, 130.20, 127.21, 119.21, 111.14, 91.82, 40.02, 77.28–76.78 ($CDCl_3$). IR (KBr) ν_{max} (cm^{-1}): 2925, 1586, 1377, 1329, 1229, 1011, 741. m/z = 310.08 $(M + H)^+$.

1-(4-(Diphenylamino)phenyl)-4,4,5,5,5-pentafluoro-3-hydroxypent-2-en-1-one (HDPAPFP): Yield: 85%. Elemental analysis (%): calculated for $C_{23}H_{16}F_5NO_2$ (433.37): C 63.74, H 3.72, N 3.23; Found: C 63.90, H 3.84, N 3.35. ^{1}H NMR ($CDCl_3$, 500 MHz) δ (ppm): 15.71 (broad, enol–OH), 7.78 (d, 2H, J = 9 Hz), 7.35 (m, 4H), 7.20 (m, 6H), 6.98 (d, 2H, J = 8.5 Hz), 6.50 (s, 1H). $^{13}C\{^{1}H\}$ NMR ($CDCl_3$, 125.7 MHz) δ (ppm): 189.63, 185.74, 153.39, 145.83, 130.10, 129.88, 129.79, 129.48, 126.39, 125.42, 123.80, 119.06, 92.45, 77.27–76.76 ($CDCl_3$). IR (KBr) ν_{max} (cm^{-1}): 3059, 1609, 1585, 1490, 1331, 1265, 1016, 697. m/z = 434.22 $(M + H)^+$.

4,5-Bis(diphenylphosphino)-9,9-dimethylxanthene oxide (DDXPO): The corresponding phosphine (5.0 mmol) was dissolved in 10 mL of 1,4-dioxane solution, to which 1.0 mL of 30% H_2O_2 (10.5 mmol) was added drop wise with vigorous stirring. The resultant mixture was then stirred for 2 h and then 10 mL of water was added to the reaction mixture to arrest the reaction. The mixture was extracted with 3 × 30 mL of dichloromethane. The oily phase was then washed with 2 × 30 mL of water to remove 1,4-dioxane. The dichloromethane layer was dried with Na_2SO_4. The solvent was removed *in vacuo*. The product was recrystallized from dichloromethane. Yield: 95%. Elemental analysis (%): calculated for $C_{39}H_{32}O_3P_2$ (610.18): C 76.71, H 5.28; Found: C 76.52, H 5.40. ^{1}H NMR ($CDCl_3$, 500 MHz) δ (ppm): 7.61 (d, 2 H, J = 8 Hz), 7.41 (m, 12 H), 7.30 (m, 8 H), 6.99 (t, 2 H, J = 7.5 Hz), 6.77 (q, 2 H, J = 7.5 Hz), 1.70 (s, 6 H). $^{31}P\{^{1}H\}$ NMR ($CDCl_3$, 202.44 MHz) δ(ppm): 30.97. IR (KBr) ν_{max} (cm^{-1}): 1727, 1670, 1436, 1401, 1229, 1190, 1114, 875, 785, 746, 719, 694. m/z = 611.31 $(M + H)^+$.

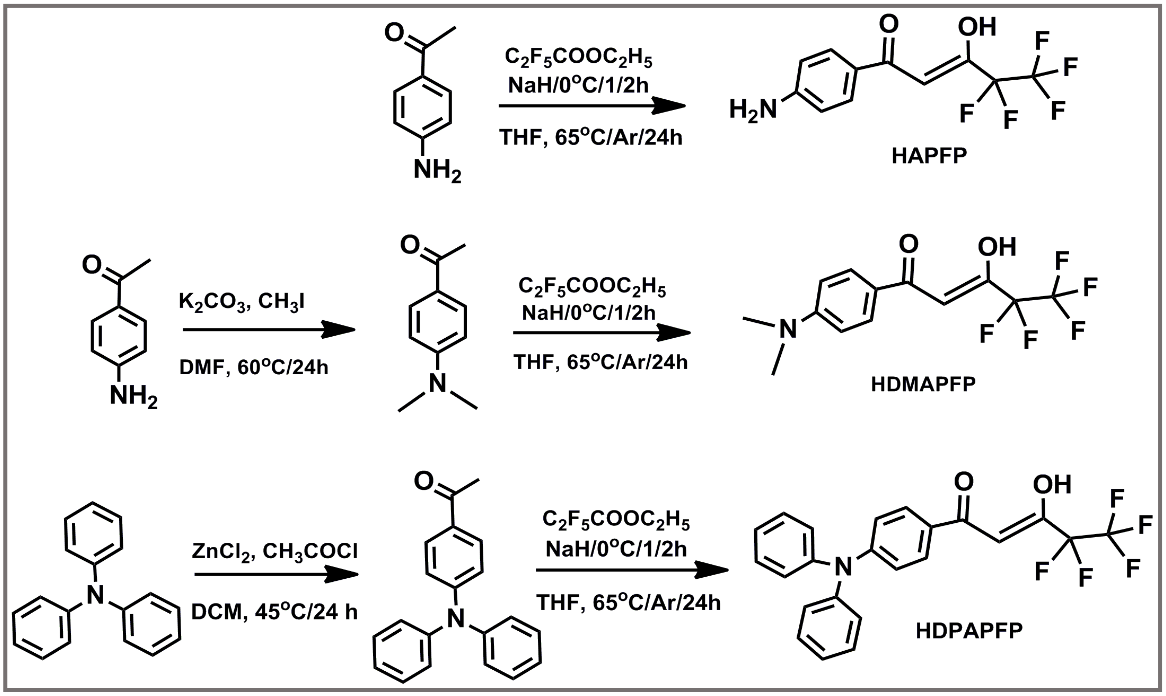

Scheme 2.1. Synthetic procedure for the β-diketonate ligands.

2.3.4. Synthesis of binary complexes

To a solution of β-diketonate ligand (3.0 mmol) in ethanol, NaOH (3.0 mmol) in water was added and stirred for 5 min. To this mixture, $Ln(NO_3)_3{\cdot}6(H_2O)$ (where Ln = Eu^{3+}, Gd^{3+}) (1.0 mmol) in 2 mL water was added drop wise and stirred for 12 h at room temperature. The resultant precipitate formed was filtered off, washed with water and dried. The products were purified by recrystallization from a chloroform solution and used for further analysis and photophysical studies. Efforts to grow single crystals of complexes were not fruitful. The synthesis method is described in Scheme 2.2.

Eu(APFP)$_3$(H$_2$O)$_2$ (1). Elemental analysis (%): calculated for $C_{33}H_{25}F_{15}N_3O_8Eu$ (1029.06): C 38.54, H 2.45, N 4.09; Found: C 38.35, H 2.53, N 3.93. IR (KBr) ν_{max} (cm^{-1}): 3435, 3320, 1712, 1523, 1328, 1216, 1039, 695. m/z = 1016.28 [Eu(APFP)$_3$ + Na + 1]$^+$.

Eu(DMAPFP)$_3$(H$_2$O)$_2$ (2). Elemental analysis (%): calculated for $C_{39}H_{37}F_{15}N_3O_8Eu$ (1113.16): C 42.10, H 3.35, N 3.78; Found: C 42.25, H 3.33, N 3.87. IR (KBr) ν_{max} (cm^{-1}): 3443, 2927, 1594, 1370, 1323, 1281, 1014, 671. m/z = 1094.44 [Eu(DMAPFP)$_3$(H$_2$O)]$^+$.

Eu(DPAPFP)$_3$(H$_2$O)$_2$ (3). Elemental analysis (%): calculated for $C_{69}H_{49}F_{15}N_3O_8Eu$ (1485.25): C 55.80, H 3.33, N 2.83; Found: C 56.01, H 3.45, N 2.91. IR (KBr) ν_{max} (cm^{-1}): 3437, 3049, 1614, 1583, 1492, 1327, 1275, 1013, 678. m/z = 1447.33 [Eu(DPAPFP)$_3$ – H]$^+$.

Gd(APFP)$_3$(H$_2$O)$_2$ (7). Elemental analysis (%): calculated for $C_{33}H_{25}F_{15}N_3O_8Gd$ (1034.06): C 38.34, H 2.44. N 4.06; Found: C 38.20, H 2.18, N 3.91. IR (KBr) ν_{max} (cm^{-1}): 3435, 3321, 1711, 1523, 1328, 1216, 1039, 695. m/z = 1016.48 [Gd(APFP)$_3$(H$_2$O)]$^+$.

Gd(DMAPFP)$_3$(H$_2$O)$_2$ (8). Elemental analysis (%): calculated for $C_{39}H_{37}F_{15}N_3O_8Gd$ (1118.16): C 41.90, H 3.35. N 3.76; Found: C 42.06, H 3.26, N 3.68. IR (KBr) ν_{max} (cm^{-1}): 3443, 2927, 1595, 1370, 1323, 1281, 1014, 671. m/z = 1141.89 [Gd(DMAPFP)$_3$(H$_2$O)$_2$ + Na]$^+$.

Gd(DPAPFP)$_3$(H$_2$O)$_2$ (9). Elemental analysis (%): calculated for $C_{71}H_{55}F_{15}N_3O_8Gd$ (1454.23): C 55.61, H 3.31. N 2.82; Found: C 55.78, H 3.43, N 2.98. IR (KBr) ν_{max} (cm^{-1}): 3433, 3054, 1615, 1584, 1492, 1327, 1276, 1013, 698. m/z = 1022.30 [Gd(DPAPFP)$_2$]$^+$.

2.3.5. Synthesis of Eu^{3+} complexes 4–6

Ternary Eu^{3+} complexes were prepared by stirring equimolar solutions of the corresponding binary complexes and DDXPO in $CHCl_3$ solution for 12 h at 70 °C. The products were isolated by solvent evaporation and purified by recrystallization from a chloroform mixture. The synthesis procedure is illustrated in Scheme 2.3.

$Eu(APFP)_3(DDXPO)$ (4). Elemental analysis (%): calculated for $C_{72}H_{53}O_9F_{15}N_3P_2Eu$ (1603.22): C 53.94, H 3.33, N 2.62; Found: C 54.06, H 3.44, N 2.65. IR (KBr) ν_{max} (cm^{-1}): 3060, 1713, 1527, 1333, 1217, 1179, 1019, 696. m/z = 1345.83 [Eu(APFP)$_2$(DDXPO) + Na]$^+$. ^{31}P NMR ($CDCl_3$, 202.44 MHz) δ (ppm): −77.55.

$Eu(DMAPFP)_3(DDXPO)$ (5). Elemental analysis (%): calculated for $C_{78}H_{65}O_9F_{15}N_3P_2Eu$ (1687.32): C 54.52, H 3.88, N 2.49; Found: C 54.39, H 4.01, N 2.45. IR (KBr) ν_{max} (cm^{-1}): 3061, 1596, 1506, 1403, 1330, 1274, 1179, 1014, 676. m/z = 1402.20 [Eu(DMAPFP)$_2$(DDXPO) + Na + 1]$^+$. ^{31}P NMR ($CDCl_3$, 202.44 MHz) δ (ppm): −82.80.

$Eu(DPAPFP)_3(DDXPO)$ (6). Elemental analysis (%): calculated for $C_{108}H_{77}O_9F_{15}N_3P_2Eu$ (2059.67): C 62.98, H 3.77, N 2.04; Found: C 63.02, H 3.92, N 2.11. IR (KBr) ν_{max} (cm^{-1}): 3061, 1622, 1588, 1524, 1492, 1327, 1274, 1178, 1013, 696. m/z = 1628.93 [Eu(DPAPFP)$_2$(DDXPO)]$^+$. ^{31}P NMR ($CDCl_3$, 202.44 MHz) δ (ppm): −86.87.

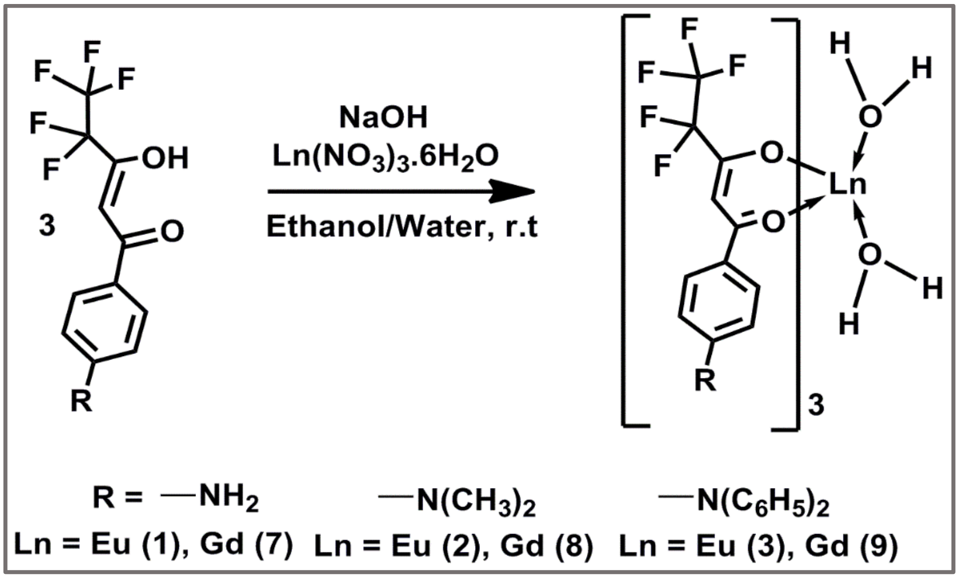

Scheme 2.2. Synthesis of Ln^{3+} (Ln = Eu, Gd) binary complexes.

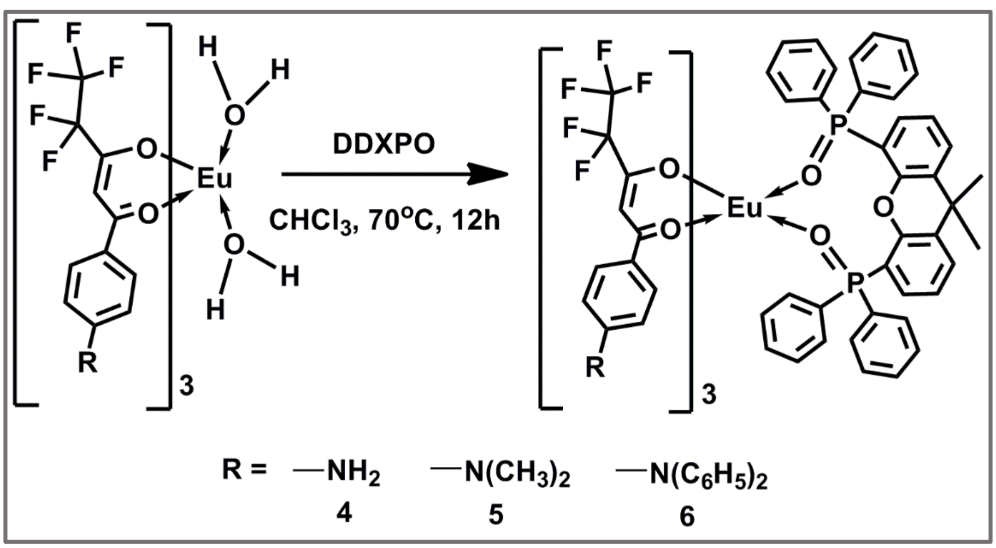

Scheme 2.3. Synthesis of ternary Eu^{3+} complexes.

2.3.6. Synthesis of $Eu(DPAPFP)_3(DDXPO)$-gel [EuC-Gel]

Tetraethyl orthosilicate (TEOS) was first mixed with ethanol, and then HCl-acidified water (pH = 2) was added to the above mixture under magnetic stirring to initiate the hydrolysis and condensation reaction. The molar ratio of TEOS/ethanol/H_2O

was maintained at 1 : 4 : 4. A transparent sol was obtained. After stirring for 3 h, an *N*,*N*-dimethylformamide (DMF) solution containing an appropriate amount of the ternary complex Eu(DPAPFP)$_3$(DDXPO) (the mass ratio of Eu^{3+} complex (**6**)/SiO_2 was 3 : 10) was added to the sol. The mixture was stirred at room temperature for 4 h. The gel was allowed to stand for 5 days and then dried at 45 °C. The gel was collected as monolithic bulks and ground into powdered material for the photophysical studies.

2.3.7. Synthesis of polymer-Eu(DPAPFP)$_3$(DDXPO)-gel (EuC-PMMA-Gel)

Similar to the EuC-Gel preparation, TEOS was first mixed with ethanol. Then HCl-acidified water (pH = 2) was added to start the hydrolysis and condensation reaction. The molar ratio of TEOS/ethanol/H_2O was 1 : 4 : 4. After stirring for 3 h, a DMF solution containing the complex Eu(DPAPFP)$_3$(DDXPO) and a polymer (PMMA) were added to the sol. The mass ratio of Eu^{3+}complex/PMMA/SiO_2 was 3 : 4 : 10. The mixture was stirred for 4 h at room temperature to make sure uniform mixing and complete hydrolysis, and then placed in a sealed container, which was kept at 45 °C until the precursor solution was converted into a monolithic gel and ground into powdered material for the photophysical studies.

2.4. Results and discussion

2.4.1. Synthesis and characterization of lanthanide complexes

Scheme 2.1 summarizes the protocols used for the synthesis of various *β*-diketonates that are used in the present study. The *β*-diketonates (HAPFP, HDMAPFP and HDPAPFP) were obtained as yellow solids in 60–85% yields by Claisen condensation of the corresponding ketones with ethyl pentafluoropropionate in the presence of a strong base, NaH. Detailed characterization of the synthesized ligands was performed by ^{1}H NMR, $^{13}C\{^{1}H\}$ NMR, $^{31}P\{^{1}H\}$ NMR, FT-IR and mass spectroscopic (ESI-MS) methods, as well as by elemental analysis. ^{1}H NMR analysis shows that the β-diketonate compounds mainly exist as enol form in deuterated chloroform solutions. In the ^{1}H NMR spectrum, a broad peak around δ 15 ppm is observed which corresponding to enolic –OH. Further, the appearance of methyne protons (-CH) as a singlet at ~6.5 ppm (δ) confirms the existence of the ligand in enolic form. The chelating ligand 4,5-bis(diphenylphosphino)-9,9-dimethylxanthene oxide (DDXPO) was synthesized according to the literature reports.[5e,f] The synthesis procedures for the Ln^{3+} (Eu^{3+} and Gd^{3+}) complexes are depicted in Schemes 2.2 and 2.3, respectively. The lanthanide complexes were characterized by FT-IR, MALDI-TOF and elemental analysis. The elemental analysis and MALDI-TOF studies of Ln^{3+} complexes (**1–9**) revealed that the central Ln^{3+} ion is coordinated to three β-diketonate ligands. In the case of ternary complexes (**4–6**), one molecule of the bidentate phosphine oxide, DDXPO, is also present in the coordination sphere, which was confirmed by FT-IR analysis. The shift in the P=O stretching frequency of DDXPO from 1190 cm^{-1} to 1179 cm^{-1} in ternary complexes **4–6** confirms the participation of phosphoryl oxygen in complex formation with the metal ion. It has been further confirmed from the $^{31}P\{^{1}H\}$ NMR spectra of complexes **4–6** that the P=O resonances are shifted upfield compared to the free ligand, indicating the involvement of phosphoryl oxygen in the coordination with the Eu^{3+} ion. The broad absorption band noted in the region 3000–3500 cm^{-1} of the FT-IR spectra of complexes (**1–3** and **7–9**) points to the existence of water molecules in the coordination sphere. On the other hand, the absence of this broad band in complexes **4–6** suggested that the water molecules have been displaced successfully by the chelating phosphine oxide ligand. The carbonyl stretching frequency of the *β*-diketonate ligands, HAPFP (1703 cm^{-1}), HDMAPFP (1586 cm^{-1}), and HDPAPFP (1609 cm^{-1}), is shifted to higher wave numbers in **1–9** (1712 cm^{-1} in **1**; 1594 cm^{-1} in **2**; 1614 cm^{-1} in **3**; 1713 cm^{-1} in **4**; 1596 cm^{-1} in **5**; 1622 cm^{-1} in **6**, 1711 cm^{-1} in **7**; 1595 cm^{-1} in **8** and 1615 cm^{-1} in **9**), thus confirming the coordination of the carbonyl oxygen to the Ln^{3+} ions.

The thermal behavior of the Ln^{3+} complexes was investigated by means of thermogravimetric analysis (TGA) under a nitrogen atmosphere, and the results are given in Figures 2.2, 2.3 and 2.4. It is clear from the thermogravimetric analysis data that complexes **1–3** and **7–9** undergo a mass loss of about 3% in the first step (90–140 °C), which corresponds to the elimination of the coordinated water molecules. On the other hand, complexes **4–6** are more stable than the precursor samples **1–3** and do not show decomposition up to 250 °C. The total weight loss that occurred in the thermal analysis of all these complexes is much higher than the calculated values for the non-volatile lanthanide(III) oxide, indicating the partial sublimation of these complexes under atmospheric pressure, which is commonly observed in the case of fluorinated *β*-diketonate complexes.[5f]

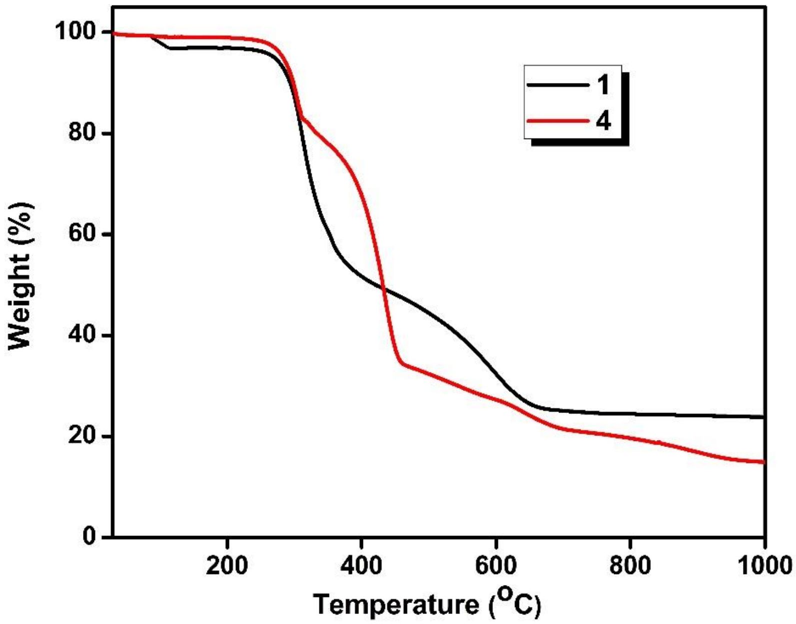

Figure 2.2. Thermogravimetric curves for Eu^{3+} complexes **1** and **4**.

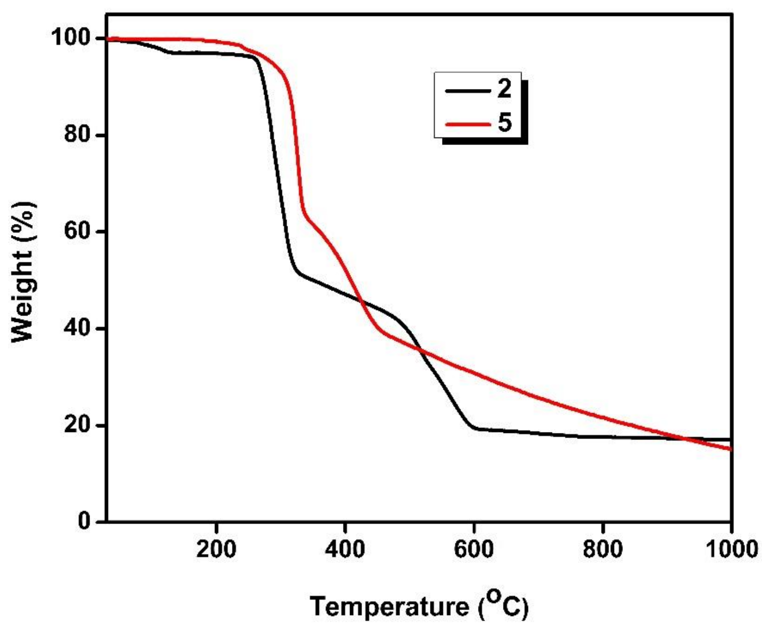

Figure 2.3. Thermogravimetric curves for Eu^{3+} complexes **2** and **5**.

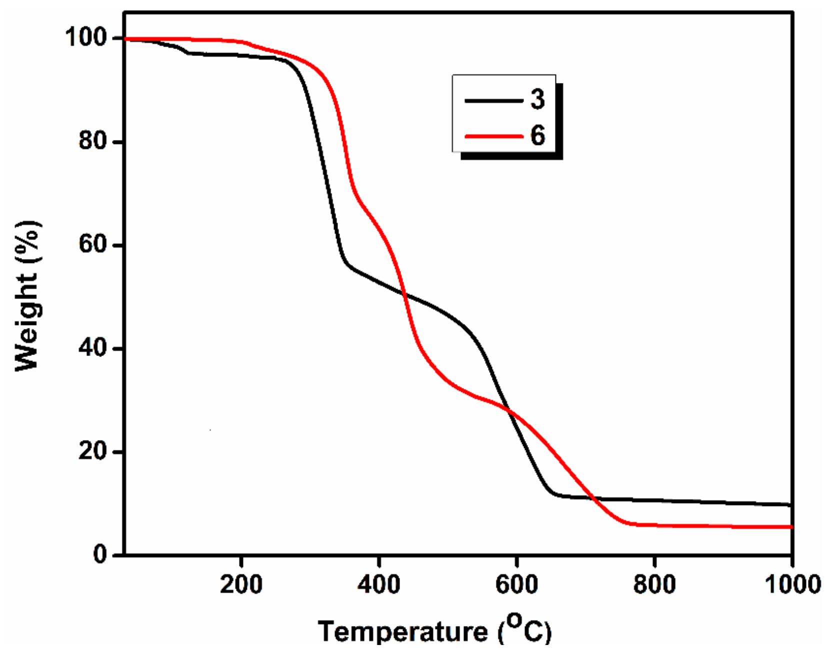

Figure 2.4. Thermogravimetric curves for Ln^{3+} complexes **3** and **6**.

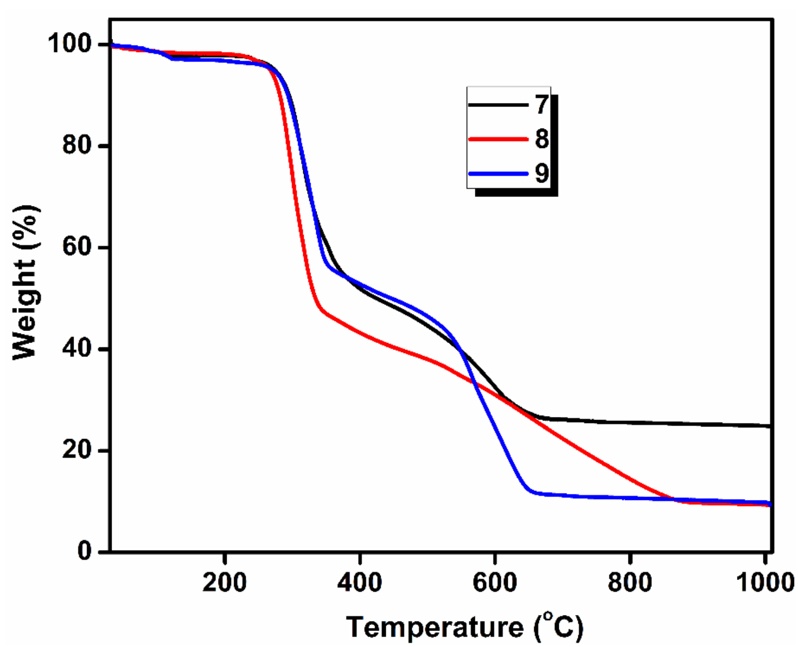

Figure 2.5. Thermogravimetric curves for Gd^{3+} complexes **7-9**.

2.4.2. Electronic spectra of the aminophenyl based β-diketonate ligands and their corresponding Eu^{3+} complexes (1–6)

The absorption spectra of the free ligands and the corresponding Eu^{3+} complexes (**1–6**) have been recorded in THF solution ($c = 5 \times 10^{-6}$ M) at 298 K and are depicted in Figure 2.6 and 2.7, respectively. The absorption profiles of the Eu^{3+} complexes in THF solution are found to be similar to that of the ligands, indicating that the singlet excited state of the ligand is not significantly affected by complexation to the Eu^{3+} ion. The main absorption band of all the β-diketonate ligands (singlet–singlet n–π^* enolic transition: 290–380 nm in HAPFP with λ_{max} = 350 nm; 340–470 nm in HDMAPFP with λ_{max} = 420 nm; 340–490 nm in HDPAPFP with λ_{max} = 425 nm), on complexation with Eu^{3+} ions, underwent a hypsochromic shift (~10 nm in **1** and **4**; ~35–45 nm in **2** and **5**; ~38–45 nm in **3** and **6**), while the short wavelength band (π–π^* transition of the aromatic moiety of the β-diketonate ligand: 250–305 nm in **1** and **4**; 275–325 nm in **2** and **5**; 275–340 nm in **3** and **6**) remains unaffected. This indicates that the electron density on the diketonate moiety has been perturbed by the imposed negative charge of deprotonation and the presence of a Lewis acidic metal centre, while the aromatic part retains the same strength.[5f,18] The electronic transitions of the aromatic moiety of the β-diketonate ligand (peak at *ca.* 250–320 nm) and the chelated phosphine oxide (peak at *ca.* 250–300 nm) units are overlapped. The presence of the ancillary ligand DDXPO not only enhances the absorption intensity but also satisfies the high coordination number of the central Eu^{3+} ion and thus improves the coordination and thermal stabilities of ternary complexes. The extinction coefficients (Table 2.1) of complexes (**1–6**) are about three times higher than that of the free ligand, in line with the formation of 3 : 1 (ligand : metal). These features point to the ligand being an adequate light-harvesting chromophore for the sensitization of Eu^{3+} luminescence.[5a–g,8]

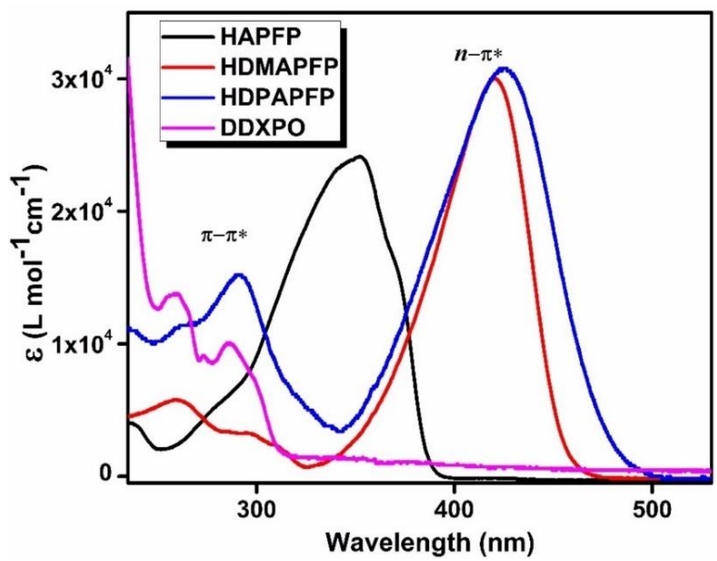

Figure 2.6. UV-visible absorption spectra of the ligands HAPFP, HDMAPFP, HDPAPFP and DDXPO in THF ($c = 5 \times 10^{-6}$ M).

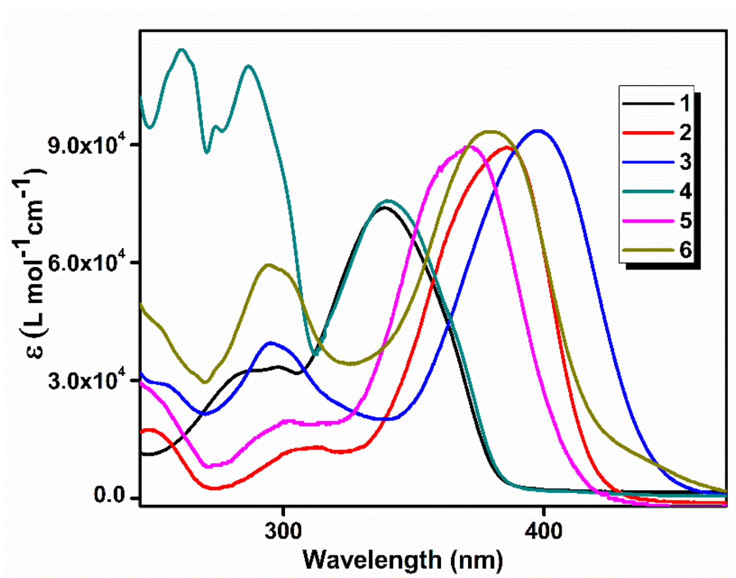

Figure 2.7. UV-visible absorption spectra of complexes **1-6** in THF ($c = 5 \times 10^{-6}$ M).

Table 2.1 Molar absorption coefficient for the *β*-diketonate ligands and their corresponding Eu^{3+} complexes

Compounds		λ_{max} (nm)	ε (L mol^{-1} cm^{-1})
HAPFP		350	2.40×10^4
HDMAPFP		420	2.96×10^4
HDPAPFP		425	3.08×10^4
$Eu(APFP)_3(H_2O)_2$	(**1**)	340	7.30×10^4
$Eu(DMAPFP)_3(H_2O)_2$	(**2**)	385	8.91×10^4
$Eu(DPAPFP)_3(H_2O)_2$	(**3**)	398	9.32×10^4
$Eu(APFP)_3(DDXPO)$	(**4**)	340	7.45×10^4
$Eu(DMAPFP)_3(DDXPO)$	(**5**)	375	8.90×10^4
$Eu(DPAPFP)_3(DDXPO)$	(**6**)	380	9.28×10^4

2.4.3. Solid-state photophysical properties of Eu^{3+} complexes 1–6

The solid-state normalized excitation spectra of the Eu^{3+} binary (**1–3**) and ternary complexes (**4–6**) recorded at 298 K are displayed in Figures 2.8 and 2.9, respectively. The excitation profiles were recorded by monitoring the intense $^5D_0 \rightarrow {}^7F_2$ (612 nm) transition of the Eu^{3+} ion. The excitation spectra of compounds (**1–6**) exhibit a broad band between 250 and 500 nm, which is attributable to the π–π^* transition of the coordinated ligands. The absence of any absorption bands due to the f–f transitions of the Eu^{3+} ion proves that the luminescence sensitization *via* excitation of the ligand is effective. The replacement of hydrogen ions in the aminophenyl based *β*-diketonate ligand with highly conjugated phenyl moieties significantly influences the π-conjugation in the complex molecules of the Eu^{3+} (**3** and **6**) and shifts the excitation window to the visible region (λ_{exc} = 400 nm), with important applications in biomedical analysis and lighting devices.[1–4] The introduction of *N*-phenyl substituents into the aminophenyl based β-diketonate ligand results in considerable bathochromic shifts in the excitation wavelength (~30 nm in **3** and **6**), suggesting substantial interactions between the *N*-phenyl and aminophenyl β-diketonate moieties. Indeed, it has been suggested, for triphenylamine and its derivatives, that there is a strong conjugation between the nitrogen lone pair electrons and the phenyl π-electrons and that the whole molecule is a new chromophore with characteristic absorption and excitation profiles.[10b,19] Here the resonance effect plays a major role compared to the electron donating effect in shifting the excitation maximum. On the other hand, the presence of an electron-donating dimethylamino group in Eu^{3+} complexes **2** and **5** moderately red shifted the excitation window in the UV region (λ_{exc} = 380 nm) as compared to the parent Eu^{3+} complexes **1** and **4** (λ_{exc} = 370 nm).[18a] The donating capacity can be described by the Hammett substituent constant, σ_p, which represents a situation where the substituent is directly attached with the reaction center in an electron demanding state. The Hammett constants, σ_p = −0.83 for $N(CH_3)_2$ and σ_p = −0.66 for NH_2, clearly explain the observed behaviour.[20]

The ambient-temperature emission spectra of Eu^{3+} complexes **1–6** excited at their corresponding excitation maxima (λ_{exc} = 370 nm for complexes **1** and **4**; λ_{exc} = 380 nm for complexes **2** and **5**; λ_{exc} = 400 nm for complexes **3** and **6**) exhibit characteristic narrow emission bands arising from the intra-configurational $^5D_0 \rightarrow {}^7F_J$ (J = 0–4) transitions of the Eu^{3+} ion (Figure 2.10). No ligand-based emission is noted in the region 400–550 nm, indicating an efficient ligand-to-metal energy transfer process. The five narrow emission peaks centered at 579, 592, 612, 652, and 701 nm are assigned to $^5D_0 \rightarrow {}^7F_0$, $^5D_0 \rightarrow {}^7F_1$, $^5D_0 \rightarrow {}^7F_2$, $^5D_0 \rightarrow {}^7F_3$ and $^5D_0 \rightarrow {}^7F_4$ transitions, respectively. Among the peaks, the intense $^5D_0 \rightarrow {}^7F_2$ peak points to a highly polarizable chemical environment around the Eu^{3+} ion and is responsible for the red emission.[5,8,21] Moreover, the presence of single and sharp peaks in the region of the $^5D_0 \rightarrow {}^7F_0$ at 579 nm indicates the existence of a single chemical environment around the Eu^{3+} ion of point group symmetry C_s, C_n or C_{nv}.[5,8,22] It can be seen from the emission spectra that the luminescence intensity of the ternary complexes (**4–6**) were significantly enhanced (7–12 fold) as compared to the precursor complexes (**1–3**) by the displacement of water molecules from the coordination sphere by the rigid chelating phosphine oxide, DDXPO.

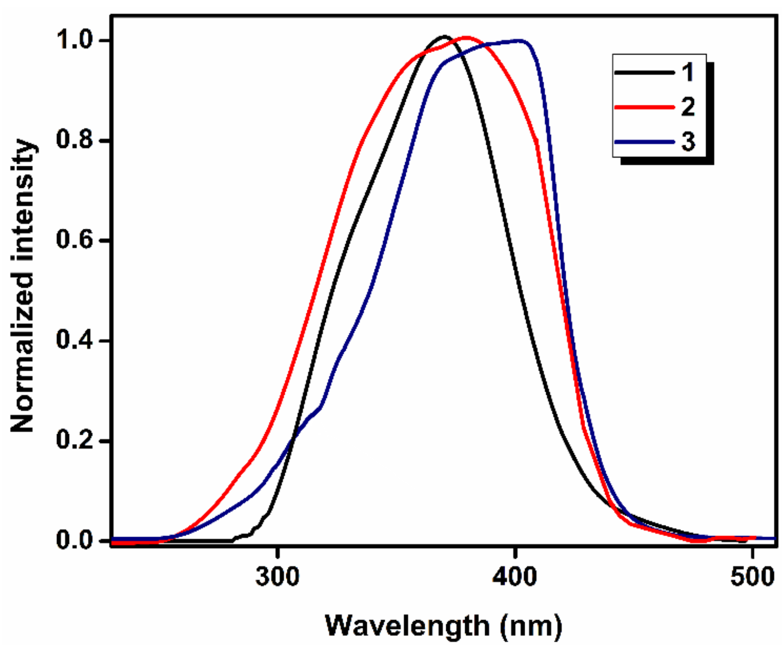

Figure 2.8. Normalized excitation spectra of Eu^{3+} binary complexes **1-3** in solid state.

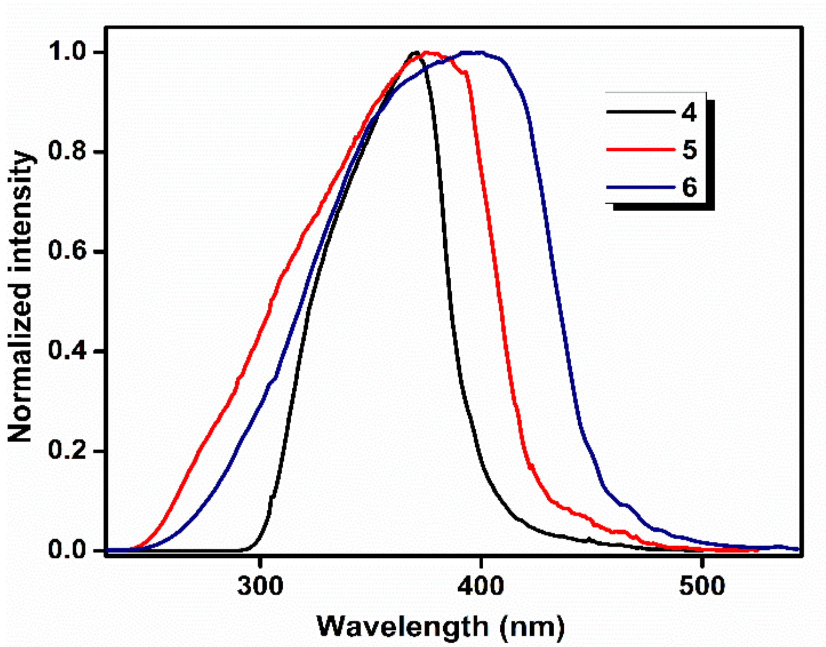

Figure 2.9. Normalized excitation spectra of Eu^{3+} ternary complexes **4-6** in solid state.

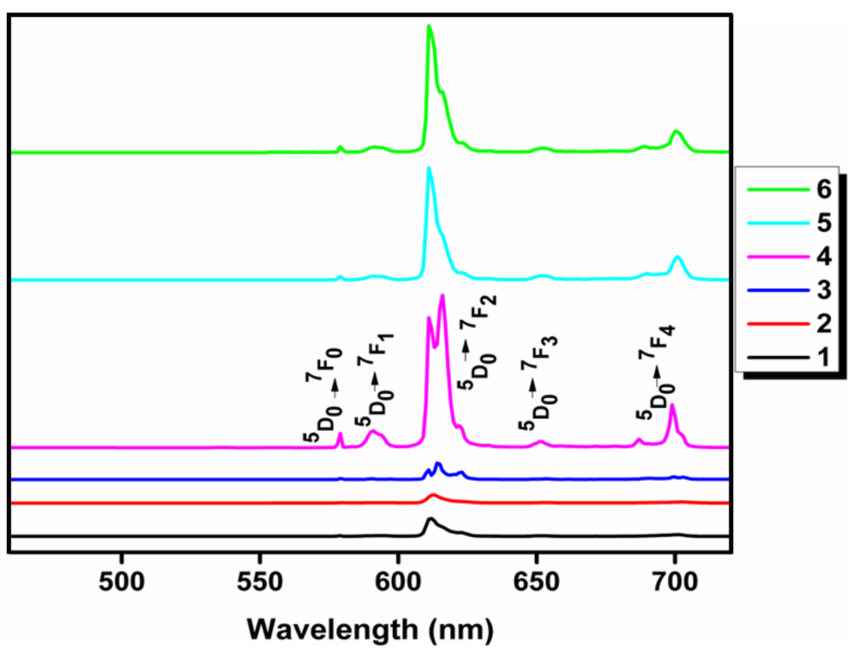

Figure 2.10. 298 K emission spectra of Eu^{3+} complexes **1-6** in solid state.

The luminescence decay times (τ_{obs}) for Eu^{3+}–β-diketonate complexes (**1–6**) were measured at room temperature using an excitation wavelength that maximizes the Eu^{3+} emission intensity and were monitored by the most intense emission line at 612 nm. The lifetime profiles for all the complexes fitted with single exponentials, thus indicating the presence of only one emissive Eu^{3+} centre. Typical decay profiles for complexes **1–6** are displayed in Figures 2.11, 2.12 and 2.13, respectively. The corresponding lifetime values are summarized in Table 2.2. The shorter $^5D_0$ lifetimes noted for Eu^{3+} complexes **1–3** may be due to the dominant non-radiative decay channels associated with vibronic coupling on account of the presence of water molecules in the coordination spheres of these complexes.[5,8,23] These values are essentially temperature dependent, with τ_{obs} (at 77 K, τ_{obs} = 362, 422 and 339 μs in **1–3**, respectively) showing approximately 2–4 fold enhancement in the case of complexes **1–3**, while going from 298 to 77 K, thereby reflecting the presence of thermally activated deactivation processes. This effect has been well documented for several other hydrated Eu^{3+}–β-diketonate complexes.[8,24] On the other hand, the lifetime values of complexes **4–6** have been significantly enhanced (3–5 times) as compared to their corresponding binary complexes. This may be due to the dramatic decrease of non-radiative decay rates as compared to their precursor complexes. However, the lifetime values of the ternary complexes (**4–6**) are almost independent of temperature (τ_{obs} = 551 μs at 298 K; 578 μs in 77 K).

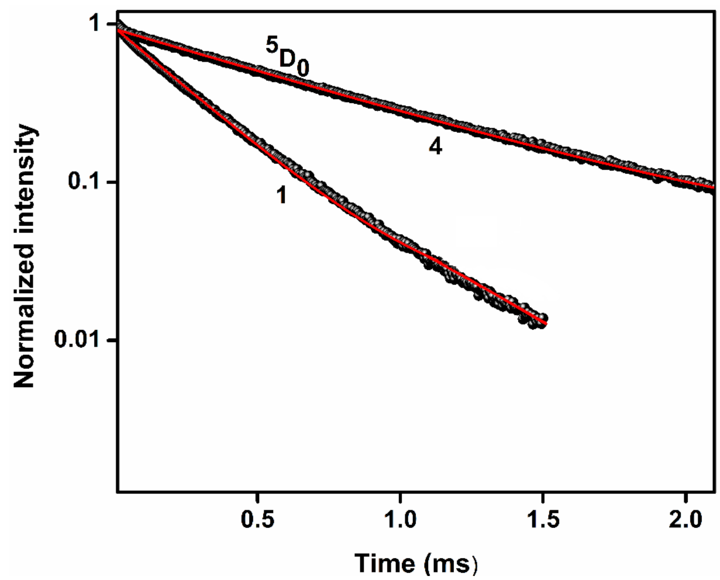

Figure 2.11 $^5D_0$ decay profiles for complexes **1** and **4** (solid-state) where emission monitored around 612 nm. The straight lines are the best fits (r^2 = 0.999) considering single-exponential behavior.

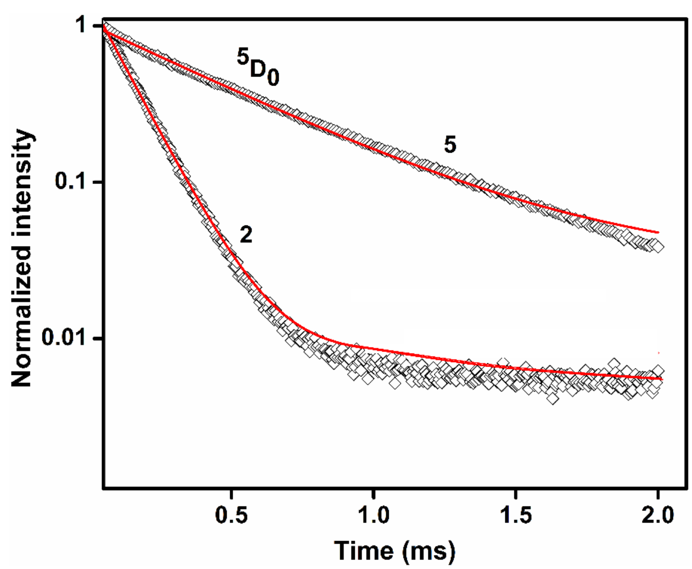

Figure 2.12. $^5D_0$ decay profiles for complexes **2** and **5** (solid-state) where emission monitored around 612 nm. The straight lines are the best fits (r^2 = 0.999) considering single-exponential behavior.

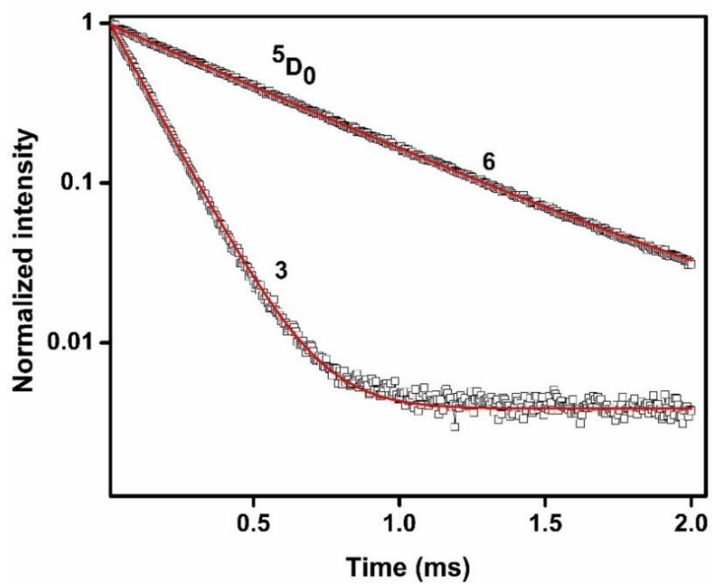

Figure 2.13. $^5D_0$ decay profiles for complexes **3** and **6** (solid-state) where emission monitored around 612 nm. The straight lines are the best fits (r^2 = 0.999) considering single-exponential behavior**.**

In order to quantify the ability of the ligands designed to sensitize the luminescence of Eu^{3+}, and to draw conclusions about the relationship between the structure and the photophysical properties, it was appropriate to analyze the emission in terms of eqn (1), where $\Phi_{overall}$ and Φ_{Ln} represent the ligand-sensitized and intrinsic luminescence quantum yields of Eu^{3+}; Φ_{sens} represents the efficiency of the ligand-to-metal energy transfer and τ_{obs}/τ_{rad} are the observed and the radiative lifetimes of Eu^{3+} ($^5D_0$):[4b–e,2]

$$\Phi_{overall} = \Phi_{sens} \times \Phi_{Ln} = \Phi_{sens} \times (\tau_{obs}/\tau_{rad}) \qquad (1)$$

The intrinsic quantum yields of Eu^{3+} could not be determined experimentally upon direct f–f excitation because of the very low absorption intensity.[4c,e,21] Therefore, the radiative lifetimes of Eu^{3+} ($^5D_0$) have been calculated from eqn (2), where *n* represents the refractive index (1.5) of the medium. $A_{MD,0}$ is the spontaneous emission probability for the $^5D_0/^7F_1$ transition *in vacuo* (14.65 s^{-1}), and I_{tot}/I_{MD} signifies the ratio of the total integrated intensity of the corrected Eu^{3+} emission spectrum to the integrated intensity of the magnetic dipole $^5D_0/^7F_1$ transition:[25]

$$1/\tau_{rad} = A_{MD,0} \times n^3 \times (I_{tot}/I_{MD}) \qquad (2)$$

The intrinsic quantum yield for the designed Eu^{3+}–β-diketonate complexes (**1–6**) has been estimated from the ratio τ_{obs}/τ_{rad} and the pertinent values are listed in Table 2. The overall quantum yields ($\Phi_{overall}$), radiative (A_{RAD}) and non-radiative (A_{NR}) decay rates and energy transfer efficiencies (Φ_{sens}) are also presented in Table 2.2. The substitution of water molecules in $[Eu(DPAPFP)_3(H_2O)_2]$ **3** by the chelating ligand (DDXPO) leads to a 4-fold enhancement in the $^5D_0$ lifetime (129 to 551 μs) and a 13-fold enhancement in the solid state quantum yield (3 to 40%). Similarly, in the case of 1-(4-(dimethylamino)phenyl)-4,4,5,5,5-pentafluoro-3-hydroxypent-2-en-1-one based Eu^{3+} complexes, the displacement of water molecules with DDXPO in $[Eu(DMAPFP)_3(H_2O)_2]$ **2** significantly enhances the $^5D_0$ lifetime (105 to 498 μs) and overall quantum yields (1 to 25%). On the other hand, a 3-fold enhancement in the $^5D_0$ lifetime (275 to 800 μs) and a 5-fold enhancement in the overall quantum yield (12 to 60%) have been noted in Eu^{3+} complex (**4**) containing 1-(4-aminophenyl)-4,4,5,5,5-pentafluoro-3-hydroxypent-2-en-1-one β-diketonate in the presence of DDXPO.

Table 2.2. The radiative ($\boldsymbol{A}_{\mathbf{RAD}}$) and non-radiative ($\boldsymbol{A}_{\mathbf{NR}}$) decay rates, $^5D_0$ lifetime (τ_{obs}), intrinsic quantum Yield ($\boldsymbol{\Phi}_{\mathbf{Ln}}$**, %**), energy transfer efficiency ($\boldsymbol{\Phi}_{\mathbf{sens}}$**, %**), and overall quantum yield ($\boldsymbol{\Phi}_{\mathbf{overall}}$**, %**) for complexes **1-6** in the solid state

Compounds		A_{RAD} (s^{-1})	A_{NR} (s^{-1})	τ_{obs} (μs)	Φ_{Ln} (%)	Φ_{sens} (%)	$\Phi_{overall}$ (%)
$Eu(APFP)_3(H_2O)_2$	(**1**)	1082	2649	275 ± 2	29	41	12 ± 1
$Eu(DMAPFP)_3(H_2O)_2$	(**2**)	963	8667	105 ± 3	10	13	1 ± 0.1
$Eu(DPAPFP)_3(H_2O)_2$	(**3**)	1505	6416	129 ± 3	19	17	3 ± 0.3
$Eu(APFP)_3(DDXPO)$	(**4**)	786	481	800 ± 3	63	95	60 ± 6
$Eu(DMAPFP)_3(DDXPO)$	(**5**)	1189	826	498 ± 2	59	42	25 ± 2
$Eu(DPAPFP)_3(DDXPO)$	(**6**)	1152	676	551 ± 1	63	63	40 ± 4

2.4.4. Energy transfer between ligands and Eu^{3+}

To demonstrate the energy transfer process of the derived Eu^{3+} complexes, the energy levels of relevant electronic states of the newly synthesized ligands have been calculated. The singlet (S_1) energy levels of the designed β-diketonate and the chelating phosphine oxide ligands were estimated by referring to the upper wavelengths of the UV-vis absorption edges of the corresponding Gd^{3+} complexes (Figure 2.14). The pertinent S_1 levels of HAPFP, HDMAPFP, HDPAPFP and DDXPO are found to be 25000 (400 nm), 23981 (416 nm), 23148 (432 nm) and 31850 cm^{-1} (313 nm), respectively. The triplet (T_1) energy levels were calculated from the position of the highest energy band in the corresponding phosphorescence spectra of the Gd^{3+} complexes (Figure 2.14).[26] Accordingly, the T_1 of the ligands HAPFP, HDMAPFP, HDPAPFP and DDXPO were found to be 21505 (465 nm), 20833 (480 nm), 20202 (495 nm) and 23470 cm^{-1} (426 nm), respectively. All these values are entirely consistent with the above results that the replacement of hydrogen atoms with electron donating methyl or π-conjugated phenyl groups in aminophenyl based β-diketonate ligands has a profound effect on the singlet and triplet states of these ligands. The energy gaps between the Eu^{3+} core ($^5D_0 \sim 17250$ cm^{-1}) and the donor ligand's T_1 levels turned out to be 4255, 3583, 2952 and 6220 cm^{-1} for HAPFP, HDMAPFP, HDPAPFP and DDXPO, respectively. The triplet energy levels of the ligands appear at appreciably higher energy than that of the $^5D_0$ state of Eu^{3+}, thus indicating that the newly developed β-diketonate ligands can act as efficient sensitizers for the Eu^{3+} ion.[26] On the other hand, the $^5D_1$ state Eu^{3+} (18800 cm^{-1}) is found to be closer to the T_1 of HDPAPFP ($\Delta E(T_1–{}^5D_1)$ = 1402 cm^{-1}), which can lead to thermally assisted back energy transfer.[27] However, the T_1 levels of HDMAPFP and HAPFP are situated slightly above the $^5D_1$ state of Eu^{3+}. The $^5D_2$ of the Eu^{3+} emitting state (21200 cm^{-1}) is higher than the T_1 state of the β-diketonate ligands, which can lead to the thermally assisted back-energy transfer from the central core.[27] It is also noticed that the energy gaps between the S_1 and T_1 levels are 3495, 3148, 2946 and 8380 cm^{-1} for HAPFP, HDMAPFP, HDPAPFP and DDXPO, respectively. Also in the diphenylamino substituted ligand, the singlet–triplet energy gap is lowered compared to the other ligands as explained before. According to Reinhoudt's empirical rule,[6] the intersystem crossing process becomes effective when $\Delta E(S_1–T_1)$ is around 5000 cm^{-1} and hence the intersystem crossing processes are efficient for these ligands. Based on the above observations the photoluminescence mechanism for the derived Eu^{3+} complexes is proposed to involve a ligand sensitized luminescence process (antenna effect).[5,8,28] The typical energy level diagram for complex **6** and the plausible energy transfer pathways are shown in Figure 2.15.

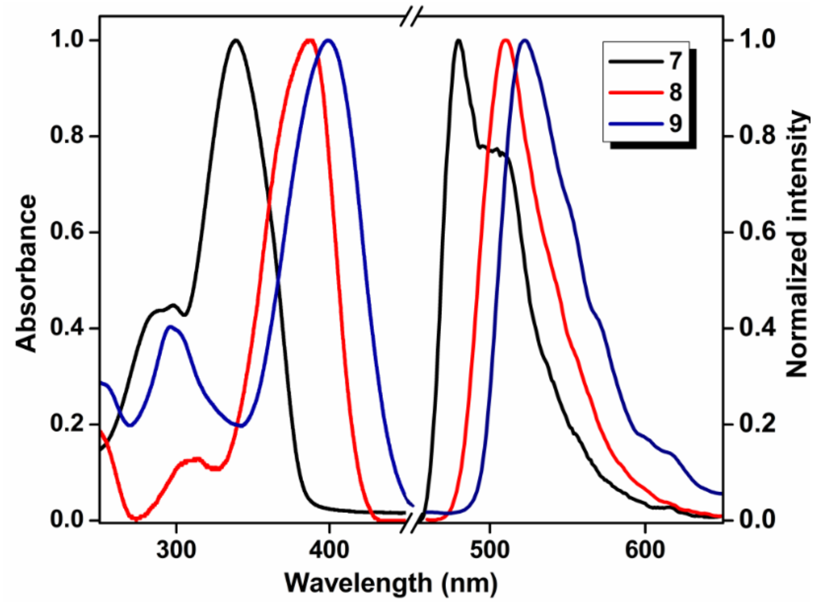

Figure 2.14. UV-vis absorption spectra at 298 K (left), and 77 K phosphorescence spectra (right) of the complexes **7-9** in THF (c = 5 × 10^{-6} M).

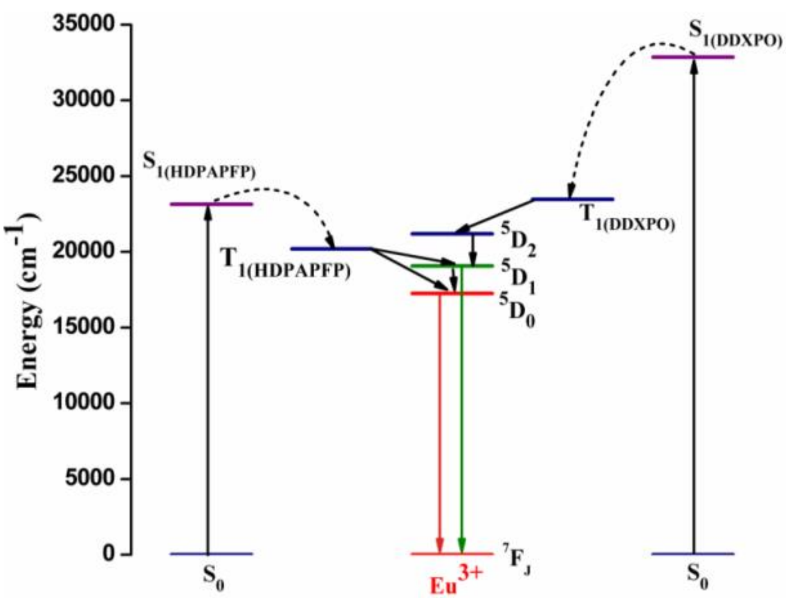

Figure 2.15. Schematic energy level diagram and energy transfer processes for the complex **6.** S_1 represents the first excited singlet state and T_1 represents the first excited triplet state.

2.4.5. Photostability of the $Eu(DPAPFP)_3DDXPO$ complex

The photostability of the visible light sensitized Eu^{3+} complex **6** was investigated by measuring the luminescence intensity at 612 nm excited at 400 nm at definite time intervals (10 min) for 3 h and the results are shown in Figure 2.16. The results demonstrated that the luminescence intensity of the complex is almost the same even after 3 h of irradiation, indicating the photostability of the Eu^{3+}complex.

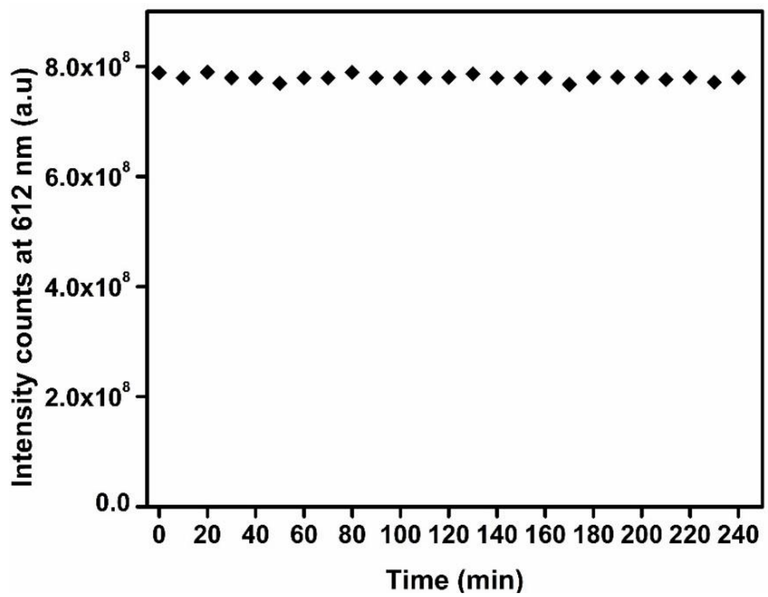

Figure 2.16. Photoluminescence intensity of the complex $Eu(DPAPFP)_3DDXPO$ in solid state as a function of irradiation time.

2.5. Synthesis, characterization and luminescence studies of the hybrid materials EuC-Gel and EuC-PMMA-Gel

The photographs of the designed hybrid gel materials are displayed in Figure 2.17. The FT-IR spectra of the $Eu(DPAPFP)_3(DDXPO)$ doped hybrid materials EuC-Gel and EuC-PMMA-Gel are shown in Figure 2.18.

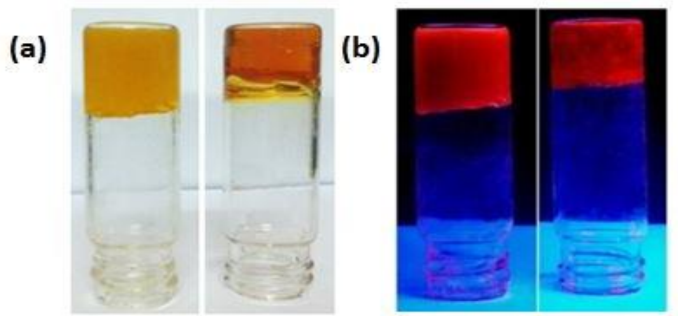

Figure 2.17. Photographs of the EuC-PMMA-Gel (left) and EuC-Gel (right) before (a) and after (b) UV irradiation.

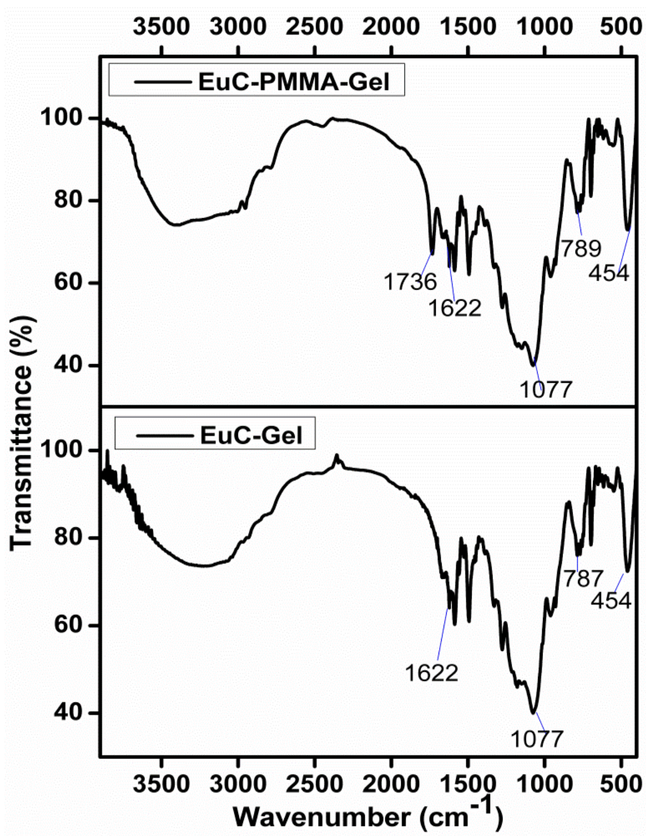

Figure 2.18. FT-IR spectra of the EuC-Gel and EuC-PMMA-Gel.

The formation of the Si–O–Si framework in the hybrid materials was confirmed by the peaks observed around 1077 cm^{-1} (ν_{as}, Si–O–Si), 787 cm^{-1} (ν_{s}, Si–O–Si) and 454 cm^{-1} (δ, Si–O–Si) and in both the hybrid materials which are characteristic of the trialkoxysilyl function.[13d,f,29] The absorption band noted at 1622 cm^{-1} for both the gels can be assigned to the C=O group vibrations of the ligand. A new band at 1736 cm^{-1} noted in the IR spectra of EuC-PMMA-Gel, ascribed to the C=O vibrations of PMMA. The above results suggest the incorporation of the polymer into hybrid material, which may bring small changes *via* coordinating with the central Eu^{3+} ions.

The XRD patterns from 10 to 70° of the hybrid materials are shown in Figure 2.19, showing that the developed hybrid materials are amorphous. The broad peaks noted in both the hybrid materials centered at 22.98° and 23.04° can be attributed to the siliceous backbone of the hybrids.[13a,29e,30-31] Further, the absence of any crystalline regions in these hybrid materials correlates with the presence of host inorganic networks. The above results clearly indicate that the hybrid materials still hold disordered sequences even after doping into the PMMA matrix, although the polymeric carbon chains of the polymers are essentially regularly ordered.

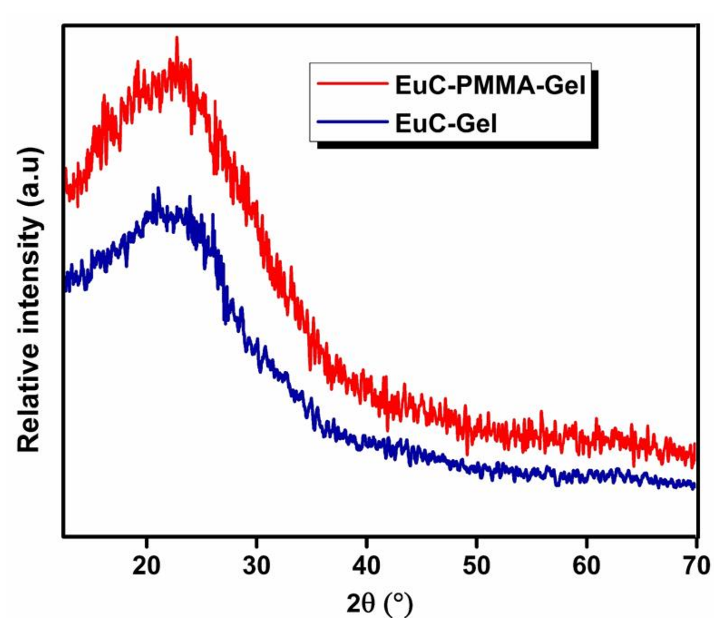

Figure 2.19. XRD patterns of the EuC-Gel and EuC-PMMA-Gel.

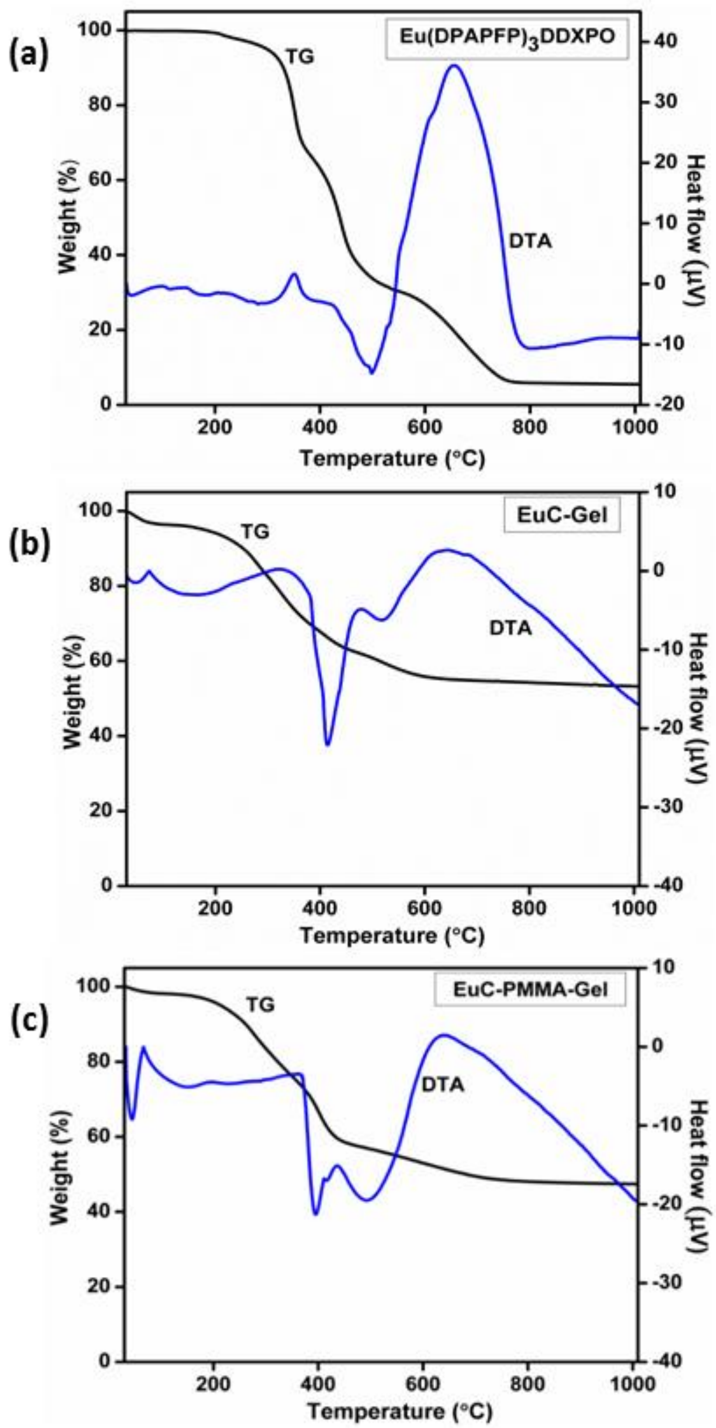

Figure 2.20. TG/DTA curves for (a) $Eu(DPAPFP)_3DDXPO$, (b) EuC-Gel and (c) EuC-PMMA-Gel.

The thermal stabilities of EuC-Gel and EuC-PMMA-Gel developed hybrid materials were investigated by TG and DTA measurements and the results are given in Figure 2.20. The DTA curve shows that the thermal stability of the Eu^{3+} ternary complex [353 °C for $Eu(DPAPFP)_3(DDXPO)$ decomposition] has been enhanced after incorporating into the hybrid material [414 °C in EuC-Gel decomposition]. It can be noted from the TG curve of EuC-PMMA-Gel that PMMA began to decompose at 398 °C. Further, when the temperature reached 445 °C, the polymer PMMA had departed from the hybrid material.[29e] The results revealed that the thermal stability of the hybrid material has been enhanced after loading into the hybrid material.

The solid-state absorption spectra of the complex ($Eu(DPAPFP)_3DDXPO$) and the hybrid materials are displayed in Figure 2.21. Compared to the Eu^{3+} ternary complex, a red-shift of the major electronic transition (from 439 to 447 nm) occurs in hybrid materials, which indicates that the electronic distributions of the system have changed when the complexes are embedded in the matrixes and the perturbation is induced by the silanol groups in the hybrid materials.

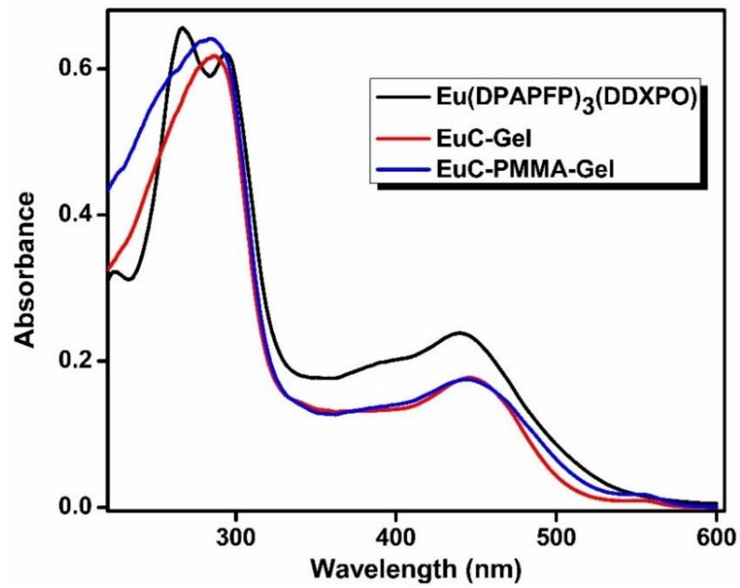

Figure 2.21. UV-visible absorption spectra of the gels (solid).

The excitation and emission spectra of the isolated hybrid materials as solids at room temperature are illustrated in Figure 2.22. The excitation spectra of the hybrid materials, which were obtained by monitoring at 612 nm, exhibit a broad excitation band between 300 and 515 nm. This band can be assigned to the π–π* electronic transition of the ligands. In the emission spectra of the hybrid materials, only characteristic emissions of Eu^{3+} ions are noted, which indicates that the energy transfer from the ligands to the central Eu^{3+} ions is efficient. The hybrid materials showed characteristic narrow band emissions of Eu^{3+} corresponding to the $^5D_0 \rightarrow {^7F_J}$ (J = 0–4) transitions. The five expected peaks of the luminescence spectra are well resolved. The content of the Eu^{3+} complex in hybrid materials and its relative luminescence intensities are listed in Table 2.3. It is interesting to note that the complex of unit mass in the silica/polymer matrix is found to be superior to that of the corresponding pure complex. The shortening of lifetimes (τ_{obs} = 305 μs in EuC-Gel and 361 μs in EuC-PMMA-Gel) in the hybrid materials has been noticed as compared to the precursor Eu^{3+} complex (τ_{obs} = 551 μs) (Figure 2.23). This might be due to the quenching of abundant O–H oscillators on the silica matrix surface to the absorbed complex, which can be clearly seen from the high values of nonradiative decay rates of the hybrid materials (A_{NR}).[29,32] The overall quantum efficiencies of these hybrid materials have been significantly decreased due to the presence of high frequency oscillators in the hybrid materials. This might be due to the quenching of abundant O–H oscillators on the silica matrix surface to the absorbed complex, which can be clearly seen from the high values of non-radiative decay rates of the hybrid materials (A_{NR}).[29,32] The overall quantum efficiencies of these hybrid materials have been significantly decreased due to the presence of high frequency oscillators in the hybrid materials.

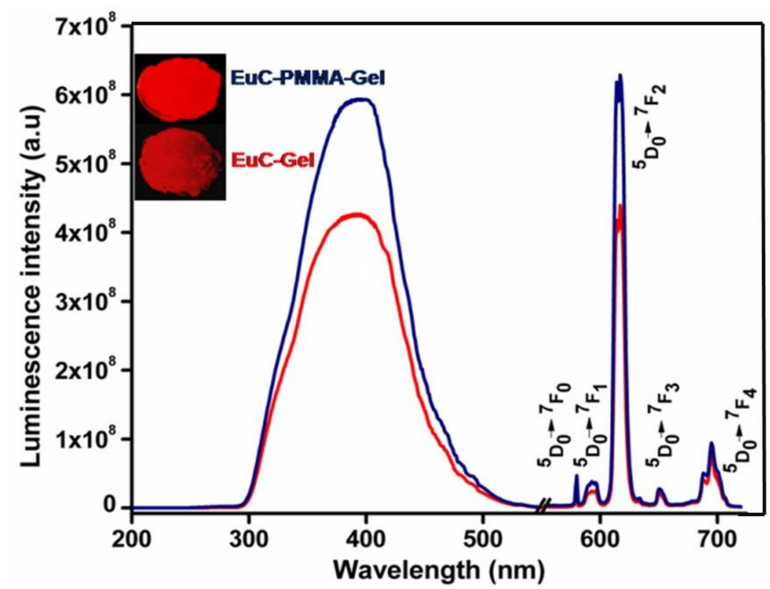

Figure 2.22. Room temperature excitation and emission spectra of hybrid materials, EuC-Gel and EuC-PMMA-Gel (Inset photographs show the gels coated on a glass plate).

Table 2.3. Luminescence intensities, content of the Eu^{3+} complex, radiative-nonradiative decay rates and the photoluminescence quantum yields of $Eu(DPAPFP)_3DDXPO$, EuC-PMMA-Gel and EuC-Gel samples

Compounds	**$Eu(DPAPFP)_3DDXPO$**	**EuC-Gel**	**EuC-PMMA-Gel**
Content of the complex **6** (wt %)	100	23.8	18.5
Relative intensity of $^5D_0 \rightarrow {}^7F_2$	8.02×10^8	4.37×10^8	6.31×10^8
Unit mass luminescence intensity	8.02×10^8	1.84×10^9	3.41×10^9
A_{RAD} (s^{-1})	1152	1031	953
A_{NR} (s^{-1})	676	2294	1849
τ_{obs} (μs)	551 ± 1	305 ± 2	361 ± 2
Φ_{Ln} (%)	63	31	34
Φ_{sens} (%)	63	56	63
$\Phi_{overall}$ (%)	40 ± 4	18 ± 2	22 ± 2

In addition, in the present work, EuC-PMMA-Gel hybrid material has been used as a phosphor to fabricate LED after coating onto a 400 nm emitting InGaN chip and the photoluminescence properties have been investigated (Figure 2.24). The LED fabricated with a 400 nm emitting chip exhibited a strong red-emission. Thus, the results indicate that EuC-PMMA-Gel hybrid material is an interesting red-emitting material excited by blue-light, making it a potential candidate for many photonic applications without using UV radiation for excitation.[7b]

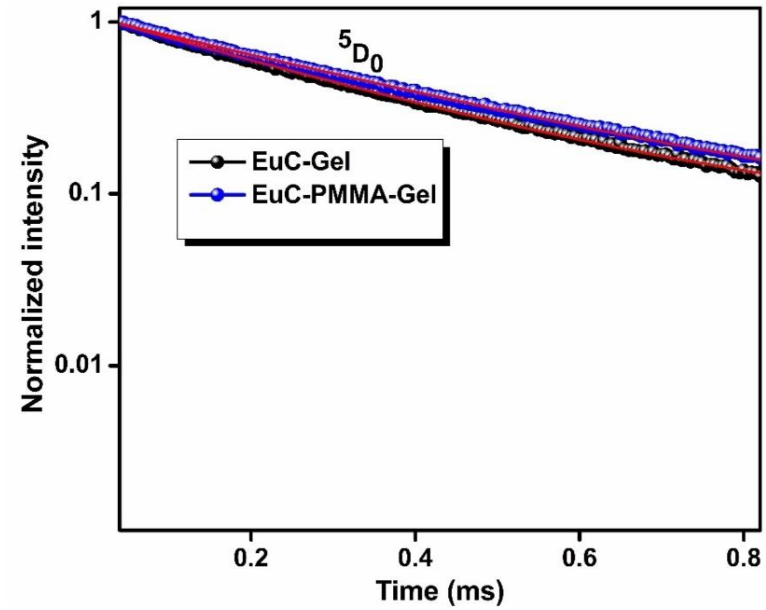

Figure 2.23. $^5D_0$ decay profiles for EuC-Gel and EuC-PMMA-Gel (solid-state) where emission monitored around 612 nm. The straight lines are the best fits (r^2 = 0.999) considering single-exponential behavior.

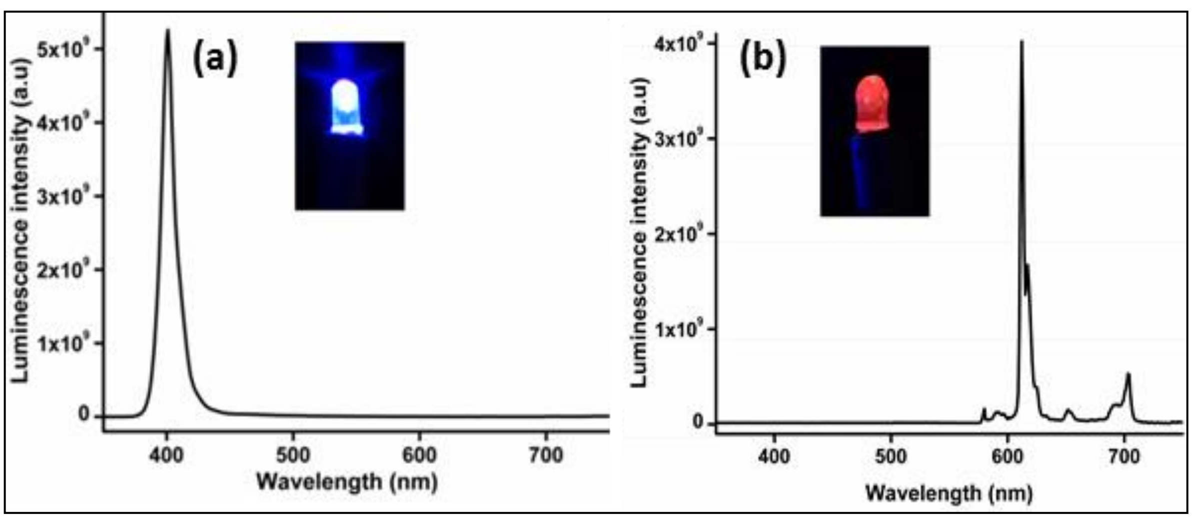

Figure 2.24. Emission spectra of the blue emitting InGaN LED (left) and EuC-PMMA-Gel coated on an InGaN chip (right). Inset: photographs of the LEDs in working state.

2.6. Conclusions

- A series of new antenna complexes of Eu^{3+} based on aminophenyl based polyfluorinated β-diketonate ligands in the absence and presence of a chelating phosphine oxide has been developed.
- Among the designed complexes, the Eu^{3+}–triphenylamine β-diketonate ternary complex exhibits intense red-emission under blue light excitation (λ_{exc} = 400 nm) with an impressive quantum yield ($\Phi_{overall}$ = 40%) and $^5D_0$ lifetime values (τ_{obs} = 551 μs). Suitably expanded π-conjugation in the complex molecules successfully red-shifted the excitation band of the Eu^{3+}–β-diketonate complexes to the visible region. Contrary to the above, the electron-donating dimethylamino group (Hammett constant: σ_p = −0.83) containing Eu^{3+}–β-diketonate complexes moderately shifted the excitation maximum in the UV region from 370 to 380 nm as compared to unsubstituted aminophenyl (Hammett constant: σ_p = −0.66) Eu^{3+} complexes.
- To improve the thermal and mechanical stability, the derived highly luminescent Eu^{3+} complex has been embedded into a hybrid silica/polymer material by the sol–gel method. The resultant hybrid material EuC-PMMA-Gel displays efficient unit mass luminescence emission (3.41×10^9) and greater thermal stability (398 °C) as compared to the precursor ternary Eu^{3+} complex [unit mass luminescence emission = 8.02×10^8; thermal stability = 353 °C].
- LED developed by coating the EuC-PMMA-Gel hybrid material on InGaN LED displays bright red-emission under blue light excitation. The present results

clearly demonstrate that Eu^{3+}-triphenylamine based β-diketonate complexes may find potential applications in many optoelectronic technologies.

2.7. References

1. (a) J.-C. G. Bünzli, *Chem. Rev*., 2010, **110**, 2729; (b) M. C. Heffern, L. M. Matosziuk and T. J. Meade, *Chem. Rev.,* 2014, **114**, 4496; (c) X. Wang, H. Chang, J. Xie, B. Zhao, B. Liu, S. Xu, W. Pei, N. Ren, L. Huang and W. Huang, *Coord. Chem. Rev*., 2014, **273**, 201; (d) J.-C. G. Bünzli and S. V. Eliseeva, *Chem. Sci*., 2013, **4**, 1939.
2. (a) J. Feng and H. Zhang, *Chem. Soc. Rev.,* 2013, **42**, 387; (b) A. de Bettencourt-Dias, *Dalton Trans*., 2007, **22**, 2229; (c) L. D. Carlos, R. A. S. Ferreira, V. de Zea Bermudez, B. J.-Lopezc and P. Escribano, *Chem. Soc. Rev.,* 2011, **40**, 536.
3. (a) S. V. Eliseeva and J.-C. G. Bünzli, *Chem. Soc. Rev*., 2010, **39**, 189; (b) S. V. Eliseeva and J.-C. G. Bünzli, *New J. Chem*., 2011, **35**, 1165; (c) L. D. Carlos, R. A. S. Ferreira, V. Z. Bermudez and S. J. L. Ribeiro, *Adv. Mater*., 2009, **21**, 509.
4. (a) C. P. Montgomery, B. S. Murray, E. J. New, R. Pal and D. Parker, *Acc. Chem. Res*., 2009, **42**, 925; (b) L. Armelao, S. Quici, F. Barigelletti, G. Accorsi, G. Bottaro, M. Cavazzini and E. Tondello, *Coord. Chem. Rev*., 2010, **254**, 487; (c) Y. Ma and Y. Wang, *Coord. Chem. Rev*., 2010, **254**, 972; (d) K. Binnemans, *Chem. Rev*., 2009, **109**, 4283; (e) J.-C. G. Bünzli and C. Piguet, *Chem. Soc. Rev*., 2005, **34**, 1048; (f) P. P. Lima, M. M. Nolasco, F. A. A. Paz, R. A. S. Ferreira, R. L. Longo, O. L. Malta and L. D. Carlos, *Chem. Mater*., 2013, **25**, 586.
5. (a) D. B. A. Raj, S. Biju and M. L. P. Reddy, *Inorg. Chem*., 2008, **47**, 8091; (b) S. Biju, D. B. A. Raj, M. L. P. Reddy and B. M. Kariuki, *Inorg. Chem*., 2006, **45**, 10651; (c) S.

Biju, M. L. P. Reddy, A. H. Cowley and K. V. Vasudevan, *Cryst. Growth Des*., 2009, **9**, 3562; (d) S. Biju, N. Gopakumar, J.-C. G. Bünzli, R. Scopelliti, H. K. Kim and M. L. P. Reddy, *Inorg. Chem*., 2013, **52**, 8750; (e) D. B. A. Raj, B. Francis, M. L. P. Reddy, R. R. Butorac, V. M. Lynch and A. H. Cowley, *Inorg. Chem*., 2010, **49**, 9055; (f) D. B. A. Raj, S. Biju and M. L. P. Reddy, *Dalton Trans.*, 2009, **36**, 7519; (g) B. Francis, D. B. A. Raj and M. L. P. Reddy, *Dalton Trans*., 2010, **39**, 8084; (h) J. A. Fernandes, R. A. Sá Ferreira, M. Pillinger, L. D. Carlos, I. S. Goncalves, and P. J. A. R.-Claro, *Eur. J. Inorg. Chem.,* 2004, **19**, 3913; (i) L. F. Smith, B. A. Blight, H.-J. Park and S. Wang, *Inorg. Chem*., 2014, **53**, 8036; (j) J. Leng, H. Li, P. Chen, W. Sun, T. Gao and P. Yan, Dalton Trans., 2014, **43**, 12228; (k) G. Shao, H. Yu, N. Zhang, Y. He, K. Feng, X. Yang, R. Cao and M. Gong, *Phys. Chem. Chem. Phys*., 2014, **16**, 695; (l) X. Chen, P. Zhang, T. Wang, and H. Li, *Chem. Eur. J*., 2014, **20**, 2551.

6. F. J. Steemers, W. Verboom, D. N. Reinhoudt, E. B. Vander Tol and J. W. Verhoeven, *J. Am. Chem. Soc*., 1995, **117**, 9408.
7. (a) P. He, H. H. Wang, S. G. Liu, J. X. Shi, G. Wang and M. L. Gong, *Inorg. Chem*., 2009, **48**, 11382; (b) P. He, H. H. Wang, H. G. Yan, W. Hu, J. X. Shi and M. L. Gong, *Dalton Trans*., 2010, **39**, 8919; (c) J. Wu, Z. Ye, G. Wang, D. Jin, J. Yuan, Y. Guan and J. Piper, *J. Mater. Chem*., 2009, **19**, 1258; (d) J. Wu, G. Wang, D. Jin, J. Yuan, Y. Guan and J. Piper, *Chem. Commun*., 2008, 365; (e) M. Shi, C. Ding, J. Dong, H. Wang, Y. Tian and Z. Hu, Phys. *Chem. Chem. Phys*., 2009, **11**, 5119; (f) M. H. V. Werts, M. A. Duin, J. W. Hofstraat and J. W. Verhoeven, *Chem. Commun*., 1999, **9**, 799.
8. (a) M. L. P. Reddy, V. Divya and R. Pavithran, *Dalton Trans*., 2013, **42**, 15249; (b) V. Divya, R. O. Freire and M. L. P. Reddy, *Dalton Trans*., 2011, **40**, 3257; (c) V. Divya,

S. Biju, R. Luxmi Varma and M. L. P. Reddy, *J. Mater. Chem*., 2010, **20**, 5220; (d) V. Divya and M. L. P. Reddy, *J. Mater. Chem. C*., 2013, **1**, 160; (e) V. Divya, V. Sankar, K. G. Raghu and M. L. P. Reddy, *Dalton Trans*., 2013, **42**, 12317.

9. (a) R. V. Deun, P. Fias, P. Nockemann, K. V. Hecke, L. V. Meervelt, and K. Binnemans, *Inorg. Chem*., 2006, **45**, 10416; (b) C. Yang, L.-M. Fu, Y. Wang, J.-P. Zhang, W.-T. Wong, X.-C. Ai, Y.-F. Qiao, B.-S. Zou, and L.-L. Gui, *Angew. Chem. Int. Ed*., 2004, **43**, 5010; (c) F. Xue, Y. Ma, L. Fu, R. Hao, G. Shao, M. Tang, J. Zhang and Y. Wang, *Phys. Chem. Chem. Phys*., 2010, **12**, 3195; (d) M. Shi, C. Ding, J. Dong, H. Wang, Y. Tian and Z. Hu, *Phys. Chem. Chem. Phys*., 2009, **11**, 5119; (e) G. Zucchi,V. Murugesan, D. Tondelier, D. Aldakov, T. Jeon, F. Yang, P. Thuéry, M. Ephritikhine and B. Geffroy, *Inorg. Chem*., 2011, **50**, 4851.

10. (a) K. Sakanoue, M. Motoda, M. Sugimoto and S. Sakaki, *J. Phys. Chem. A*., 1999, **103**, 5551; (b) J.-S. Yang, S.-Y. Chiou, and K.-L. Liau, *J. Am. Chem. Soc*., 2002, **124**, 2518.

11. (a) L.-N. Sun, J.-Bo Yu, G.-L. Zheng, H.-J. Zhang, Q.-G. Meng, C.-Y. Peng, L.-S. Fu, F.-Y. Liu and Y.-N. Yu, *Eur. J. Inorg. Chem*., 2006, 3962; (b) A.-S. Chauvin, F. Gumy, I. Matsubayashi, Y. Hasegawa, and J.-C. G. Bünzli, *Eur. J. Inorg. Chem*., 2006, 473; (c) Y. Hasegawa, Y. Wada, S. Yanagid, J*. Photochem. Photobiol. C*., 2004, **5**, 183; (d) Y. Hasegawa, T. Ohkubo, K. Sogabe, Y. Kawamura, Y. Wada, N. Nakashima and S. Yanagida, *Angew. Chem., Int. Ed*., 2000, **39**, 357.

12. (a) S. Biju, M. L. P. Reddy, A. H. Cowley and K. V. Vasudevan, *J. Mater. Chem*., 2009, **19**, 5179; (b) S. Sivakumar and M. L. P. Reddy, *J. Mater. Chem*., 2012, **22**, 10852; (c) S. Biju, R. O. Freire, Y. Kyung Eom, R. Scopelliti, J.-C. G. Bünzli and H. K. Kim, *Inorg. Chem*., 2014, **53**, 8407; (d) R. Shunmugam and G. N. Tew, *J. Am. Chem. Soc*., 2005,

127, 13567; (e) B. Chen and J. Feng, *J. Phys. Chem. C.,* 2015, **119**, 7865; (f) W. Fan, J. Feng, S. Song, Y. Lei, L. Zhou, G. Zheng, S. Dang, S. Wang and H. Zhang, *Nanoscale.*, 2010, **2**, 2096; (g) J. Kai, D. F. Parrab and H. F. Brito, *J. Mater. Chem*., 2008, **18**, 4549; (h) O. Moudam, B. C. Rowan, M. Alamiry, P. Richardson, B. S. Richards, A. C. Jones and N. Robertson, *Chem. Commun*., 2009, 6649.

13. (a) D. Haranath, S. Mishra, A. G. Joshi, S. Sahai and V. Shanker, *Nano-Micro Lett*., 2011, **3**, 141; (b) P. P. Lima, R. A. S. Ferreira, R. O. Freire, F. A. Almeida Paz, L. Fu, S. Alves Jr, L. D. Carlos and O. L. Malta, *ChemPhysChem*., 2006, **7**, 735; (c) J. D. Mackenzie and E. P. Bescher, *Acc. Chem. Res*., 2007, **40**, 810; (d) X. Guo, H. Guo, L. Fu, H. Zhang, L. D. Carlos, R. Deng and J. Yu, *J. Photochem. Photobiol. A*., 2008, **200**, 318; (e) L. D. Carlos, R. A. Sá Ferreira, J. P. Rainho, V. de Zea Bermudez, *Adv. Funct. Mater*., 2002, **12**, 819; (f) L. N. Sun, H. J. Zhang, Q. G. Meng, F. Y. Liu, L. N. Fu, C. Y. Peng, J. B. Yu, G. L. Zheng and S. B. Wang, *J. Phys. Chem. B.*, 2005, **109**, 6174.

14. (a) D. B. A. Raj, S. Biju and M. L. P. Reddy, *J. Mater. Chem*., 2009, **19**, 7976; (b) P. Escribano, B. J.-Loṕez, J. P.-Aragó, E. Cordoncillo, B. Viana and C. Sanchez, *J. Mater. Chem*., 2008, **18**, 23; (c) B. Yan and Y.-J. Li, *J. Mater. Chem*., 2011, **21**, 18454; (d) L. Sun, W. Mai, S. Dang, Y. Qiu,W. Deng, L. Shi,W. Yanaand H. Zhang, *J. Mater. Chem*., 2012, **22**, 5121; (e) P. Lenaerts, A. Storms, J. Mullens, J. D'Haen, C. G.-Walrand, K. Binnemans, and K. Driesen, *Chem. Mater*., 2005, **17**, 5194; (f) E. DeOliveira, C. R. Neri, O. A. Serra, and A. G. S. Prado, *Chem. Mater*., 2007, **19**, 5437; (g) D. Zhang, X. Wang, Z.-an Qiao, D. Tang, Y. Liu, and Q. Huo, *J. Phys. Chem. C*., 2010, **114**, 12505.

15. (a) L. Maggini, H. Traboulsi, K. Yoosaf, J. Mohanraj, J. Wouters, O. Pietraszkiewicz, M. Pietraszkiewicz, N. Armaroliand D. Bonifazi, *Chem. Commun*., 2011, **47**, 1625;

(b) L. Maggini, J. Mohanraj, H. Traboulsi, A. Parisini, G. Accorsi, N. Armaroli and D. Bonifazi, *Chem. Eur. J.*, 2011, **17**, 8533; (c) X. Xin, M. Pietraszkiewicz, O. Pietraszkiewicz, O. Chernyayeva, T. Kalwarczyk, E. Gorecka, D. Pociecha, H. Li and R. Hołyst, *Carbon.*, 2 0 1 2, **50**, 4 3 6; (d) B. Sitharaman, S. Rajamani and Pramod, K. Avti, *Chem. Commun*., 2011, **47**, 1607; (e) C. Zhao, Y. Song, K. Qu, J. Ren, and X. Qu, *Chem. Mater*., 2010, **22**, 5718; (f) J. Mohanraj and N. Armaroli, *J. Phys. Chem. Lett*., 2013, **4**, 767; (g) L. Maggini, F. M. Toma, L. Feruglio, J. M. Malicka, T. D. Ros, N. Armaroli, M. Prato and D. Bonifazi, *Chem.–Eur. J.*, 2012, **18**, 5889.

16. (a) J. C. De Mello, H. F. Wittmann and R. H. Friend, *Adv. Mater.*, 1997, **9**, 230; (b) L.-O. Pålsson and A. P. Monkman, *Adv. Mater.*, 2002, **14**, 757; (c) B. K. Shah, D. C. Neckers, J. Shi, E. W. Forsythe and D. Morton, *Chem. Mater.*, 2006, **18**, 603.
17. (a) M. Cölle, J. Gmeiner, W. Milius, H. Hillebrecht and W. Brütting, *Adv. Funct. Mater.*, 2003, **13**, 108; (b) N. S. Saleesh Kumar, S. Varghese, N. P. Rath and S. Das, *J. Phys. Chem. C*, 2008, **112**, 8429; (c) S. V. Eliseeva, O. V. Kotova, F. Gumy, S. N. Semenov, V. G. Kessler, L. S. Lepnev, J.-C. G. Bünzli and N. P. Kuzmina, *J. Phys. Chem. A.*, 2008, **112**, 3614.
18. (a) N. M. Shavaleev, R. Scopelliti, F. Gumy and J.-C. G. Bünzli, *Eur. J. Inorg. Chem.,* 2008, **9**, 1523; (b) A. W. Woodward, A. Frazer, A. R. Morales, J. Yu, A. F. Moore, A. D. Campiglia, E. V. Jucov, T. V. Timofeevab and K. D. Belfield, *Dalton Trans*., 2014, **43**, 16626; (c) D. Nie, Z. Chen, Z. Bian, J. Zhou, Z. Liu, F. Chen, Y. Zhao and C. Huang, *New J. Chem*., 2007, **31**, 1639.
19. (a) C. M. Whitaker, E. V. Patterson, K. L. Kott and R. J. McMahon, *J. Am. Chem. Soc*., 1996, **118**, 9966; (b) G. Park, C. S. Ra and B. R. Cho, *Bull. Korean Chem. Soc*., 2003,

24, 1671; (c) J. E. Haley, D. M. Krein, J. L. Monahan, A. R. Burke, D. G. McLean, J. E. Slagle, A. Fratini and T. M. Cooper, *J. Phys. Chem*., 2011, **115**, 265; (d) L.-H. Ma, Z.-B. Chen, Y.-B. Jiang, *Chem. Phys. Lett*., 2003, **372**, 104-113; (e) G.-J. Huang and J.-S. Yang, *Chem. Asian J.*, 2010, **5**, 2075; (f) J.-S. Yang, K.-L. Liau, C.-M.Wang and C.-Y. Hwang, *J. Am. Chem. Soc*., 2004, **126**, 12325.

20. (a) X. Mou, Y. Wu, S. Liu, M. Shi, X. Liu, C. Wang, S. Sun, Q. Zhao, X. Zhoua and W. Huang, *J. Mater. Chem*., 2011, **21**, 13951; (b) C. Hansch, A. Leo and R. W. Taft, *Chem. Rev*., **97**, 165; (c) T. Karatsu, M. Takahashi, S. Yagai and A. Kitamura, *Inorg. Chem*., 2013, **52**, 12338.
21. (a) M. H. V. Werts, R. T. F. Jukes and J. W. Verhoeven, *Phys. Chem. Chem. Phys*., 2002, **4**, 1542; (b) Z. Ahmed and K. Iftikhar, *J. Phys. Chem. A.*, 2013, **117**, 11183; (c) E. E. S. Teotonio, H. F. Brito, M. C. F. C. Felinto, L. C. Thompson, V. G. Young, O. L. Malta, *J. Mol. Struct.*, 2005, **751**, 85.
22. (a) J. Shi, Y. Hou, W. Chu, X. Shi, H. Gu, B. Wang, and Z. Sun, *Inorg. Chem*., 2013, **52**, 5013; (b) G. Shao, H. Yu, N. Zhang, Y. He, K. Feng, X. Yang, R. Cao and M. Gong, *Phys. Chem. Chem. Phys.,* 2014, **16**, 695; (c) J. Kai, D. F. Parra and H. F. Brito, *J. Mater. Chem*., 2008, **18**, 4549.
23. (a) G. F. de Sa, O. L. Malta, C. de Mello Donega, A. M. Simas, R. L. Longo, P. A. Santa-Cruz and E. F. da Silva Jr., *Coord. Chem. Rev*., 2000, **196**, 165; (b) B. Makhinson, A. K. Duncan, A. R. Elam, A. de Bettencourt-Dias, C. D. Medley, J. E. Smith, and E. J. Werner, *Inorg. Chem*., 2013, **52**, 6311.

24. (a) A. Dossing, *Eur. J. Inorg. Chem*., 2005, 1425; (b) A. Beeby, I. M. Clarkson, R. S. Dickins, S. Faulkner, D. Parker, L. Royle, A. S. de Sousa, J. A. G. Williams and M. Woods, *J. Chem. Soc. Perkin Trans*., 1999, **2**, 493.

25. N. M. Shavaleev, S. V. Eliseeva, R. Scopelliti and J.-C. G. Bünzli, *Inorg. Chem.*, 2010, **49**, 3927.

26. (a) Q.-Y. Yang, M. Pan, S.-C. Wei, C.-W. Hsu, J.-M. Lehn and C.-Y. Su, *CrystEngComm*., 2014, **16**, 6469; (b) M. Shi, F. Li, T. Yi, D. Zhang, H. Hu and C. Huang, *Inorg. Chem.*, 2005, **44**, 8929; (c) S. I. Klink, L. Grave, D. N. Reinhoudt, and F. C. J. M. van Veggel, *J. Phys. Chem. A.,* 2000, **104**, 5457; (d) H. Xin, M. Shi, X. C. Gao, Y. Y. Huang, Z. L. Gong, D. B. Nie, H. Cao, Z. Q. Bian, F. Y. Li, and C. H. Huang, *J. Phys. Chem. B.*, 2004, **108**, 10796.

27. (a) N. Armaroli, G. Accorsi, F. Barigelletti, S. M. Couchman, J. S. Fleming, N. C. Harden, J. C. Jeffery, K. L. V. Mann, J. A. McCleverty, L. H. Rees, S. R. Starling and M. D. Ward, *Inorg. Chem.*, 1999, **38**, 5769; (b) M. Latva, H. Takalo, V.-M. Mukkala, C. Matachescu, J. C. Rodriguez-Ubis and J. Kankare, *J. Lumin.*, 1997, **75**, 149.

28. (a) J.-M. Lehn, *Angew. Chem. Int. Ed.*, 1990, **29**, 1304; (b) S. Petoud, S. M. Cohen, J.-C. G. Bünzli and K. N. Raymond, *J. Am. Chem. Soc.*, 2003, **125**, 13324; (c) A. R. Ramya, D. Sharma, S. Natarajan and M. L. P. Reddy, *Inorg. Chem*., 2012, **51**, 8818.

29. (a) L.-N. Sun, H.-J. Zhang, J.-B. Yu, Q.-G. Meng, F.-Y. Liu and C.-Y. Peng, *J. Photochem. Photobiol. A*., 2008, **193**, 153; (b) L. Sun, Y. Qiu, T. Liu, J. Z. Zhang, S. Dang, J. Feng, Z. Wang, H. Zhang and L. Shi, *ACS Appl. Mater. Interfaces.*, 2013, **5**, 9585; (c) X. Guo, H. Guo, L. Fu, L. D. Carlos, R. A. S. Ferreira, L. Sun, R. Deng and H. Zhang, *J. Phys. Chem. C*., 2009, **113**, 12538; (d) J. Xu, Y. Ma, L. Jia , X. Huang, Z. Deng, H.

Wana, W. Liu and Yu Tang, *Materials Chemistry and Physics*., 2012, **133**, 78; (e) X. Huang, Q. Wang, X. Yan, J. Xu, W. Liu, Q. Wang and Y. Tang, *J. Phys. Chem. C*., 2011, **115**, 2332.

30. L. Guo, B. Yan, J.-L. Liu, K. Sheng and X.-L. Wang, *Dalton Trans*., 2011, **40**, 632.
31. P. C. R. Soares-Santos, H. I. S. Nogueira, V. FeĺÍix, M. G. B. Drew, R. A. Sá Ferreira, L. D. Carlos and T. Trindade, *Chem. Mater*., 2003, **15**, 100.
32. J. G.-Torres, P. B.-Jimenez, E. T.-Calleja, M. Kennedy, H. Ahmed, J. Doran, D. G.-Tauste, L. Bautista and M. D. Pirriera, *J. Photochem. Photobiol. A*., 2014, **283**, 8.

Chapter 3

Chapter 3

Visible-light excitable highly luminescent molecular plastic materials derived from Eu^{3+}-biphenyl based β-diketonate ternary complex and poly(methylmethacrylate)

3.1. Abstract

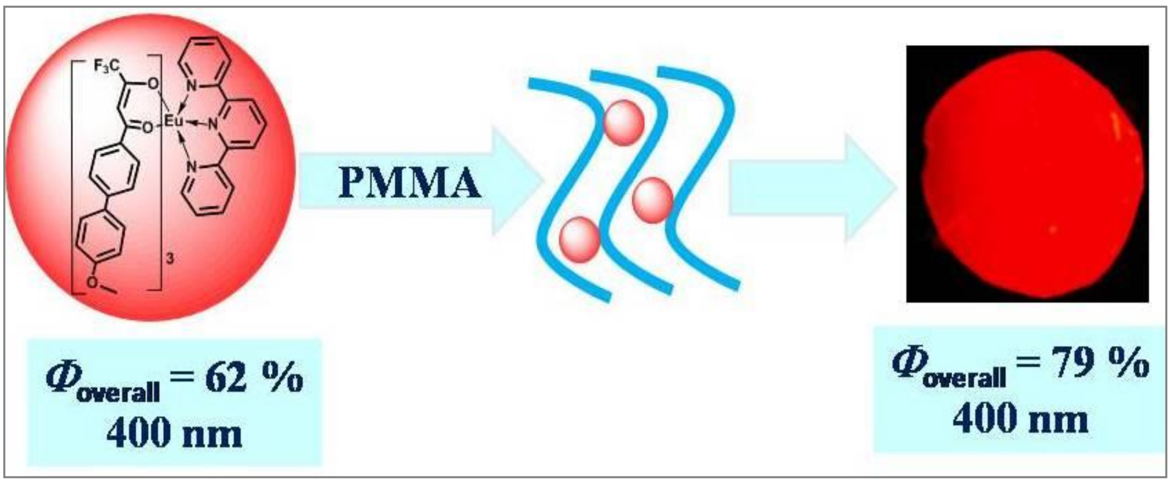

In the present work, a β-diketonate ligand, namely, 1-(4'-methoxy-[1,1'-biphenyl]-4-yl)-4,4,4-trifluoro-3-hydroxybut-2-en-1-one (HMeOBPhTFB), which contains a conjugated methoxy-substituted biphenyl unit, as well as a polyfluorinated alkyl group, was synthesized and utilized for the construction of two new Eu^{3+} complexes [Eu(MeOBPhTFB)$_3$(H_2O)(C_2H_5OH)] ***1*** *and [Eu(MeOBPhTFB)$_3$(TPY)]* ***2*** *where TPY denotes 2,2':6',2"-terpyridine. The synthesized compounds are well characterized by various spectroscopic techniques, and their solid-state photophysical properties were investigated. For comparison, Eu^{3+} complexes {[Eu(BPhTFB)$_3$(H_2O)(C_2H_5OH)]* ***3*** *and [Eu(BPhTFB)$_3$(TPY)]* ***4****} were also designed involving an unsubstituted biphenyl based β-*

*diketonate ligand, 1-[1,1'-biphenyl]-4-yl)-4,4,4-trifluoro-3-hydroxybut-2-en-1-one (HBPhTFB). The results disclosed that the methoxy-substituted biphenyl based polyfluorinated Eu^{3+}-β-diketonate complexes significantly red-shifted the excitation maximum to the visible region (λ_{exc} = 400 nm) with promising solid-state quantum yield ($\Phi_{overall}$ = 62% for **2**) as compared to simple Eu^{3+}-biphenyl β-diketonate ternary complex (λ_{exc} = 382 nm for **3** and **4**). In the current work, attempts also have been made to isolate luminescent molecular plastic materials by incorporating the unique photophysical properties of the developed visible-light excitable Eu^{3+}-β-diketonate complex (**2**) with the mechanical, thermal, and chemical stability, and flexibility and a film-forming tendency of poly(methylmethacrylate) [PMMA]. The developed molecular plastic materials were characterized and evaluated their photoluminescence properties. Most importantly, the newly constructed polymer films exhibit remarkable quantum yields (75–79%) under blue-light excitation as compared to many of the existing Eu^{3+} based polymeric materials.*

T. V. Usha Gangan, S. Sreenadh and M. L. P. Reddy, *J. Photochem. Photobiol. A: Chem.,* 2016, **328**, 171–181.

3.2. Introduction

Due to their excellent photophysical properties, Eu^{3+}-*β*-diketonate complexes are among the most meticulously studied class of coordination compounds. The considerable attention they have been attracting until now stems from their ease of synthesis, intense absorption transitions and the variety of potential practical applications ranging from biomedicine[1] to material sciences.[2] The forbidden nature of the f–f transitions in trivalent europium ions results in a very weak intensity of the metal-centered absorption bands. This weak absorbance can, however, be overcome by coordinating chromophore-containing ligands to the Eu^{3+} ion which, upon irradiation, transfer energy to the metal center, typically *via* the ligand triplet excited state, thereby populating the Eu^{3+} emitting levels in a process known as the "antenna effect".[3] As a result, a significant number of Eu^{3+}-*β*-diketonate complexes have been isolated and investigated their photoluminescence properties.[4] However, the optical excitation window for many of the reported luminescent Eu^{3+} complexes are found to be limited to UV region (<390 nm) due to the energy constraints arose from the photophysics of Eu^{3+} ions as emphasized by Reinhoudt et al.[5] For application in biosensing or bioimaging, over the years great efforts have been made on the development of luminescent Eu^{3+} complexes that are capable of being efficiently excited by visible-light, because the blue-light is less harmful to biological tissue, allowing deep penetration, causing less background fluorescence and thus lowering the interferences from biological samples.[3c] Thus, one of the challenges in the photophysics of 4f elements is to design and develop visible-light excitable Eu^{3+}-*β*-diketonate complexes, which is in high demand for less-harmful labeling reagents in the field of life sciences. Indeed, some of the latest studies have revealed that the excitation window can be shifted to longer wavelengths in Eu^{3+}-β-diketonate complexes by appropriate molecular engineering and suitably expanded π-conjugation in the β-diketonate ligands.[3c,6] Reddy and coworkers reviewed recent advances on the development of visible-light sensitized luminescent Eu^{3+}-β-diketonate complexes and their applications towards bioprobes for cellular imaging.[7] In this context, Divya and Reddy have developed a novel visible-light excited red-emitting luminescent Eu^{3+}-phenathrene-based fluorinated β-diketonate complex with high solid-state quantum yield (75%).[8] Recently, a new family of Eu^{3+}-complexes based on aminophenyl polyfluorinated β-diketonate ligands in the absence and presence of a chelating phosphine oxide has been isolated in our laboratory and investigated their photophysical properties.[9] Among the developed compounds, the Eu^{3+}-triphenylamine based β-diketonate ternary complex displays intense red emission under blue-light excitation, (λ_{exc} = 400 nm) with an overall quantum yield of 40%. In the later studies, visible-light excited carbazole-based Eu^{3+}-β-diketonate complexes *via* molecular engineering have also been disclosed.[10] The results demonstrated that suitably expanded π-conjugation in the developed Eu^{3+}-carbazole based β-diketonate complexes with a red-shift in the excitation maximum to the visible region (λ_{exc} = 420 nm) with a moderate quantum yield (34–42%). Nevertheless, many of the visible-light excitable Eu^{3+}-β-diketonate complexes so far known display poor quantum yields. Thus, there is a growing demand for the development of new Eu^{3+} complexes with high quantum yields that are based on robust visible-light excitable β-diketonate ligands.

The compounds with aromatic–aromatic bond appended with functional moieties have attracted considerable interest owing to their intriguing structural motifs and unique luminescence properties.[11] The intermolecular interactions in the solid state may promote the coplanar arrangements of aromatic rings in the biphenyl compounds, which may be accountable for the noted conjugation. Further, investigations disclosed that complexation with cations can control the conformation of the biphenyl.[12] It is also well documented that the incorporation of electron-donating methoxy group on the phenyl ring of the biphenyl system allows oxygen electrons to be part of the delocalized system through resonance and increases the conjugation of the chromophore.[6j,10,13,14] The replacement of C-H bonds in a *β*-diketonate ligand with low-energy C-F oscillators reduces the vibrational energy and further promotes the spin-orbit coupling through heavy atom effect, which facilitates the intersystem crossing in lanthanide complexes and thus improves the photoluminescence quantum yield.[7a,15,16] These factors have inspired us to incorporate simultaneously highly conjugated methoxy-substituted biphenyl and trifluoromethyl units into the *β*-diketonate ligand system and synthesize a *β*-diketonate ligand. The resultant antenna molecule expected to display efficient luminescence under visible-light excitation upon coordination with trivalent europium ions. Therefore, in the current study a *β*-diketonate ligand, namely, 1-(4′-methoxy-[1,1′-biphenyl]-4-yl)-4,4,4-trifluoro-3-hydroxybut-2-en-1-one (HMeOBPhTFB) was designed and utilized for the synthesis of new visible-light excitable Eu^{3+}-*β*-diketonate complexes in the presence and absence of an ancillary ligand, 2,2′:6′,2′′-terpyridine and investigated their solid-state photophysical properties. For comparison, Eu^{3+}-coordination compounds were also prepared involving an unsubstituted biphenyl based *β*-diketonate ligand system.

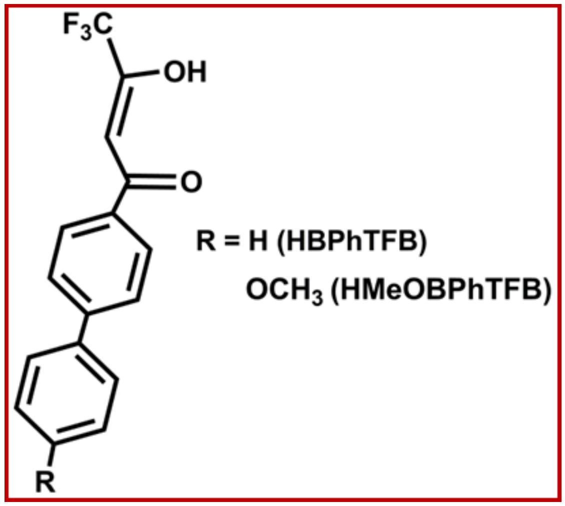

Figure 3.1. Structure of the ligands.

It is noteworthy to mention that the Eu^{3+}-*β*-diketonate complexes have always been excluded from the practical applications, mainly due to their low thermal stability, limited photostability and poor mechanical properties. The polymers are ideal matrices for Eu^{3+}complexes, because their several attractive features including mechanical strength, flexibility, ease of processing and controllable cost.[21,24,16-20] To overcome the above-cited limitations, in the present study, the newly developed visible-light excitable Eu^{3+}-*β*-diketonate compound was embedded into a PMMA matrix and developed molecular plastic materials and studied their thermal and photophysical properties.

3.3. Experimental Section

3.3.1. Materials and instrumentation

The reagents used in this study were commercially available and used as purchased: europium(III) nitrate hexahydrate, 99.9% (Alfa Aesar); gadolinium(III) nitrate hexahydrate, 99.999% (Sigma-Aldrich); (4-acetylphenyl)boronic acid, 97%

(Sigma-Aldrich), iodobenzene, 98% (Sigma-Aldrich), iodoanisole, 96% (Sigma-Aldrich); ethyl trifluoroacetate, 99% (Sigma-Aldrich); poly(methylmethacrylate), 98% (Sigma-Aldrich); sodium hydride 60% dispersion in mineral oil (Sigma-Aldrich); sodium carbonate, 99.5% (Sigma-Aldrich).

Elemental analyses were performed with an Elementar – vario MICRO cube elemental analyzer. FT-IR spectra were recorded on a Perkin-Elmer Spectrum two FT-IR spectrometer using KBr pellets. The synthesized compounds were characterized by ^{1}H NMR (500 MHz) and $^{13}C\{^{1}H\}$ NMR (125.7 MHz) using a Bruker 500 MHz NMR spectrometer in chloroform-*d* solution. The chemical shifts are reported in parts per million relative to tetramethylsilane, $SiMe_4$ for ^{1}H NMR and $^{13}C\{^{1}H\}$ NMR spectra. Electro spray ionization (ESI) mass spectra were recorded on a Thermo Scientific Exactive Benchtop LC/MS Orbitrap Mass Spectrometer and the thermogravimetric analyses were performed on a TG/DTA-6200 (SII Nano Technology Inc., Japan). The absorbances of the ligands were measured in THF solution on a UV–vis spectrophotometer (Shimadzu, UV-2450). The photoluminescence (PL) spectra were recorded on a Spex-Fluorolog FL22 spectrofluorimeter equipped with a double grating 0.22 m Spex 1680 monochromator and a 450 W Xe lamp as the excitation source operating in the front face mode. The lifetime and phosphorescence measurements were carried out by using a SPEX 1040 D phosphorimeter. The phosphorescence spectra were monitored after a delay after flash of 50 μs. The overall quantum yield ($\Phi_{overall}$) was measured using an integrating sphere in a SPEX Fluorolog spectrofluorimeter as previously reported in literature.[9,21] The estimated error for the quantum yields is ±10%.

3.3.2 Synthetic procedures for the ketones

The corresponding ketone was prepared by Suzuki-Miyaura coupling reaction. In a round bottom flask, one equivalent of iodoanisole or iodobenzene was taken and dissolved in 25 mL of dry THF. To that 1.2 equivalents of (4-acetylphenyl)boronic acid and 0.06 equivalents of tetrakis-(triphenylphosphine)palladium(0) were added. A solution of 5% Na_2CO_3 (10 mL) was added to that mixture and refluxed with stirring for 24 h, under the nitrogen atmosphere. After cooling to room temperature, the mixture was poured into water, and extracted with dichloromethane. The organic layer was dried over Na_2SO_4. The solvent was removed and the crude product was purified by silica column chromatography with ethyl acetate: *n*-hexane as the eluent (1:99) to give the final product.

1-([1,1′-biphenyl]-4-yl)ethanone. Yield: 72%. ^{1}H NMR ($CDCl_3$, 500 MHz): δ (ppm) 7.89 (m, 2H), 7.68 (m, 4H), 7.44 (m, 2H), 7.13 (m, 1H), 2.53 (s, 3H). ^{13}C{^{1}H} NMR (125.7 MHz, $CDCl_3$) δ (ppm): 197.77, 145.79, 139.88, 135.86, 128.96, 128.92, 128.24, 127.28, 115.23, 26.66. m/z = 197 (M + 1)$^+$.

1-(4′-methoxy-[1,1′-biphenyl]-4-yl)ethanone. Yield: 60%. ^{1}H NMR ($CDCl_3$, 500 MHz): δ (ppm) 8.03 (m, 2H), 7.64 (m, 4H), 7.01 (m, 2H), 3.87 (s, 3H) 2.63 (s, 3H). ^{13}C{^{1}H} NMR (125.7 MHz, $CDCl_3$) δ (ppm): 196.48, 159.81, 145.51, 135.78, 132.92, 131.03, 129.34, 128.60, 114.96, 55.84, 25.53. m/z = 227 (M + 1)$^+$.

3.3.3. Synthesis of ligands

The ligands, 1-([1,1′-biphenyl]-4-yl)-4,4,4-trifluoro-3-hydroxybut-2-en-1-one (HBPhTFB) and 1-(4′-methoxy-[1,1′-biphenyl]-4-yl)-4,4,4-trifluoro-3-hydroxybut-2-en-1-one (HMeOBPhTFB) were synthesized by Claisen condensation reaction (Scheme 3.1) as reported in literature.[4,9]

1-([1,1′-biphenyl]-4-yl)-4,4,4-trifluoro-3-hydroxybut-2-en-1-one (HBPhTFB). Yield: 64%. Elemental analysis (%): calculated for $C_{16}H_{11}F_3O_2$ (292.25): C 65.76, H 3.59; Found: C 66.01, H 3.86, ^{1}H NMR ($CDCl_3$, 500 MHz) δ (ppm): 15.15 (broad, enol–OH), 8.03 (d, 2H, J = 8.5 Hz), 7.74 (d, 2H, J = 8.5 Hz), 7.65 (m, 2H), 7.48 (m, 3H), 6.62 (S, 1H). ^{13}C{^{1}H} NMR (125.7 MHz, $CDCl_3$) δ (ppm): 185.66, 177.50, 146.91, 131.50, 129.07, 128.61, 128.23, 127.61, 127.2, 116.05, 92.23, 77.26-76.76 ($CDCl_3$). FT-IR (KBr) ν_{max} (cm^{-1}): 3033, 2918, 2849, 1605, 1486, 1319, 1288, 1213, 1150, 1066, 772, 689. m/z = 293 (M + 1)$^+$.

1-(4′-methoxy-[1,1′-biphenyl]-4-yl)-4,4,4-trifluoro-3-hydroxybut-2-en-1-one (HMeOBPhTFB). Yield: 52%. Elemental analysis (%): calculated for $C_{17}H_{13}F_3O_3$ (322.08): C 63.06, H 4.07; Found: C 63.31, H 3.97, ^{1}H NMR ($CDCl_3$, 500 MHz) δ (ppm): 15.31 (broad, enol–OH), 8.00 (d, 2H, J = 8.5 Hz), 7.69 (d, 2H, J = 8.5 Hz), 7.60 (m, 2H), 7.01 (m, 2H), 6.60 (S, 1H), 3.88 (s, 3H). ^{13}C{^{1}H} NMR (125.7 MHz, $CDCl_3$) δ (ppm): 185.68, 182.10, 160.24, 146.52, 136.42, 131.74, 130.79, 128.42, 128.28, 126.96, 114.53, 92.10, 55.42, 77.27-76.76 ($CDCl_3$). FT-IR (KBr) ν_{max} (cm^{-1}): 3038, 2970, 2917, 2846, 1600, 1496, 1296, 1217, 1150, 1108, 799, 669. m/z = 323 (M + 1)$^+$.

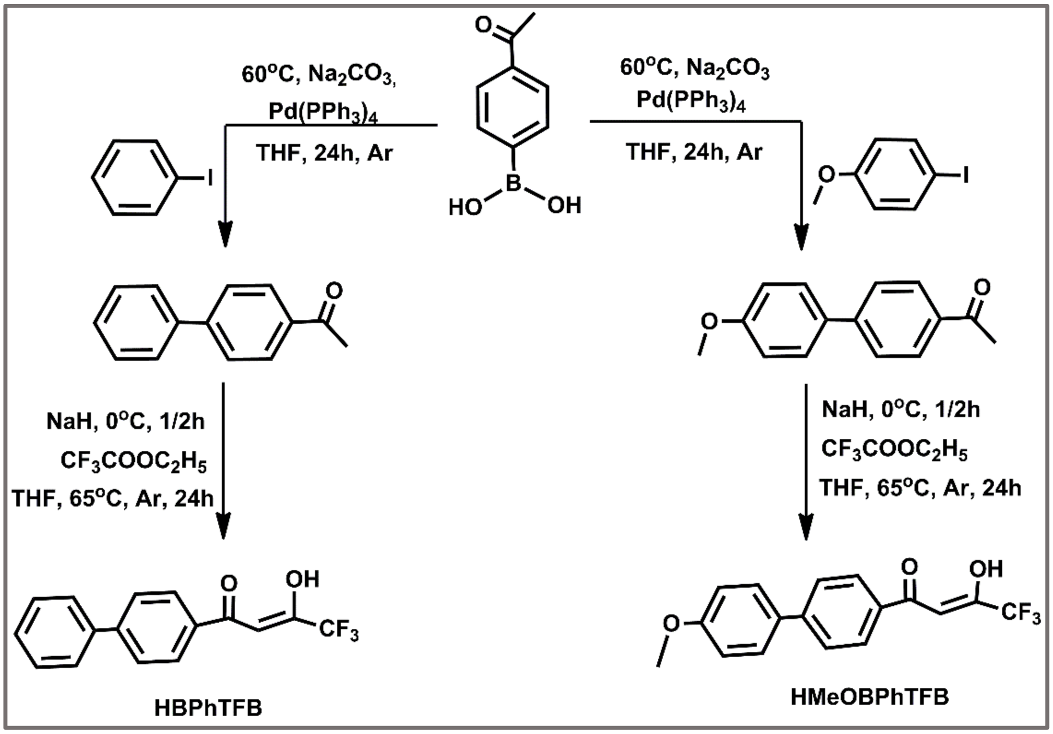

Scheme 3.1. Synthesis of the ligands.

3.3.4. Synthesis of binary complexes

NaOH (3.0 mmol) in water was added to a solution of corresponding β-diketonate ligand (3.0 mmol) in ethanol and stirred for 10 min. To this mixture, $Ln(NO_3)_3{\cdot}6(H_2O)$ (where Ln = Eu^{3+}, Gd^{3+}) (1.0 mmol) in ethanol was added drop wise and stirred for 12 h at room temperature. A light yellow colored precipitate was formed by adding excess amount of water. The resultant precipitate was filtered off, washed with water and dried. The products were purified by recrystallization from dichloromethane solution and used for further analysis and photophysical studies. The synthesis procedure is given in Scheme 3.2.

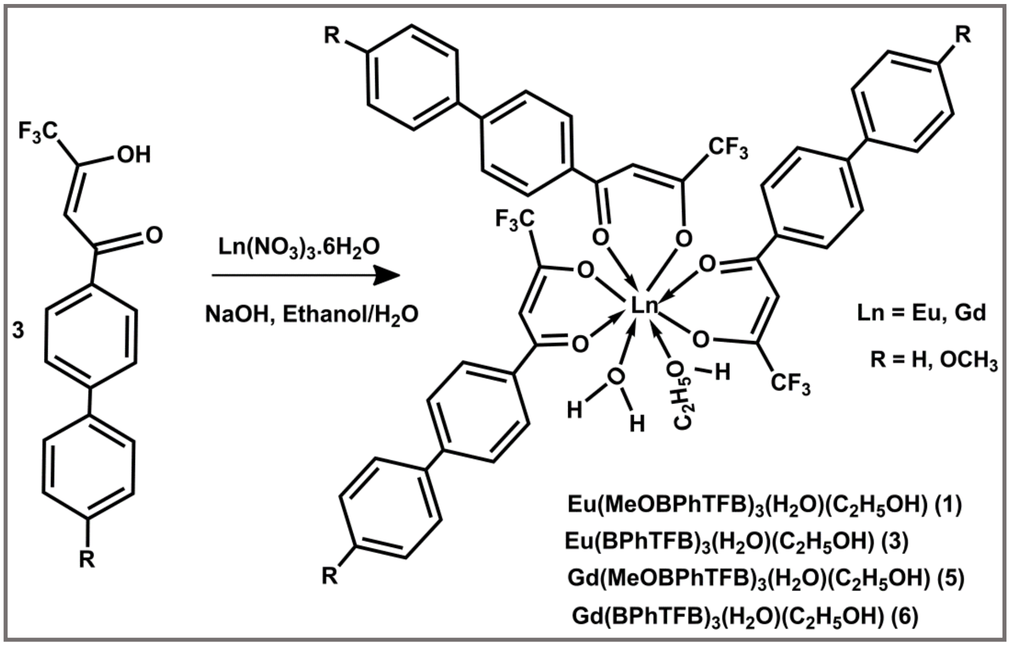

Scheme 3.2. Synthesis of the Ln^{3+} (Ln = Eu, Gd) binary complexes.

$Eu(MeOBPhTFB)_3(H_2O)(C_2H_5OH)$ (1). Elemental analysis (%): calculated for $C_{53}H_{44}F_9O_{11}Eu$ (1179.86): C 53.95, H 3.76; Found: C 54.23, H 3.94. FT-IR (KBr) ν_{max} (cm^{-1}): 3419, 3036, 2959, 2911, 2839, 1615, 1602, 1557, 1530, 1496, 1299, 1199, 1138, 793, 667. m/z = 1116 $[Eu(MeOBPhTFB)_3]^+$.

$Eu(BPhTFB)_3(H_2O)(C_2H_5OH)$ (3). Elemental analysis (%): calculated for $C_{50}H_{38}F_9O_8Eu$ (1089.78): C 55.11, H 3.51; Found: C 54.93, H 3.68. FT-IR (KBr) ν_{max} (cm^{-1}): 3411, 3031, 2928, 1618, 1603, 1557, 1486, 1319, 1296, 1196, 1140, 1073, 766, 689. m/z = 1025 $[Eu(BPhTFB)_3\text{-}1]^+$.

$Gd(MeOBPhTFB)_3(H_2O)(C_2H_5OH)$ (5). Elemental analysis (%): calculated for $C_{53}H_{44}F_9O_{11}Gd$ (1185.15): C 53.71, H 3.74; Found: C 54.03, H 3.81. FT-IR (KBr) ν_{max} (cm^{-1}): 3418, 3061, 2961, 2921, 2841, 1614, 1602, 1560, 1530, 1495, 1317, 1296, 1193, 1138, 790, 667. m/z = 1122 $[Gd(MeOBPhTFB)_3 + 1]^+$.

Gd(BPhTFB)$_3$(H$_2$O)(C$_2$H$_5$OH) (6). Elemental analysis (%): calculated for $C_{50}H_{38}F_9O_8Gd$ (1095.07): C 54.84, H 3.50; Found: C 54.87, H 3.46. FT-IR (KBr) ν_{max} (cm^{-1}): 3418, 3032, 2922, 1617, 1601, 1556, 1486, 1316, 1296, 1196, 1140, 1073, 766, 689. m/z = 1054 [Gd(BPhTFB)$_3$ + Na + 1]$^+$.

3.3.5. Synthesis of ternary Eu^{3+} complexes 2 and 4

Like earlier literature reports,[4,9] ternary complexes were synthesized by refluxing equimolar solutions of corresponding binary complexes and terpyridine in chloroform solution for 12 h at 70 °C. Solvent was removed in rotary-evaporator and purified by recrystallization from a chloroform solution. The synthesis procedure is illustrated in Scheme 3.3.

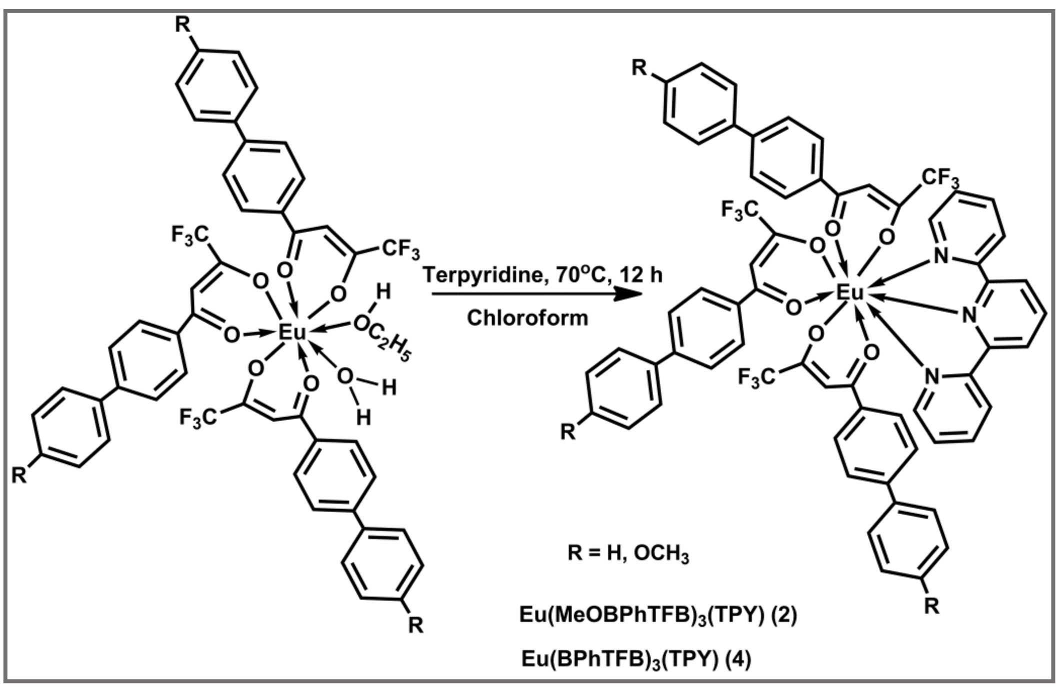

Scheme 3.3. Synthesis of the Eu^{3+} ternary complexes **2** and **4**.

Eu(MeOBPhTFB)$_3$(TPY) (2). Elemental analysis (%): calculated for $C_{66}H_{47}O_9F_9N_3Eu$ (1349.04): C 58.76, H 3.50, N 3.11; Found: C 58.72, H 3.84, N 2.82. FT-IR (KBr) ν_{max} (cm^{-1}): 3034, 2958, 2917, 2847, 1640, 1620, 1602, 1581, 1556, 1492, 1298, 1248, 1184, 1137, 786, 665. m/z = 1027 [Eu(MeOBPhTFB)$_2$(TPY)]$^+$.

Eu(BPhTFB)$_3$(TPY) (4). Elemental analysis (%): calculated for $C_{63}H_{41}O_6F_9N_3Eu$ (1258.97): C 60.10, H 3.28, N 3.34; Found: C 59.82, H 3.47, N 3.08. FT-IR (KBr) ν_{max} (cm^{-1}): 3030, 2919, 2849, 1638, 1621, 1602, 1580, 1555, 1484, 1316, 1295, 1188, 1138, 1071, 764, 687. m/z = 968 [Eu(BPhTFB)$_2$(TPY)]$^+$.

3.3.6. Preparation of luminescent polymer films

PMMA powder and required amount of Eu(MeOBPhTFB)$_3$(TPY) (3, 5, 7 and 9% (w/w)) were dissolved in 10 mL of chloroform solution. After stirring for 30 min at 70 °C, the solution was dried at room temperature to obtain the transparent polymer films. The prepared polymer films were represented as PMMA@3Eu, PMMA@5Eu, PMMA@7Eu and PMMA@9Eu.

3.4. Results and discussion

3.4.1. Synthesis and characterization of ligands and their corresponding lanthanide complexes

The ligands 1-([1,1′-biphenyl]-4-yl)-4,4,4-trifluoro-3-hydroxybut-2-en-1-one (HBPhTFB) and 1-(4′-methoxy-[1,1′-biphenyl]-4-yl)-4,4,4-trifluoro-3-hydroxybut-2-en-1-one (HMeOBPhTFB) were successfully synthesized in two steps starting from commercially available 4-acetylphenylboronic acid as summarized in Scheme 3.1. The designed biphenyl based β-diketonate ligands were identified by ^{1}H NMR and ^{13}C NMR spectroscopy, electrospray ionization mass spectrometry (ESI–MS), FT-IR spectroscopy and elemental analysis. ^{1}H NMR analysis indicates that both the β-diketonate ligands exist as enol form in chloroform-*d* solution. This can be confirmed by the presence of broad peak at δ 15.15 ppm for HBPhTFB and 15.31 ppm for HMeOBPhTFB which corresponding to enolic –OH. Further, the absence of methylene protons at ~3.7 ppm confirms the existence of the ligand in enolic form. The protocols used for the syntheses of binary and ternary lanthanide complexes (Ln = Eu^{3+} and Gd^{3+}) are outlined in the Scheme 3.2 and Scheme 3.3, respectively. The elemental analysis and ESI–MS data of all the lanthanide complexes revealed that in each case Ln^{3+} ion has reacted with the corresponding β-diketone ligand in a metal-to-ligand mole ratio of 1:3. In the case of ternary Eu^{3+}-β-diketonate complexes (**2** and **4**), one molecule of terpyridine is also present in the coordination sphere. The FT-IR spectra of the binary complexes (**1**, **3**, **5** and **6**) show a broad absorption band in the 3000–3500 cm^{-1} region, indicating the presence of solvent molecules in the coordination sphere of the Ln^{3+} ion. The presence of coordinated water molecule in the case of binary Eu^{3+}-β-diketonate complexes has been further ascertained by ^{1}H NMR analysis (a broad peak noted at about 3.02 ppm in **1** of Figure 3.2 and 2.50 ppm in **3** of Figure 3.3). However, the absence of the above broadband in the case of Eu^{3+} ternary complexes implies that the ancillary ligand, terpyridine displaced the solvent molecules successfully. Also, the strong bands at 1581, 1436 and 736 cm^{-1} noted in the ternary complexes confirm the presence of coordinated terpyridine.[22]

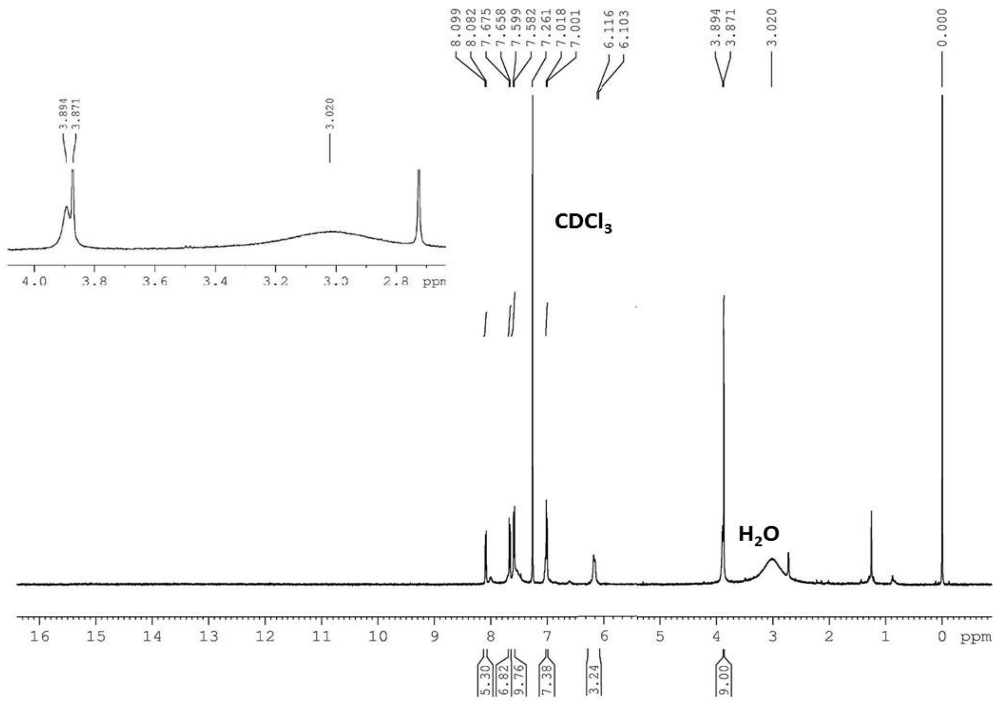

Figure 3.2. ^{1}H NMR spectrum of $Eu(MeOBPhTFB)_3(H_2O)(C_2H_5OH)$ in $CDCl_3$.

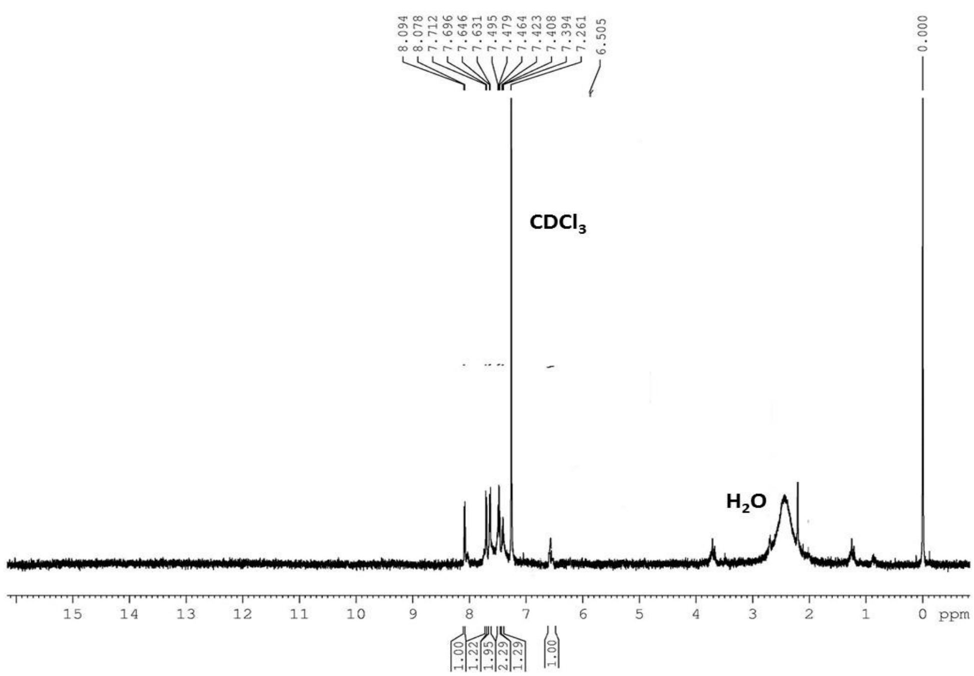

Figure 3.3. ^{1}H NMR spectrum of $Eu(BPhTFB)_3(H_2O)(C_2H_5OH)$ in $CDCl_3$.

The carbonyl stretching frequency of the biphenyl based β-diketonate ligands (1605 cm^{-1} for HBPhTFB and 1600 cm^{-1} for HMeOBPhTFB) are shifted to higher wavenumbers (1615 cm^{-1} in **1**, 1620 cm^{-1} in **2**, 1618 cm^{-1} in **3** and 1621 cm^{-1} in **4**) in all the Eu^{3+} complexes indicating the involvement of carbonyl oxygen in the complex formation with the Eu^{3+} ion.

The thermal behavior of the synthesized biphenyl based Eu^{3+}-β-diketonate complexes (**1–4**) were evaluated by thermogravimetric analysis (30–1000 °C range in a nitrogen atmosphere), and the corresponding thermograms are depicted in Figure 3.4 and 3.5. It is evident from the thermogravimetric analysis that both the binary Eu^{3+} complexes **1** and **3** undergoes a mass loss about ~5.3% (calculated ~5.4%) in the first step (90–140 °C), which corresponds to the loss of coordinated solvent and water molecules. In contrast, Eu^{3+} ternary complexes **2** and **4** are more stable than binary complexes, and they undergo decomposition only above 220 °C, indicating that there are no coordinated solvent molecules in these complexes. These trends are in good agreement with the FT-IR spectral data. The total weight loss noted in the thermal analysis of the complexes is found to be much lower than the calculated value for the non-volatile europium oxide, implying the partial sublimation of these compounds under atmospheric pressure which is well documented in many of the lanthanide fluorinated β-diketonate complexes.[4e,9,23]

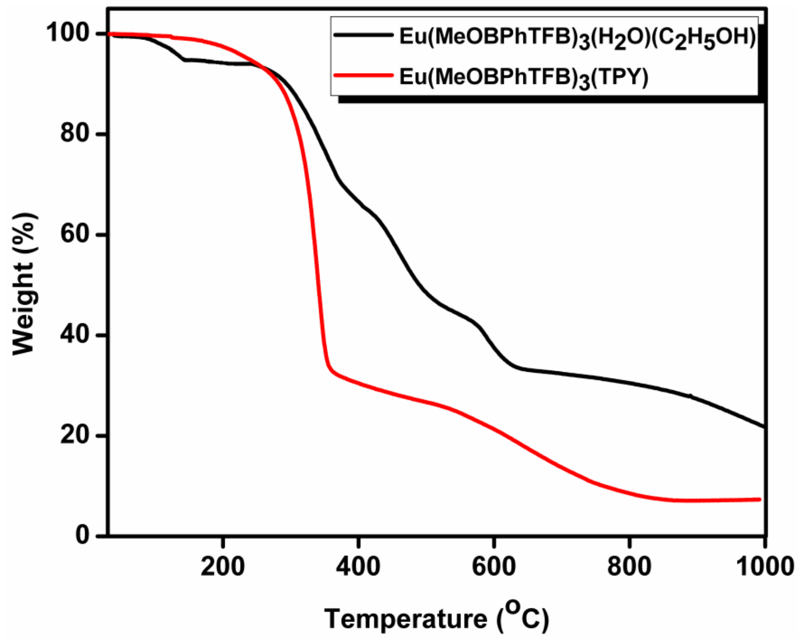

Figure 3.4. Thermogravimetric curves for Eu^{3+} complexes $Eu(MeOBPhTFB)_3(H_2O)(C_2H_5OH)$ (**1**) & $Eu(MeOBPhTFB)_3(TPY)$ (**2**).

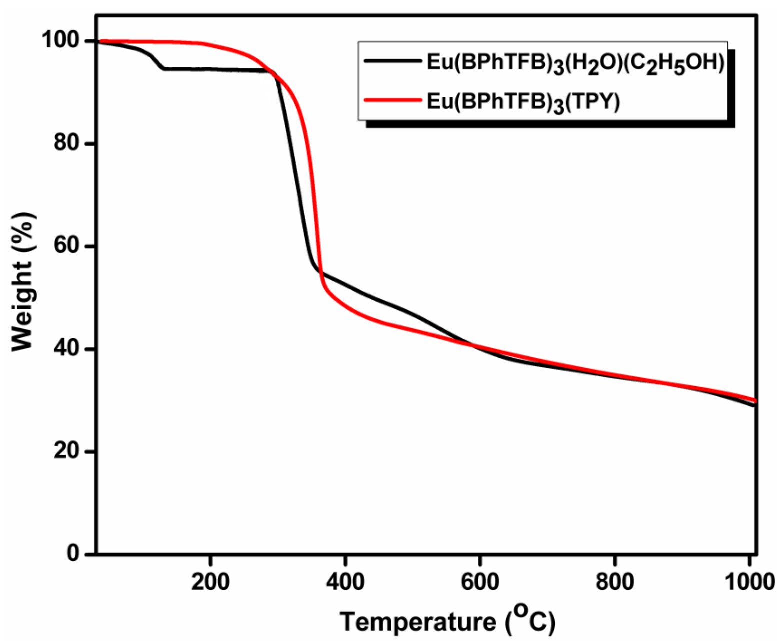

Figure 3.5. Thermogravimetric curves for Eu^{3+} complexes $Eu(BPhTFB)_3(H_2O)(C_2H_5OH)$ (**3**) & $Eu(BPhTFB)_3(TPY)$ (**4**).

3.4.2. Electronic spectra of the Eu^{3+}-β-diketonate complexes

The UV–vis absorption spectra of the β-diketonate ligands and their corresponding Eu^{3+}complexes, which were recorded in acetonitrile solution ($c = 5 \times 10^{-6}$ M) at 298 K, are displayed in Figures 3.6 and 3.7. The pertinent spectral features are summarized in Table 3.1. The absorption maxima at 345 and 358 nm noted for the ligands HBPhTFB and HMeOBPhTFB are attributable to the singlet–singlet $^1\pi$-π^* enolic transition assigned to the β-diketonate moiety.[4a,b,10,23] It is notable that the UV–vis absorption maximum band is red-shifted (13 nm) in the case of methoxy-substituted biphenyl based β-diketonate ligand, thus pointing out that the degree of conjugation enhances and that the $^1\pi$-π^* energy level is lowered by the introduction of electron-donating methoxy moiety at the 4′ position of the biphenyl based β-diketonate ligand.[6j,9,10,12] Besides, the molar absorption coefficient of the HMeOBPhTFB ligand also significantly enhanced as compared to the parent ligand (ε = 34463 L mol^{-1} cm^{-1} for HBPhTFB and 46945 L mol^{-1} cm^{-1} for HMeOBPhTFB, calculated at their absorption maximum). The absorption profiles of the Eu^{3+}-β-diketonate complexes are found to be identical to that one observed for the free ligands, indicating that the singlet excited states of the ligands are not significantly affected upon coordination to the Eu^{3+} ion. However, a small blue shift that is detectable in the absorption maximum of all the complexes is a consequence of perturbation induced by the coordination of Eu^{3+} ion to the ligand.[4d,h,6g,24] The absorption coefficients for the complexes are three times larger than those of the free ligands, thus indicating the presence of three β-diketonate ligands in the coordination sphere of the lanthanide ion. Furthermore, the large molar absorption coefficients noted for the developed ligands disclose that the β-diketonate ligands have a strong potential to absorb light.

Table 3.1. Molar absorption coefficient for the ligands and their corresponding Eu^{3+} complexes **1-4**

Compounds	**λ_{max} (nm)**	**ε (L mol^{-1} cm^{-1})**
HMeOBPhTFB	358	46945
HBPhTFB	345	34463
Eu(MeOBPhTFB)$_3$(H$_2$O)(C$_2$H$_5$OH) (**1**)	345	143205
Eu(MeOBPhTFB)$_3$(TPY) (**2**)	345	148292
Eu(BPhTFB)$_3$(H$_2$O)(C$_2$H$_5$OH) (**3**)	340	102573
Eu(BPhTFB)$_3$(TPY) (**4**)	340	105064

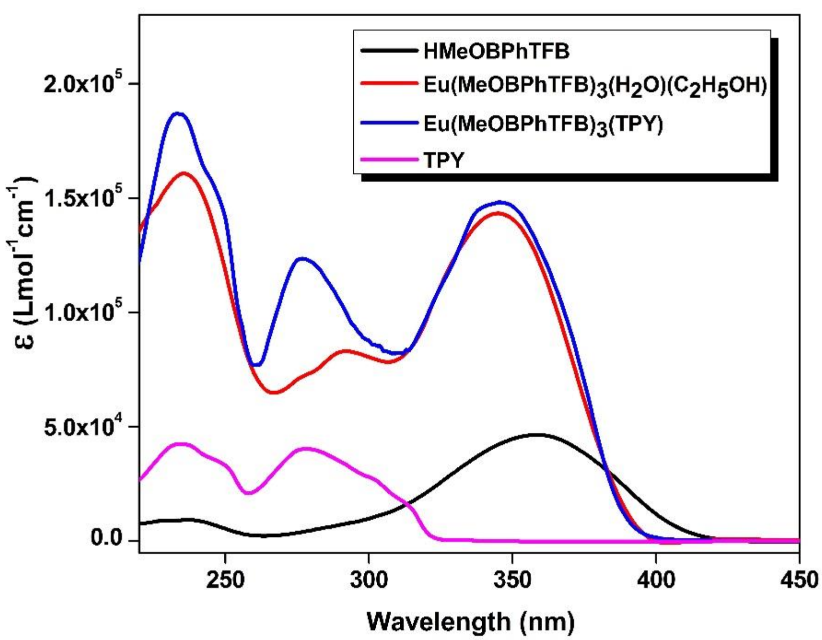

Figure 3.6. UV-visible absorption spectra of the ligands, HMeOBPhTFB, TPY and corresponding Eu^{3+} complexes (**1-2**) in THF (c = 5 × 10^{-6} M).

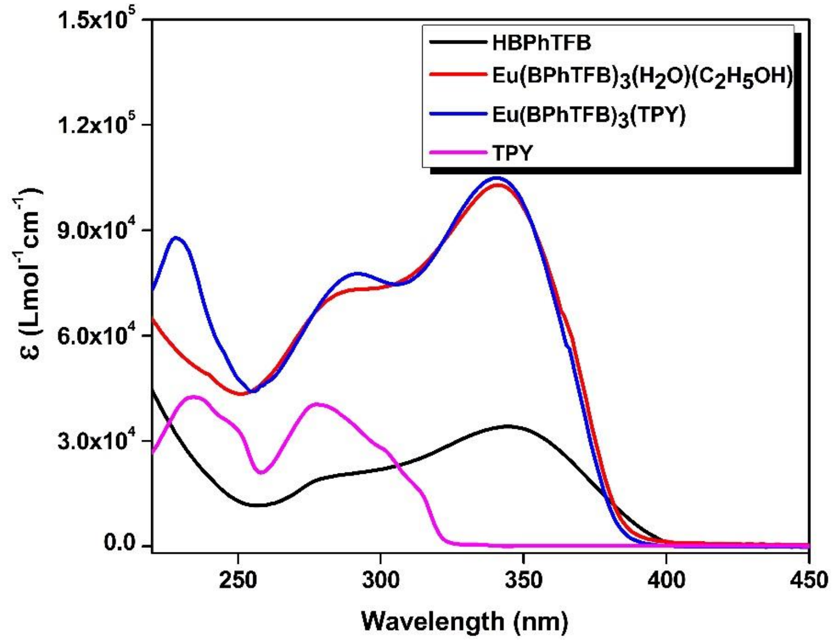

Figure 3.7. UV-visible absorption spectra of the ligands, HBPhTFB, TPY and corresponding Eu^{3+} complexes (**3**-**4**) in THF ($c = 5 \times 10^{-6}$ M).

3.4.3. Steady state photoluminescence

To understand the energy transfer mechanism in the developed Eu^{3+}-biphenyl based β-diketonate complexes it is required to determine the singlet and triplet energy levels of the β-diketonate ligands. The singlet (S_1) energy levels of these ligands are estimated by reference to the wavelengths of the UV–vis absorption edges of the Gd^{3+} biphenyl based β-diketonate complexes (**5** and **6**).[25] The relevant values are found to be 26178 cm^{-1} (382 nm) and 25641 cm^{-1} (390 nm) for HBPhTFB and HMeOBPhTFB, respectively (Figure 3.8). The triplet energy levels (T_1) of the developed β-diketonate ligands were calculated by reference to the lower wavelength emission edges (480 nm: 20833 cm^{-1}, 492 nm: 20325 cm^{-1} for HBPhTFB and HMeOBPhTFB, respectively) from the low-temperature phosphorescence spectra of the Gd^{3+} complexes of the pertinent β-

diketonates.[66-69] Because there is a large gap (32000 cm^{-1}) between the $^8S_{7/2}$ ground state and the first $^6P_{7/2}$ excited state of the Gd^{3+} ion, it cannot accept any energy from the first excited triplet state of the ligand *via* intramolecular ligand-to-metal energy transfer. Thus, the phosphorescence spectra of the Gd^{3+} complexes reveal the triplet energy levels of the *β*-diketonate ligand in the Eu^{3+} complexes. It is also noticed that the energy gap between the S_1 and T_1 levels are 5345, 5316 cm^{-1} for HBPhTFB and HMeOBPhTFB, respectively. These values are in accordance with the Reinhoudt's empirical rule,[5] that the intersystem crossing process becomes effective when $\Delta E(S_1\text{-}T_1)$ is around 5000 cm^{-1}. Thus, the intersystem crossing processes are efficient for these ligands. The energy gaps between the Eu^{3+} core ($^5D_0$ ~17250 cm^{-1}) and the donor ligand's T_1 levels turns out to be 3583, 3075 cm^{-1} for HBPhTFB and HMeOBPhTFB, respectively. According to the empirical rule pointed out by Latva, for an optimal ligand-to-metal energy transfer process $2500 < \Delta E(T_1\text{-}^5D_0) < 4000$ cm^{-1} for Eu^{3+}.[26] It is interesting to note that the triplet energy levels of the developed *β*-diketonate ligands lay above the energy of the main emitting level of $^5D_0$ for Eu^{3+}, thus demonstrate that these ligands can act as antenna molecules for the sensitization of Eu^{3+} ions.

The room-temperature (298 K) solid-state excitation spectra of Eu^{3+}-*β*-diketonate complexes (**1–4**) recorded by monitoring the intense $^5D_0 \rightarrow {}^7F_2$ transition of Eu^{3+} are depicted in Figures 3.9a and 3.10a, respectively. The excitation profiles of unsubstituted biphenyl based Eu^{3+} complexes **3** and **4** exhibit a broad band in the 300–475 nm region (centered at 382 nm) because of the π-π^* electronic transitions of the coordinated *β*-diketonate ligand. In addition, a sharp band corresponding to f–f transition is also seen at 464 nm ($^5D_2 \longleftarrow {}^7F_{0,1}$).[4e] Most importantly, in the case of Eu^{3+} complexes **1** and **2** upon substitution of electron-donating methoxy group at 4′ position of the biphenyl based β-diketonate ligand strikingly shifts the excitation window to visible region (300–490 nm) with an excitation maximum 400 nm. The red-shift observed in the excitation window can be attributed to the donating methoxy group on the phenyl ring, which allows the oxygen electrons as a part of the whole delocalization process and enhances conjugation of the chromophore molecule.[6j,10,12] These findings specify that methoxy- substituted biphenyl based β-diketonate Eu^{3+} complexes (**1** and **2**) are propitious red-emitting materials for luminescent applications such as bioimaging and solid-state lighting without UV radiation.

The emission spectra of Eu^{3+}-β-diketonate complexes (**1**–**4**) (Figures 3.9b and 3.10b) excited at their corresponding excitation maxima (λ_{exc} = 382 nm for **3** and **4** and 400 nm for **1** and **2**) show characteristics of the metal ion emissions in the 550–725 nm wavelength region, and displays well resolved peaks that are due to the transitions from the metal-centered $^5D_0$ excited state to the ^7F_J ground state multiplet. Maximum peak intensities at 579, 593, 615, 653 and 697 nm were noted for the J = 0, 1, 2, 3, 4 transitions, respectively. The so-called ‘hypersensitive transition’ (J = 2) observed at 615 nm is found to be intense, and is responsible for the observed red emission in these complexes. Further, the intensity of the $^5D_0 \rightarrow {}^7F_2$ transition (electric-dipole) is greater than that of the $^5D_0 \rightarrow {}^7F_1$ transition (magnetic-dipole), which indicates that the coordination environment of the Eu^{3+} ion is devoid of an inversion center.[6d,28-30] It can also be noted from the emission spectra that the luminescence intensity of the Eu^{3+} ternary complexes (**2** and **4**) significantly enhanced as compared to the Eu^{3+} binary complexes (**1** and **3**) by the displacement of solvent molecules from the complexes by the ancillary ligand terpyridine.[29-30] Further, no broad emission bands related to β-diketonate ligands are observed in the blue region, indicating the efficient energy transfer from the ligand to the emitting level of the metal ion. It is worth mentioning that the emission intensity specifically at 615 nm of the Eu^{3+} ternary complex (**2**) with a methoxy-substitution at the 4′ position (9.03×10^8) has been greatly enhanced (about three fold) as compared to Eu^{3+}-biphenyl based β-diketonate complex (**4**) without a methoxy substitution (3.05×10^8). This enhancement is easily understood by the modification of the molecular structure of the ligand. The substitution of 4′ positional hydrogen atom with methoxy moiety leads to increase in electron density in the biphenyl ring and thus increases the electron transition probability.[12-13] Based on their emission spectra, the CIE chromaticity coordinates (Figure 3.11) for all the Eu^{3+} complexes are calculated to be the same, $x = 0.67$ and $y = 0.32$, which are very close to the NTSC standard CIE values for red ($x = 0.67$, $y = 0.33$).[12,28b]

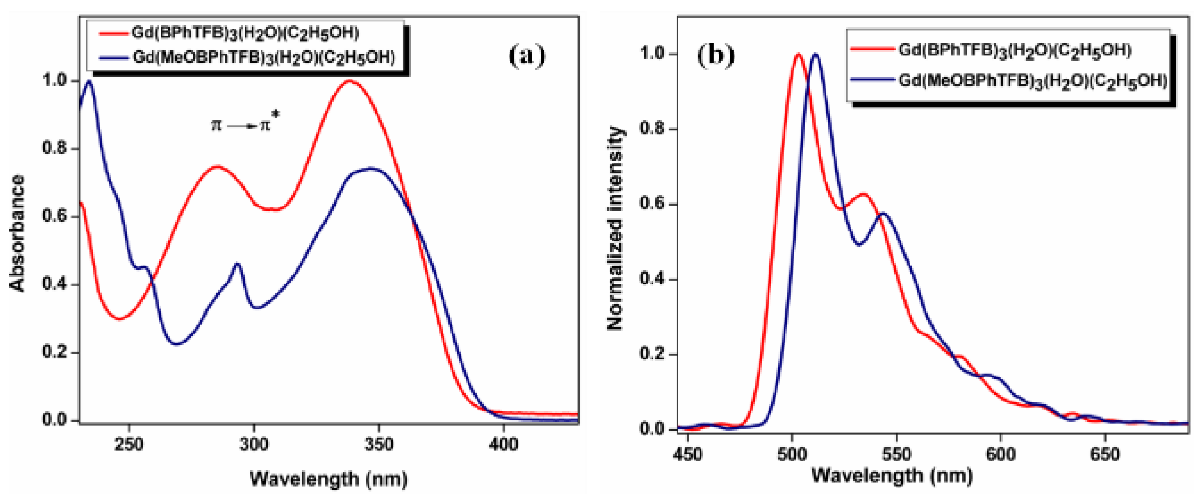

Figure 3.8. (a) UV-vis absorption spectra at 298K and (b) 77K phosphorescence spectra of the $Gd(BPhTFB)_3(H_2O)(C_2H_5OH)$ (red) and $Gd(MeOBPhTFB)_3(H_2O)(C_2H_5OH)$ (blue) complexes.

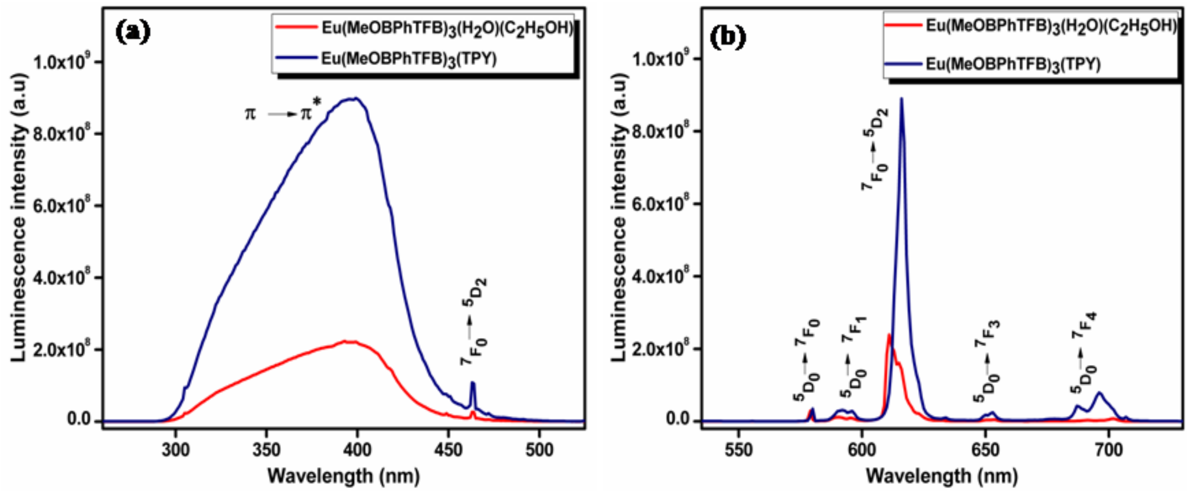

Figure 3.9. 298 K (a) excitation and (b) emission spectra of Eu^{3+} complexes $Eu(MeOBPhTFB)_3(H_2O)(C_2H_5OH)$ (**1**) and $Eu(MeOBPhTFB)_3(TPY)$ (**2**) in solid-state.

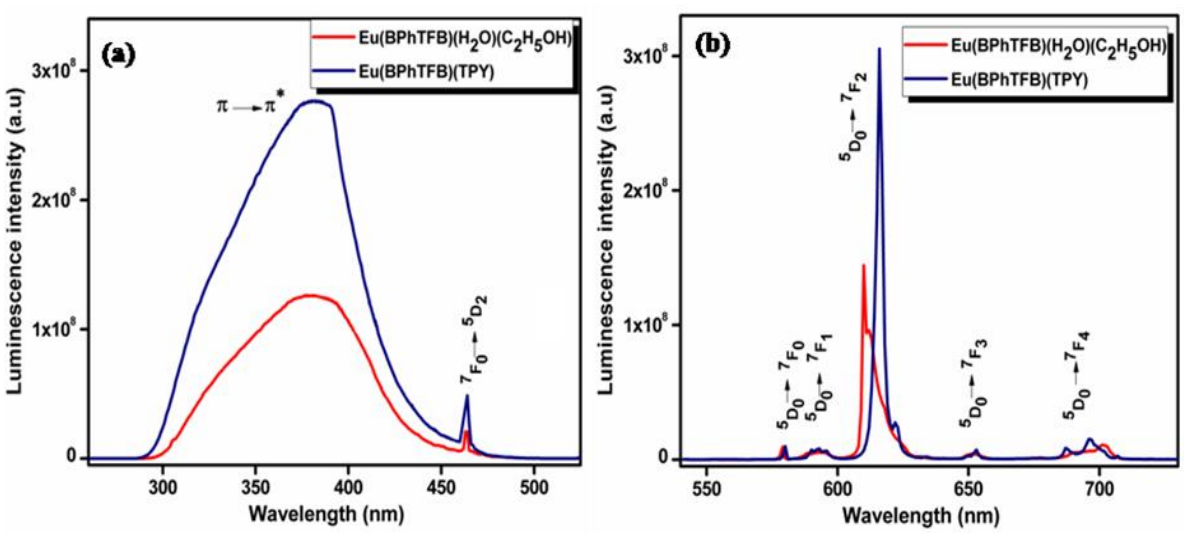

Figure 3.10. 298 K (a) excitation and (b) emission spectra (b) of Eu^{3+} complexes $Eu(BPhTFB)_3(H_2O)(C_2H_5OH)$ (**3**) and $Eu(BPhTFB)_3(TPY)$ (**4**) in solid-state.

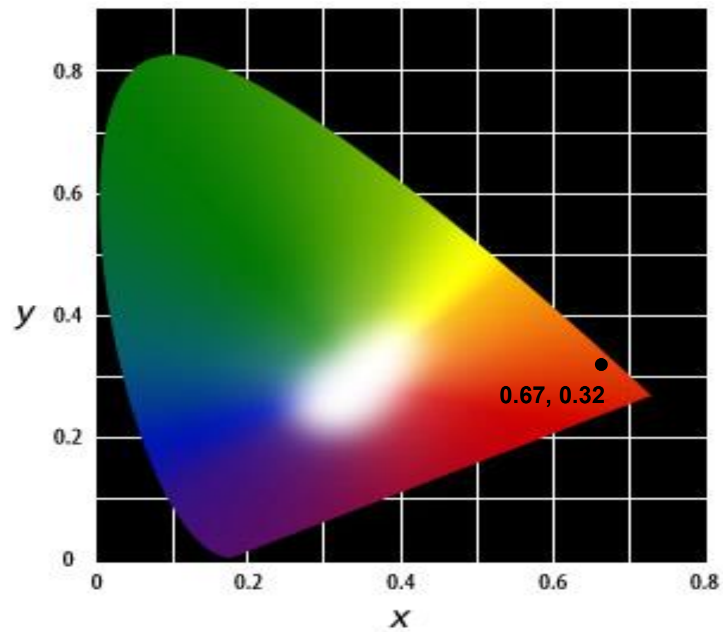

Figure 3.11. CIE chromaticity diagram showing the colour of the Eu(MeOBPhTFB)$_3$(TPY) complex (**2**).

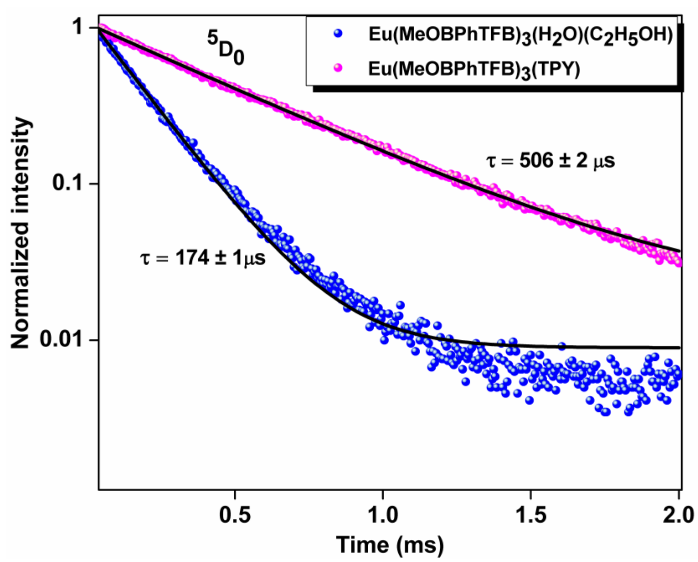

Figure 3.12. 298 K $^5D_0$ decay profiles for complexes Eu(MeOBPhTFB)$_3$(H_2O)(C_2H_5OH) (**1**) and Eu(MeOBPhTFB)$_3$(TPY) (**2**) (solid-state) (emission monitored around 615 nm). The straight lines are the best fits (r^2 = 0.999) considering single-exponential behavior.

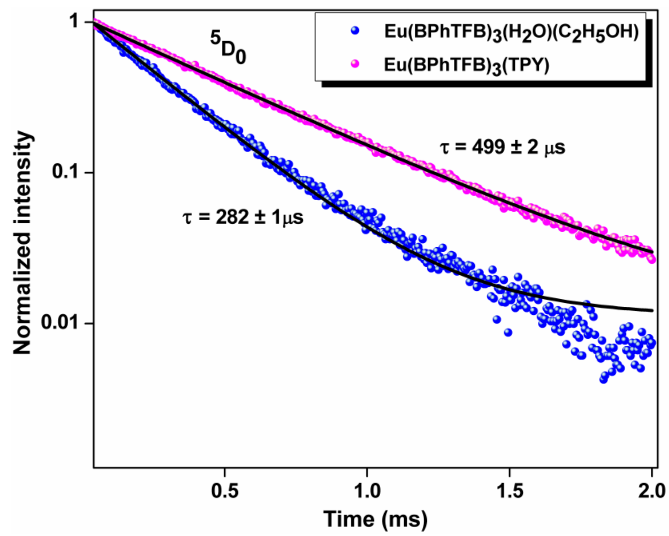

Figure 3.13. 298 K $^5D_0$ decay profiles for complexes Eu(BPhTFB)$_3$(H$_2$O)(C$_2$H$_5$OH) (**3**) & Eu(BPhTFB)$_3$(TPY) (**4**) (solid-state) (emission monitored around 615 nm). The straight lines are the best fits (r^2 = 0.999) considering single-exponential behavior.

In the current study, the various photophysical parameters summarized in Table 3.2 of the newly developed Eu^{3+} complexes were calculated by the procedures described in our previous publications.[7b,9,21a] The observed luminescence decay profiles (τ_{obs}) for all the Eu^{3+}-β-diketonate complexes at 298 K (Figures 3.12 and 3.13) are found to be single exponential functions, indicating the presence of only one emissive Eu^{3+} center.[9,20] The relatively shorter lifetime observed for binary Eu^{3+} complexes (**1** and **3**) may be caused by dominant non-radiative decay channels associated with the vibronic coupling due to the presence of solvent molecules, as well documented in many of the binary Eu^{3+}-β-diketonate complexes.[7-10,31] On the other hand, longer lifetime values have been noted for ternary Eu^{3+} complexes (**2** and **4**) because of the absence of solvent molecules. These trends are in good agreement with the observed radiative and non-radiative decay rates of the complexes (Table 3.2).

Table 3.2 The radiative (**A_{RAD}, s^{-1}**) and non-radiative (**A_{NR}, s^{-1}**) decay rates, $^5D_0$ lifetime (**τ_{obs}, μs**), intrinsic quantum yield (**Φ_{Ln}, %**), energy transfer efficiency (**Φ_{sen}, %**), overall quantum yield (**$\Phi_{overall}$, %**) and colour coordinates for Eu^{3+} complexes in the solid-state (λ_{exc} = 400 nm).

Compounds	**A_{RAD} (s^{-1})**	**A_{NR} (s^{-1})**	**τ_{obs} (μs)**	**Φ_{Ln} (%)**	**Φ_{sen} (%)**	**$\Phi_{overall}$ (%)**	**CIE$_{(x,y)}$**
$Eu(MeOBPhTFB)_3(H_2O)(C_2H_5OH)$ (**1**)	1152	4608	174 ± 1	20	95	19 ± 2	0.67, 0.32
$Eu(MeOBPhTFB)_3(TPY)$ (**2**)	1171	813	506 ± 2	59	~100	62 ± 6	0.67, 0.32
$Eu(BPhTFB)_3(H_2O)(C_2H_5OH)$ (**3**)	948	2698	282 ± 1	26	77	20 ± 2	0.66, 0.33
$Eu(BPhTFB)_3(TPY)$ (**4**)	1165	843	499 ± 2	58	91	53 ± 5	0.66, 0.33

The substitution of solvent molecules in the Eu^{3+}-tris(1-(4′-methoxy-[1,1′-biphenyl]-4-yl)-4,4,4-trifluoro-3-hydroxybut-2-en-1-one) complex **1** by a chelating ancillary ligand, 2,2′:6′,2′′-terpyridine leads to an approximately 3-fold enhancement in the absolute quantum yield (from 19 to 62%). The substantial contribution of the chelating terpyridine ligand to the overall sensitization of the Eu^{3+}-centered luminescence in **2** is confirmed by (i) an increase in the intrinsic quantum yield by a factor of 3, which results from removal of quenching effect of the O.H vibrations and (ii) the significant enhancement of Φ_{sens} from 95 to 100%. Furthermore, due to the extended conjugation induced by the substitution of the electron-donating methoxy group at 4′ position of biphenyl based *β*-diketonate ligand, Eu^{3+} complex **2** notably exhibits visible-light sensitized red luminescence with an overall quantum yield 62 ± 6% when excited at 400 nm. Indeed, this overall quantum yield also found to be superior to that of parent Eu^{3+} ternary complex ($\Phi_{overall}$ = 53 ± 5% at 400 nm). Most significantly, the overall quantum yield obtained in the present investigation is found to be promising as compared to many of the recently reported visible-light excited Eu^{3+}-β-diketonate complexes (Table 3.3).

Table 3.3. Comparison of the results of the current work with previous reports with respect to quantum yields ($\Phi_{overall}$, %) and excitation maxima (λ_{exc}, nm) of various Eu^{3+}-β-diketonate complexes.

S. No.	Publication	System	Solid-state quantum yield ($\Phi_{overall}/\lambda_{exc}$)
1	Current work	Visible-light excitable highly luminescent molecular plastic materials derived from Eu^{3+}-biphenyl based β-diketonate ternary complex and poly(methylmethacrylate).	62% at 400 nm
2	*Dalton Trans.*, 2015, **44**, 15924	Tuning of excitation wavelength in Eu^{3+}-aminophenyl based polyfluorinated β-diketonate complexes: Red-emitting Eu^{3+}-complex encapsulated in silica/polymer hybrid material excited by blue-light	40% at 400 nm
3	*RSC Adv.*, 2015, **5**, 90720	Achieving visible-light excitation in carbazole based Eu^{3+}–β-diketonate complexes *via* molecular engineering	42% at 400 nm
4	*Phys. Chem. Chem. Phys.* 2014, **16**, 695	Synthesis and photophysical properties of europium(III)–β-diketonate complexes applied in LEDs	24% at 425 nm
5	*Dalton Trans.* 2011, **40**, 3257	Tuning of the excitation wavelength from UV to visible region in Eu^{3+}-β-diketonate complexes: Comparison of theoretical and experimental photophysical properties	19% at 400 nm
7	*J. Mater. Chem. C,* 2013, **1**, 160	Visible-light excited red emitting luminescent nanocomposites derived from Eu^{3+}-phenathrene-based fluorinated β-diketonate complexes and multi-walled carbon nanotubes	75% at 415 nm
8	*J. Lumin.*, 2010, **130**, 35	A red europium(III) ternary complex for InGaN-based light-emitting diode	17% at 395 nm

3.4.4. Characterization and photophysical properties of $Eu(MeOBPhTFB)_3(TPY)$ doped PMMA polymer films

PMMA displays superior mechanical and optical properties that aid its application in optical devices. In addition, PMMA comprises carbonyl groups along with its carbon-chain that can strongly interact with Eu^{3+} ions and displace ligand water molecules. Therefore, in the present study visible-light excitable Eu^{3+}-tris(methoxy-substituted biphenyl-β-diketonate)(terpyridine) complex has been embedded into PMMA polymer films with a view to improving its mechanical and emission properties.[4g,16-17,32]

PMMA was doped with a ternary Eu^{3+} complex **2** in proportions of 3, 5, 7 and 9% (w/w), and characterized by FT-IR spectroscopy and the results are shown in Figure 3.14. For the PMMA film and the samples (PMMA@3Eu, PMMA@5Eu PMMA@7Eu PMMA@9Eu), the absorption bands noted in the range 2900–3000 cm^{-1} corresponds to CH vibrations. The band at 1726 cm^{-1} for the PMMA film belongs to CO vibration, whereas for the Eu^{3+} complex doped PMMA films, it shifts to 1733 cm^{-1}.[17,33] Figure 3.15 displays the TGA thermograms for PMMA film (solution casting) and PMMA film doped with 7% of Eu^{3+} complex (solution casting). It is observed that the solution cast PMMA film shows ~10% weight loss at 166 °C, which is attributed to the entrapped solvent removal from the polymer matrix. Further, Eu^{3+} complex doped PMMA film exhibits ~10% weight loss at 238 °C.[16] Thus, TGA infers that the Eu^{3+} complex doped films have improved thermal stability as compared to precursor PMMA film.

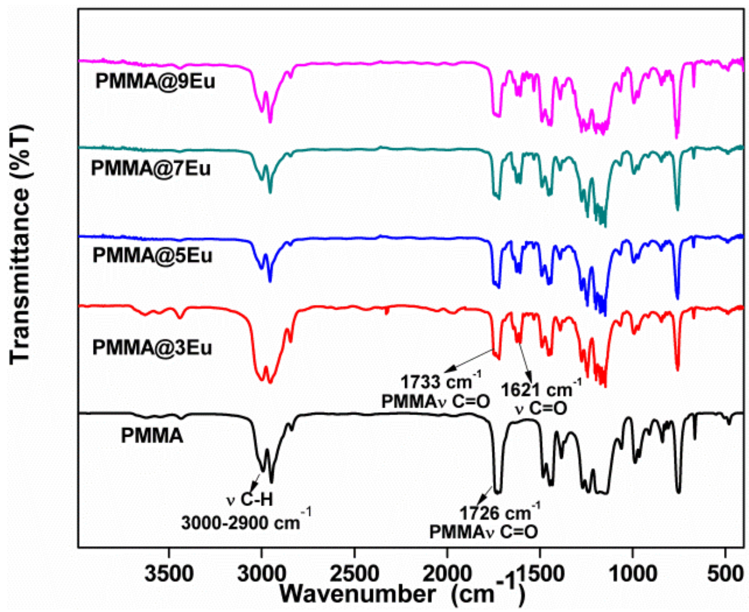

Figure 3.14. FT-IR Spectra for the PMMA film, 3, 5, 7 and 9 w/w% Eu(MeOBPhTFB)$_3$(TPY) doped PMMA films.

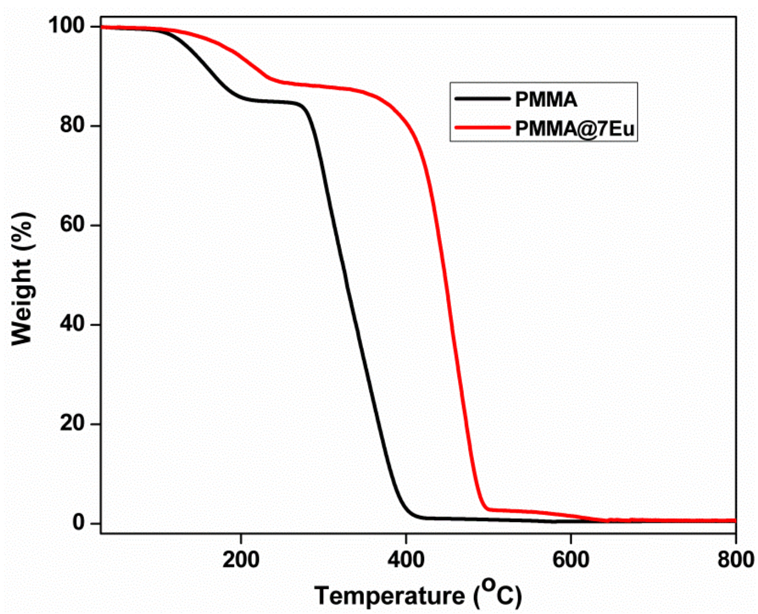

Figure 3.15. Thermogravimetric curves for pure PMMA (black) and Eu^{3+} complex doped PMMA film (PMMA@7Eu) (red).

Figure 3.16a illustrates the room temperature (298 K) excitation profiles of PMMA polymer films embedded with Eu^{3+} complex **2** at different concentrations (3, 5, 7 and 9 w/w%), by monitoring the emission at $^5D_0 \rightarrow {}^7F_2$ (615 nm) transition. The excitation spectra are dominated by an intense broad band in the region 300–450 nm (λ_{exc} = 385 nm) which can be ascribed to absorptions of both PMMA and methoxy-substituted biphenyl based *β*-diketonate ligand. However, the excitation spectra of the polymer film doped with complex **2** are blue-shifted (~15 nm) as compared to solid state spectrum of the Eu^{3+}complex **2.** This behavior may be due to a change of symmetry of the complex.[20] The emission spectra of PMMA doped with Eu^{3+} complex **2** at variety of concentrations (3, 5, 7 and 9 w/w%), and excited at 400 nm exhibit well defined emission peaks characteristic of the $^5D_0 \rightarrow {}^7F_J$ (J = 0–4) transition of Eu^{3+} ion in the wavelength region 550–715 nm (Figure 3.16).

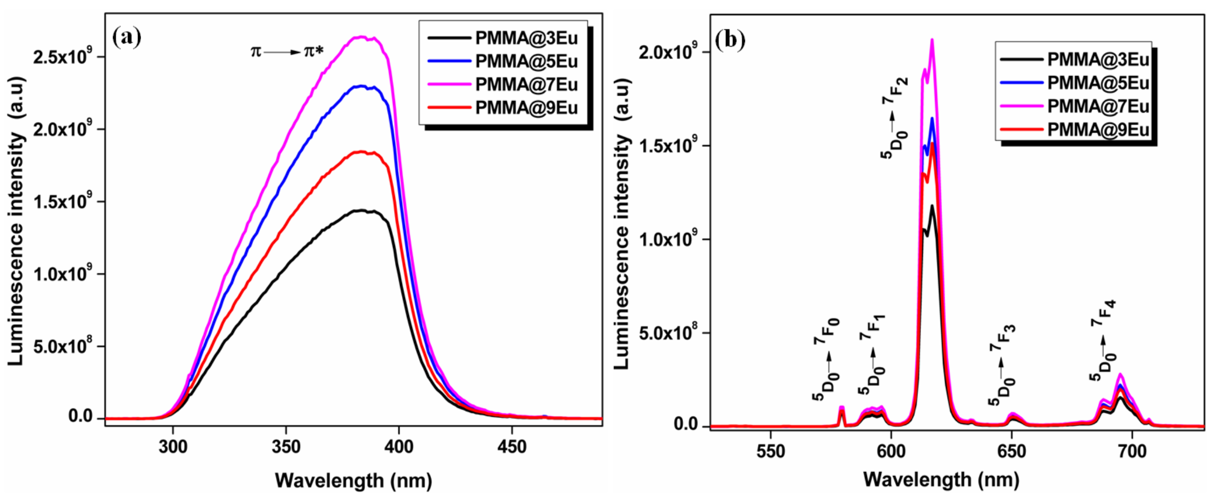

Figure 3.16. 298 K (a) excitation and (b) emission spectra of 3%, 5%, 7% and 9% $Eu(MeOBPhTFB)_3(TPY)$ doped PMMA films.

As can be noted from the emission profiles, the luminescence intensity at 615 nm increases with increase in the concentration of Eu^{3+} compound **2** and reaches a maximum at 7 w/w% (1.7 times). Further, an increase in the Eu^{3+} concentration decreases the luminescence intensity.[4d,20,23] This may be due to the energy transfer between the Eu^{3+} ions themselves is a non-radiative process, which is responsible for the decrease in the Eu^{3+} emission, especially at 9 w/w%. The overall quantum yield, radiative and non-radiative decay rates, intrinsic quantum yield and energy transfer efficiencies of the PMMA film doped with Eu^{3+} complex **2** at different concentration are summarized in Table 3.4. The overall quantum yield of the polymer films (75–79%) excited under blue- light (400 nm) was found to be remarkably enhanced as compared to the precursor Eu^{3+} complex **2** ($\Phi_{overall}$ = 62%).

Table 3.4 The radiative ($\boldsymbol{A_{RAD}}$, $\mathbf{s^{-1}}$) and non-radiative ($\boldsymbol{A_{NR}}$, $\mathbf{s^{-1}}$) decay rates, $^5D_0$ lifetime ($\boldsymbol{\tau_{obs}}$, **μs**), intrinsic quantum yield ($\boldsymbol{\Phi_{Ln}}$, **%**), energy transfer efficiency ($\boldsymbol{\Phi_{sen}}$, **%**), overall quantum yield ($\boldsymbol{\Phi_{overall}}$, **%**) of 3%, 5%, 7% and 9% Eu^{3+} complex doped PMMA films (λ_{exc} = 400 nm).

Compounds	$\boldsymbol{A_{RAD}}$ ($\mathbf{s^{-1}}$)	$\boldsymbol{A_{NR}}$ ($\mathbf{s^{-1}}$)	$\boldsymbol{\tau_{obs}}$ (**μs**)	$\boldsymbol{\Phi_{Ln}}$ (**%**)	$\boldsymbol{\Phi_{sen}}$ (**%**)	$\boldsymbol{\Phi_{overall}}$ (**%**)
PMMA@3Eu	994	280	788 ± 4	78	96	75 ± 8
PMMA@5Eu	972	290	792 ± 5	77	99	76 ± 8
PMMA@7Eu	980	230	823 ± 4	81	98	79 ± 8
PMMA@9Eu	982	420	714 ± 5	70	100	70 ± 7

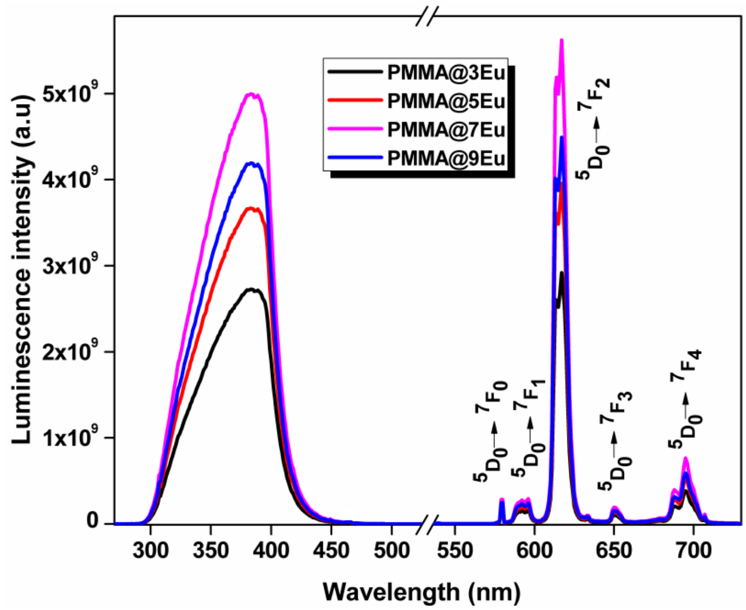

Figure 3.17. 298 K excitation and emission spectra of Eu^{3+} complexes doped PMMA films (λ_{ex} = 385 nm).

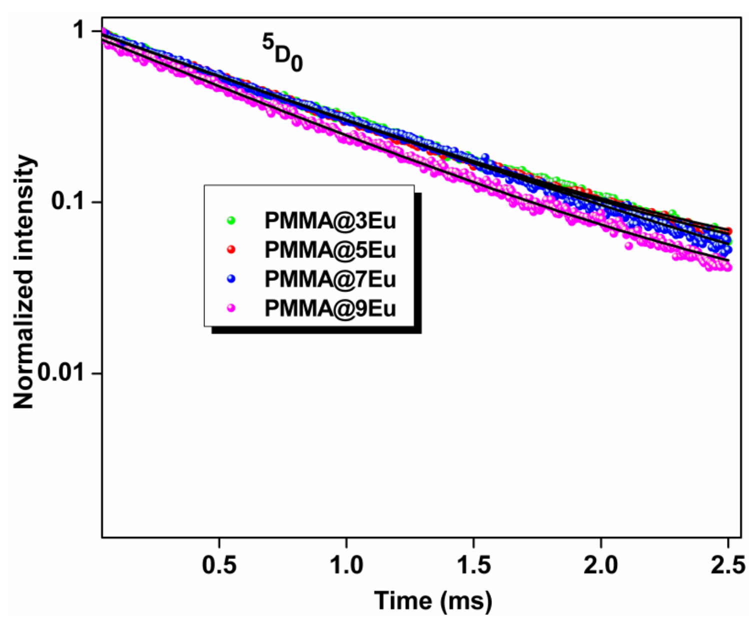

Figure 3.18. $^5D_0$ decay profiles for 3, 5, 7 and 9 w/w% $Eu(MeOBPhTFB)_3(TPY)$ doped PMMA films, where emission monitored around 615 nm. The straight lines are the best fits (r^2 = 0.999) considering single-exponential behavior.

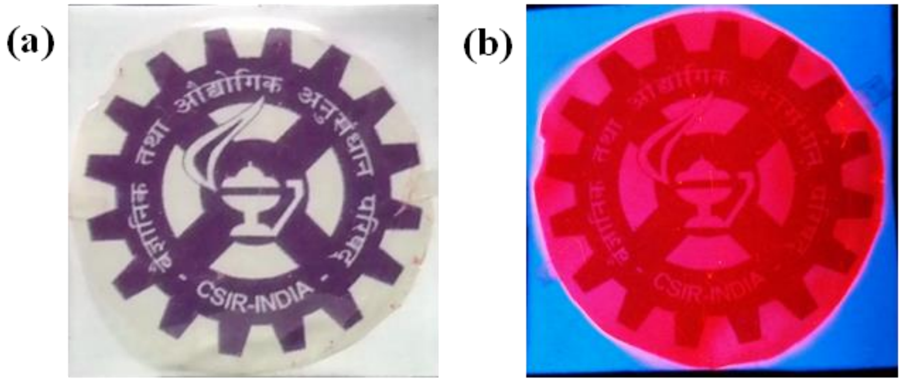

Figure 3.19. Photograph of the transparent PMMA film doped with 7 w/w% Eu(MeOBPhTFB)$_3$(TPY) a) before UV irradiation and b) after UV irradiation.

To the best of our knowledge, no reports have been seen in the open literature regarding investigations on the photophysical properties of Eu^{3+}-compounds doped PMMA polymer films, especially excited under visible-light, which exhibit exceptionally high photoluminescence quantum yields as noted in the current study. Further, the intrinsic quantum yields noted in the current hybrid polymer films are found to be exceptionally higher than that reported elsewhere[6e] for Eu^{3+}-tris(1-(4′-methoxy-[1,1′-biphenyl]-4-yl)-4,4,4-trifluoro-3-hydroxybut-2-en-1-one)(phen) complex doped into silicone rubber (38.8%). The quantum yields of the polymer films also have been calculated at the excitation maximum 385 nm and the corresponding excitation and emission profiles are given in Figure 3.17. Exceptionally very high quantum yield of about 98% has been noted for the 7 w/w% Eu^{3+}complex doped PMMA polymer film when excited at 385 nm. The $^5D_0$ lifetimes of the Eu^{3+} complex doped films (Figure 3.18) are higher than that of the parent compound **2**. In addition, the non-radiative decay rates have been significantly lowered in the doped films and hence the intrinsic quantum yields also greatly improved (78–81%) in the doped polymer films. The Photograph of the

PMMA film doped with 7 w/w% Eu(MeOBPhTFB)$_3$(TPY) under normal light and after UV irradiation is shown in Figure 3.19.

3.5. Conclusions

- In summary, a new visible-light excited (λ_{exc} = 400 nm) Eu^{3+}-tris(1-(4′-methoxy-[1,1′-biphenyl]-4-yl)-4,4,4-trifluoro-3-hydroxybut-2-en-1-one)(2,2':6',2"-terpyridine) ternary complex was developed, which display intense metal centered luminescence with remarkable solid-state quantum yield (62%). Consequently, the synthesized Eu^{3+} ternary complex may find potential applications in bioimaging and organic light emitting diodes (OLEDs).
- The newly designed Eu^{3+} ternary complex incorporated PMMA polymer films exhibit exceptionally high photoluminescence quantum yield under wide excitation wavelengths (PL quantum yield 98% at λ_{exc} = 385 nm and 79% at λ_{exc} = 400 nm). This indicates that the PMMA with high molecular weight enwraps the Eu^{3+} ternary complex and keeps the donor-acceptor close, which results in the effective intermolecular energy transfer and, consequently, the high quantum yields.
- The photoluminescence quantum yields noted for the Eu^{3+} compound doped PMMA polymer films under blue-light excitation are found to be promising as compared to earlier reports. Thus, the derived luminescent molecular plastic materials show considerable promise for use in polymer light emitting diodes and active polymer optical fibers.

3.6. References

1. (a) L. Wu, X. Qu, *Chem. Soc. Rev.,* 2015, **44,** 2963; (b) J.-C. G. Bünzli, *Chem. Rev.,* 2010, **110**, 2729; (c) H.-S. Peng, D. T. Chiu, *Chem. Soc. Rev.,* 2015, **44,** 4699; (d) O. S. Wolfbeis, *Chem. Soc. Rev.,* 2015, **44**, 4743; (e) A. J. Amoroso, S. J. A. Pope, *Chem. Soc. Rev.,* 2015, **44,** 4723.
2. (a) J. Feng, H. Zhang, *Chem. Soc. Rev.,* 2013, **42,** 387; (b) K. Binnemans, *Chem. Rev.,* 2009, **109**, 4283; (c) L. D. Carlos, R. A. S. Ferreira, V. D. Z. Bermudez, S. J. L. Ribeiro, *Adv. Mater.,* 2009, **21**, 509; (d) W. Guan, W. Zhou, J. Lu, C. Lu, *Chem. Soc. Rev*., 2015, **44**, 6981; (e) S. V. Eliseeva, J.-C. G. Bünzli, *Chem. Soc. Rev*., 2010, **39,** 189.
3. (a) S. I. Weissman, *J. Chem. Phys.,* 1942, **10**, 214; (b) J.-C. G. Bunzli, S. V. Eliseeva, *Springer Ser. Fluoresc.,* 2011, **7**, 1; (c) K. Binnemans, *Handb. Phys. Chem. Rare Earths.,* 2005, **35**, 107; (d) Y. Ma, Y. Wang, *Coord. Chem. Rev.,* 2010, **254**, 972; (e) J.-C. G. Bünzli, C. Piguet, *Chem. Soc. Rev.,* 2005, **34**, 1048; (f) P. A. Tanner, C. K. Duan, *Coord. Chem. Rev.,* 2010, **254**, 3026; (g) L. Armelao, S. Quici, F. Barigelletti, G. Accorsi, G. Bottaro, M. Cavazzini, E. Tondello, *Coord. Chem. Rev.,* 2010, **254,** 487.
4. (a) R. Pavithran, N. S. Saleesh Kumar, S. Biju, M. L. P. Reddy, S. A. Junior, and R. O. Freire, *Inorg. Chem.,* 2006, **45**, 2184; (b) D. B. A. Raj, S. Biju, M. L. P. Reddy, *Inorg. Chem.,* 2008, **47,** 8091; (c) S. Biju, D. B. A. Raj, M. L. P. Reddy, B. M. Kariuki, *Inorg. Chem.,* 2006, **45,** 10651; (d) D. B. A. Raj, B. Francis, M. L. P. Reddy, R. R. Butorac, V. M. Lynch, A. H. Cowley, *Inorg. Chem.,* 2010, **49**, 9055; (e) D. B. A. Raj, S. Biju, M. L. P. Reddy, *Dalton Trans.,* 2009, 7519; (f) S. Biju, M. L. P. Reddy, A. H. Cowley, K. V. Vasudevan, *Cryst. Growth Des.,* 2009, **9,** 3562; (g) E. S. Andreiadis, N. Gauthier, D.

Imbert, R. Demadrille, J. Pecaut, M. Mazzanti, *Inorg. Chem.,* 2013, **52**, 14382; (h) J. Shi, Y. Hou, W. Chu, X. Shi, H. Gu, B. Wang, Z. Sun, *Inorg. Chem.,* 2013, **52**, 5013; (i) C. C. L. Pereira, S. Dias, I. Coutinho, J. P. Leal, L. C. Branco, C. A. T. Laia, *Inorg. Chem.,* 2013, **52,** 3755; (j) C. Freund, W. Porzio, U. Giovanella, F. Vignali, M. Pasini, S. Destri, A. Mech, S. Di Pietro, L. Di Bari, P. Mineo, *Inorg. Chem.,* 2011, **50,** 5417.

5. F. J. Steemers, W. Verboom, D. N. Reinhoudt, E. B. van der Tol, J. W. Verhoeven, *J. Am. Chem. Soc.,* 1995, **117**, 9408.
6. (a) L. Jiang, J. Wu, W. Guilan, Z. Ye, W. Zhang, D. Jin, J. Yuan, J. Piper, *Anal. Chem.,* 2010, **82,** 2529; (b) J. Wu, Z. Ye, G. Wang, D. Jin, J. Yuan, Y. Guan, J. Piper, *J. Mater. Chem.,* 2009, **19**, 1258; (c) J. Wu, G. Wang, D. Jin, J. Yuan, Y. Guan, J. Piper, *Chem. Commun.,* 2008, 365; (d) M. Shi, C. Ding, J. Dong, H. Wang, Y. Tian, Z. Hu, *Phys. Chem. Chem. Phys.,* 2009, **11,** 5119; (d) P. He, H. H. Wang, S. G. Liu, J. X. Shi, G. Wang, M. L. Gong, *Inorg. Chem.,* 2009, **48**, 11382; (e) M. H. V. Werts, M. A. Duin, J.W. Hofstraat, J. W. Verhoeven, *Chem. Commun.,* 1999, 799; (f) W. Deng, D. Jin, K. Drozdowicz-Tomsia, J. Yuan, E. M. Goldys, *Langmuir,* 2010, **26**, 10036; (g) A. W. Woodward, A. Frazer, A. R. Morales, J. Yu, A. F. Moore, A. D. Campiglia, E. V. Jucov, T. V. Timofeeva, K. D. Belfield, *Dalton Trans.*, 2014, **43**, 16626; (h) T. Valta, E. M. Puputti, I. Hyppänen, J. Kankare, H. Takalo, T. Soukka, *Anal. Chem.,* 2012, **84**, 7708; (i) L. Tian, Z. Dai, Z. Ye, B. Song, J. Yuan, *Analyst.,* 2014, **139**, 1162; (j) G. Shao, H. Yu, N. Zhang, Y. He, K. Feng, X. Yang, R. Cao, M. Gong, *Phys. Chem. Chem. Phys.,* 2014, **16,** 695.
7. (a) M. L. P. Reddy, V. Divya, R. Pavithran, *Dalton Trans.,* 2013, **44,** 15249; (b) V. Divya, R. O. Freire, M. L. P. Reddy, *Dalton Trans.,* 2011, **40,** 3257.
8. V. Divya, M. L. P. Reddy, *J. Mater. Chem. C.,* 2013, **1**, 160.

9. T. V. Usha Gangan, M. L. P. Reddy, *Dalton Trans.,* 2015, **44**, 15924.

10. B. Francis, C. Heering, R.O. Freire, M. L. P. Reddy, C. Janiak, *RSC Adv.,* 2015, **5**, 90720.

11. (a) H. Zhang, B. Yang, Y. Zheng, G. Yang, L. Ye, Y. Ma, X. Chen, *J. Phys. Chem. B,* 2014, **108,** 9571; (b) D.-D. Kong, L.-S. Xue, R. Jang, B. Liu, X.-G. Meng, S. Jin, Y-P. Ou, X. Hao, S.-H. Liu, *Chem. - A Eur. J.,* 2015, **21**, 9895; (c) A. Specht, F. Bolze, L. Donato, C. Herbivo, S. Charon, D. Warther, S. Gug, J.-F Nicoud, M. Goeldner, *Photochem. Photobiol. Sci.,* 2012, **11**, 578; (d) J. Wang, G. Cooper, D. Tulumello, A. P. Hitchcock, *J. Phys. Chem. A.,* 2005, **109**, 10886.

12. P. He, H. H. Wang, H. G. Yan, W. Hu, J. X. Shi, M.L. Gong, *Dalton Trans.,* 2010, **39**, 8919.

13. E. Cogné-Laage, J. F. Allemand, O. Ruel, J. B. Baudin, V. Croquette, M. Blanchard-Desce, L. Jullien, *Chem. - A Eur. J.,* 2004, **10**, 1445.

14. A. S. Chauvin, F. Gumy, I. Matsubayashi, Y. Hasegawa, J.-C.G. Bünzli, *Eur. J. Inorg. Chem.,* 2006, 473.

15. L. N. Sun, J. B. Yu, G. L. Zheng, H. J. Zhang, Q. G. Meng, C. Y. Peng, L.-S. Fu, F.-Y Liu, Y.-N Yu, *Eur. J. Inorg. Chem.,* 2006, 3962.

16. J. Kai, M. C. F. C. Felinto, L. A. O. Nunes, O. L. Malta, H. F. Brito, *J. Mater. Chem.,* 2011, **21,** 3796.

17. E. B. Gibelli, J. Kai, E. E. S. Teotonio, O. L. Malta, M. C. F. C. Felinto, H. F. Brito, *J. Photochem. Photobiol. A Chem.,* 2013, **251,** 154.

18. S. Biju, R. O. Freire, Y.K. Eom, R. Scopelliti, J.-C.G. Bünzli, H. K. Kim, *Inorg. Chem.,* 2014, **53,** 8407.

19. S. Biju, Y. K. Eom, J.-C. G. Bünzli, H. K. Kim, *J. Mater. Chem. C.,* 2013, **1**, 6935.

20. S. Sivakumar, M. L. P. Reddy, *J. Mater. Chem.,* 2012, **22**, 10852.

21. (a) A. R. Ramya, D. Sharma, S. Natarajan, M. L. P. Reddy, *Inorg. Chem.,* 2012, **51**, 8818; (b) A. R. Ramya, M. L. P. Reddy, A. H. Cowley, K. V. Vasudevan, *Inorg. Chem.,* 2010, **49**, 2407; (c) B. L. Pålsson, A. P. Monkman, *Adv. Mater.,* 2002, **14,** 757–758.
22. (a) V. Divya, V. Sankar, K. G. Raghu, M. L. P. Reddy, *Dalton Trans.,* 2013, 42, 12317–12323; (b) D. A. Turchetti, M. M. Nolasco, D. Szczerbowski, L. D. Carlos, L. C. Akcelrud, *Phys. Chem. Chem. Phys.,* 2015, 17, 26238.
23. T. M. George, M. J. Sajan, N. Gopakumar, M. L. P. Reddy, *J. Photochem. Photobiol. A: Chem.,* 2016, **317**, 88.
24. (a) A. Bellusci, G. Barberio, A. Crispini, M. Ghedini, M. La Deda, D. Pucci, *Inorg. Chem.,* 2005, **44**, 1818; (b) H.-F. Li, P.-F. Yan, P. Chen, Y. Wang, H. Xu, G.-M. Li, *Dalton Trans.,* 2012, **41**, 900.
25. (a) S. I. Klink, L. Grave, D. N. Reinhoudt, F. C. J. M. Van Veggel, *J. Phys. Chem. A,* 2000, **104**, 5457; (b) M. Shi, F. Li, T. Yi, D. Zhang, H. Hu, C. Huang, *Inorg. Chem.,* 2005, **44,** 8929; (c) H. Xin, M. Shi, X. C. Gao, Y. Y. Huang, Z. L. Gong, D. B. Nie, H. Cao, Z. Q. Bian, F. Y. Li, C. H. Huang, *J. Phys. Chem. B.,* 2004, **108**, 10796; (d) L. M. Ying, A. Yu, X. Zhao, Q. Li, D. Zhou, C. Huang, *J. Phys. Chem.,* 1996, **100**, 18387.
26. M. Latva, H. Takalo, V.-M. Mukkala, C. Matachescu, J. C. R.-Ubis, J. Kankarea, *J. Lumin.,* 1997, **75**, 149.
27. (a) N. M. Shavaleev, R. Scopelliti, F. Gumy, J.-C.G. Bunzli, *Inorg. Chem.,* 2009, **48**, 6178; (b) T. D. Pasatoiu, A. M. Madalan, M. U. Kumke, C. Tiseanu, M. Andruh, *Inorg. Chem.,* 2010, **49**, 2310.
28. (a) E. S. Andreiadis, N. Gauthier, D. Imbert, R. Demadrille, J. Pe, *Inorg. Chem.,* 2013, **52**, 14382-14390; (b) Z. Wang, H. Liang, L. Zhou, H. Wu, M. Gong, Q. Su, *Chem. Phys.*

Lett., 2005, **412**, 313.

29. (a) S. V. Eliseeva, D. N. Pleshkov, K. A. Lyssenko, L. S. Lepnev, J.-C. G. Bünzli, N. P. Kuzmina, *Inorg. Chem.,* 2011, **50**, 5137; (b) A. J. Amoroso, M.W. Burrows, R. Haigh, M. Hatcher, M. Jones, U. Kynast, K. M. A. Malik, D. Sendor, *Dalton Trans.,* 2007, 1630.
30. (a) N. M. Shavaleev, S. V. Eliseeva, R. Scopelliti, J.-C.G. Bünzli, *Inorg. Chem.,* 2015, **54**, 9166; (b) N. M. Shavaleev, S. V. Eliseeva, R. Scopelliti, J.-C. G. Bünzli, *Inorg. Chem.,* 2010, **49**, 3927.
31. A. Dossing, *Eur. J. Inorg. Chem.,* 2005, 1425.
32. (a) G. Zucchi, V. Murugesan, D. Tondelier, D. Aldakov, T. Jeon, F. Yang, P. Thuery, M. Ephritikhine, B. Geffroy, *Inorg. Chem.,* 2011, **50**, 4851; (b) A. K. Singh, S. K. Singh, H. Mishra, R. Prakash, S. B. Rai, *J. Phys. Chem. B,* 2010, **114**, 13042; (c) W. Li, P. Yan, G. Hou, H. Li, G. Li, *Dalton Trans.,* 2013, **42**, 11537.
33. H.-J. Zhang, R.-Q. Fan, X.-M. Wang, P. Wang, Y.-L. Wang, Y.-L. Yang, *Dalton Trans.,* 2015, **44**, 2871.
34. F. Xie, H. Liang, G. Zhong, F. Deng, *Optoelectron. Adv. Mat.,* 2010, **4**, 685.

Chapter 4

Synthesis, characterization and photoluminescence properties of Eu^{3+}-β-diketonate complexes derived from 3-hydroxy-1-(4-methoxyphenyl)-3-(naphthalen-2-yl)prop-2-en-1-one and various bidentate nitrogen donors

4.1. Abstract

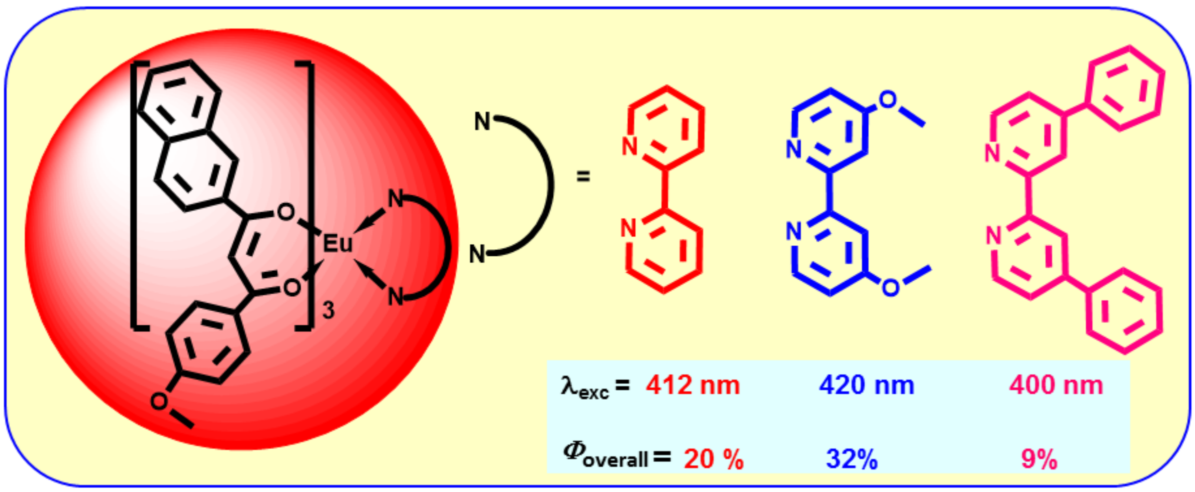

In this work, a visible-light excitable β-diketonate ligand, 3-hydroxy-1-(4-methoxyphenyl)-3-(naphthalen-2-yl)prop-2-en-1-one (HMeOPNP) was synthesized and utilized for the construction of a series of new Eu^{3+} *complexes of the general formula* $Eu(MeOPNP)_3(L)$ *[where L =* H_2O*, 2,2-bipyridine (BPY), 4,4'-dimethoxy-2,2-bipyridine (MeOBPY) and 4,4'-diphenyl-2,2-bipyridine (PhBPY)] in the presence and the absence of various derivatives of bipyridines as ancillary ligands. The designed* Eu^{3+} *complexes have been characterized by various spectroscopic techniques and investigated their photophysical properties with a view to understanding the structure–property relationships in these systems. The*

substitution of conjugated naphthyl moiety as well as methoxyphenyl group at 1,3-positions, respectively of the β-diketonate ligand notably extended the excitation window of the binary complex Eu(MeOPNP)$_3$(H$_2$O)$_2$ to visible region (λ_{exc} = 410 nm) with a quantum yield of 6 %. In the presence of an electron-donating methoxy substituted bipyridine as an ancillary ligand, the excitation window of Eu(MeOPNP)$_3$(MeOBPY) has been further shifted to longer wavelengths in the visible region [(λ_{exc} = 420 nm; $\Phi_{overall}$ = 32%)] with an enhanced luminescence intensity as compared to unsubstituted ternary complex Eu(MeOPNP)$_3$(BPY) [(λ_{exc} = 412 nm; $\Phi_{overall}$ = 20%)]. The red-shifted excitation window is attributed to the presence of donating methoxy group, which allows the oxygen electrons to be a part of the whole delocalized system through resonance and enhances the conjugation of the chromophore. On the contrary, when electron-withdrawing phenyl groups substituted bipyridine used as an ancillary ligand, the excitation window of Eu(MeOPNP)$_3$(PhBPY) has been drastically shifted to the lower wavelength region (λ_{exc} = 400 nm) with diminished quantum yield ($\Phi_{overall}$ = 9%) as compared to Eu(MeOPNP)$_3$(BPY). This may be due to the fact that the bulky phenyl substituents on the 4,4'-position of the bipyridine system severely hinders co-planarity and as a result attenuate any extended π-interactions in this system. As an integral part of this work, the photophysical properties of the visible light excitable Eu^{3+} complex, Eu(MeOPNP)$_3$(MeOBPY) was investigated under biologically relevant pH conditions [pH 7.4, % DMSO: % PBS = 1: 99; c = 1 x 10^{-4} M].

Communicated to Journal of Photochemistry and Photobiology A: Chemistry

4.2. Introduction

Since Kido reported the Eu^{3+}-β-diketonate complex-based electroluminescence devices in 1991,[1] many Eu^{3+}-β-diketonate complexes have received great interest due to their characteristic luminescence properties and extremely sharp, intense emission in the visible region.[2-4] However, the excitation window appears to be limited to the near UV region in most of the popular Eu^{3+}-β-diketonate systems due to the energy constraints posed by the photophysics of sensitized Eu^{3+} luminescence.[5] Therefore, one of the growing challenges in the study of luminescent europium complexes is to develop visible-light excitable systems, which may find potential applications in fluorescence-based bioassays.

Polycyclic arene such as naphthalene has an intense π- π stacking and interacting tendency owing to its plane and enlarged π-conjugation system, it is considered to be favorable to enhance molecular interaction and charge transport by directed molecular self-assembly.[6] The increased π-conjugation in the chromophoric molecule red-shift the absorbance spectra and allows visible light absorption, which is less phototoxic compared to higher energy UV excitation.[7] Therefore, previously naphthalene appended chromophoric ligands have been utilized successfully in optoelectronic lanthanide complexes[8] and in visible-light absorbers for temperature sensitive Eu^{3+} complexes.[9] Compared to phenyl moiety, the methoxyphenyl counterpart has the same chemical structure except that the later has an electron-donating methoxy group on the benzene ring to explore the substituent effect.[10] With the above considerations, in the present work, in order to explore the effect of the appending planar π-system as well as electron-donating methoxy group, a β-diketonate ligand namely, 3-hydroxy-1-(4-

methoxyphenyl)-3-(naphthalen-2-yl)prop-2-en-1-one has been designed and utilized for the construction of a series of coordination complexes of Eu^{3+} and investigated their photophysical properties.

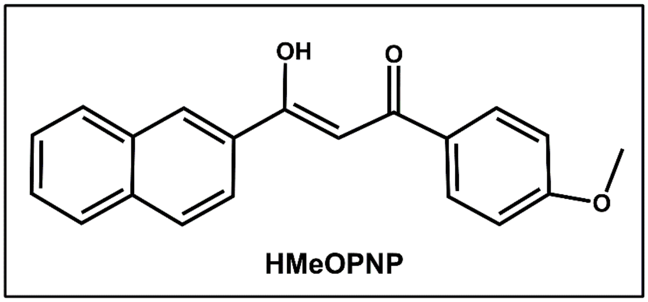

Figure 4.1. Structures of the β-diketonate ligand.

Over the last thirty years 2,2'-bipyridine complexes of virtually every metal ion in the periodic table have been described. This chelating ligand presents two nitrogen atoms to the metal centre in an almost identical configuration, with only the rotation in the pyridyl - pyridyl bond being restricted upon complex formation. This results in extremely stable species, even with the more labile metal ions.[11] Also it is highly possible to tailor desirable optoelectronic properties of such molecules by manipulation of the parent chromophore, which includes conjugation length control and the introduction of electron donating or withdrawing groups into the chemical structure.[12] These factors motivated to develop various derivatives of 2,2'-bipyridine ligand by introducing electron-withdrawing and electron-donating group at 4,4'-position and utilize as ancillary ligand in Eu^{3+}-β-diketonate complexes with an aim to displace successfully water molecules from the coordination sphere of the hydrated Eu^{3+}-β-diketonate complexes. In the current study, a series of ternary Eu^{3+} complexes have been isolated, characterized and investigated their photophysical properties with a purpose of studying the structure-property relationships among these complexes.

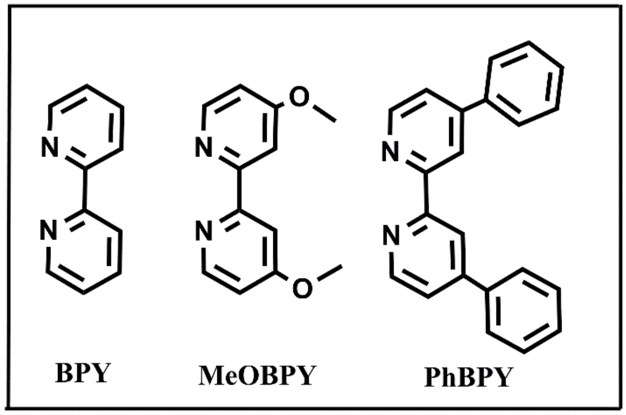

Figure 4.2. Structures of the ancillary ligands.

4.3. Experimental Section

4.3.1. Materials and instrumentations

All the reagents were used as received without further purification and are listed here: Eu^{3+} nitrate hexahydrate, 99.9% (Alfa Aesar); gadolinium(III) nitrate hexahydrate, 99.999% (Sigma-Aldrich); lanthanum(III) nitrate hexahydrate, 99.99% (Alfa Aesar); 2-Naphthoic acid, >98% (TCI Chemicals); 4-methoxyacetophenone, 99% (Sigma-Aldrich); sodium hydride 60% dispersion in mineral oil (Sigma-Aldrich); 2,2′-bipyridine, 99% (Sigma-Aldrich); 4,4′-dimethoxy-2,2′-bipyridine, 97% (Sigma-Aldrich); 4,4′-diphenyl-2,2′-bipyridine, technical grade (Sigma-Aldrich).

Elementar - vario MICRO cube elemental analyzer was used to perform Elemental analyses. FT-IR spectra were carried out on a Perkin-Elmer Spectrum two FT-IR spectrometer using KBr pellets. The synthesized compounds were characterized by ^{1}H

NMR (500 MHz) and ^{13}C NMR (125.7 MHz) using a Bruker 500 MHz NMR spectrometer in chloroform-*d* solution. The chemical shifts are reported in ppm reference to tetramethylsilane, $SiMe_4$ for ^{1}H NMR and ^{13}C NMR spectra. Electro spray ionization (ESI) mass spectra were recorded on a Thermo Scientific Exactive Benchtop LC/MS Orbitrap Mass Spectrometer and the TG/DTA-6200 (SII Nano Technology Inc., Japan) was used to study the thermal stability of the prepared complexes. The absorbance of the ligands and the complexes were measured in THF solution on a UV-vis spectrophotometer (Shimadzu, UV-2450). The solid-state absorption spectral studies of the β-diketonate ligand and the europium complexes were carried out in a UV–vis Spectrophotometer (Shimadzu UV-3600 with an integrating sphere attachment, ISR- 2200) using barium sulfate as a reference (the reflectance is monitored and converted to absorbance by Kubelka-Munk equation). The photoluminescence (PL) spectra were recorded on a Spex-Fluorolog FL22 spectrofluorimeter equipped with a double grating 0.22 m Spex 1680 monochromator and a 450W Xe lamp as the excitation source operating in the front face mode. The lifetime and phosphorescence measurements were carried out by using a SPEX 1040 D phosphorimeter. The overall quantum yield ($\Phi_{overall}$) was measured using an integrating sphere in a SPEX Fluorolog spectrofluorimeter as reported in the literature. The estimated error for the quantum yields is ± 10%.[13]

All the spectroscopic measurements were also performed in buffer solution at pH = 7.4 [% DMSO: % PBS = 1: 99; $c = 1 \times 10^{-4}$ M] at room temperature. The overall quantum yields of the sensitized Eu^{3+} emission of the complexes were measured in a DMSO: PBS solution at room temperature relative to a reference solution of quinine sulfate in 1 N H_2SO_4 ($\Phi_{overall}$ = 54.6%). Corrections were made for the refractive index of the solvent.

All solvents were of the spectroscopic grade. The overall luminescence quantum yields of the complexes were calculated according to the well-known equation,[14]

$$\Phi_{overall} = \frac{n^2 A_{ref} I}{n_{ref}^2 A I_{ref}} \Phi_{ref}$$

where *n*, *A*, and *I* denote the refractive index of the solvent, the absorbance at the excitation wavelength and the area of the emission spectrum, respectively, and Φ_{ref} represents the quantum yield of the standard quinine sulfate solution. The subscript ref denotes the reference, and the absence of a subscript implies an unknown sample. The refractive index is assumed to be equivalent to that of the pure solvent: 1.33 for water at room temperature. All data reported are averages of at least three independent measurements.

4.3.2. Synthetic procedure for the ligand

Synthesis of methyl 2-naphthoate: 2 g of 2-naphthoic acid was dissolved in 20 ml methanol and added catalytic amounts of conc. H_2SO_4. The reaction mixture was then stirred at 70 °C for 48 h (Scheme 4.1). After cooling to room temperature, the mixture was poured into ice-cold water, ester precipitated out, filtered, dried and used for further synthesis step.

Yield: 92%. ^{1}H NMR ($CDCl_3$, 500 MHz): δ (ppm): 8.02 (s, 1H), 7.96 (d, 1H, *J* = 7.5 Hz), 7.89 (d, 1H, *J* = 8.5 Hz), 7.87 (d, 2H, *J* = 7.5 Hz), 7.59 (t, 2H, *J* = 8 Hz), 3.98 (s, 3H). $^{13}C\{^{1}H\}$ NMR (125 MHz, $CDCl_3$) δ (ppm): 167.29, 135.52, 132.50, 131.07, 129.36, 128.24, 127.76, 127.40, 126.64, 125.23, 77.26-76.76 ($CDCl_3$), 52.13. *m/z* = 187 $(M+H)^+$.

Synthesis of 3-hydroxy-1-(4-methoxyphenyl)-3-(naphthalen-2-yl)prop-2-en-1-one (HMeOPNP): The ligand was synthesized by Claisen condensation reaction between methyl 2-naphthoate and 4-methoxyacetophenone as reported in literature (Scheme 4.1).[4]

Yield: 69%. Elemental analysis (%): calculated for $C_{20}H_{16}O_3$ (304.11): C 78.93, H 5.30; Found: C 78.73, H 5.32. ^{1}H NMR ($CDCl_3$, 500 MHz) δ (ppm): 17.09 (broad, enol–OH), 8.52 (s, 1H), 8.01 (m, 4H), 7.90 (m, 2H), 7.57 (m, 2H), 6.99 (d, 2H, J = 9 Hz), 6.94 (s, 1H), 3.89 (s, 3H). ^{13}C{^{1}H} NMR (125.7 MHz, $CDCl_3$) δ (ppm): 186.23, 183.79, 163.28, 135.21, 132.80, 132.79, 129.38, 129.32, 128.41, 128.29, 128.04, 128.00, 127.78, 126.76, 123.23, 114.02, 92.73, 77.26-76.76 ($CDCl_3$), 55.51. FT-IR (KBr) ν_{max} (cm^{-1}): 3047, 2974, 2936, 2842, 1585, 1520, 1498, 1450, 1344, 1295, 1249, 1175, 1029, 950, 792, 636. m/z = 305 (M+1)$^+$.

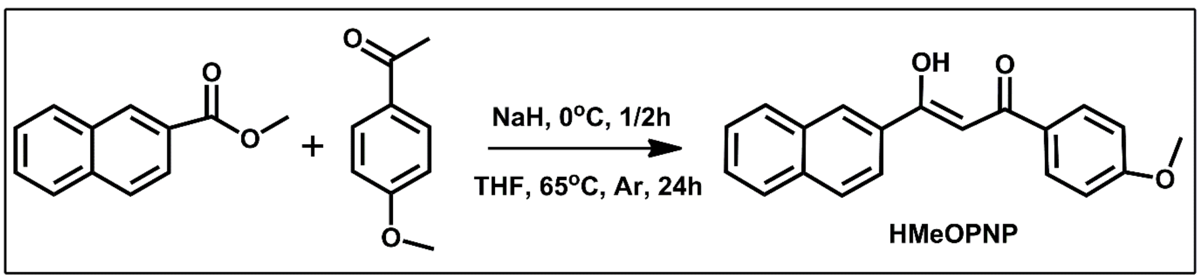

Scheme 4.1. Synthetic procedure for the β-diketonate ligand.

4.3.3. Synthesis of binary complexes 1-3.

The β-diketonate ligand was dissolved in methanol. To that NaOH (3.0 mmol) in water was added and stirred. After 15 min, $Ln(NO_3)_3{\cdot}6(H_2O)$ (where Ln = Eu, Gd, La) (1.0 mmol) in methanol was added drop-wise and stirred for 12 h at room temperature (Scheme 4.2). The resultant precipitate was filtered off, washed with water and dried.

The products were purified by recrystallization from dichloromethane-methanol solution and used for further analysis and photophysical studies.

$Eu(MeOPNP)_3(H_2O)_2$ (1). Elemental analysis (%): calculated for $C_{60}H_{49}O_{11}Eu$ (1098.25): C 65.53, H 4.50; Found: C 65.70, H 4.43. FT-IR (KBr) ν_{max} (cm^{-1}): 3425, 3053, 2959, 2936, 2834, 1600, 1588, 1524, 1494, 1464, 1343, 1291, 1245, 1174, 1030, 959, 787, 633. *m/z* = 1062 $[Eu(MeOPNP)_3+1]^+$.

$Gd(MeOPNP)_3(H_2O)_2$ (2). Elemental analysis (%): calculated for $C_{60}H_{49}O_{11}Gd$ (1103.25): C 65.32, H 4.48; Found: C 65.43, H 4.68. FT-IR (KBr) ν_{max} (cm^{-1}): 3423, 3051, 2958, 2935, 2834, 1601, 1587, 1524, 1496, 1465, 1343, 1292, 1246, 1174, 1033, 959, 786, 634. *m/z* = 1063 $[Gd(MeOPNP)_3]^+$.

$La(MeOPNP)_3(H_2O)_2$ (3). Elemental analysis (%): calculated for $C_{60}H_{49}O_{11}La$ (1084.23): C 66.42, H 4.55; Found: C 66.50, H 4.42. ^1H NMR ($CDCl_3$, 500 MHz) δ (ppm): 8.53 (s, 1H), 8.02 (m, 7H), 7.98 (m, 5H), 7.91 (m, 7H), 7.56 (m, 7H), 7.01 (m, 6H), 6.95 (s, 3H), 3.90 (s, 9H), 3.48 (H_2O). FT-IR (KBr) ν_{max} (cm^{-1}): 3429, 3053, 2957, 2936, 2834, 1603, 1588, 1523, 1494, 1464, 1343, 1291, 1245, 1171, 1030, 958, 785, 633. *m/z* = 1047 $[La(MeOPNP)_3-1]^+$.

4.3.4. Synthesis of ternary complexes 4-9.

All these complexes were prepared by stirring equimolar concentration of binary complexes **1** and **3** with bidentate nitrogen donors in chloroform at 70 ^oC. After 12 h, the solvent was evaporated and pure product was obtained by recrystallization from the dichloromethane-methanol mixture. The synthetic procedure is illustrated in Scheme 4.3.

Eu(MeOPNP)$_3$(BPY) (4). Elemental analysis (%): calculated for $C_{70}H_{53}O_9N_2Eu$ (1218.30): C 69.02, H 4.39, N 2.30; Found: C 68.92, H 4.30, N 2.24. FT-IR (KBr) ν_{max} (cm^{-1}): 3055, 2961, 2936, 2836, 1601, 1588, 1548, 1523, 1494, 1461, 1440, 1343, 1288, 1246, 1172, 1029, 959, 785, 632. *m/z* = 916.32 [Eu(MeOPNP)$_2$(BPY)+1]$^+$.

Eu(MeOPNP)$_3$(MeOBPY) (5). Elemental analysis (%): calculated for $C_{72}H_{57}O_{11}N_2Eu$ (1278.32): C 67.66, H 4.49, N 2.19; Found: C 67.54, H 4.59, N 2.08. FT-IR (KBr) ν_{max} (cm^{-1}): 3055, 2963, 2938, 2836, 1602, 1589, 1549, 1523, 1494, 1461, 1440, 1343, 1287, 1243, 1171, 1033, 959, 786, 633. *m/z* = 1008.31 [Eu(MeOPNP)$_2$(BPY)+Na]$^+$.

Eu(MeOPNP)$_3$(PhBPY) (6). Elemental analysis (%): calculated for $C_{82}H_{61}O_9N_2Eu$ (1370.36): C 71.87, H 4.49, N 2.04; Found: C 71.69, H 4.29, N 1.93; FT-IR (KBr) ν_{max} (cm^{-1}): 3055, 2968, 2935, 2836, 1602, 1589, 1548, 1523, 1494, 1461, 1439, 1343, 1288, 1242, 1172, 1140, 1033, 959, 786, 632. *m/z* = 1068.23 [Eu(MeOPNP)$_2$(PhBPY)+1]$^+$.

La(MeOPNP)$_3$(BPY) (7). Elemental analysis (%): calculated for $C_{70}H_{53}O_9N_2La$ (1204.28): C 69.77, H 4.43, N 2.32; Found: C 69.92, H 4.32, N 2.26. ^{1}H NMR ($CDCl_3$, 500 MHz) δ (ppm): 8.53 (s, 3H), 7.99 (m, 14H), 7.91 (m, 9H), 7.56 (m, 9H), 7.00 (m, 7H), 6.95 (s, 3H), 3.95 (s, 9H). FT-IR (KBr) ν_{max} (cm^{-1}): 3056, 2963, 2935, 2836, 1601, 1588, 1548, 1523, 1494, 1461, 1440, 1343, 1288, 1246, 1171, 1029, 960, 785, 632. *m/z* = 902.21 [La(MeOPNP)$_2$(BPY)+1]$^+$.

La(MeOPNP)$_3$(MeOBPY) (8). Elemental analysis (%): calculated for $C_{72}H_{57}O_{11}N_2La$ (1264.30): C 68.35, H 4.54, N 2.21; Found: C 68.54, H 4.59, N 2.09.

^1H NMR ($CDCl_3$, 500 MHz) δ (ppm): 8.55 (s, 3H), 8.02 (m, 12H), 7.88 (m, 7H), 7.50 (m, 5H), 7.01 (m, 6H), 6.95 (s, 6H), 6.83 (s, 3H), 3.91 (s, 9H), 3.83 (s, 6H). FT-IR (KBr) ν_{max} (cm^{-1}): 3055, 2963, 2938, 2836, 1602, 1589, 1549, 1523, 1494, 1462, 1440, 1343, 1287, 1243, 1171, 1035, 959, 786, 634. *m/z* = 983.23 [La(MeOPNP)$_2$(MeOBPY)+Na]$^+$.

La(MeOPNP)$_3$(PhBPY) (9). Elemental analysis (%): calculated for $C_{82}H_{61}O_9N_2Eu$ (1356.34): C 72.56, H 4.53, N 2.06; Found: C 72.69, H 4.29, N 2.13. ^1H NMR ($CDCl_3$, 500 MHz) δ (ppm): 8.73 (m, 2H), 8.53 (s, 3H), 7.96 (m, 24H), 7.57 (m, 12H), 7.00 (m, 8H), 6.95 (s, 3H), 3.90 (s, 9H). FT-IR (KBr) ν_{max} (cm^{-1}): 3055, 2968, 2935, 2836, 1602, 1589, 1548, 1523, 1494, 1461, 1439, 1343, 1288, 1242, 1172, 1140, 1033, 959, 786, 632. *m/z* = 1054.34 [La(MeOPNP)$_2$(PhBPY)+1]$^+$.

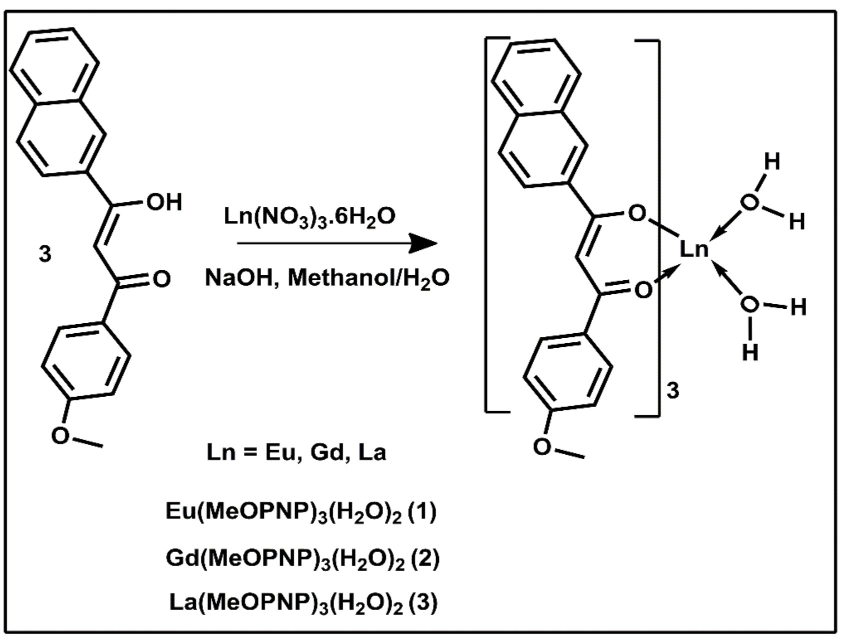

Scheme 4.2. Synthesis of Ln^{3+} (Ln = Eu, Gd, La) binary complexes.

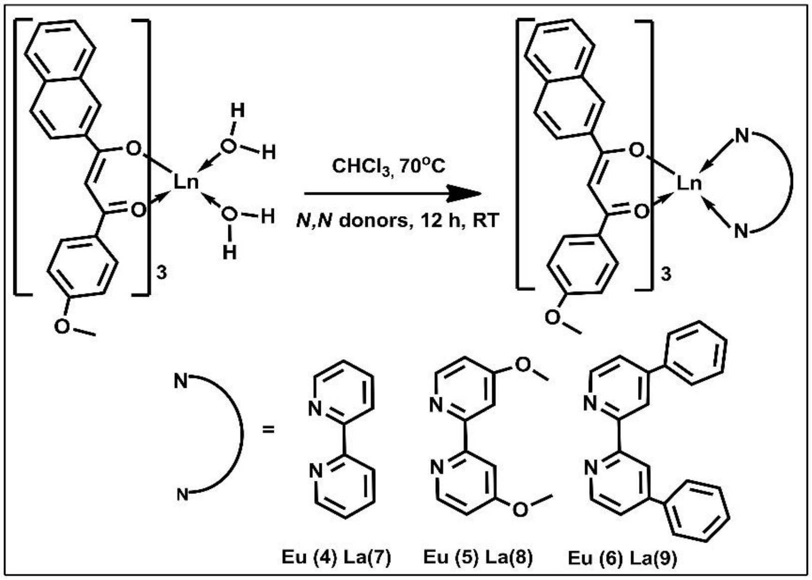

Scheme 4.3. Synthesis of ternary Ln^{3+} (Ln = Eu, La) complexes **4**-**9**.

4.4. Results and discussion

4.4.1. Synthesis and characterization of lanthanide complexes

The preparation process of the *β*-diketonate ligand and lanthanide complexes are shown in Schemes 4.1, 4.2 and 4.3, respectively. The synthesized ligand has been characterized by ^{1}H NMR, ^{13}C NMR, FT-IR and mass spectroscopic (ESI-MS) methods, as well as by elemental analysis. The derived *β*-diketonate compound mainly exists as enol form in chloroform-*d* solutions which is clear from the ^{1}H NMR data. In the ^{1}H NMR spectrum of HMeOPNP, a broad peak at δ 17.09 ppm corresponding to enolic –OH has been observed. Further, the appearance of methyne protons as a singlet at δ 6.94 ppm confirms the existence of the ligand in enolic form. The lanthanide complexes were characterized by FT-IR, ESI-MS, and elemental analysis. The elemental analysis and ESI-MS studies of Ln^{3+} complexes (**1**-**9**) (where Ln = Eu, Gd, La) revealed that the central Ln^{3+} ion is coordinated to three *β*-diketonate ligands. The FT-IR spectral studies for the complexes were performed and exhibit a broad absorption band in the region 3000 – 3500 cm^{-1} for the binary complexes (**1**, **2** and **3**) indicating the presence of coordinated water molecules. On the other hand, the absence of this broad band in complexes **4-9** inferred that the water molecules have been displaced successfully by the chelating bipyridine derivatives. The carbonyl stretching frequency of the β-diketonate ligand, HMeOPNP (1595 cm^{-1}) is shifted to higher wave numbers in **1–9** (~1602 cm^{-1}), thus disclosing the coordination of the carbonyl oxygen to the Ln^{3+} ions. In the ternary complexes **4-9**, the strong band near 1548 cm^{-1} were attributed to C=N stretching vibrations of bipyridine derivatives. [15] All these evidences indicate that the Eu^{3+} ion coordinated to the ligand *via* the nitrogen atoms of bipyridine and the carbonyl oxygen atoms of the β-diketonates.[15]

In order to further understand the coordination behaviour of europium complexes, ^{1}H NMR studies were performed for the lanthanum complexes **3** and **7-9**. The ^{1}H NMR spectrum of lanthanum complex $La(MeOPNP)_3(H_2O)_2$ (**3**) give the characteristic signals which is in accordance with the presence of three β-diketonate moieties coordinated to the central lanthanide ion (NMR data is given in the experimental section). The ^{1}H NMR signal for methyne proton (–CH) of HMeOPNP resonates at 6.95 ppm (δ) and the aromatic protons resonates in the range 8.53 to 7.01 ppm (δ). The absence of enolic -OH peak at δ 17.09 ppm in the lanthanum complexes confirms the coordination of HMeOPNP ligands with the Ln^{3+} ion. In addition, a broad signal around 3.48 ppm is observed in the NMR spectrum signifying the presence of coordinated water molecule. The proton signals appeared in the lanthanum complexes **7-9** indicate the existence of three HMeOPNP moieties and one bipyridine derivative in the corresponding ternary complexes. Moreover, no signals for the coordinated water molecule are noted in the ternary complexes **7-9**, which validates the replacement of coordinated water molecules by the chelating bipyridine ligands in the complexes.

Thermal behaviour of the synthesized Eu^{3+}-β-diketonate complexes (**1** and **4-6**) were investigated by thermogravimetric analysis in the temperature range 30-1000 °C under nitrogen atmosphere. As shown in Figure 4.3, a weight loss of about ~3.55% (calculated ~3.27%) was observed in the range 90-150 °C for the binary Eu^{3+}-β-diketonate complex **1**, corresponding to the loss of bound water molecules. No significant weight loss was observed for the Eu^{3+} complexes **4-6** until temperature of 230 °C, indicating that coordinated water molecules are not present in these complexes.[16] This observation is in good agreement with the FT-IR spectral data also. Further increase in temperature lead to decomposition of the complex in the temperature range 240-1000 °C corresponding to the loss of organic moieties present in the complexes.

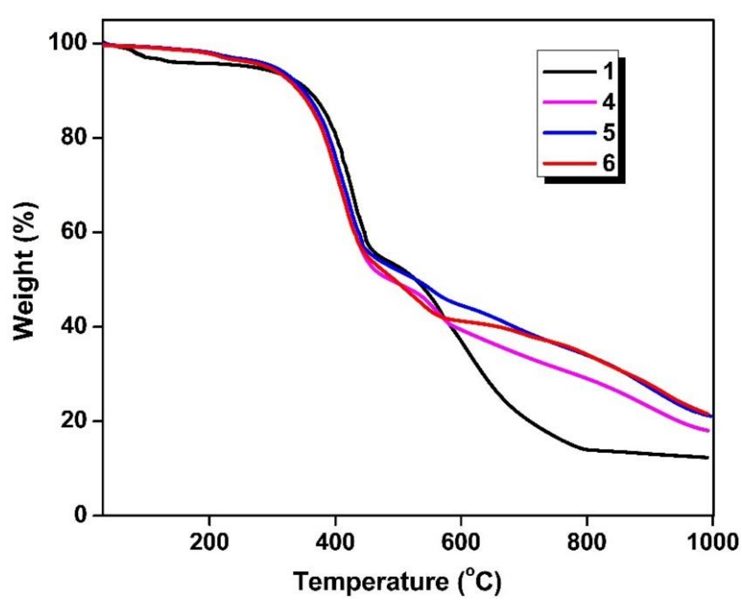

Figure 4.3. Thermogravimetric curves for Eu^{3+} complexes **1** and **4**-**6**.

4.4.2. Electronic spectra of the ligand and Eu^{3+} complexes

The solid-state UV-vis absorption studies of β-diketonate ligand and Eu^{3+} complexes were carried out at room temperature to understand the effect of increased conjugation of organic ligands. The respective spectra are shown in Figure 4.4. The absorption spectrum of the ligand HMeOPNP shows two intense broad bands in the range 200-300 nm assigned to the π-π* transition of the aromatic moiety of the ligand and 300-440 nm corresponding to the π-π* transition of the β-diketonate part of the ligand. All the europium complexes (**1**, **4**-**6**) exhibit spectral features similar to the ligand, indicating that the complexation of the β-diketonate with europium ion does not significantly alter the energy states of the β-diketonate ligand. However, a red shift is observed in the higher wavelength absorption band (red shifted up to 470 nm) for the europium complexes; probably arising from the intense π-π* transition of the conjugated chromophore due to the chelation between the europium ion and organic ligands. The absorption maximum of the electron donating dimethoxy bipyridine substituted europium complex **5** show a bathochromic shift of about ~10 nm towards the visible region (λ_{max} = 420 nm) when compared to unsubstituted europium complex **4** (λ_{max} = 410 nm). In contrast, the electron withdrawing phenyl group substituted complex **6** display a blue shifted absorption maximum (λ_{max} = 397 nm). Moreover, co-planarity of the phenyl ring with respect to the bipyridine moiety is lost due to the bulkiness of the molecules which reduce any extended conjugation. Red-shifted absorbance allows for visible light absorption, which is less harmful compared to UV absorption, enhancing the possible applications for the synthesized complex.

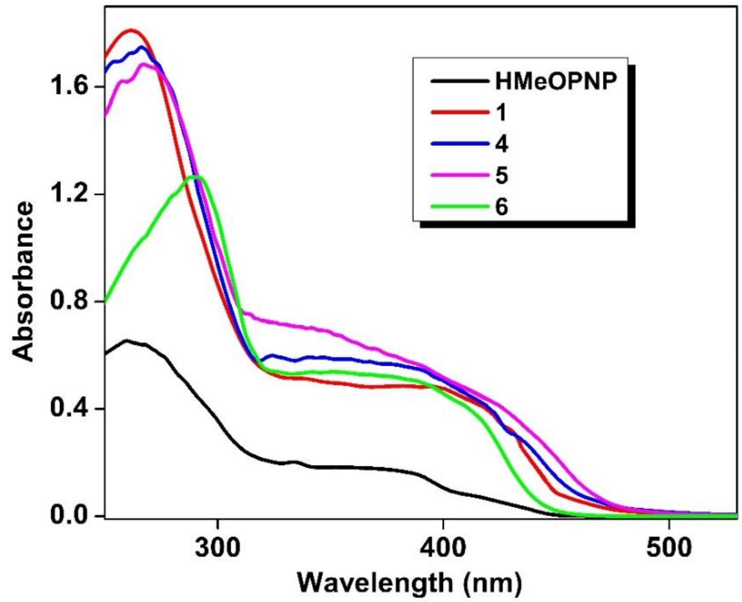

Figure 4.4. Solid-state UV-vis absorption spectra of the β-diketonate ligand, HMeOPNP and Eu^{3+} complexes **4-6**.

In order to define the light absorbing ability of the β-diketonate ligand, molar absorption coefficient is calculated from the UV-vis absorption spectra in THF solution at a concentration, c = 5 × 10^{-6} M. The β-diketonate ligand, HMeOPNP display a high absorption coefficient of 30283 L mol^{-1} cm^{-1} (calculated at the absorption maximum λ_{max} = 365 nm) indicate that it has a strong ability to absorb light. The magnitude of molar absorption coefficient of all the Eu^{3+} complexes are larger than those of the free ligand by about three times, indicating the presence of three β-diketonate ligands in the coordination sphere of the lanthanide ion. The molar absorption coefficient values for the β-diketonate ligand and the corresponding Eu^{3+} complexes are given in Table 4.1.

Table 4.1 Molar absorption coefficient for the ligand and the corresponding Eu^{3+} complexes.

Compounds		ε ($L\ mol^{-1}\ cm^{-1}$) calculated at λ_{max} (nm) = 365 nm
HMeOPNP		30223
$Eu(MeOPNP)_3(H_2O)_2$	(**1**)	92853
Eu(MeOPNP)$_3$(BPY)	(**4**)	96907
Eu(MeOPNP)$_3$(MeOBPY)	(**5**)	97726
Eu(MeOPNP)$_3$(PhBPY)	(**6**)	96454

4.4.3. Steady-state photoluminescence

The solid-state excitation spectra of Eu^{3+} complexes at room temperature were recorded by monitoring the intense $^5D_0 \rightarrow {}^7F_2$ transition of Eu^{3+} at 612 nm and are shown in Figure 4.5. The results demonstrate that due to the presence of conjugated naphthalene moiety and electron donating methoxy group on the phenyl counterpart, the excitation spectrum of the binary Eu^{3+} complex **1** exhibit a broad band between 270 and 500 nm with an excitation maximum of λ_{exc} = 410 nm, corresponding to the π-π^* transition of the coordinated ligands.[6,10] The introduction of bidentate nitrogen donors in the coordination sphere of Eu^{3+} complex **1** have a significant influence on the excitation spectra of the ternary complexes **4**-**6**. The difference in excitation spectra of the complexes can be ascribed to the different π-π^* transitions of the coordinated ligands originating from the various substituents on the pyridyl ring. Compared with binary complex **1**, Eu^{3+} complex **4** exhibit a broad excitation spectrum with λ_{exc} = 412 nm, whereas, the dimethoxy substituted bipyridine containing Eu^{3+} ternary complex **5** display a notable red-shift of about 10 nm with an excitation maximum of λ_{exc} = 420 nm.

This observed red-shift is due to the presence of two electron donating methoxy groups on bipyridine moiety which increases the conjugation length of the whole molecule.[18] This red-shift would make the complex avoid UV irradiation-induced photodecomposition in photoluminescence applications. A blue-shift (λ_{exc} = 400 nm) is observed in the excitation spectrum of complex **6**, which can be due to the electron withdrawing effect and nonplanar arrangement of phenyl group present in the bipyridine ligand. The steric effect of the bulky substituent hinders the ability for the peripheral phenyl rings to become coplanar with the bipyridyl fragment and reduce the intra-ligand delocalization, consequently blue-shifting the excitation maximum.[19] The excitation spectra of all the complexes exhibit a sharp peak at ~464 nm corresponds to the $^5D_2 \leftarrow {}^7F_{0,1}$ transition of europium ion and is much weaker than the ligand excitation. This observation suggests that sensitization of europium by ligands are much more efficient than the direct excitation of the europium complex.[17a]

The emission spectra of Eu^{3+}-β-diketonate complexes (**1, 4**-**6**) (Figure 4.5) excited at their corresponding excitation maxima show characteristic Eu^{3+} ion emissions in the 550-725 nm wavelength region. The well-resolved peaks observed are due to the f-f transitions from the metal-centered $^5D_0$ excited state to the ^7F_J ground state multiplet. Maximum peak intensities at 579, 593, 612, 653 and 697 nm were noted for the J = 0, 1, 2, 3, 4 transitions, respectively. A prominent feature that may be noted in these spectra was the very high intensity of $^5D_0 \rightarrow {}^7F_2$ transition at 612 nm responsible for the observed red emission in these complexes. Further, the intensity of the $^5D_0 \rightarrow {}^7F_2$ transition (electric-dipole) is greater than that of the $^5D_0 \rightarrow {}^7F_1$ transition (magnetic-dipole), which indicates that the coordination environment of the Eu^{3+} ion is devoid of an inversion center.[20] It can also be noted from the emission spectra that the luminescence intensity of the Eu^{3+} ternary complexes (**4-6**) is significantly enhanced as compared to the Eu^{3+} binary complexes (**1**), on displacement of the solvent molecules from the complexes by the bidentate nitrogen donor. It is clear from the emission spectra that presence of electron donating methoxy group at the 4,4'-position in the bipyridine molecule has significantly enhanced the emission intensity of Eu^{3+} complex **5** (8.8×10^8) compared to simple bipyridine complex **4** (5.7×10^8 at 412 nm). This observation is due to the enhanced basicity of the coordinating nitrogen atoms upon the substitution with two electron-donating groups (OCH_3).[4b] On the other hand, the bulky 4,4'-diphenyl-2,2'-bipyridine substituted Eu^{3+} complex show a lowered emission intensity of 2.0×10^8. The emission intensity follows the order, complex **1**<**6**<**4**<**5**. Further, no broad emission bands related to β-diketonate ligand is observed in the blue region, indicating the efficient energy transfer from the ligand to the emitting level of the metal ion. The intensity ratio of the hypersensitive $^5D_0 \rightarrow {}^7F_2$ transition to the magnetic dipole allowed $^5D_0 \rightarrow {}^7F_1$ transition (I_{7F2}/I_{7F1}) reflects the nature and symmetry of the first coordination sphere. The intensity ratio for (I_{7F2}/I_{7F1}) complex **1** is 12.89 in the presence of coordinated water molecules, while it is increased to 16.98 for **4**, 15.86 for **5**, and 15.60 for **6**. The results indicate that the introduction of bipyridine ligands into the coordination sphere of the complex **1** leads to an effective reduction of the symmetry around Eu^{3+} ions.[21] However, the high intensity ratio is responsible for the brilliant red emission of the complexes.

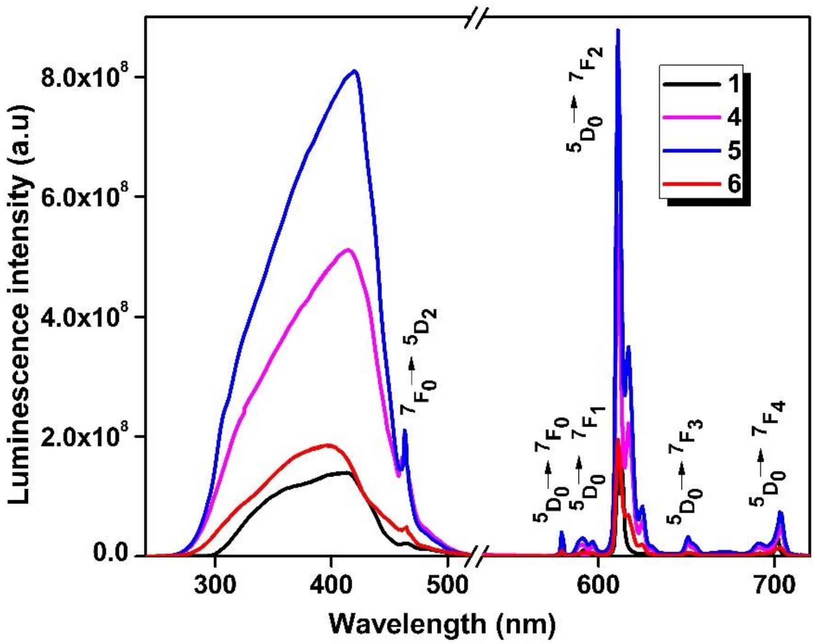

Figure 4.5. Room temperature excitation and emission spectra of Eu^{3+} complexes **1**, **4-6** in the solid-state.

The room temperature luminescence decay curves of the $^5D_0$ level for Eu^{3+} complexes **1**, **4**-**6** were investigated by monitoring the intense emission at 612 nm ($^5D_0 \rightarrow {}^7F_2$) and are given in Figure 4.6. These curves can be described by single exponential kinetics, thus indicating that the Eu^{3+} ion in the complexes is located in the same parity sites. As explained in previous literature reports, luminescence lifetime of ternary europium complexes **3**-**5**, enhanced up on introduction of bidentate nitrogen donors. This may be due to the replacement of the coordinated water molecule by bidentate nitrogen donors, thereby decreasing the non-radiative deactivation, suggesting that the introduction of secondary ligand enhances the photoluminescence stability of the overall coordination system.[22] The ternary complex **5** also display higher excited state lifetime value (τ_{obs} = 380 ± 1 μs at 298 K for **5**) compared to the Eu^{3+} complexes **4** and **6**. The lifetime values for the emission of all Eu^{3+} complexes are listed in Table 4.2.

To understand more about the sensitization ability of these ligands, further investigations about the luminescent process were carried out. The overall quantum yield (Φ_{overall}) of a europium complex is determined by two aspects: (i) efficiency of energy transfer from excited state of antenna ligand to emitting Eu^{3+} level (Φ_{sens}) and (ii) efficiency of Eu^{3+}-centered emission, the intrinsic quantum yield (Φ_{Ln}). The values were calculated according to the emission spectra and room temperature lifetime and are tabulated in Table 4.2. The substitution of solvent molecules in the complex **1** by a chelating ancillary ligand, bipyridine leads to an approximately 2-4-fold enhancement in the absolute quantum yield (from 6% for complex **1** to 9-32% for complexes **4**-**6**, respectively),[23] which is in good agreement with the results from their luminescence emission intensity. Furthermore, the two methoxy substituents on the bipyridine moiety enhanced the photoluminescence properties of ternary Eu^{3+} complex **5** in comparison with other ternary Eu^{3+} complexes, probably due to the increase in electron density which improve the radiative process.[4b] Examination of the radiative and non-radiative decay rate constants, derived from the observed lifetime and quantum yield, reveals that the increase in quantum yield is due to both an increase in A_{RAD} and a decrease in A_{NR} in complex **5**.[19]

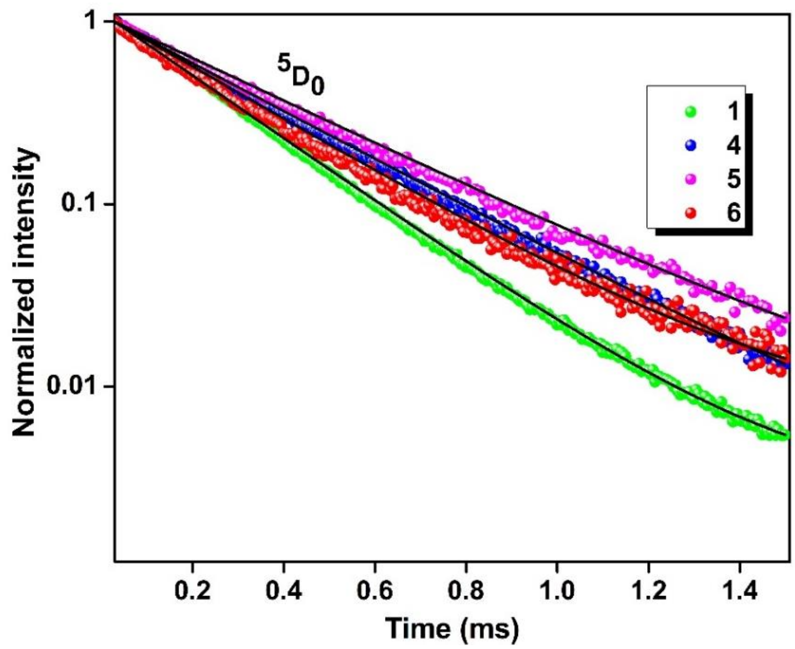

Figure 4.6 $^5D_0$ decay profiles for complexes **1** and **4-6** (solid-state) where emission monitored around 612 nm. The straight lines are the best fits (r^2 = 0.999) considering single-exponential behavior.

Table 4.2 The radiative (***A*RAD**, s^{-1}) and non-radiative (***A*NR**, s^{-1}) decay rates, $^5D_0$ lifetime (τ_{obs}, µs), intrinsic quantum yield (Φ_{Ln}, %), energy transfer efficiency (Φ_{sen}, %), overall quantum yield ($\Phi_{overall}$, %) and colour coordinates for Eu^{3+} complexes in the solid-state excited at their excitation maximum.

Compounds	A_{RAD} (s^{-1})	A_{NR} (s^{-1})	τ_{obs} (µs)	Φ_{Ln} (%)	Φ_{sen} (%)	$\Phi_{overall}$ (%)
$Eu(MeOPNP)_3(H_2O)_2$ (**1**)	823	3292	240 ± 1	20	30	6 ± 1
$Eu(MeOPNP)_3$(BPY) (**4**)	1031	2093	317 ± 1	33	60	20 ± 2
$Eu(MeOPNP)_3$(MeOBPY) (**5**)	1049	1865	344 ± 2	36	89	32 ± 3
$Eu(MeOPNP)_3$(PhBPY) (**6**)	1025	2391	274 ± 1	30	30	9 ± 1

The energy levels of the significant electronic states should be estimated in order to explain the energy transfer processes in europium complexes. The energy transfer is effective, when there is an energy level match between the triplet states of the ligands and the ground state of Eu^{3+}. The ligand centered triplet state is determined from the lower wavelength emission edge of the low temperature phosphorescence spectra of gadolinium complex (Figure 4.7).[24] The triplet state is estimated to be 20121 cm^{-1} which corresponds to its lower wavelength emission edge of 496 nm. The singlet energy level of the ligand was 24571 cm^{-1} (406 nm), which was calculated from the higher wavelength absorbance edges of the UV-vis spectra of the gadolinium complex (Figure 4.7). Because the lowest excited state, $^6P_{7/2}$ (32 000 cm^{-1}), of Gd^{3+} is too high to accept energy from the ligand, the data obtained from the phosphorescence spectrum actually reveal the triplet energy level (T_1) of HMeOPNP in lanthanide complexes. According to Reinhoudt's empirical rule, it is known that intersystem crossing becomes effective when the energy gap between the S_1 and T_1 levels $\Delta E(S_1\text{-}T_1)$ is around ~5000 cm^{-1}. The energy gap $\Delta E(S_1\text{-}T_1)$ is found to be 4450 cm^{-1}, indicating that the intersystem crossing processes are efficient for this ligand. The energy gaps between the Eu^{3+} core ($^5D_0$ ~17250 cm^{-1}) and the donor ligand's T_1 levels turn out to be 2870 cm^{-1}. According to the empirical rule pointed out by Latva, for an optimal ligand-to-metal energy transfer process $2500 < \Delta E(T_1\text{-}^5D_0) < 4000$ cm^{-1} for Eu^{3+}. It is interesting to note that the triplet energy levels of the developed β-diketonate ligands lie above the energy of the main emitting level of $^5D_0$ for Eu^{3+}, thus demonstrating that this ligand can act as antenna molecules for the sensitization of Eu^{3+} ions.[24] Also, the triplet energies of ancillary ligands are situated above the metal excited state (T_1 of bipyridine derivative ~ 22000 cm^{-1}) indicating that it could participate in the energy transfer process in complexes **4**, **5** and **6**, which makes the ligand-to-metal energy transfer process efficient. Hence the synthesized ligand obeys all the necessary criteria for an efficient antenna molecule.

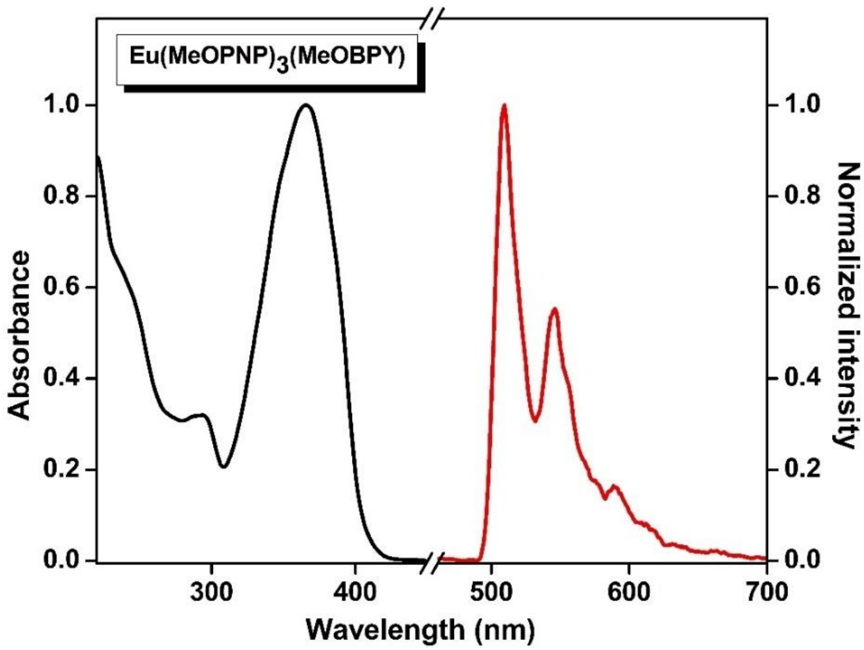

Figure 4.7. UV-vis absorption spectra at 298 K (left), and 77 K phosphorescence spectra (right) of the complex **2** in THF ($c = 5 \times 10^{-6}$ M).

4.4.4. Photoluminescence measurement of complex 5 in buffer solution [% DMSO: % PBS = 1: 99; c = 1 x 10^{-4} M]

The absorption spectra of the Eu^{3+} complex **5** was investigated in DMSO: PBS buffer solution (%DMSO: %PBS = 1: 99, $c = 1\times10^{-4}$ M) under physiological pH conditions (pH = 7.4) (Figure 4.8). The absorption profile show similar spectral features as observed in THF solution indicating that use of DMSO: PBS buffer solution does not significantly alter the coordination sphere. The Eu^{3+} complex show a promising molar absorption coefficient observed of 52443 L mol^{-1} cm^{-1}

(λ_{max} = 370 nm) indicating that absorption capacity of the HMeOPNP ligand retained even in DMSO: PBS buffer solution.

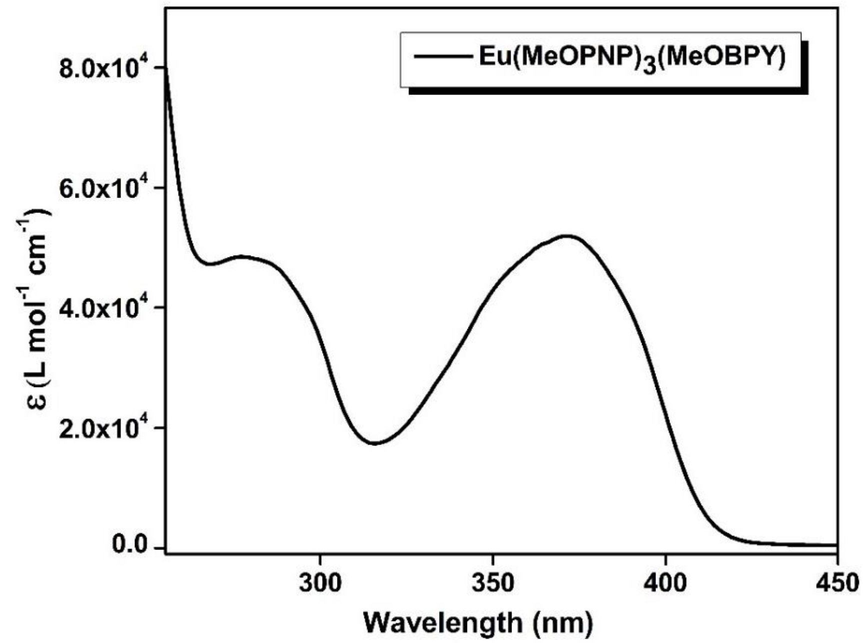

Figure 4.8. UV-visible absorption spectra of the Eu^{3+} complex **5** in buffer solution (%DMSO: %PBS = 1: 99, c = 1×10^{-4} M).

The excitation and emission profiles of the visible-light excitable europium complex **4** recorded in buffer solution of pH 7.4 [% DMSO: % PBS = 1: 99; c = 1 x 10^{-4} M] at 298 K are shown in Figure 4.9. The excitation spectrum was recorded by monitoring the $^5D_0 \rightarrow {}^7F_2$ (612 nm) transition of the Eu^{3+}. The excitation spectrum exhibit a broad band between 300 to 450 nm, which can be designated to the π–π* transition of the β-diketonate ligand. The absence of any absorption bands due to the f-f transitions of the Eu^{3+} ion clearly indicates a very efficient luminescence sensitization *via* the ligand excitation. The room temperature (298 K) emission spectrum of the europium complex was also recorded in a buffer solution (pH = 7.4) at λ_{exc} = 405 nm, which shows the characteristic emission peaks of Eu^{3+}. Only a negligible ligand emission is observed in the emission spectra indicating that the ligand transfers the absorbed energy effectively to the emitting level of metal ion.

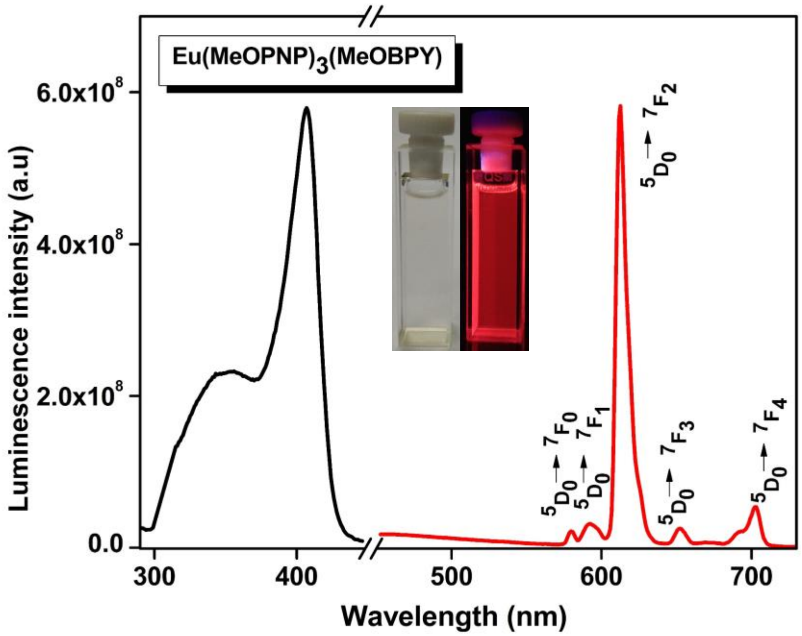

Figure 4.9. Solution-state excitation (left) and emission spectra (right) Eu(MeOPNP)$_3$(MeOBPY) in a buffer solution of pH 7.4 [% DMSO : % PBS = 1: 99; c = 1 × 10^{-4} M] at 298 K, emission monitored at around 612 nm (λ_{exc} = 405 nm). Inset: photograph of the complex **5** in buffer solution under day light and UV light with 365 nm excitation).

The luminescent lifetime of the visible-light excitable Eu^{3+} complex **5** was measured in buffer solution and is shown in Figure 4.10. The result shows a single exponential decay curve indicating the presence of only one emitting species in the coordination sphere. The lifetime observed is τ_{obs} = 322 ± 2 μs.

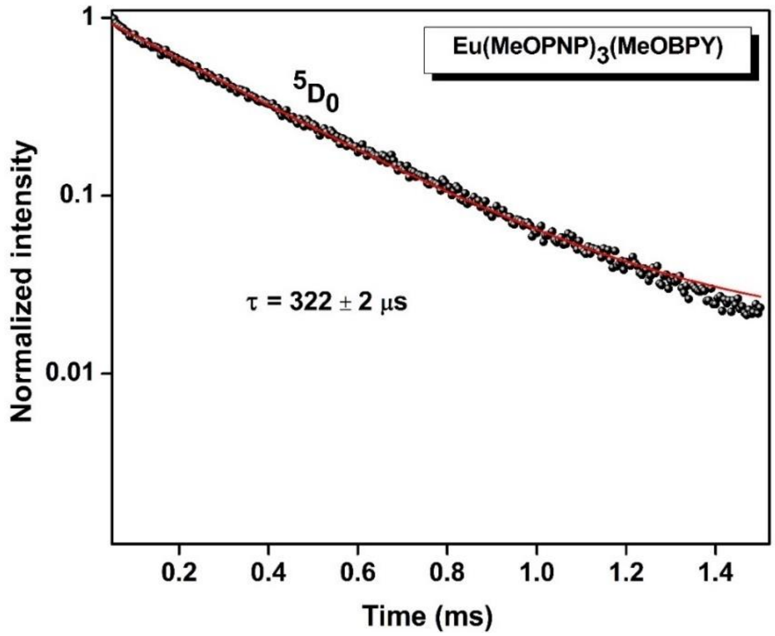

Figure 4.10. The $^5D_0$ decay profile for the complex **5** in a buffer solution of pH 7.4 [% DMSO: % PBS =1: 99; c = 1 x 10^{-4} M] at 298 K, excited at 405 nm. The emission was monitored at 612 nm.

The overall quantum yields estimated under biological pH condition excited at 405 nm with respect to the reference standard Quinine Sulfate (in 1 N H_2SO_4, $\Phi_{overall}$ = 54.6%) was found to be $\Phi_{overall}$ = 24 ± 2%.

4.4.5. Photostability of the Eu^{3+} complex $Eu(MeOPNP)_3(MeOBPY)$ (5) in buffer solution

The photo-stability of the Eu^{3+} complex **5** was investigated by measuring photoluminescence intensity at 612 nm in a buffer solution of pH 7.4 [% DMSO: % PBS = 1: 99; c = 1 x 10^{-4} M] at 298 K, as a function of irradiation time. The excitation wavelength was λ_{exc} = 405 nm and irradiated for 5 h. The results are given in Figure 4.11. These results confirmed that the emission intensity of the complex at 612 nm remains approximately the same even after 5 h of continuous irradiation indicating the stability of the Eu^{3+} complex towards photo-irradiation. These results suggest that the complex **5** can be used as a new class of stable agent for applications in cellular imaging.[25]

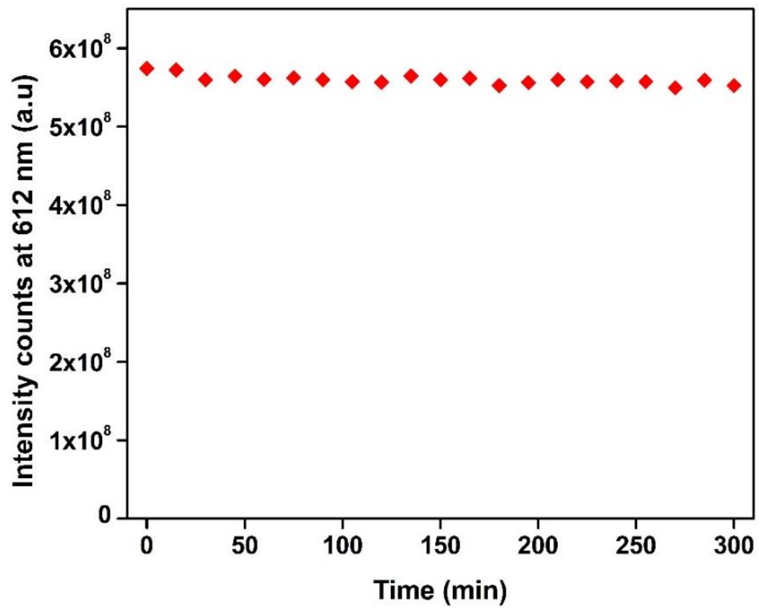

Figure 4.11. Photoluminescence intensity of complex **5** at 612 nm in a buffer solution of pH 7.4 [% DMSO: % PBS = 1: 99; c = 1 x 10^{-4} M] at 298 K, as a function of irradiation time. λ_{exc} = 405 nm.

4.5. Conclusions

- A series of new ternary Eu^{3+} complexes $Eu(MeOPNP)_3(MeOBPY)$, $Eu(MeOPNP)_3(BPY)$ and $Eu(MeOPNP)_3(PhBPY)$ based on a visible-light excitable β-diketonate ligand, 3-hydroxy-1-(4-methoxyphenyl)-3-(naphthalen-2-yl)prop-2-en-1-one (HMeOPNP) and bidentate nitrogen donors were synthesized. Photophysical properties of the europium complexes were thoroughly studied in order to understand the electronic effect of substituents on the bipyridine molecules.

- The result demonstrate that all the complexes exhibited visible-light excitation with Eu(MeOPNP)$_3$(MeOBPY) being the most red shifted (λ_{exc} = 420 nm) followed by Eu(MeOPNP)$_3$(BPY) (λ_{exc} = 412 nm) and Eu(MeOPNP)$_3$(PhBPY) (λ_{exc} = 400 nm). Enhanced conjugation induced by the participation of the lone pair of the oxygen atom leads to the observed red-shift in λ_{exc} for Eu(MeOPNP)$_3$(MeOBPY), while lack of co-planarity and hence decreased π-interactions in the chromophore due to steric effects of the bulky phenyl substituents on the 4,4'-position of the bipyridine system results in blue-shift in λ_{exc} for Eu(MeOPNP)$_3$(PhBPY).
- The substitution of solvent molecules by bidentate nitrogen ligands in Eu(MeOPNP)$_3$(H_2O)$_2$ complex greatly enhances the metal-centered luminescence quantum yields and lifetime values. Compared to previously reported naphthalene based systems, the newly synthesized complexes show a redshifted absorption and excitation spectra with promising quantum yields.
- Photostability investigations under continuous irradiation of the visible-light excitable complex Eu(MeOPNP)$_3$(MeOBPY) dissolved in buffer solution mimicking biological media revealed high stability for the complex, rendering the possibility of its use in applications like bio-imaging.

4.6. References

1. Y. Kido, K. Nagai, Y. Okamoto, T. Skothein, *Chem. Lett.*, 1991, **235**, 1267.

2. (a) X. Jiang, A. K.-Y. Jen, D. Huang, G. D. Phelan, T. M. Londergan and L. R. Dalton, *Synth. Met.,* 2002, **125**, 331; (b) F. Liang, Q. Zhou, Y. Cheng, L. Wang, D. Ma, X. Jing and F. Wang, *Chem. Mater*., 2003, **15**, 1935; (c) L. Fu, R. A. S. Ferreira, N. J. O. Silva, A. J. Fernandes, P. Ribeiro-Claro, I. S. Goncalves, V. D. Z. Bermudez and L. D. Carlos, *J. Mater. Chem.*, 2005, **15**, 3117; (d) C. P. Montgomery, B. S. Murray, E. J. New, R. Pal and D. Parker, *Acc. Chem. Res*., 2009, **42**, 925; (e) L. Armelao, S. Quici, F. Barigelletti, G. Accorsi, G. Bottaro, M. Cavazzini and E. Tondello, *Coord. Chem. Rev*., 2010, **254**, 487; (f) Y. Ma and Y. Wang, *Coord. Chem. Rev*., 2010, **254**, 972; (g) K. Binnemans, *Chem. Rev*., 2009, **109**, 4283; (h) J.-C. G. Bünzli and C. Piguet, *Chem. Soc. Rev*., 2005, **34**, 1048; (i) P. P. Lima, M. M. Nolasco, F. A. A. Paz, R. A. S. Ferreira, R. L. Longo, O. L. Malta and L. D. Carlos, *Chem. Mater*., 2013, **25**, 586.
3. (a) J.-C. G. Bünzli, *Chem. Rev*., 2010, **110**, 2729; (b) M. C. Heffern, L. M. Matosziuk and T. J. Meade, *Chem. Rev.,* 2014, **114**, 4496; (c) X. Wang, H. Chang, J. Xie, B. Zhao, B. Liu, S. Xu, W. Pei, N. Ren, L. Huang and W. Huang, *Coord. Chem. Rev*., 2014, **273**, 201; (d) J.-C. G. Bünzli and S. V. Eliseeva, *Chem. Sci*., 2013, **4**, 1939; (e) J. Feng and H. Zhang, *Chem. Soc. Rev.,* 2013, **42**, 387; (f) A. de Bettencourt-Dias, *Dalton Trans*., 2007, **22**, 2229; (g) L. D. Carlos, R. A. S. Ferreira, V. de Zea Bermudez, B. J.-Lopezc and P. Escribano, *Chem. Soc. Rev.,* 2011, **40**, 536; (h) S. V. Eliseeva and J.-C. G. Bünzli, *Chem. Soc. Rev*., 2010, **39**, 189; (i) S. V. Eliseeva and J.-C. G. Bünzli, *New J. Chem*., 2011, **35**, 1165; (J) L. D. Carlos, R. A. S. Ferreira, V. Z. Bermudez and S. J. L. Ribeiro, *Adv. Mater*., 2009, **21**, 509.
4. (a) D. B. A. Raj, S. Biju and M. L. P. Reddy, *Inorg. Chem*., 2008, **47**, 8091; (b) S. Biju, D. B. A. Raj, M. L. P. Reddy and B. M. Kariuki, *Inorg. Chem*., 2006, **45**, 10651; (c) S. Biju, M. L. P. Reddy, A. H. Cowley and K. V. Vasudevan, *Cryst. Growth Des*., 2009, **9**, 3562; (d) S.

Biju, N. Gopakumar, J.-C. G. Bünzli, R. Scopelliti, H. K. Kim and M. L. P. Reddy, *Inorg. Chem*., 2013, **52**, 8750; (e) D. B. A. Raj, B. Francis, M. L. P. Reddy, R. R. Butorac, V. M. Lynch and A. H. Cowley, *Inorg. Chem*., 2010, **49**, 9055; (f) D. B. A. Raj, S. Biju and M. L. P. Reddy, *Dalton Trans.*, 2009, **36**, 7519; (g) B. Francis, D. B. A. Raj and M. L. P. Reddy, *Dalton Trans*., 2010, **39**, 8084; (h) M. L. P. Reddy, V. Divya and R. Pavithran, *Dalton Trans*., 2013, **42**, 15249.

5. F. J. Steemers, W. Verboom, D. N. Reinhoudt, E. B. Vander Tol and J. W. Verhoeven, *J. Am. Chem. Soc*., 1995, **117**, 9408.
6. (a) Y. Zhang, H. Tan, M. Xiao, X. Bao, Q. Tao, Y. Wang, Y. Liu, R. Yang and W. Zhu, *Org. Electron.*, 2014, **15**, 1173; (b) O. P. Lee, A. T. Yiu, P. M. Beaujuge, C.H. Woo, T.W. Holcombe, J. E. Millstone, J. D. Douglas, M. S. Chen and J. M. J. Fréchet, *Adv. Mater.,* 2011, **23** 5359; (c) Z. L. Wu, A. Y. Li, B. H. Fan, F. Xue, C. Adachi and J. Ouyang, *Sol. Energy Mater. Sol. Cells*, 2011, **95**, 2516; (d) D. B. Mi, J. B. Park, F. Xu, H. U. Kim, J. H. Kim and D. H. Hwang, *Bull. Korean Chem. Soc.*, 2014, **35**, 1647; (e) Y. Zhang, X. Bao, M. Xiao, H. Tan, Q. Tao, Y. Wang, Y. Liu, R. Yang and W. Zhu, *J. Mater. Chem. A*, 2015, **3**, 886.
7. (*a*) P. He, H. H. Wang, S. G. Liu, J. X. Shi, G. Wang and M. L. Gong, *Inorg. Chem*., 2009, **48**, 11382; (*b*) P. He, H. H. Wang, H. G. Yan, W. Hu, J. X. Shi and M. L. Gong, *Dalton Trans*., 2010, **39**, 8919; (*c*) J. Wu, Z. Ye, G. Wang, D. Jin, J. Yuan, Y. Guan and J. Piper, *J. Mater. Chem*., 2009, **19**, 1258; (*d*) J. Wu, G. Wang, D. Jin, J. Yuan, Y. Guan and J. Piper, *Chem. Commun*., 2008, 365; (*e*) M. Shi, C. Ding, J. Dong, H. Wang, Y. Tian and Z. Hu, *Phys. Chem. Chem. Phys*., 2009, **11**, 5119; (*f*) M. H. V. Werts, M. A. Duin, J. W. Hofstraat and J. W. Verhoeven, *Chem. Commun*., 1999, **9**, 799; (g) V. Divya, S. Biju, R. Luxmi Varma and M.

L. P. Reddy, *J. Mater. Chem*., 2010, **20**, 5220; (*h*) V. Divya, R. O. Freire and M. L. P. Reddy, *Dalton Trans*., 2011, **40**, 3257.

8. M. D. McGehee, T. Bergstedt, C. Zhang, A. P. Saab, M. B. O'Regan, G. C. Bazan, V. I. Srdanov and A. J. Heeger, *Adv. Mater.,* 1999, **11**, 1349.
9. H. Peng, M. I. Stich, J. Yu, L. Sun, L. H. Fischer, and O. S. Wolfbeis, *Adv. Mater.,* 2010, **22**, 716.
10. (a) S. Xu, R. E. Evans, T. Liu, G. Zhang, J. N. Demas, C. O. Trindle, and C. L. Fraser, *Inorg. Chem.,* 2013, **52**, 3597; (b) C. A. DeRosa, J. Samonina-Kosicka, Z. Fan, H. C. Hendargo, D. H. Weitzel, G. M. Palmer, and C. L. Fraser, Macromolecules, 2015, **48**, 2967.
11. N. C. Fletcher, *J. Chem. Soc*., *Perkin Trans.,* 2002, **1,** 1831.
12. (a) V.-M. Mukkala and J. J. Kankare, *Helv. Chim. Acta,* 1992, **75**, 1578; (b) Z. Chen, F. Ding, F. Hao, M. Guan, Z. Bian, B. Ding and C. Huang, *New J. Chem.*, 2010, **34**, 487; (c) W.-S. Han, J.-K. Han, H.-Y. Kim, M. J. Choi, Y.-S. Kang, C. Pac, and S. O. Kang, *Inorg. Chem.,* 2011, **50**, 3271.
13. (a) J. C. De Mello, H. F. Wittmann and R. H. Friend, *Adv. Mater.*, 1997, **9**, 230; (b) L.-O. Pålsson and A. P. Monkman, *Adv. Mater.*, 2002, **14**, 757; (c) B. K. Shah, D. C. Neckers, J. Shi, E. W. Forsythe and D. Morton, *Chem. Mater.*, 2006, **18**, 603; (*d*) M. Cölle, J. Gmeiner, W. Milius, H. Hillebrecht and W. Brütting, *Adv. Funct. Mater.*, 2003, **13**, 108; (e) N. S. Saleesh Kumar, S. Varghese, N. P. Rath and S. Das, *J. Phys. Chem., C*, 2008, **112**, 8429; (f) S. V. Eliseeva, O. V. Kotova, F. Gumy, S. N. Semenov, V. G. Kessler, L. S. Lepnev, J.-C. G. Bünzli and N. P. Kuzmina, *J. Phys. Chem. A.*, 2008, **112**, 3614.

14. (a) S. R. Meech and D. Phillips, *J. Photochem.*, 1983, **23**, 193; (b) D. F. Eaton, *Pure Appl. Chem.*, 1988, **60**, 1107; (c) G. A. Crosby and J. N. Demas, *The J. Phys. Chem.*, 1971, **75**, 991; (d) V. Divya, V. Sankar, K. G. Raghu and M. L. P. Reddy, *Dalton Trans.*, 2013, **42**, 12317; (e) J. Bao, H. Tian, R. Tang, *Inorg. Chim. Acta*, 2013, **401**, 19.
15. (a) D. Wang, Y. Pi, C. Zheng, L. Fan, Y. Hu and X. Wei, *J. Alloys Compd.,* 2013, **574**, 54; (b) D. Wang, C. Zheng, L. Fan, Y. Hu and J. Zheng, *Spectrochim. Acta. Part A,* 2014, **117**, 245; (c) D. A. Turchetti, M. M. Nolasco, D. Szczerbowski, L. D. Carlos and L. C. Akcelrud, *Phys. Chem. Chem. Phys.*, 2015, **17**, 26238.
16. (a) J. Wu, Z. Ye, G. Wang, D. Jin, J. Yuan, Y. Guan and J. Piper, *J. Mater. Chem.,* 2009, **19**, 1258; (b) A. S. Chauvin, F. Gumy, I. Matsubayashi, Y. Hasegawa and J.-C. G. Bünzli, *Eur. J. Inorg. Chem.,* 2006, 473; (c) N. M. Shavaleev, R. Scopelliti, F. Gumy and J.-C. G. Bunzli, *Inorg. Chem.,* 2009, **48**, 6178.
17. (a) A. Specht, F. Bolze, L. Donato, C. Herbivo, S. Charon, D. Warther, S. Gug, J.-F Nicoud and M. Goeldner, *Photochem. Photobiol. Sci.,* 2012, **11**, 578.; (b) L. N. Sun, J. B. Yu, G. L. Zheng, H. J. Zhang, Q. G. Meng, C. Y. Peng, L.-S Fu, F.-Y Liu and Y.-N Yu, *Eur. J. Inorg. Chem.,* 2006, 3962.
18. (a) G. Shao, H. Yu, N. Zhang, Y. He, K. Feng, X. Yang, R. Cao and M. Gong, *Phys. Chem. Chem. Phys.,* 2014, **16,** 695; (b) B. Francis, C. Heering, R. O. Freire, M. L. P. Reddy and C. Janiak, *RSC Adv.*, 2015, **5**, 90720; (c) T. V. Usha Gangan, S. Sreenadh and M. L. P. Reddy, *J. Photochem. Photobiol. A*, 2016, **328**, 171.
19. N. H. Damrauer, T. R. Boussie, M. Devenney, and J. K. McCusker, *J. Am. Chem. Soc.,* 1997, **119**, 8253.

20. (a) H. Xin, M. Shi, X.C. Gao, Y.Y. Huang, Z.L. Gong, D.B. Nie, H. Cao, Z. Q. Bian, F. Y. Li, C. H. Huang, *J. Phys. Chem. B,* 2004, **108**, 10796; (b) K. P. F. Siqueira, P. P. Lima, R. A. S. Ferreira, L. D. Carlos, E. M. Bittar, F. M. Matinaga, R. Paniago, K. Krambrock, R. L. Moreira and A. Dias, *J. Phys. Chem. C,* 2015, **119**, 17825.
21. L. M. Ying, A. Yu, X. Zhao, Q. Li, D. Zhou and C. Huang, *J. Phys. Chem.,* 1996, **100**, 18387.
22. (a) M. Latva, H. Takalo, V.-M. Mukkala, C. Matachescu, J. C. R.-Ubis and J. Kankarea, *J. Lumin.,* 1997, **75**, 149; (b) N. M. Shavaleev, R. Scopelliti, F. Gumy and J.-C.G. Bunzli, *Inorg. Chem.,* 2009, **48**, 6178; (c) T. D. Pasatoiu, A. M. Madalan, M. U. Kumke, C. Tiseanu and M. Andruh, *Inorg. Chem.,* 2010, **49**, 2310; (d) E. S. Andreiadis, N. Gauthier, D. Imbert, R. Demadrille and J. Pe, *Inorg. Chem.,* 2013, **52**, 14382; (e) Z. Wang, H. Liang, L. Zhou, H. Wu, M. Gong and Q. Su, *Chem. Phys. Lett.,* 2005, **412**, 313.
23. (a) S. V. Eliseeva, D. N. Pleshkov, K. A. Lyssenko, L. S. Lepnev, J.-C. G. Bünzli and N. P. Kuzmina, *Inorg. Chem.,* 2011, **50**, 5137; (b) A. J. Amoroso, M. W. Burrows, R. Haigh, M. Hatcher, M. Jones, U. Kynast, K. M. A. Malik and D. Sendor, *Dalton Trans.,* 2007, 1630; (c) N. M. Shavaleev, S. V. Eliseeva, R. Scopelliti and J.-C. G. Bünzli, *Inorg. Chem.,* 2015, **54**, 9166; (d) N. M. Shavaleev, S. V. Eliseeva, R. Scopelliti and J.-C. G. Bünzli, *Inorg. Chem.,* 2010, **49**, 3927.
24. (a) S. I. Klink, L. Grave, D. N. Reinhoudt and F. C. J. M. Van Veggel, *J. Phys. Chem. A,* 2000, **104**, 5457; (b) M. Shi, F. Li, T. Yi, D. Zhang, H. Hu and C. Huang, *Inorg. Chem.,* 2005, **44**, 8929; (c) H. Xin, M. Shi, X. C. Gao, Y. Y. Huang, Z. L. Gong, D. B. Nie, H. Cao, Z. Q. Bian, F. Y. Li and C. H. Huang, *J. Phys. Chem. B.,* 2004, **108**, 10796; (d) L.

M. Ying, A. Yu, X. Zhao, Q. Li, D. Zhou and C. Huang, *J. Phys. Chem.,* 1996, **100**. 18387.

25. (a) S. Pandya, J. Yu and D. Parker, *Dalton Trans.*, 2006, 2757; (b) M. P. Coogan and V. F.-Moreira, *Chem. Commun*., 2014, **50**, 384.

Papers Presented at Conferences

1. Tuning of excitation wavelength in Eu^{3+}-aminophenyl based polyfluorinated β-diketonate complexes: a red-emitting Eu^{3+}-complex encapsulated in silica/polymer hybrid material excited by blue light. **T. V. Usha Gangan** and M. L. P. Reddy.
   Presented a paper at the poster session in the *International Symposium on Photonic Applications and Nanomaterials (ISPAN-2015)* during 28-30 October **2015**, organized by Sree Chitra Tirunal Institute for Medical Sciences and Technology, Thiruvananthapuram.

2. Tuning of excitation wavelength in Eu^{3+}-aminophenyl based polyfluorinated β-diketonate complexes: a red-emitting Eu^{3+}-complex encapsulated in silica/polymer hybrid material excited by blue light. **T. V. Usha Gangan** and M. L. P. Reddy.
   Presented a poster at the *National Conference on Analytical Science for Technological Excellence and Environmental Sustainability* organized by the Indian Society of Analytical Scientists, held in Munnar, Kerala, India during September 24-26, **2015 (Best poster award)**.

3. Tuning of excitation wavelength from UV to visible region in Eu^{3+}-aminophenyl based polyfluorinated β-diketonate complexes by molecular engineering. **T. V. Usha Gangan**, Ricardo O. Freire and M. L. P. Reddy.
   Presented a poster at the *International Conference on Science, Technology and Applications of Rare earths (ICSTAR 2015)* organized by Rare Earths Association of India (REAI) held at Thiruvananthapuram during April 23-25, **2015**.

4. Tunable White Light Emission from Mixed Lanthanide Coordination Polymers. A. R. Ramya, **T. V. Usha Gangan**, M. L. P. Reddy.

Presented a paper at the *International Conference on Luminescence and its Applications (ICLA)*, Bangalore, February 9-12, **2015**.

List of Publications

1. Tuning of the excitation wavelength in Eu^{3+}-aminophenyl based polyfluorinated *β*-diketonate complexes: a red-emitting Eu^{3+}-complex encapsulated in a silica/polymer hybrid material excited by blue light; **T. V. Usha Gangan** and M. L. P. Reddy
   Dalton Transactions, 2015, **44**, 15924-15937.

2. Visible-light excitable highly luminescent molecular plastic materials derived from Eu^{3+}-biphenyl based *β*-diketonate ternary complex and poly(methylmethacrylate); **T. V. Usha Gangan,** S. Sreenadh and M. L. P. Reddy
   Journal of Photochemistry and Photobiology A: Chemistry, 2016, **328**, 171–181.

3. Synthesis, characterization and photoluminescence properties of Eu^{3+}-*β*-diketonate complexes derived from 3-hydroxy-1-(4-methoxyphenyl)-3-(naphthalen-2-yl)prop-2-en-1-one and various bidentate nitrogen donors; **T. V. Usha Gangan** and M. L. P. Reddy
   Communicated to Journal of Photochemistry and Photobiology A: Chemistry